THE UNIVERSITY OF CHICAGO

TRANSKINGDOM INTERACTIONS REGULATE BEHAVIOR ACROSS THE LIFESPAN

A DISSERTATION SUBMITTED TO

THE FACULTY OF THE DIVISION OF THE SOCIAL SCIENCES

IN CANDIDACY FOR THE DEGREE OF

DOCTOR OF PHILOSOPHY

DEPARTMENT OF PSYCHOLOGY

BY

KENNETH GAYOSA ONISHI

CHICAGO, ILLINOIS

JUNE 2021

Dedication

Truly, nothing is done is isolation. I will be forever grateful for the community of people who made my time at The University of Chicago a remarkable one. I have the upmost gratitude for my loving family. My parents, Felie Gayosa Onishi and Hiroshi Onishi who are always a phone call or short drive away. Even though you have no idea of what I've been doing the last 10 years of my life, I appreciate your support. My brother, Royden Gayosa Onishi, whose genuine nature and determination serves as a model for my strong work ethic. It has been a privilege to spend so much of our adult lives together and I will forever cherish our brotherly bond. You've taught me about making rational financial decisions, a computer scientist's mindset, N+1, and so much more about developing patience in politics and the random happenings on the interwebs. As our paths diverge, I will always love you and will always be just a phone call away.

I'm thankful for my friends who have been forgiving of my regular absence at get-togethers. To my childhood friends, Charlie Levy, Ashley Mueller, Paul Shin, Zeno Shin, John Volpendeseta, and Patrick Yuk – you've kept me in check while in the echo chamber that makes up UChicago politics. Mike Werner, your grit and dark humor, despite the rollercoaster of a life you've lived, has always served as a grounding point, everyday stressors look small when compared to the way unexpected illness can change a life. To my college friends, Nghi Le, Janki Nagarsheth, and Navya Pyati, you make celebrations special. Erin Cable and Jae Peiso, thank you for being true friends during graduate school. Huy Tram Nguyen, you're the best thing that could have happened to me during my final year of graduate school. I give thanks to you all, I cannot imagine going through the ups and downs of graduate school without your combined support.

It’s courageous to be hopeful, because you know one day your heart will be broken.

Table of Contents

List of Figures

List of Tables

Acknowledgments

There are many people to thank for the culmination of this document. Jennifer Stevenson, you took a chance on a naïve undergraduate at The University of Illinois at Chicago and changed the trajectory of my life. Jason Yee, thank you for taking an orphan student under your wing and helping me develop my interests in psychoneuroimmunology and introducing me to Brian. Erin Cable – you've supported my growth both personally and academically. Thank you for lending me your ear and serving as a ray of positivity despite the many obstacles of graduate school. I will forever be grateful for you playing along with my antics of keeping energy levels and morale high as we approached the 20 hour mark of our around-the-clock collections – playing Egyptian Rat Screw, racing office chairs around the building, and singing Mumford & Sons at the top of our lungs as we struggled to stay awake during incubations are all memories I'll always look fondly upon, *ain't no doubt about it*. Tyler Stevenson, your guidance and never-ending love for science and caring nature is truly an inspiration that I hope to instill in future generations of scientists. Katya Fraizer, Megan Kennedy, Vanessa Leone, and Eugene Chang – thank you for sharing with me the world of microbiota, I am so incredibly thankful to have you all as teachers and collaborators.

To my lab mates. Stephanie Dimitroff, Karen Smith, Kelly Faig, Freddy Rockwood, Colleen Wohlrab, and Anita Restrepo Lachman – thank you for letting me attend lab meetings and journal club. I've learned so much by intellectual osmosis from you all. JP Riggle, Dana Beach, and Jharnae Love – thank you for keeping the lab afloat and putting up with my pickiness throughout the years. To the many undergraduates who I've had the pleasure of working with, Feyza Yucel, Carina Elvira, Andrew Maneval, Mary Claire Tuohy, Aashna Mukerji, Jen Novo, Evelina Sterina, Abena Appah-Sampong, Lauren Capra, Joseph Gary, Andrew Scasny, Julie

Klock, Dora Lin, and the dozens more, thank you for your time and efforts, the lab would not be a fraction of its productivity without you all.

I have so much appreciation for my committee. Brian, it is difficult to imagine how much I've grown during our time together. From setting up the ClockLab system, coordinating dozens of students, and pushing the limits of sleep deprivations for the sake of chronobiology, I've been able to see how far I can push my limits. I will be forever thankful for the autonomy you granted me both as lab manager and graduate student. For better or for worse, I will be scarred by your OCD-tendencies to double- (triple- or quadruple-) check everything. Greg Norman, thank you for your endless support and mentoring. I am grateful for the lab community you've created which allowed me to exercise the psychophysiologist part of my brain. Leslie Kay, you have my gratitude for always being dependable, approachable, and a source of reason in the IMB. Boaz Keysar, thank you for reading my dissertation. It is with hope and gratitude that I was able to cross paths with you and Linda Ginzel. I don't think there is a more important life skill than what I learned in Negotiations, and both you and Linda have truly made me a better leader. You all have my appreciation for supporting me as I've grown during my time at The University of Chicago.

My thanks to Elsevier (Onishi et al 2020). Chapter 6 was published in Brain, Behavior, and Immunity, Volume 83, pages 33-43. Circadian and circannual timescales interact to generate seasonal changes in immune function was authored by Kenneth G Onishi, Andrew C Maneval, Erin C Cable, Mary Claire Tuohy, Andrew J Scasny, Evelina Sterina, Jharnae A Love, Jonathan P Riggle, Leah K Malamut, Aashna Mukerji, Jennifer S Novo, Abena Appah-Sampong, Joseph B Gary, and Brian J Prendergast. Copyright Elsevier (2020).

Abstract

Every mammalian cell in the body contains a timekeeper – a molecular clock that tracks time-of-day information. It is well-established that interactions between central (SCN) and peripheral oscillators can influence the mammalian circadian rhythms in physiology and behavior. These experiments examine how the environment influences circadian rhythms in both behavior and physiology. Chapter 3 tests the hypothesis that the gut microbiota is a component of the circadian network by chronotyping mice born and reared devoid of bacteria (germ free mice) and comparing those to 'normal' SPF mice. Chapter 4 examines the role of gut microbiota in mediating the effects of high fat diet on circadian rhythms by chronotyping both bacterially replete and germ free mice fed either a normal chow or high fat diet. Chapter 5 examines the influence of gestational sickness on circadian rhythms in mice with different gut microbiota composition, using a mouse model of maternal immune activation in mice obtained from different rodent vendors known for their differential presence of gut microbiota species. Chapter 6 examines interacting timescales that generate seasonal rhythms in immune function. Seasonally breeding rodents, Siberian hamsters (Phodopus sungorus) were immune challenged every three hours of the circadian cycle in both winterlike and summerlike photocycles. Chapter 6 examines both innate and adaptive immune traits and how seasonal and daily timescales interact to produce rhythmic changes in immune function. Together, these experiments explore transkingdom interactions and their influence on host behavior.

Chapter 1: General Introduction and Background

All biological functions are oriented in time. From single-cell processes optimized to occur in a specific sequence, to organismal behavior coordinated to a specific time of day, biological rhythms are ubiquitous across kingdoms (Young 2001). Species, unicellular and multicellular, use light information to entrain to geological time (Ouyang et al 1998, Pittendrigh & Minis 1972). From daily cycles of predation to food availability, the timing of behavior has consequences for fitness (Spoelstra et al 2016). Indeed, the timing of physiological processes and behaviors have profound implications for health and disease (Arendt 2010, Roenneberg & Merrow 2016).

In optimal conditions, behavior and physiology maintain a stable phase relationship with environmental conditions. Accomplishing this requires two processes: (1) a functional organismal circadian network that internalizes timing cues from the environment to maintain a stable phase relationship between environmental cues and organismal physiology and (2) stable environmental conditions which an organism can entrain to (Pittendrigh 1960). Desynchrony of an organism's biological rhythms with environmental conditions can impair fitness (Ouyang et al 1998, Pittendrigh & Minis 1972, Spoelstra et al 2016).

The following research program examines environmental influences on the circadian network and the development of behavioral rhythms. Additionally, the influence of environmental stressors on the development of the circadian network is studied. First, the role of gut microbiota on circadian rhythms is examined: I test the hypothesis that intestinal microbiota acts as a component of the organismal circadian network (Chapter 3). Second, the influence of high fat diet, independent of and dependent on gut microbiota is explored (Chapter 4). Third, circadian rhythms in offspring that experienced gestational illness were examined; this was done

in the context of defined maternal and offspring microbiomes (Chapter 5). Finally, the interactions between circadian and circannual rhythms were examined in a seasonally breeding rodent model (Chapter 6). In order to provide context for this work, background in circadian rhythms, immune function, gut microbiota, and gestational sickness is first considered.

Circadian Rhythms

Homeostasis, Allostasis, and Biological Rhythms

Homeostasis refers to the complex, coordinated physiological reactions which maintain steady states within an organism. In a view espoused by Cannon (1929), complex, multicellular organisms can be viewed as complex systems, with a multifaceted *milieu interne*, or internal environment. Changes in the external environment can create disturbances in the system that make up an organism's *milieu interne*. Compensatory changes to the system are typically kept within narrow limits as automatic adjustments are made within the organism. Examples of homeostatic functions include temperature regulation and blood serum ion concentrations. Deviations from homeostasis trigger negative feedback mechanisms that continue to act on a system until the desired set-point has been re-achieved (Cannon 1929).

Allostasis, defined as "maintenance of stability through change," expands upon the homeostatic framework by differentiating between variables with relatively static levels (such as blood pH and oxygen saturation) from those that are dynamically regulated in an ever-changing environment (such a daily fluctuations in ambient temperature). Allostasis is an equilibrium by which regulatory mediators reactively deviate from basal levels to engage mechanisms in response to stressors that result in the reestablishment of homeostasis (McEwen & Wingfield 2010). Most mediators of allostasis exhibit robust biological rhythms. Biological rhythms

preserve homeostasis by synchronizing internal physiological processes with predictable changes in the environment, and temporally-organizing physiology to promote survival and optimize energetic resources. Temporal variability of physiology with a stable period (period – time to complete one sleep-wake cycle), many with a period of ~24 hrs, enables individuals to optimize physiology and behavior by actively anticipating predictable daily changes in the environment (Mohawk et al 2012).

Circadian rhythms (abbreviated hereafter as 'CRs') are cycles in biology and behavior that exhibit a period of approximately 24 hours (usually between 23-25 hours, unless the individual has been subjected to extreme manipulations such as genomic mutation, deuterium oxide treatment). To adapt and respond appropriately to daily environmental changes, organisms have evolved internal timing systems that entrain to the 24-hour day. In mammals, these rhythms are ubiquitous and controlled by an innate oscillator, a circadian clock, which is localized within the brain in the suprachiasmatic nucleus (SCN) of the hypothalamus. This endogenous clock generates self-sustaining rhythms in neural electrical and neuropeptide activity with a period of about (*circa*) one day (*dies*), or a frequency of about one cycle per day (~24 hours). Circadian rhythms readily serve two adaptive functions: (1) they allow internal physiology to maintain a specific phase relationship with recurrent, daily changes in the external biotic (food availability, predator presence) and abiotic (e.g., temperature, humidity, light, solar radiation) environment and (2) they allow internal coordination between and among physiological systems distributed throughout the body (Pittendrigh 1993). This 'circadian network' – loosely defined as the coordinated activity of all circadian oscillators in the organism – allows individuals to anticipate recurrent environmental changes and adjust their physiological state accordingly, providing an

obvious adaptive advantage in a sufficiently cyclic environment (Daan & Pittendrigh 1976, Pittendrigh & Daan 1976b, Pittendrigh & Daan 1976c).

Circadian rhythms contribute to Darwinian fitness. With few exceptions, species across kingdoms feature diverse molecular mechanisms that synchronize organismal physiology to diurnal environmental fluctuations (Young 2001). Indeed, endogenous circadian rhythms with a period similar to that of daily environmental fluctuations improve fitness. For example, fruit flies *Drosophila melanogaster* with a wildtype period (often called 'tau' or τ in reference to the Greek letter "t", for "time") of 24 hours exhibit a shorter lifespan when housed in an artificial 'day' that deviates substantially from 24 hr (e.g., 27-, 21-, 13.5 hr days), in contrast to mutant flies with circadian tau (τ) that resonates with the environmental day (Pittendrigh & Minis 1972). Additionally, cyanobacteria expressing circadian periods similar to that of the ambient light:dark cycle were favored under competition with cyanobacteria expressing circadian periods that are dissimilar from the ambient cycle (Ouyang et al 1998). Finally, mice with a shorter endogenous period (~20 hours) showed increased mortality relative to wildtype mice with a 24-hour tau (τ) over the course of one year when both were housed in an outdoor enclosure and exposed to natural, solar days (Spoelstra et al 2016). Collectively these findings suggest that endogenous circadian periods that resonate with environmental photoperiods improve Darwinian fitness.

Properties of Circadian Rhythms

A functional circadian network can be conceptualized as having three essential properties: (1) an endogenous, free-running cycle in the absence of external cues (2) the ability to entrain to external environmental cues (*Zeitgebers*) and (3) the ability to confer phase to the rest

of the body. Most circadian clocks also compensate for changes in temperature. Circadian rhythms are innate and persist in constant environmental conditions (Pittendrigh 1960).

Free-Running Rhythms

In constant darkness, circadian rhythms are self-sustained oscillations in physiology with a period of about 24 hours. Absent environmental time cues, circadian rhythms 'free-run' at the speed of the organism's endogenous period and persist in constant conditions, without a *Zeitgeber* or 'time giver.' The period of this cycle in constant conditions is the organism's free-running rhythm or tau (τ); tau is the amount of time to complete one rest-active cycle. The use of constant conditions as an experimental tool allows to disentanglement of rhythmic processes that are endogenously generated from those that are merely caused (driven by, or 'masked') by external, environmental cues (Pittendrigh & Daan 1976b). The circadian network that keeps organismal time is composed of multiple, distributed oscillators located both in the CNS and in peripheral tissues (Takahashi et al 2008). Once an adequate *Zeitgeber* is introduced, the pacemaker entrains to it, and all organismal rhythms entrain as well (Daan & Pittendrigh 1976, Pittendrigh & Daan 1976b). See Figures 3 to 5 for visualizations in a light:dark cycle and constant darkness conditions.

Entrainment

The environment changes over time; rhythmic changes in the light:dark cycle and temperature are evident in most ecological niches. Temporal adaptation is fundamental for survival of individuals that need to entrain their physiology and behavior to environmental cues. Entrainment represents an organism's adaptation to cyclical changes in the environment. The

prominent photic *Zeitgeber*, light, has been well-studied in entrainment (Albrecht 2012, Pittendrigh & Daan 1976c), though mammals also entrain to food availability and social contact (Mistlberger 1994, Paul et al 2015). During entrainment, the endogenous period of a biological rhythm (lowercase Greek 't': tau, τ; i.e., the speed at which the circadian rhythm free-runs in the absence of an environmental *Zeitgeber*) takes on the period of the entraining stimulus (uppercase 't': T). In order for an organism to entrain to environmental cues, it must reset the phase of an otherwise free-running circadian pacemaker each day, by an amount that corrects for the difference between the period of the environmental time cue and that of the endogenous pacemaker. Light is the principal entraining agent for circadian rhythms. For a circadian rhythm to be stably entrained, a phase shift equal to the difference between τ and T must occur every day (Daan & Pittendrigh 1976, Pittendrigh & Daan 1976b).

In mammals, the master circadian pacemaker is located in the nucleus suprachiasmaticus (nSC; but more commonly referred to as the 'suprachiasmatic nucleus' and abbreviated as 'SCN') of the hypothalamus. The SCN is both necessary and sufficient for rhythmic behavior in mammals. Electrolytic ablation of the SCN (SCNx) in rats results in the loss of circadian rhythms in locomotor activity (Stephan & Zucker 1972). Further, mutant Syrian hamsters have an endogenous tau of 20 hours (i.e., tau mutants); when wild type hamsters with a 24 hour tau (τ) are transplanted with SCN from fetal tau mutants with a 20 hour tau (τ), previously wild type hamsters with a 24 hour tau (τ) show rhythms in locomotor activity with a 20 hour tau (τ), a tau (τ) duration similar to the donor tau mutant (Ralph et al 1990). The observation that tau can be transplanted via the SCN tissue is strong evidence that the SCN is sufficient for the generation of circadian period.

The SCN facilitates entrainment to the light:dark cycle via photic input pathways primarily via the photopigment melanopsin, which is localized in non-image-forming ganglion cells of the retina. Rods and cones in the retina are well-known for their role in vision. Mice without both rods and cones show unaltered phase-shifting responses to light (Freedman et al 1999). Mice lacking melanopsin (*Opn4*$^{-/-}$ mice) show no differences in circadian rhythms compared to their wild type counterparts when housed in constant darkness or in a 12:12 light:dark cycle. However, *Opn4*$^{-/-}$ mice show attenuated phase resetting in response to light pulses (Panda et al 2002). The photic signals from the retina terminating in the SCN, the monosynaptic retinohypothalamic tract (RHT), trace the signals that comprise the SCN's light entrainment pathway via phase shifts in response to light (Hendrickson & Boothe 1976). Together, these data suggest that neither melanopsin, nor rods and cones are necessary for photoentrainment, but that either is sufficient.

The SCN is a collection of 20,000 neurons which form the circadian pacemaker in mammals. Daily oscillators of thousands of coupled clock neurons in the SCN each contain a molecular and biochemical oscillator with a period of about 24 hours (Liu et al 1997). The principal *Zeitgeber* for the mammalian circadian clock, light, shifts the phase of the oscillation in individual clock neurons, which in turn induce shifts in the collective rhythms of the SCN. Light stimulation of the retina during subjective night leads to the release of neurotransmitters glutamate (Glu) and pituitary adenylate cyclase-active protein (PACAP) at the terminal synapses of the RHT in the SCN. Only a fraction of clock cells in the SCN receives light input leading to the activation of proteins that reset the circadian autoregulatory transcription-translation feedback loop (TTFL) with the majority of cells receiving input in the ventrolateral 'core' region (Meijer & Schwartz 2003), primarily in neurons that express vasoactive intestinal polypeptide

(VIP). The expression of neuropeptides within the SCN are not homogenous; rather, the SCN are composed of functionally and phenotypically differentiated cells. While the SCN oscillations are synchronized, they do not share a common phase. These individual cellular oscillations are coupled with specific phase relationships to produce consistent circadian oscillations within the SCN. The dorsomedial 'shell' cells show a PERIOD (see below for molecular clock) peak 2-3 hours before the ventrolateral 'core' cells. The neurotransmitters for SCN synchronization include VIP, arginine vasopressin (AV), GABA, ghrelin-releasing peptide (GRP) and gap junctions (Welsh et al 2010). As a result, a spatiotemporal wave of TTFL gene expression peaks in the dorsomedial SCN in advance of the ventrolateral region of the SCN (Evans et al 2011, Evans et al 2013, Yamaguchi et al 2003).

The Molecular Circadian Clock

The majority of cells in the body, if not all, possess a molecular circadian clock. The circadian transcription-translation feedback loop (TTFL) revolves around the timed transcription of PERIOD (PER) and CRYPTOCHROME (CRY) genes, activated by BMAL/CLOCK dimers, and subsequent accumulation of PER and CRY proteins that progressively inhibit BMAL1/CLOCK dimer activity. The degradation of PER and CRY proteins removes the inhibition from BMAL1/CLOCK and begins a new 24 hour cycle (Takahashi et al 2008). See Figure 2 for schematic of the TTFL. The SCN's sensitivity to the phase resetting properties of light are dependent on the phase of the oscillation at which the stimulus is presented.

Phase Response Curves

Phase response curves (PRCs) provide information about the circadian clock's sensitivity to a *Zeitgeber* at different phases of the circadian cycle and characterize the phase shift induced by exposure to a *Zeitgeber* at different phases of the cycle (Daan & Pittendrigh 1976, Johnson 1999). PRCs for light are produced by first transferring an organism from a light:dark cycle to a room in constant darkness, measuring its free-running rhythm, then providing a light pulse (of a specific intensity and duration) at different phases of the circadian cycle. Responsiveness to a light pulse is mostly consolidated to the subjective night, a time in which the circadian system is not expecting light. In the presence of a light:dark cycle, Zeitgeber Time (ZT) refers to the time, in hours, after lights on; where in a 12:12 light:dark cycle, ZT00 is the time lights turn on and ZT12 is the time lights turn off. In constant darkness, light pulses (light exposure of varying intensity and duration) are delivered at different circadian times (CTs), also known as projected Zeitgeber Times (pZT). pZTs refer to the expected time of light delivery based off the previous day's photocycle. PRCs are species-specific and stimulus-specific (Johnson 1999). When put into constant conditions, nocturnal species that are active during the dark phase show more responsiveness (phase resetting) to photic (i.e., light) cues during their active (dark) phase, and more sensitivity to non-photic cues (i.e., social cues, food, novel running wheel) during their inactive (light) phase. The amplitude of the shift (i.e., the number of hours by which the start of the next clock cycle is shifted) is dependent on the time at which the light stimulus occurs during the organism's circadian phase as well as the duration and saliency of the *Zeitgeber* presentation (Daan & Pittendrigh 1976). In the following examples lights were expected to be on from ZT00 to ZT12 (subjective day) and expected to be off from ZT12 to ZT00 (subjective night). Light pulses early in the subjective night (e.g., pZT15) produce a high amplitude phase delay, whereas

light pulses later in the subjective night (e.g., pZT19), generate a high amplitude phase advance (Daan & Pittendrigh 1976).

The "Web of Circadian Pacemakers"

In multicellular organisms, every region or organ exhibits robust circadian rhythms in clock gene expression and metabolic activity. Under steady state conditions, these organ-level rhythms are synchronized within the whole body. They form a hierarchically structured circadian network, with the circadian clocks in the brain (i.e., the SCN) as the master coordinator (Figure 1). Because individual cells contain circadian clocks, these single-cell oscillators must be synchronized within the tissue. In turn, entire tissues and organs are kept in a stable phase relationship with each other to make use of time information for the entire multicellular organism. To build a coherent circadian system, such that all tissues in the entire organism are in the same phase (or at least have stable phase relations with one another), cellular clocks must be able to respond to stimuli, integrate the phase information regarding when the stimulus occurred in their molecular clock mechanism, and transfer clock information to other cells (Schibler & Sassone-Corsi 2002). This organization is present at the systems level where light is detected by the retina then transmitted to the SCN. There, light signals are integrated to adjust the information about time or phase of solar day. Subsequently, this elicits a change in the onset of the molecular clock in the SCN and behavior in following cycles (Meijer & Schwartz 2003). There are three hallmarks of organization in a circadian network: (1) the perception of the environmental input integration of time-related information into the autonomous circadian network, (2) transmission of adjusted timing information to metabolic and physiological processes, and (3) subsequent feedback of tissue information to the circadian network

(Pittendrigh 1960). The circadian network must continuously adapt to and synchronize with the environment and the body's internal signals in order to organize individual cellular clocks and coordinate tissue networks into a coherent, functional organismal-level network that regulates behavior and physiology. The SCN synchronizes peripheral oscillators to ensure temporally coordinated physiology. Further, peripheral oscillators may be connected among themselves and may communicate back to the central pacemaker in the SCN (Schibler & Sassone-Corsi 2002).

The SCN is not necessary for the generation of peripheral tissue circadian oscillations, but it is essential for their persistent coordination (Balsalobre et al 2000). Across kingdoms, different genes drive molecular oscillations, suggesting multiple independent origins of circadian clocks' responsiveness to light (Paranjpe & Sharma 2005). One core function of the circadian system is to synchronize the clocks within an organism. While the mechanisms of SCN communication pathways remain poorly understood, the SCN is necessary and sufficient to drive rhythmic oscillations in locomotor activity (Ralph et al 1990, Stephan & Zucker 1972). The SCN is traditionally thought to be positioned at the top of the circadian hierarchy, with SCN lesions (SCNx) resulting in arrhythmic locomotor behavior (Stephan & Zucker 1972). However, in addition to the light-responsiveness of the SCN pacemaker oscillator, peripheral mammalian cells also house circadian oscillations that do not respond directly to changes in the light:dark cycle, but rather are sensitive to various chemical, electrical or temperature cues, communicated from interoceptive and exteroceptive routes (Balsalobre et al 2000, Brown et al 2002). Indeed, persistent circadian rhythms, absent any input have been documented in multiple peripheral tissues *in vitro* (recorded outside a living organism), via oscillations in reporter molecules linked to core clock genes, such as the commonly used PER2::luc fusion protein. PER2::luc allows for quantification of daily PER2 protein expression in tissues via luminescence. In the behaviorally

arrhythmic SCNx mouse, circadian oscillations in PER2::LUC were detected in kidney, liver and submandibular glands. While amplitude of PER2::LUC was dampened in SCNx mice, the free-running period of peripheral clocks were similar to activity rhythms recorded before the SCNx. This indicates that the organismal level circadian network still functions absent the SCN, but its properties are fundamentally altered (Tahara et al 2012).

Food Entrainable Oscillator

The precise timing of food appearance is a salient signal for organizing physiology and behavior of many organisms in nature. In the laboratory, rodents readily entrain to timed feeding. When food is freely available, nocturnal species eat during the dark phase – a circadian rhythm controlled by the SCN and entrained by light (Challet 2019, Mistlberger 1994). However, when light signals are not concordant with food availability (i.e., if nocturnal animals are fed only during the day), then peripheral organs that regulate metabolism synchronize with environmental food availability instead of with the light:dark cycle. In nocturnal animals such as rats, mice and hamsters, when food is experimentally made only available during the light phase, a major component of locomotor activity shifts to the phase of food availability (i.e., daytime) (Mistlberger 1994, Schibler et al 2003). Metabolism shifts as well. When mice or rats are restricted to one daily meal during in their light phase, peripheral organ clocks shift and animals become active during the day. This shifted activity, which precedes food delivery in the rest phase, is known as food anticipatory activity (FAA) (Mistlberger 1994, Stephan 2002).

Food serves as a powerful *Zeitgeber* for peripheral tissue-level circadian clocks, and it does so without affecting the molecular rhythms in the SCN. A circadian oscillator distinct from the SCN generates food anticipatory activity (FAA). The substrates that mediate this anticipatory

behavior have collectively come to be termed the food entrainable oscillator (FEO). The FEO is a component of the circadian network of clocks, but its precise anatomical localization remains elusive. Abundant evidence has identified an SCN-independent FEO in rodents: SCNx rats and mice exposed to time-feeding continue to exhibit FAA, indicating the central SCN light-entrained pacemaker is distinct from behavioral rhythms that entrain to food (Stephan et al 1979, Storch & Weitz 2009). The FEO can be disentangled from the light entrainable oscillator (LEO) when examining rats trained to a light:dark T cycle with a 24 hour period and feeding T cycle with a 26 hour period. Rhythmic clock gene expression in peripheral organs phase shift (i.e., liver, esophagus, stomach, colon) to a new phase, which aligns with the 26 hour cycle of food intake rather than light, but the TTFL molecular clock rhythms of the SCN and cornea remain unaltered under timed feeding (Davidson et al 2003, Stokkan et al 2001), further indicating the separability of the FEO and the LEO, and the tissue-specific responsiveness of the circadian network to light and food. Although the SCN may not shift phase under timed feeding, timed feeding can entrain a disrupted SCN rhythm following exposure to constant light conditions (LL; a circadian manipulations known for induing arrythmia in nocturnal rodents), indicating food delivery as an entrainment cue into the SCN (Lamont et al 2005, Mistlberger 1994). Collectively, these data suggest distinct mechanisms driving the FEO and LEO.

Whereas the exact mechanisms for FAA remain elusive, studies suggest both leptin and body composition play a role in the emergence of FAA. Leptin is a hormone released from adipocytes that decreases appetite and increases energy expenditure (Friedman & Halaas 1998). Leptin-deficient *ob/ob* mice are obese and have decreased locomotor activity, and leptin administration in these mice increases locomotor activity and decreases adiposity. While total activity in *ob/ob* mice is reduced, food intake is increased (Pelleymounter et al 1995). Food

anticipatory activity is augmented in *ob/ob* mice, and leptin administration completely eliminates FAA in wild type mice collectively establishing a major role for leptin in FAA (Ribeiro et al 2011).

By all accounts, the FEO operates via properties that are non-overlapping with the mechanisms that mediate the canonical molecular clock and its TTFL. Clock gene mutations alter circadian rhythms in light-entrainable locomotor rhythms (Takahashi et al 2008), although clock gene rhythms are not necessary for food entrainment or for the expression of FAA. Mice missing core circadian clock genes such as *per1*$^{-/-}$; *per2*$^{-/-}$ or *bmal1*$^{-/-}$ knockouts continue to show FAA in the presence of light:dark cycles (Mendoza et al 2010, Storch & Weitz 2009). Even absent photic environmental cues (i.e., in constant darkness), *bmal1*$^{-/-}$ and *per2*$^{-/-}$ knockout mice continue to show FAA in constant darkness, excluding the possibility that a circadian clock responsive to light contributes to FAA (Storch & Weitz 2009). Though in an abrupt shift from *ad libitum* (unlimited) feeding to timed, daytime feeding *bmal1*$^{-/-}$ mice fail to exhibit FAA (Fuller et al 2008, Mistlberger et al 2008), a gradual shift to timed, daytime feeding results in a typical FAA emergence (Storch & Weitz 2009). Further studies in *per2*$^{-/-}$ mice show normal FAA behavior, while, paradoxically, *per2*^{Brdm1} mutant mice do not show FAA (Feillet et al 2006), which may result from widespread effects on locomotor activity independent of defects in circadian clock function, especially in light of evidence that *per2*^{Brdm1} encodes a functional PER2 protein with abnormal properties (Shearman et al 2000). A complete deletion of clock genes in *bmal1*$^{-/-}$ or *per1*$^{-/-}$/*per2*$^{-/-}$ does not attenuate the emergence of FAA in mice, though a mutation of the *per2* gene in *per2*^{Brdm1} mice eliminates FAA in locomotor activity. These data indicate that deletions of individual clock genes (both in the positive and negative arms of the circadian molecular feedback loop) do not influence the emergence of FAA behavior, but a *per2* mutation

in *per2* ^{Brdm1} mice abolishes anticipation of mealtime (Feillet et al 2006, Storch & Weitz 2009). Together, these data indicate that deletion of canonical clock genes are not necessary for the emergence of FAA (Storch & Weitz 2009). Although, a more nuanced role of the molecular clock components and their role in the emergence of FAA remains to be elucidated.

Sex Differences in Circadian Rhythms

Decades of biomedical research has omitted the use of females in pre-clinical research, out of a belief that females show increased variability compared to their male counterparts due to their hormonal cycles. Male biased studies where only males are included in their report outnumber female-only studies 5.5 to 1 (Beery & Zucker 2011). However, this sex disparity in basic scientific research lacks merit as it relates to increased variability in female rodents, where a meta-analysis performed showed no increases in variability among female mice compared to their male counterparts (Prendergast et al 2014). Circadian rhythm research is no exception to the disparities in the number of male-only and female-only studies. However, the influence of chromosomal sex and gonadal hormones has been addressed in decades of research on biological timing.

Free-running period, tau (τ), varies between sexes. The influence of sex hormones on circadian period has been well-established in rats and hamsters, where ovariectomy (the removal of the main source of circulating estradiol in these rodents) lengthens period, and an estradiol implant shortens period (Albers 1981, Morin et al 1977). Surgically or chemically castrated (male) or ovariectomized (female) mice show inconsistent effects on period (Butler et al 2012, Daan et al 1975, Jechura et al 2000, Kuljis et al 2013). While all species have an endogenous

circadian period very close to 24 hours, differences in period due to sex hormones are well-established in some rodent species while others require further clarification.

Activity onset (the time at which daily activity begins) varies between sexes. Inter-day variability in activity onset is considerably greater in females than in males, and is closely tied to the phase of the estrous cycle the female is in. Activity onset is most advanced on the day (or night, in nocturnal animals) of ovulation, the day of elevated estradiol levels (Blattner & Mahoney 2014). This advanced phase of activity on the day of estrus (or night of proestrus) might play an evolutionary advantage where earlier wakefulness may lead to improved mate selection. The exact mechanism by which estradiol and other sex hormones confer their phase advancing effect in female mice has yet to be determined. It may be that the SCN shifts a little each day under the direct influence of estradiol, as indicated by a shortened period following estradiol administration in some rodent studies (Krizo & Mintz 2014).

Little information on sex differences in food anticipatory activity (FAA) have been reported in mice. Food anticipatory behavior is not SCN-dependent (see above). Sex differences in mice have shown that when using a high fat food as a meal for FAA, males exhibited FAA and females did not. While female mice did not show anticipation of a daily high fat meals during the training days, they did show increased activity at scheduled mealtime when that meal was withdrawn during the probe trial of 48 hours of food deprivation (Hsu et al 2010).

Immune Function

Mammals are constantly exposed to microorganisms that have the potential to cause host sickness. When pathogenic microbes have access to vulnerable sites for passage into the body, the result can be profound disease or death. Whether these foreign pathogens induce host

sickness is dependent on both aggressiveness of the pathogen and strength of the immune system (Hart 1988, Hart 2011). The immune system is a network of diverse cell types that circulate through networks of the lymphatic system, blood vessels and tissues such as brain, skin, and gut. The function of the immune system is to protect the organism from invasion by exogeneous microscopic life forms or particles and to rid the body of defective or damaged cells (Janeway & Medzhitov 2002).

Innate Immune System

There are two arms to the immune system: the innate immune system and the adaptive immune system. The innate immune system serves as the organism's endogenous, built-in resistance to pathogens; it is fast-acting and requires no previous experience (i.e., previous pathogen exposure) to elicit an immune response. Innate immunity covers many areas of host defense against pathogenic microbes, including the recognition of pathogen-associated molecular patterns (PAMPs), molecules on the surface of pathogenic microbes. Innate immunity lies behind most inflammatory responses, triggered by macrophages, leukocytes, and mast cells through their innate immune receptors (Janeway & Medzhitov 2002). This arm of the immune system restricts tissue damage and infection to the site of the pathogen entry. It involves phagocytes such as macrophages and neutrophils that engulf foreign or infected cells. Macrophages serve as antigen presenting cells (APCs) in the innate immune system; they break down invading pathogens and present features of the pathogen on their cell membranes for other immune cells to recognize (Janeway & Medzhitov 2002). Phagocytes recognize foreign substances, but they do so in a nonspecific way. They recognize general features of foreign substances, rather than a single antigenic site. After recognition, some macrophages are activated and release a number of

products that function in defense. Macrophages release nitric oxide which interferes with mitochondrial respiration and proliferation of the cells surrounding it. Activated macrophages also release proinflammatory cytokines: small signaling proteins used to regulate immune responses (Janeway & Medzhitov 2002). Cytokines, such as interleukin-6 (IL-6) and tumor necrosis factor alpha (TNFα), localize actions that facilitate the development of an inflammatory reaction at the wound site. Proliferation of T and B cells are not required for the initial stages of the innate immune response and the initiation of an innate immune response can be detected within an hour of contact with the appropriate pathogen (Konsman et al 2002). The innate immune system has diverse mediators and structures; it includes physical barriers such as skin, but also phagocytes, complement immune system cells, and cellular receptors such as toll-like receptors (TLRs). The collective activity of the innate immune system functions to prevent infection, eliminate pathogens, and initiate an inflammatory process. One of the major intersections between psychology and immunology lies in the relationship between the activity of the innate immune system and the brain: innate immune signaling molecules (i.e., cytokines), which are initially generated to cause local inflammation and activate cellular immune processes, also result in profound behavioral changes in the infected host organism (Dantzer et al 2008, Hart 1988).

Cytokines - molecules secreted by immune cells - orchestrate a complex set of cellular cascades throughout the entire organism to combat infection and injury. This organismal reaction is often called the acute phase response (APR) to infection. The APR is part of the early defense of the innate immune system, activated by infection. When responding to pathogens, the innate immune response produces cytokines generated by activated immune cells (e.g., macrophages, T cells). Proinflammatory cytokines such as IL-1β and TNFα have numerous effects throughout the

body, including their participation in the APR (Dantzer et al 2008, Hart 1988). The APR results in complex reactions that aim to reestablish homeostasis. Physiological changes that occur during the initial hours of infection and innate immune activation include fever, increased slow-wave sleep, shifts away from liver protein synthesis toward projection of acute-phase proteins, and increased leukocyte activity. Fever occurs even in primitive organisms and is highly adaptive (Kluger & Rothenburg 1979). Increasing body temperature is advantageous, as many microorganisms proliferate best at or below the body temperature of the host (Zwietering et al 1991), slight increases in body temperature can cause microorganisms to proliferate more slowly. Fever increases the intensity of immunological responses to infection by increasing cellular activity of immune cell division and enzymatic-dependent reactions (Small et al 1986). Increases in body temperature entail a large metabolic cost, up to 13% for every 1°C increase (DuBois 1921). Cytokines can lead to an increase in a set point of body temperature such that an organism feels cold under previously 'normal' environmental temperature. This will lead an organism to attempt to arrive at a new thermal equilibrium by reducing heat loss and increasing heat production. Animals shiver to increase metabolism, shift blood flow away from the periphery, or curl up to maintain increased temperature (Kluger 1978).

The cytokines that induce alterations in immune cell function during the innate immune response also generate sickness behaviors (Hart 1988). Sickness behaviors function to reduce the energetic costs of survival and to reduce exploratory motivation, and so that heat and energy expenditure will be limited to allocate available energy toward maintaining an increased temperature. Decreases in locomotor activity, social interaction and sexual behavior function to reduce the energy used in behavior and reduce surface area to minimize heat loss (Hart 1988). Decreased food intake, or anorexia, is important to reduce plasma iron in order to inhibit

bacterial proliferation, as bacteria require iron to replicate (Kluger & Rothenburg 1979); as an adaptive response to bacterial invaders, iron is actively sequestered in the liver during infection (Hart 1988). However, decreases in food intake may also be a maladaptive byproduct of the overall reduction in hedonic drive whose primary adaptive significance lies in decreasing energy expenditure. Increases in sympathetic nervous system activity and the hypothalamic-pituitary-adrenal axis responses are also hallmarks of the APR: catecholamines and glucocorticoids are produced at higher levels to liberate energy from bodily stores, leading to depletion of body mass (mainly in the form of stored fat), but they also catalyze the conversation of glycogen to glucose in order to break down muscle proteins into amino acids (Rabasa & Dickson 2016). These metabolic processes are capable of freeing up energy for use in fever and cell proliferation, and homeostatic maintenance of other bodily functions during periods of anorexia that commonly follow innate immune activation (Maier & Watkins 1998). The way pathogens and the immune system influence behavior indicates communication between the immune and central nervous systems (Dantzer et al 2008).

Adaptive Immune System

Adaptive immunity refers to the slower acquired immunity by exposure to pathogens. This arm of the immune system requires presentation of foreign microbes and their cell surface markers to mount a robust immune response in the future. T cells, a class of lymphocytes, arise from the bone marrow and migrate to the thymus where they mature. After maturation, T cells circulate through the blood and lymphatic system, and reside in secondary immune organs (i.e., spleen and lymph nodes). Each T cell has a selective receptor on its surface that can recognize and bind a single, unique antigen (Banchereau et al 2000, Iwasaki & Medzhitov 2004, Maier &

Watkins 1998).

Immunological memory allows species to mount rapid immune responses to pathogens (and their surface antigens) upon secondary exposure, even after long intervals have passed since a primary exposure occurred (Gray 2002). One type of immune response which relies on the formation of T cell-dependent immunological memory is the delayed-type hypersensitivity (DTH) response. DTH responses involve cellular activation of CD4+ T-helper cells and cytotoxic CD8+ T cells (Actor & Ampel 2009). DTH response involves two stages, a sensitization stage and a challenge stage. During the initial skin sensitization or exposure, skin dendritic cells (DCs) are activated and migrate to skin-draining lymph nodes where DCs present the antigen to major histocompatibility molecules and prime antigen-specific T cells. Presentation of an antigen modifies cell-surface and intracellular molecules of skin DCs, which migrate to regional lymph nodes to initiate primary T cell response to the antigen. Memory T lymphocytes are created, and later a reaction to the eliciting stimulus (challenge or secondary phase) during which memory T cells augment the immune response to the same pathogen (and their surface antigen) during the DTH reaction. During the challenge stage, the antigen modifies skin DCs which recruit and activate antigen-specific T cells to the involved area of exposure. Memory T cells potentiate proinflammatory cytokine secretion and accessory cell recruitment upon subsequent exposure to the same antigen (Gaspari et al 2016). DTH responses play a crucial role in clearing bacterial and viral infections (Gray 2002).

Immune Mechanisms Within the Central Nervous System

Sickness behaviors in response to pathogen exposure are orchestrated by the brain's ability to integrate information from the peripheral immune response. Peripheral immune

responses are communicated to the brain through numerous pathways. First, cytokines in the periphery activate local afferent vagal nerves during abdominal and visceral infections (Bluthé et al 1994, Watkins et al 1994). The vagus nerve transmits immune information from the periphery to the brain, confirmed in subdiaphragmatic vagotomy (SDx) experiments. When the vagus nerve is severed below the diaphragm, cardiac and pulmonary function are not compromised, vagal afferents are shown to mediate the activation of numerous brain regions in response to peripheral LPS injection, measured by attenuated expression of c-fos in the primary projections of the vagus nerve (Wan et al 1994). Second, toll-like receptors on microglia lining the circumventricular organs and choroid plexus respond to circulating pathogen-associated molecular patterns by producing pro-inflammatory cytokines (Quan et al 1998). The cytokines produced by the cells adjacent to the blood-brain barrier can enter the brain by diffusion (Vitkovic et al 2000). Third, great increases in proinflammatory cytokine production can enter transporter cells lining the blood brain barrier and bind in the brain (Banks 2009).

Inflammation in the periphery can result in increased cytokine release in the brain. When information about a pathogen (communicated via cytokine or neural pathways) is transmitted to the brain, microglia (the brain's resident immune cell) produce proinflammatory cytokines in response. Systemic administration of LPS results in proinflammatory cytokine expression in the brain (van Dam et al 1992). Additionally, administering individual cytokines in the brain, absent peripheral infection, induces sickness behaviors (Anforth et al 1998, Palin et al 2008). Further, disruption of the inflammatory TNFα-activated JNK pathway in the central nervous system via intracerebroventricularly administration of JNK pathway disruptor, D-JNKI-1, prevents sickness behaviors (Palin et al 2008). The sickness behaviors orchestrated by the brain are adaptive strategies critical to host survival (Dantzer & Kelley 2007).

Circadian Control of the Immune System

Many aspects of immune function exhibit robust daily oscillations. In common with changes in behavior and other aspects of physiology, there exist stark diurnal oscillations in immune function (Lange et al 2010, Scheiermann et al 2013). For example, leukocyte subpopulations oscillate in a circadian manner. Circadian patterns of immunity depend on whether a given species is diurnal or nocturnal. Circulating blood leukocyte concentrations are high in the blood during the rest phase and low during the active phase (Dhabhar et al 1994). Further, naïve T cells and production of proinflammatory cytokines peak during the inactive phase, where cytotoxic effector leukocytes and production of anti-inflammatory cytokine IL-10 peak during the active phase (Lange et al 2010). In terms of the deployment and trafficking of blood leukocytes, the number of leukocytes in circulation peak during the rest phase: released from immune tissue into the blood at the beginning of the resting phase, depending on local sympathetic innervations and the decline on circulating glucocorticoids (Scheiermann et al 2012).

The frequency and timing of the rhythms varies by species and cell type. Nocturnal species exhibit decreased circulating blood leukocyte concentrations during the dark (active) phase and increases during the light (inactive) phase (Johnson et al 2004), whereas diurnal species exhibit the antiphase waveform (Dimitrov et al 2009). However, not all immune cells follow this pattern, increases in CD4+ and CD8+ T cells are seen during the dark phase, with a negative correlation between cortisol and total T cell counts. Glucocorticoids exert a clear role in leukocyte trafficking, with decreases in total blood CD4+ and CD8+ cells in response to cortisol infusion in humans (Dimitrov et al 2009). Glucocorticoids play a major role in the orchestration of the large-scale redistribution of immune cells, although the effect of glucocorticoids depend

on the specific immune cell type (Kawate et al 1981, Scheiermann et al 2013). The presence of blood leukocytes trafficked into the skin and organs during the active phase presumably allows for more rapid responses to pathogen exposure (Viswanathan & Dhabhar 2005).

Daily cycles figure prominently in the adaptive organization of biology. Just as behavior changes seasonally and daily, so too does physiology. As indicated above, the immune system alters its responsiveness to pathogens depending on time-of-day (Logan & Sarkar 2012, Scheiermann et al 2013). Additionally, administration of the same high dose of lipopolysaccharide (LPS; a gram-negative bacterial mimic) to mice housed in a 12:12 light:dark cycle is 100% lethal when given 1 hour before lights off, but results in only 25% mortality when administered during the midpoint of the dark phase (Marpegan et al 2009). In a hamster model of circadian arrythmia, daily oscillations of leukocytes are consistently elevated throughout the circadian cycle (Prendergast et al 2013). Response to simulated gram-negative bacteria infection vary (Prendergast et al 2015) and the responsiveness of individual immune cells changes as a function of circadian phase (Gibbs et al 2012a). Further, SCNx rats show attenuated fever response in the dark phase when injected with LPS at ZT03 (*Zeitgeber Time*, hours after lights on; here, 3 hours after lights on) compared to sham-SCNx rats (Wachulec et al 1997). Circadian rhythms are important for normal immune responses, though patterns of peak responses to pathogens vary as a function of species, pathogen dose, phase of circadian challenge, sickness response, and pathogen type (Scheiermann et al 2013, Tognini et al 2017).

Seasonal Photoperiodic Changes in Immune Function

Daily alterations in behavior and physiology revolve around the Earth's rotation on its axis and change depending on time-of-day. Additionally, Earth's rotation around the Sun causes

months of limited resources during the wintertime in some non-equatorial regions (Nelson 2004, Nelson & Demas 2004). In this dynamic environment, organisms exhibit robust and predictable physiological and behavioral changes which optimize their Darwinian fitness. In complex multicellular animals, these changes are orchestrated by the central nervous system, a critical node for the integration of environmental stimuli and endogenous signals. The input into the hypothalamus coordinates a diverse range of physiological systems, and environmental and internal signals to appropriately time adaptive changes in physiology and behavior (Hut & Beersma 2011).

Seasonal rhythms in reproduction are one strategy that many temperate zone species use for the propagation of their species and maximizing the use of seasonally changing energy reserves (Nelson & Demas 1996). The timing of seasonal reproduction requires extensive neuroendocrine plasticity in response to seasonal, social and hormonal cues. The annual change in daylength (commonly referred to as 'photoperiod') provides a predictive, noise-free cue which indicates the time-of-year. Scores of species possess the ability to internalize photoperiodic cues in order to engage in seasonal changes in physiology and behavior (Follett 2015). Seasonality results in the generation of predictable changes in the CNS and periphery; driven by, and driving, annual changes in gene expression in a cell-specific manner (Stevenson 2017).

Laboratory mice possess robust circadian rhythms, and thus are suitable models for investigations of circadian biology, but they exhibit little-to-no physiological changes over the course of the year, and thus are not a useful model system in which to examine the biological substrates of seasonal rhythms (Stevenson & Prendergast 2015). Siberian hamsters (*Phodopus sungorus*), in contrast, exhibit robust changes in immune and reproductive function when photoperiod is manipulated in the laboratory, and thus have been adopted as a common model

species for investigations of seasonal biological rhythms (Martin et al 2008, Nelson 2004, Stevenson & Prendergast 2015).

In non-equatorial regions, winter brings with it annual changes in abundance of foraging options. In winter, species are exposed to harsh conditions such as low temperature, coincident with reduced food and water availability. With increased metabolic demands, Siberian hamsters cease to breed during the short days of winter. Long (>14 hours of light per day) days stimulate, and short (<13 hours of light per day) days inhibit, reproductive physiology (Nelson 2004). They also undergo significant decreases in body mass. This adaptive strategy may have evolved because maintenance of small body size throughout winter requires less food, and less heat loss as a result of reduced surface-to-volume ratio (Martin et al 2008, Nelson 2004).

Seasonally breeding species adjust their sickness responses prior to winter by using daylength to anticipate energetically demanding conditions. Fever and anorexia are limited by food availability during the short days as a result of fewer energetic reserves during winter (Heldmaier et al 1982). Exposure to gram-negative bacterial mimic, lipopolysaccharide (LPS), activates the immune system and initiates several physiological and behavioral responses that constitute the acute phase response (APR). These include iron-withholding, reduction in food and water intake, and reduced interest in sexual, parental and other social interactions (Hart 1988). Attenuation of the APR is seen in Siberian hamsters housed in short day, by attenuated anorexic response, less iron intake alongside decreases in proinflammatory cytokines IL-6 and IL-1β following LPS injection, compared to their long day counterparts (Bilbo et al 2002b). Behaviors such as decreased activity and increased sleep to conserve energy allow for tissue repair during metabolically demanding times. Although mounting an immune response requires substantial energetic costs, anorexia following infection is thought to reduce energy spent

foraging, reduce surface area where heat can escape, and reduce concentrations of iron in the blood (Exton 1997). Food preferences change following LPS administration; intake of foods low in iron, such as carbohydrates and fats are preferred over proteins which are high in iron (Arnaud et al 1995). Mice that reduce food intake during bacterial infection recover more quickly than mice that maintain normal food intake (Exton 1997). In hamsters housed under short winter daylengths, adaptive cell-mediated immune responses are strikingly enhanced: for example, DTH responses are substantially greater in hamsters that have undergone complete seasonal adaptation to short daylengths (Bilbo et al 2002a, Prendergast et al 2004). Indeed, both the innate and adaptive arms of the immune system show striking attenuation and augmentation, respectively, as a result of changing photoperiods in Siberian hamsters (Onishi et al 2020).

Gut Microbiota

Mammals coexist in a mutualistic relationship with foreign microbes, the microbiota (also referred to as microbiome), which constitutes a complex microbial community residing in and on the organism. The largest contiguous population of microbes are found in the gut, largely in the distal colon. This ‘gut microbiota,’ is composed of microorganisms from diverse kingdoms, mainly bacteria (Palmer et al 2007). The composition and development of intestinal microbes is dependent on multiple factors such as birth delivery route, environmental bacteria, food intake, and time-of-day (Sekirov et al 2010). Consumption of different diets allows the study of high fat and high carbohydrate diet on microbiota (Backhed et al 2007).

The composition of the gut bacteria influences behavior, and vice versa (Nicholson et al 2012, Parkar et al 2019). The use of germ free mice that lack microbiota allows examination of the necessity of these bacteria in select aspects of host physiology and behavior (Bäckhed et al

2004). The gut-brain axis integrates neural, hormonal and immunological signaling between the gut and the brain (Mayer 2011). Communication between the brain and the gut is bidirectional, enabling coordination of complementary processes between the immune system, central nervous system and gut microbiota (Nicholson et al 2012, Sekirov et al 2010).

Microbiota Composition and Development

The intestinal microbiota is composed of a wide range of bacteria, mainly anaerobes (Harris et al 1976, Savage 1970, Sekirov et al 2010). In humans, the gut microbiota is mainly composed of Bacteroidestes and Firmicutes, with relatively small numbers of Proteobacteria and Cyanobacteria (Eckburg et al 2005). Colonization of the intestinal tract with microbes begins immediately after birth. When passed through the birth canal, infants are exposed to a complex of microbial communities that influence their intestinal gut microbiota population. Indeed, infants delivered through cesarean section possess different microbial populations compared with vaginally delivered infants (Ruan et al 2016). It is thought that colonization after vaginal birth is involved in shaping the composition of the gut microbiota into adulthood. Infant gut microbiota composition shifts greatly during the first few years of life and then stabilizes to resemble those of young adults (Palmer et al 2007). The host genotype plays a role in the development of offspring gut microbiota, as the similarity between fecal profiles of monozygotic twins are higher than genetically unrelated individuals (Zoetendal et al 2001).

Diet also profoundly shapes the gut microbiota, rendering some populations more capable of proliferation at the expense of less-adept populations. Diet affects both the relative (species diversity) and absolute abundance (total numbers) of gut bacteria (Korem et al 2015). Dietary fiber, or glycans, form the primary nutritional sources for microbes in the distal intestine. The

mammalian genome encodes for limited carbohydrate-active enzymes that can break glycans into usable carbohydrates. As a result, glycans such as starch and fructo-oligosaccharides reach the large intestine in their undigested forms. In contrast, the gut microbiota is estimated to encode for tens of thousands of carbohydrate-active enzymes (Cantarel et al 2012). Degradation of glycans liberates glucose. Concentration of intestinal glycan is significantly correlated with microbe abundance for specific bacteria that can break down glycans including Clostridia, Bacteroidia and Fusobacteria (Eilam et al 2014). Low fiber diets disrupt intestinal barrier function in mice, which is rescued by fiber supplements (Desai et al 2016, Schroeder et al 2018, Zou et al 2018). Bacteria use of dietary fiber results in the production of short-chain fatty acids (SCFAs), which play an important role in maintaining regulatory T (T_{reg}) cell immune homeostasis (Smith et al 2013). These T_{reg} cells in turn have an important role in maintaining homeostasis in the gut, with deficiencies leading to intestinal inflammation and dysbiosis (He et al 2017).

A high fat diet (HFD) negatively impacts metabolism in part via the gut microbiota; indeed, HFD can have adverse effects on gut microbiota by increasing systemic inflammation. Moderate increases of plasma concentration of LPS in response to HFD is defined as metabolic endotoxemia and influences host inflammation (Cani et al 2007). Four weeks of HFD results in increases of LPS-expressing bacteria, which leads to elevated LPS concentrations in the gut and serum of mice (Neal et al 2006). LPS then chronically signals TLR4 and CD14 (both LPS receptors) to promote weight gain and adiposity, and increased inflammation in white adipose tissue macrophages. Low-concentration LPS infusion for four weeks increases body, liver and adipose mass to similar levels as mice fed a HFD. CD14-deficient mice resist most of the LPS-

and HFD-induced features of metabolic disease indicating that metabolic endotoxemia dysregulates inflammatory tone and triggers body weight gain (Cani et al 2007).

Gut microbiota composition is vital in HFD-induced metabolic endotoxemia. Antibiotic treatment reduces metabolic endotoxemia and cecal LPS content in HFD-fed mice (Cani et al 2008). A HFD also increases intestinal permeability by reducing the expression of genes that code for tight junction proteins. *In vivo* intestinal permeability measured using a fluorescent sugar, dextran (size: 4 kilodaltons), quantified from serum one hour after oral gavage, show increased serum dextran in HFD-fed mice relative to mice fed a normal diet (Cani et al 2008). High fat diet changes gut microbiota towards decreasing numbers of Bifidobacterial, a genus of bacteria shown to reduce intestinal LPS levels in mice and increase mucosal barrier permeability (Griffiths et al 2004, Wang et al 2006). Interactions with HFD and gut microbiota are seen when antibiotic treatment reduces metabolic endotoxemia and cecum contents of LPS in HFD-fed mice, which correlates with reduced body mass, adipose tissue and inflammation – indicating the serum LSP comes from bacteria responsive to antibiotic (Cani et al 2008).

The adverse effects of HFD on body composition are mediated by the immune system. A HFD in wild type mice results in increased LPS levels in the intestinal lumen as well as in circulating plasma by altering gut microbiota composition and increasing intestinal wall permeability through induction of toll-like receptor 4 (TLR4; triggering downstream immune signaling). The importance of TLR4 is underscored when $TLR4^{-/-}$ mice fed a HFD do not show increased endotoxin or proinflammatory cytokine levels, indicating a role for gram-negative commensal microbes and associated LPS in increasing inflammation (Kim et al 2012). Further, irradiated (a procedure shown to abolish host bone marrow) wild type mice transplanted with bone marrow from $TLR4^{-/-}$ mice results in chimera mice deficient in bone marrow TLR4 (BMT-

TLR4$^{-/-}$), mice with a hematopoietic cell-specific deletion of *tlr4*. A HFD results in obesity in chimeric mice transplanted with bone marrow from wild type mice (BMT-WT), with increased adipose inflammation and liver cytokine levels compared to BMT-*tlr4*$^{-/-}$ mice. This suggests that TLR4 signaling in hematopoietic-derived cells is important for HFD-induced obesity (Saberi et al 2009). Moreover, plasma LPS concentrations exhibit a circadian rhythm. In control mice, diurnal fluctuations of serum LPS show a peak (10 EU/mL of endotoxin) during the last four hours of the dark phase, with lower levels at all other times of day (6 EU/mL of endotoxin). High fat diet eliminates this diurnal rhythm, with LPS levels remaining elevated at 8 EU/mL throughout the day (Cani et al 2007). The gut microbiota links HFD to an increased propensity for intestinal inflammation.

There are several methods to alleviate the adverse effects of HFD. Nondigestible dietary fibers such as oligofructose can attenuate the effects of HFD (Cani et al 2006). Supplementation of HFD mice with short-chain fatty acids (SCFA), especially butyrate, prevents diet-induced obesity and protects against inflammation (Gao et al 2009, Lin et al 2012, Lu et al 2016). This process may be a result of regulating inflammation by promoting and regulating T_{reg} cells. Over-representation of LPS-expressing bacteria as a result of HFD is associated with decreased levels of SCFAs butyrate and propionate, which both contribute to increase CD4+ Foxp3+ cells (T_{reg} cells; immune cells with anti-inflammatory effects) when CD4+ cells from the gut, spleen or lymph nodes are exposed to either SCFA (Arpaia et al 2013).

Gut-Brain Axis

Gut microbiota influences development of host physiology. Germ free (GF) mice, born and reared in a sterile environment, are devoid of commensal microbes of any kind. These mice

have been used to demonstrate the influence of microbes on brain development (Bercik et al 2011b). Both GF mice or mice depleted of intestinal microbiota via treatment with broad-spectrum antibiotics exhibit alterations in HPA axis reactivity compared to control mice that possess a 'normal' gut microbiota. In response to restraint stress, GF mice exhibit exaggerated corticosterone levels relative to 'normal,' control specific pathogen free (SPF) mice. A complete microbiota transplant from SPF mice into GF reversed this exaggerated corticosterone response, but only when GF mice are introduced bacteria at 6 to 8 weeks of age, but not at 14 weeks of age (Sudo et al 2004). This suggests that phenotypes restored to SPF-like levels in conventionalization of GF mice (ex-GF mice) have a sensitive period.

Gut microbes have a striking impact on emotional behavior of mice. GF mice display reduced anxiety-like behavior in a light/dark box, where GF mice spend more time in the light chamber compared to SPF mice (Diaz Heijtz et al 2011). Further, mouse strain differences in some behaviors could be attributed to gut microbiota composition, not genetic differences. Mice of the BALB/c strain exhibit increased anxiety-like behavior compared to Swiss mice from US National Institutes of Health (NIH). However, GF BALB/c mice exhibit more exploratory behavior than SPF BALB/c mice when colonized with microbiota from SPF NIH Swiss mice. Conversely, GF NIH Swiss mice colonized with microbiota from SPF BALB/c mice exhibit a decrease in exploratory behavior compared to SPF NIH Swiss mice (Bercik et al 2011a). These data suggest that the intestinal microbiota represents an important factor that influences behavior, independent of genetic background.

Gut microbiota modulates behavior through multiple mechanisms (Bercik et al 2011a, Bravo et al 2011). One possible route is via the vagus nerve, which is implicated as a major communication pathway between the gut microbiota and the brain (Bercik et al 2011b, Bravo et

al 2011). Mice fed Lactobacillus rhamnosus (JB-1) bacteria show reduced stress-induced corticosterone and anxiety- and depressive-like behaviors. Thirty minutes after forced swim test, mice fed JB-1 released about half the corticosterone to control mice. Mice fed JB-1 also showed more entries to the open arms of an elevated plus maze and less time immobile during the forced swim test compared to control mice. The effect of JB-1 is mediated by the vagus nerve, where the positive effects of JB-1 are eliminated in mice subject to subdiaphragmatic vagotomy prior to supplement feed (Bravo et al 2011). Additionally, chronic colitis associated with anxiety-like behavior is absent in mice subdiaphragmatic vagotomized (SDx) prior to feeding 3% dextran sodium sulfate (a treatment protocol known to induce inflammation in the colon) (Bercik et al 2011b). Direct neural signaling from the gut to the brain relies on vagal receptors that sense regulatory gut peptides, inflammatory molecules and bacterial metabolites to relay signals to the central nervous system (de Lartigue et al 2011). Toll-like receptors (TLRs) that recognize viral RNA (TLR3 and TLR7) and LPS (TLR4) are present in the enteric nervous system (Barajon et al 2009, Brun et al 2013).

Another possible route of brain-gut communication is through soluble mediators. The use of the non-absorbable antibiotics neomycin, bacitracin, and primaricin induces a transient shift in intestinal microbiota. The altered microbial profile results in mice with increased exploratory behavior and BDNF (brain derived neurotrophic factor; molecule implicated in brain plasticity) in the hippocampus. These changes cannot be attributed to the antibiotics in circulation since SPF mice injected with antimicrobials and GF mice given the same antimicrobials via oral gavage did not result in behavioral changes from the lower levels of exploratory behavior observed in control mice. Additionally, these changes are vagus nerve-independent in that antimicrobial treatment with or without subdiaphragmatic vagotomy (SDx) still showed

increased exploratory behavior (Bercik et al 2011a). Communication may be mediated by microbially derived molecules such as short-chain fatty acids and tryptophan metabolites (e.g., serotonin) (Tolhurst et al 2012). These molecules propagate signals through interactions with the intestinal epithelium and sensory neurons. Additionally, some cross the intestinal barrier, enter systemic circulation and may even cross the blood-brain barrier (Haghikia et al 2015). The intestinal microbiome produces neurotransmitters such as GABA, serotonin, norepinephrine and dopamine, though if they all reach CNS-receptors has not yet been determined (Barrett et al 2012, Furness et al 2013, Özogul 2011, Shishov et al 2009).

Gut microbiota can influence host behavior via secreted metabolites. Serotonin production is one example of communication between the gut microbiota, enterochromaffin cells of the intestinal epithelium and the CNS. Serotonin is a neurotransmitter in the CNS. The predominate site for serotonin synthesis, storage and release is the enterochromaffin cells of the intestinal mucosa. Within the intestinal mucosa, serotonin activates neural reflexes involved with intestinal secretion, motility and sensation (Costedio et al 2007). Intestinal microbiota play an important role in serotonin production as SPF mice possess approximately 3-fold higher serum serotonin as compared to GF mice (Wikoff et al 2009). The essential amino acid tryptophan is a key precursor to serotonin. Because the host is unable to produce tryptophan, diets that contain tryptophan serve as the primary regulator of its activity. Gut microbiota contributes to peripheral availability of serotonin, and colonization with bacteria normalizes plasma tryptophan but does not change hippocampal levels (Clarke et al 2013). Together, these data suggest that communication from gut microbiota to the brain to influence behavior are dependent on the specific microbes involved. Some influence behavior changes are mediated via the vagus nerve

(Bercik et al 2011b, Bravo et al 2011), whereas others through different modes of communication (Bercik et al 2011a).

Gut microbiota can influence host behavior via the immune system. The intestinal microbiota imprints and instructs the mucosal immune system throughout the life of the host (Macpherson & Harris 2004). The intestinal microbiota also influences immune activation at sites beyond the gastrointestinal tract, which might influence host susceptibility to immune-mediated conditions (Salzman 2011). The integrity of the adaptive immune system is crucial for normal learning and memory in mice (Derecki et al 2010). Alterations in the intestinal microbiota influence behavior by influencing cytokine levels in systemic circulation and the brain, which can induce sickness behaviors. Under normal conditions, the innate mucosal immune system and the microbiota coexist with one another, but introduction of disturbances such as antibiotics can alter peripheral cytokine production (Honda & Takeda 2009).

Immune System Development

The intestine's primary function is to digest food, absorb nutrients and discard waste. The intestine is not a homogenous organ, rather several anatomically and functionally specialized segments with distinct environmental pressures (Mowat & Agace 2014). The surface of the small intestine is covered by microvilli, absorptive epithelial cells containing nutrient transporters and enzymes needed to digest dietary components. The large intestine lacks villi and has little digestive function, with its main role being the reabsorption of water and elimination of undigested food. Additionally, the large intestine is the main reservoir for trillions of commensal bacteria essential for health. While important for nutrient assimilation, the intestine also represent a vulnerable site of entry for many pathogens (Mowat & Agace 2014).

The composition of intestinal surface changes along the length of the gastrointestinal tract. The frequency of mucus-producing goblet cells progressively increases moving distal in the intestines. Goblet cells make up at least 25% of epithelial cells in the distal colon, while only less than 10% in the proximal portion of the small intestine. In the colon, bacteria can be found in the outer mucus later but do not normally penetrate the inner layer (Hansson 2012, Johansson et al 2008). The production of mucus is controlled by cytokines such as interferon-gamma, IL-9, and IL-13. Mucus is antimicrobial, forming a highly charged gel that acts as a physical barrier and composed to mucin glycoproteins directly toxic to many bacteria (Mowat & Agace 2014).

In addition to absorptive and barrier functions, the intestines are important for host immunity. The constantly changing and dynamic environment of the intestine represents a key challenge to the immune system and the intestine contains the greatest number and diversity of immune cells (Mowat & Agace 2014). Intestinal epithelial cells express pattern recognition receptors that can recruit and active immune cells (Rescigno 2011). For example, TLR2 is highly expressed by epithelial cells in the proximal colon and decreases towards the distal colon (Oliveira-Nascimento et al 2012, Wang et al 2010). In contrast, TLR4 and CD14 are expressed at higher levels in the colon than in the small intestine (Ortega-Cava et al 2003), though the function of the pattern recognition receptors on the intestinal epithelium are still obscure (Mowat & Agace 2014).

The gut microbiota contribute to development of the immune system (Macpherson & Harris 2004). In the intestinal tract, a single epithelial layer, reinforced only with a mucus lining, separates the commensal bacteria from invading the rest of the host. At times, bacteria from the intestine can translocate outside of the epithelial layer (O'Boyle et al 1998); when this occurs they are typically killed rapidly by host macrophages (Macpherson & Uhr 2004). Germ free (GF)

mice have an altered immune system. Germ free mice possess less immune cell development in the bone marrow, resulting in delayed clearance of systemic bacterial infection (Lammas et al 2000). The bone marrow immune cell pool correlates with complexity of intestinal microbiota and is adjusted with the number of TLR (pathogen-sensing) receptors present in blood serum (Balmer et al 2014). Microglia, the resident immune cells of the brain, display several defects in GF mice, such as reduced *in vitro* IL-1β, IL-6, and TNFα expression in response to LPS compared to SPF mice (Erny et al 2015). Commensal bacteria play a critical role in secondary lymphoid development in Peyer's patches, where intestinal Peyer's patches in GF mice are smaller with less CD4+ cells compared to SPF mice (Macpherson et al 2001). Additionally, the spleen and lymph nodes are deformed and show reduced levels of IgG antibodies (Benveniste et al 1971).

Host immunocompetence is critical to maintain host-microbe mutualism. When administered oral gavage of *E. Coli* K-12, mice lacking TLR adaptor molecules MYD88 and TICAM1, both important for intracellular immune signaling, have more bacteria in their spleens compared to wild type SPF mice - indicating a failure to compartmentalize the bacteria solely to the intestinal tract in immunocompromised *myd88*$^{-/-}$ *ticam*$^{-/-}$ mice that lack proper innate immune signaling (Slack et al 2009). Innate recognition of bacteria in the blood and peripheral tissue results in an acute phase response, but the trillions of bacteria in the gut do not normally induce pathological inflammatory responses. Many layers of defense compartmentalize commensal bacteria within the gut (Mueller & Macpherson 2006).

The lamina propria and intestinal epithelium are effector sites of the intestinal immune system. Together, the intestinal lamina propria and intestinal epithelium contain the largest population of T cells and macrophages in the body (Mowat & Agace 2014). The lamina propria

is made up of loosely packed connective tissue just below the intestinal epithelium layer that forms the scaffolding for the villi, and contains the blood supply, lymph draining and nervous supply for the mucosa. It also contains B cells, T cells and numerous innate immune cell populations such as dendritic cells and macrophages. Between the intestinal epithelium's enterocytes are numerous intraepithelial lymphocytes (IELs) that have a wide range of regulatory and effector activities (Camerini et al 1993). IELs include T cell populations along the small intestine, while mouse colonic epithelium contain fewer IELs compared to the small intestine (Suzuki et al 2000). GF mice have dramatically reduced numbers of IELs, though the small versus large intestine ratio of IELs is maintained (Suzuki et al 2002).

The microbiota contributes to host immune reactivity by colonizing the mucosal entry sites of pathogens to prevent invasion of the ecosystem by foreign microbes, a mechanism known as colonization resistance. One example of colonization resistance is the intestinal immunity to viral infection that occurs when the host immune response is altered due to antibiotic-induced depletion of intestinal bacteria. Host antiviral innate immunity is achieved through interferon pathways. Commensal bacteria suppress IFN-λ, and antibiotic treatment can decrease IFN- λ which will, in turn, increase the host antiviral activity in the intestine (Baldridge et al 2015). Is some cases, the lack of intestinal bacteria may, in fact, benefit the host immune response.

One prominent bacterial species, segmented filamentous bacteria (SFB), induces immune cell differentiation in the lamina propria of the small intestine. At appropriate concentrations IL-6 and other growth factors, antigen-activated CD4+ T cells upregulate RORγ and express Th17 cell cytokines (Zhou et al 2008). CD4+ T-helper cells that produce IL-17 (Th17 cells) are potent inflammatory effectors that protect against fungal and foreign bacterial invaders. Th17 cell

differentiation is blunted by oral antibiotic administration, due to decreases in SFB populations. Mice from Jackson Laboratories (JAX; Bar Harbor, ME, USA) possess no SFB, whereas mice from Taconic Biosciences (Tac) possessed this bacterium when tested from fecal and small intestine samples. A result of this difference in SFB is that JAX mice have very few Th17 cells in the lamina propria, while Tac mice indeed possess increased Th17 cells. Th17 cell deficiency is rescued in JAX and germ free mice when co-housed with Tac mice, indicating coprophagia feces of mice containing SFB will transfer this microbial species to cage mates (Ivanov et al 2009, Ivanov et al 2008). Even though SFB does not come into direct contact with the mucosal lamina propria, the intestinal tissue appears to produce signaling molecules when SFB is attached to its epithelium layer. This attachment of SFBs to intestinal epithelium cells promote the differentiation of CD4+ T-helper cells to Th17 cells in the lamina propria, which, in turn, promote proinflammatory cytokine IL-17a production in response to infection (Atarashi et al 2015, Bel & Hooper 2015, Sano et al 2015). This is just one of many examples that gut microbiota species train host immune function (Belkaid & Hand 2014).

Diurnal Rhythms of Intestinal Tract and Microbiota

Gastrointestinal functions show circadian rhythmicity. In humans, gastric acid secretion increases in the evening and colonic motility increases in the morning (Moore & Wolfe 1973). In mice, DNA synthesis show circadian rhythmicity in the intestinal tract, with peak DNA synthesis gradually phase delayed by up to 8 hours between the tongue and the anus, suggestive of food intake (L. A. Scheving et al 1980, Scheving 2000, Scheving et al 1978). Further, core clock genes *Per1* and *Per3* mRNA peaks also possess shifted phase delay as colon tissues were collected more distally (Hoogerwerf et al 2007). *Clock* mRNA obtained from proximal, mid and

distal colon display a gradual delaying of clock gene peak as tissue is collected more distally, though was without circadian rhythmicity in constant darkness. Further, subdiaphragmatic vagotomy did not alter colonic clock gene expression compared to mice that received sham surgery (Hoogerwerf et al 2007).

The gut microbiota exhibits daily fluctuations in composition. Host circadian rhythms that drive feeding cycles are accompanied by compositional and functional shifts in gut microbiota (Zarrinpar et al 2014). Absolute abundance in oscillations include Bacteroidetes, Firmicutes, and Vurrucomicrobia phyla (Zarrinpar et al 2014). Genetic ablation of the host molecular clock *Per1* and *Per2* genes (in combination) or circadian disruption via jet-lag leads to aberrant microbiota diurnal fluctuations and impaired feeding rhythms. Further, timed feeding of nocturnal mice during the light phase results in a 180-degree (12-hour) shift in microbiota rhythms. Circadian feeding behavior influences microbiota rhythmicity as diurnal oscillations were restored by restricting the feeding of *per1*$^{-/-}$*/per2*$^{-/-}$ mice to the dark phase (Thaiss et al 2014). Deletion of the core clock gene *bmal1* abolished the circadian rhythms in fecal microbiota. Additionally, high fat diet can reduce the amplitude of circadian rhythms in feeding behavior as well as microbiota rhythmicity (Zarrinpar et al 2014). Further, timed feeding protects against obesity and metabolic disorders in response to high fat diet; when high fat feeding is consolidated to the active phase in mice, some daily fluctuations in gut microbiota composition are restored (Hatori et al 2012, Zarrinpar et al 2014). Since host circadian rhythms in physiology and behavior can be entrained by time restricted feeding (Stephan 2002), it's unsurprising that feeding in the dark (active) phase partially restores host circadian rhythms. Together, environmental circadian disruption, molecular clock mutation, and diet-induced obesity all

attenuate microbial circadian rhythms (Leone et al 2015, Voigt et al 2014, Voigt et al 2016, Zarrinpar et al 2014).

Neurodevelopmental Disorders

The gut microbiota influences development of neuropathology. Maternal obesity during pregnancy is associated with increased risk of neuropathology in offspring, mediated by shifts in gut microbiota populations and hypothalamic gene expression. Maternal high fat diet (MHFD) shifts microbial community and negatively impacts offspring social behavior. In a three-chamber social test, mice have the choice to spend more time with a novel sex- and age-match conspecific or a neutral, inanimate object. Wild type mice typically spend more time exploring the chamber containing the novel, social conspecific. MHFD offspring spend less time exploring the novel sex- and age-matched conspecific compared to the neutral object (Buffington et al 2016). Co-housing 3 control offspring with 1 MHFD offspring for four weeks following weaning is sufficient to return microbiota of the MHFD to levels indistinguishable from control offspring. This co-housing also returns social behavior of MHFD offspring back to levels of control offspring. Colonization of GF mice with control fecal transplant at 4 weeks of age showed normal social behavior, but a transplant at week 8 did not restore normal social behavior. In contrast, colonization of GF mice with MHFD fecal transplant remained socially impaired, when transplanted at 4 or 8 weeks of age. This decrease in social behavior observed in MHFD offspring may be mediated through oxytocin, as control offspring possess more oxytocin producing cells compared to MHFD offspring. These data identify a neurodevelopmental window during which GF microbial reconstitution via coprophgia (consumption of feces) effectively improves social behavior (Buffington et al 2016).

In an animal model of maternal immune activation (MIA; detailed below), MIA offspring also possess increased intestinal permeability and altered gut microbiota composition. Administration of human gut bacterium Bacteroides fragilis NCTC 9343 to MIA offspring every other day for 6 days post-weaning ameliorates microbiota dysbiosis and restores behavioral abnormalities in open field arena, pre-pulse inhibition, marble burying test, and ultrasonic vocalization tests (Hsiao et al 2013).

The gut microbiota is critical in development of behavioral phenotypes in MIA offspring. The presence of SFBs promote differentiation of Th17 cells that produce IL-17 and IL-22 in the lamina propria mucosal lining. Colonization with SFB is correlated with increased inflammation and anti-microbial defenses (Ivanov et al 2009). Additionally, mice from different commercial mouse vendors possess marked differences in proportion of SFBs and Th17 cells in the small intestine; Jackson Laboratory (JAX) have very low numbers of Th17 cells compared to the genetically identical C57BL/6 mouse obtained from Taconic (Tac) Biosciences (Ivanov et al 2008). The importance of SFB in neurodevelopmental disorders is underscored by contrasting results obtained in genetically identical mice with different microbiota compositions in maternal immune activation (MIA) model of neuropathology. In the mouse model of MIA, pregnant mice that are injected with polyinosinic:polycytidylic acid (PIC; viral infection mimic) on gestational day 12.5 results in offspring with behavioral phenotypes similar to those diagnosed with autism. MIA offspring show increased repetitive behavior, anti-social behavior and less exploratory behavior (Shi et al 2003). This aberrant behavior is a result of which leads to elevated serum levels of IL-6 and IL-17a in the pregnant mouse and developing fetuses (Choi et al 2016, Hsiao et al 2012).

IL-17a is a critical inflammatory mediator in MIA. MIA offspring born of mice lacking T cell-derived IL-17a are not born with MIA-typical, behavioral deficits. Further, intraventricular IL-17a administration in fetuses is sufficient to elicit abnormalities in behavioral assays. Since SFB is necessary for the expression of Th17 cells and, in turn, proinflammatory cytokine IL-17a, the presence of SFB is necessary for MIA-typical offspring with social deficits and repetitive behavior (Choi et al 2016). The immune system plays a vital role in this model for neuropathology as irradiation of MIA offspring followed by bone marrow transplant from control offspring reduces repetitive and anxiety-like behavior (Hsiao et al 2012).

Gestational Maternal Immune Activation (MIA)

A successful pregnancy requires the maternal immune system to adapt properly in order to avoid rejection of the semi-allogenic fetus without compromising the ability to protect the mother and fetus against infection. Maternal immune regulation is influenced by numerous factors such as genetic, environmental, paternal, and fetal factors. The female immune response necessitates immune tolerance to promote sperm survival. Preparation for pregnancy begins even before insemination, in which regulatory T cells (T_{regs}) accumulate in the uterus each time a female approaches estrus, in preparation for possible insemination (Kallikourdis & Betz 2007). Following insemination, epithelial cells in the cervix and uterus active cytokine synthesis to induce a reaction that resembles a classic inflammatory response. The consequence of the cytokine cascade is the recruitment and activation of macrophages, granulocytes and dendritic cells that have immune regulatory and tissue remodeling roles that improve receptivity of the implanting embryo (Robertson 2005). The fetus-placental interface is important for embryo and mother survival. Both maternal and fetal macrophages are important in the regulation of immune

cell activity during all stages of pregnancy (Brown et al 2014). Regulatory T cells are recruited from maternal peripheral blood to the fetal-maternal interface, where they contribute to local regulation of fetus-specific responses (Tilburgs et al 2008). Lower T_{regs} cell counts at the uterus are associated with reproductive disorders such as infertility and miscarriages (Guerin et al 2009, Sasaki et al 2004). Indeed, maternal immune flexibility is important for healthy development of the fetus. Maternal macrophages are mostly decidual (in the uterus), whereas fetal macrophages are placental. Maternal macrophages are involved in placental development and have roles in the vascularization, clearance of infections and apoptotic debris, and tissue remodeling (Svensson-Arvelund & Ernerudh 2015).

Early life events like those experienced *in utero* have the ability to shape the fetus for life after birth (Fisher et al 2012). The field of fetal programming has evolved based on the idea that experience during the perinatal period can modulate or 'program' the typical course of development (O'Donnell & Meaney 2017). Indeed, in the fetal brain, microglia are important for synaptic plasticity via remodeling synaptic connections by clearance of debris and play a major role in synaptic pruning (Paolicelli et al 2011, Schafer et al 2012). The idea is framed as the developmental origins of health and disease (DOHaD) hypothesis, which suggests that the quality of fetal development shapes individual differences in the risk for chronic illness over the lifespan (O'Donnell & Meaney 2017). For example, optimal fetal growth is associated with better metabolic health (Bateson et al 2014). The maternal and fetal immune systems have been identified as key factors in the emergence of aberrant behavior in offspring mice born of mothers exposed to pathogens during pregnancy.

Cytokines and Epidemiological Data on Neuropathology

Infections during pregnancy can lead to adverse outcomes for offspring. As mentioned above, exposure to foreign pathogens results in sickness behaviors in the host organism, adaptive behavioral responses that conserve energy to combat infection. Behavioral effects in the acute phase response involve activation of inflammatory signaling pathways in the brain. Chronically elevated proinflammatory cytokines and altered circadian rhythms are associated with numerous neuropsychiatric disorders (Alesci et al 2005). Increases in inflammatory cytokines are implicated in depression in those both medically ill and medically healthy individuals. Epidemiological data reveal a positive correlation of maternal levels of cytokines IL-8 and TNFα with schizophrenia (Brown et al 2004, Buka et al 2001). Given the connection between proinflammatory cytokines and abnormal development, it is plausible to conclude that systemic inflammation may induce aberrant behavioral phenotypes. Correlations from epidemiological studies implicating MIA to abnormal development are supported by rodent models of maternal immune activation (Kentner et al 2019).

Animal Models for Maternal Immune Activation

To better understand epidemiological findings that sickness during pregnancy increases neurodevelopmental risk in offspring, animal models involving several species and immunostimulants have been developed. These models examine the effects of maternal infection on central nervous system function and behavior in offspring. Both bacterial and viral infections during pregnancy have been modeled. Gestational age of immunostimulant delivery varies across studies (Estes & McAllister 2016). Animal models for maternal immune activation (MIA) examine the offspring (henceforth ‘MIA offspring’) born from pregnant dams administered LPS

(glycoprotein of gram-negative cell wall; bacterial mimic that binds to TLR4), PIC (polyIC; polyinosinic:polycytidylic acid; dsRNA; viral mimic that binds to TLR3), or influenza (live virus) during gestation. Maternal immune activation can be defined as measured levels of inflammatory markers that exceed normal range. All immunostimulants show alterations in behavior, brain morphology and neurotransmitter production in offspring born from immune activated dams compared to offspring born of vehicle-treated pregnant dams (Boksa 2010). In mice, the 19 days of gestation results in a mouse brain that is known to be less developed than the brain of the human neonate. Mapping the developmental stage equivalents between differences species is not exact, as rates of development across species are trait-specific. The 1st and 2nd halves of rat gestation (which have similar gestational period in mice, 21 days), approximate the 1st and 2nd trimesters of human pregnancy (Avishai-eliner, Brunson, Sandman, Baram, & Brunson, 2002; Clancy, Finlay, Darlington, & Anand, 2007; Romijn, Hofman, & Gransbergen, 1991). While there are variations in methodology of the generation of MIA offspring, several methods of eliciting maternal sickness results in offspring with disrupted development and behavior (Kentner et al 2019).

MIA mouse models have also been argued to have relevance to CNS development in patients diagnosed with autism spectrum disorder (ASD). In one MIA model, pregnant mice intranasally infused with live influenza virus on embryonic day 9.5 produce offspring with numerous behavioral differences compared to offspring born of mice administered intranasal PBS. MIA offspring display nearly eight-fold less time in the center of the open field arena and show less than half the social contact in the social interaction test, compared to control offspring (Shi et al 2005). ASD is a class of neurodevelopmental disorders characterized by deficits in social interactions, language and communication, and increased repetitive behaviors (Schwartzer

et al 2013). MIA offspring show decreases in social interaction, increase ultrasonic vocalizations, and increased repetitive behavior in the marble burying test compared to controls (Kentner et al 2019) suggesting face validity of using a mouse MIA model in the study of ASD. Further, construct validity is observed as the MIA model mimics a known disease-related risk factor for ASD, maternal immune activation (Estes & McAllister 2016).

Maternal influenza is unlikely acting directly on the developing fetus, as the virus is not detected in the brain or placenta in offspring mice born of MIA mothers (Shi et al 2005, Williams & Mackenzie 2009) or in the placenta of human offspring born from mothers with proven influenza A infections (Irving et al 2000). Since influenza infection remains compartmentalized to the respiratory tract and viruses raise proinflammatory cytokine levels not only in the respiratory tract but also in maternal serum, it is thought that the maternal inflammatory response that alters fetal behavioral development, rather than viral exposure to the fetus (Shi et al 2005, Van Reeth 2000).

Instead of using live influenza virus, administration of immunostimulants such as dsRNA PIC during pregnancy results in similar activation of maternal inflammatory cascades which result in MIA offspring behavioral phenotypes. The use of live influenza virus or PIC administration to pregnant mice both showed similar abnormal offspring behavioral symptoms and cytokine expression (Shi et al 2003). Pregnant mice injected with 20 mg/kg PIC on embryonic day 12.5 causes deficits in pre-pulse inhibition and latent inhibition in adult offspring. Additionally, PIC offspring show less activity, fewer entrances to the center of the open field arena, and decreased social behavior. To determine the influence of specific cytokines on MIA offspring phenotypes, pregnant mice were injected with IL-6, IL-1β, TNFα, or IFNγ. Only IL-6 injections caused deficits in pre-pulse inhibition and latent inhibition, whereas the other cytokine

injections were without effect. To further examine the influence of cytokines on MIA offspring's aberrant phenotypes, pregnant mice were co-injected a cytokine-neutralizing antibody targeted against IL-6, IL-1β, or IFNγ at the same time as PIC injection. Pregnant mice injected with anti-IL-1β and anti-INF-γ concurrent with PIC resulted in offspring with the same phenotype as offspring mice with mothers administered solely PIC. Interestingly, anti-IL-6 at the same time of gestational PIC administration prevents the pre-pulse inhibition, latent inhibition, and exploratory and social deficits caused by maternal PIC administration (Hsiao & Patterson 2011, Smith et al 2007). These data demonstrate that IL-6 is critical for mediating the effects of MIA on developmental of MIA offspring behavioral abnormalities.

The placenta's role in the occurrence of neuropsychiatric disorders has been suggested by the concordance rate of schizophrenia in monochorionic (two embryos share a single placenta) twins is 60% whereas dichorionic (each embryo has its own placenta) twins is only 10.7% (Davis et al 1995). This indicates that the uterine environment may underlie the etiologies for psychiatric disorders. Indeed, radioactively labelled IL-6 (^{125}IL-6) crosses the placental barrier in rodents, allowing direct exposure of this cytokine to the fetus. ^{125}IL-6 administered during mid-gestation in rats results in a marked increase of detectable ^{125}IL-6 compared to administration in late gestation, indicating the placental barrier is more permeable to IL-6 earlier in development compared to late gestation (Dahlgren et al 2006). This change in placental permeability aligns with previous reports showing that PIC administered in late gestation (embryonic day 17; E17) does not result in aberrant behavioral alterations seen when the same dose does in early pregnant mouse gestation (E9) (Meyer et al 2008b). Further, after pregnant mice are injected with PIC, their placentas show a 17- and 4-fold increase of IL-6, 3 and 24 hours-post injection compared to saline injected controls. Placenta from MIA dams show increased *il-6* mRNA. To disentangle the

contributing effects of the mother (bloodstream, decidual cells, uterine immune cells) and/or the fetus (bloodstream, endothelial cells) IL-6 KO mice were utilized and placenta IL-6 protein was measured following gestational injection. IL-$6^{+/-}$ females and IL-$6^{-/-}$ males were mated and injected with PIC or saline on E12.5. Additionally, IL-$6^{-/-}$ females and IL-$6^{+/-}$ males were mated. The data show that even if offspring showed a homozygous IL-6 knockout, IL-6 in the placenta is still increased and results in aberrant behaviors seen in MIA-typical offspring. Thus, the IL-6 protein response to MIA in the placenta is maternally-derived (Hsiao & Patterson 2011). Further, IL-6Rα placental knockout prevents MIA-induced behavioral abnormalities in offspring, showing placental IL-6 signaling critical for MIA-typical offspring (Wu et al 2017).

The presence of anti-inflammatory cytokines can reverse some effects of IL-6 induced MIA. Indeed, IL-6 plays a vital role in MIA offspring phenotypes. The balance between anti- and pro-inflammatory signaling at the maternal-fetal interface may play a role in the long-lasting effects of offspring born of MIA mothers; anti-inflammatory cytokines may even attenuate adverse effects of MIA. Transgenic macIL-10*tg* mice that constitutively overexpress anti-inflammatory IL-10 in macrophages result in MIA offspring with less severe behavioral deficits compared to wild type MIA offspring. Increased IL-10 leads to autocrine deactivation of macrophages accompanied by attenuated pro-inflammatory cytokine reactions. Pregnant macIL-10*tg* were injected with PIC or vehicle on E9 and fetal brains collected 5 hours later. Wild type fetal brains showed increases in TNFα, IL-1β, and IL-6 following maternal immune insult, while macIL-10*tg* fetal brains showed no increase in pro-inflammatory TNFα and similar IL-1β and IL-6 results as those seen in wild type fetal brains, with stark increased of anti-inflammatory IL-10. While MIA macIL-10*tg* fetal brains show decreased TNFα and increased IL-10 compared to their wild type MIA controls, cytokine levels taken at 100 days of age did not show changes in

cytokine concentration between any of the four groups. In the open field test, MIA decreased exploratory behavior (entries to center arena) in wild type mice; while macIL-10*tg* offspring treated with saline during gestation already show a decrease in exploratory behavior similar to wild type MIA offspring whereas macIL-10*tg* MIA offspring mice are rescued of this phenotype. A similar trend is seen in latent inhibition, in which macIL-10*tg* prevents MIA-induced deficits in LI, but leads to a loss of LI in the absence of MIA. These data show that less inflammation does not always lead to typical behavioral development, rather, a balance between pro- and anti-inflammatory markers is important for successful development (Meyer et al 2008a).

Influence of Maternal Immune Activation on Offspring Immune Function

In addition to its role in host defense and the acute phase sickness response, cytokines play an important role in central nervous system (CNS) development and function. Brain region-specific changes in cytokine expression are present during ontogenesis. MIA causes long-lasting and region-specific changes of brain cytokine levels in offspring that vary over embryonic and postnatal development. MIA offspring exhibit elevated cytokines in the frontal and cingulate cortices at birth, but this is followed by decreases during later intervals of synaptogenesis and plasticity, and a return to elevations in adulthood. MIA increases of cytokine levels in brain regions examined (frontal cortex, cingulate cortex and hippocampus) do not correlate with serum cytokine levels (Garay et al 2013). In MIA rat offspring, IL-6 expression peaks in the cortex on embryonic day 18, whereas it peaks in the hippocampus on 21 days of age (Pousset 1994). Additionally, IL-1β is expressed at high levels in the CNS during pre- and post-natal development, with lower levels in adulthood (Giulian D 1988, Mizuno et al 1994, Vela 2002). These data show changes in CNS cytokine expression, independent of immune insult.

In addition to CNS changes, MIA (PIC 20mg/kg on E12.5) leads to decreases in splenic T_{regs} and hyper-responsive CD4+ T cells with elevated IL-6 and IL-17a production *in vitro* from cells obtained from 3 and 52 week old mice compared to control offspring (Hsiao et al 2012). To examine if peripheral immune abnormalities found in MIA offspring contribute to development of typical MIA behaviors, bone marrow transplants were performed. Before the transplants, MIA-typical and control-typical offspring behavior were confirmed in their respective groups. All offspring mice were then irradiated. Following irradiation, MIA mice, received transplantation with bone marrow from control mice, MIA chimeras no longer exhibited behavioral abnormalities in marble burying, social preference, or open field test. Irradiation of control mice transplanted with bone marrow from donor MIA offspring restored repetitive marble burying to levels observed in saline controls (Hsiao et al 2012). These data support a link between cellular immune dysregulation and typical MIA offspring behavioral deficits.

Immune System and Microbiota Mediate MIA Offspring Phenotypes

Even within animal models, the results of MIA on offspring behavior and physiology are variable (Meyer et al 2009). Indeed, not all illness during pregnancy result in offspring with mental illness. Certain variables across animal studies are not consistent and may explain results of some studies showing the full array of typical MIA offspring phenotypes whereas other studies show MIA offspring with less aberrant behaviors (Kentner et al 2019). Some variables shown to influence the expression of MIA phenotypes are: gestational immune insult time during pregnancy (Samuelsson et al 2004), choice of live or mimic immunogen (Shi et al 2003), high molecular weight PIC vs low molecular weight PIC (Careaga et al 2018), strain of mouse (Schwartzer et al 2013), gut microbiota composition (Kim et al 2017) and sex of offspring (Xuan

& Hampson 2014) studied. It has even been shown that different caging systems result in different results in the generation of typical MIA offspring phenotypes (Mueller et al 2018). As it is known that immune reactions vary in intensity depending on circadian phase (Tognini et al 2017), it is possible that circadian timing of MIA may influence the effect of gestational sickness on offspring. It may be that environmental and genetic co-factors are necessary for adverse, long-term alterations in offspring.

The immune system and gut microbiota both play a role in the generation of MIA offspring. T helper 17 (Th17) cells are responsible for immune responses against extracellular bacteria and fungi, and their dysregulation may underlie various inflammatory and autoimmune disorders (Wilke et al 2011). Elevated levels of IL-17a are present in serum of children with autism, and IL-17a levels correlate with the severity of autism symptoms (AL-Ayadhi & Mostafa 2012). MIA (mice, PIC 20mg/kg E12.5) offspring with lymphocytes developed into Th17 cells produce higher levels of IL-17a upon *in vitro* activation (Mandal et al 2010). Additionally, MIA offspring born of IL-6 KO dams show no increases in IL-17a, consistent with IL-6 acting upstream of IL-17a. Blocking IL-17a with an antibody prior to PIC administration restores MIA offspring's ultrasonic vocalizations, social interaction and marble burying tests to levels similar to those observed in control offspring (Choi et al 2016). To examine mechanisms by which MIA leads to T cell activation with increased IL-17a in the maternal circulation, examination to gut microbiota were performed.

Maternal gut microbiota, specifically maternal intestinal segmented filamentous bacteria (SFB), are critical for typical MIA offspring phenotypes in rodents. Elimination of the majority of intestinal microbes via wide spectrum antibiotic, vancomycin, treatment prior to PIC administration prevented offspring from developing cortical patches and behavior deficits (USV,

marble burying, open field test, and social interaction) typically seen in MIA offspring born of pregnant mice that possess SFB. Additionally, vancomycin treatment in pregnant mothers injected with PIC show decreased Th17 cells in the small intestine with reductions in maternal IL-17a; these MIA offspring do not show aberrant MIA-typical behaviors. This shows that presence of commensal bacteria (i.e. SFB) in pregnant mice sensitive to vancomycin is crucial for induction of several typical MIA offspring phenotypes. C57BL/6 mice from Taconic Biosciences (Tac) have abundant Th17 cells in their small intestine, owing to presence of SFB; in contrast, genetically identical mice from Jackson Laboratories (JAX) lack SFB and have no intestinal Th17 cells (Ivanov et al 2008). The lack of Th17 cells is accompanied by no maternal serum IL-17a increases in JAX mice. In contrast to offspring from PIC-injected Tac mothers that showed MIA-typical abnormal behaviors, mice born from PIC-injected JAX mothers did not show any of the MIA-associated behavioral phenotypes. It was further determined that co-housing JAX and Tac mice or giving JAX mothers a bacterial SFB gavage from Tac mice resulted in offspring with the same behavior deficits seen in offspring born of Tac PIC-injected offspring. Further, IL-17a antibody administration following PIC injection on E12.5, prevents MIA-associated behaviors in offspring (Kim et al 2017). These data show that SFB plays an important role in the behavioral deficits typically developed in offspring born of PIC-injected mothers.

The brain mechanisms governing some MIA phenotypes, especially those linked to autism, lies in inflammation of cortical patches. As indicated above, pregnant dams injected with PIC on E12.5 result in increased serum IL-17a. Additionally, isolated cultures of placenta- and decidua-associated mononuclear cells showed upregulation IL-17a in PIC-treated pregnant dams compared to cells of control dams in *ex vivo* exposure to T cell receptor activators

phorbolmyristate acetate (PMA) and ionomycin. Cortex *in situ* hybridization show increased IL-17a. MIA resulted in disorganized cortical cytoarchitecture which persist in adulthood (Choi et al 2016). These cortical abnormalities in MIA offspring show cortical patches in the dysgranular zone of the primary somatosensory cortex (S1DZ). The presence and size of cortical patches are predictive of MIA-induced behaviors and their severity. Increasing neural activity in S1DZ with optogenetics ChR2 in control offspring resulted in increased marble burying, impaired sociability and reduced time spent in the center of the open field test. Inhibiting the PV+ GABAergic inhibitory interneurons acting on the S1DZ using optogenetics, causes a net increase of activity of S1DZ and also recapitulated aberrant MIA behavioral phenotypes in control (mice not exposed to maternal sickness) offspring. Additionally, reduction of S1DZ neural activity in MIA offspring using NpHR rescues MIA behaviors to levels of control offspring (Shin Yim et al 2017). Together, these data suggest increased neural activity in the S1DZ region are responsible for aberrant MIA behavioral phenotypes.

Maternal immune activation models that utilize several immunostimulants (e.g., live virus, viral mimics, or bacterial mimics) all show behavioral and morphological alterations in MIA-offspring when compared to control treated offspring (Boksa 2010). These findings suggest that it is a universal immune response to numerous pathogens that contributes to neurodevelopmental abnormalities, not the specific immunogen (Kentner et al 2019). It is reasonable to conclude that scores of immunogens can result in abnormal offspring development. At the very least, these studies utilizing different immunogens shows construct validity for MIA to induce abnormal development (Estes & McAllister 2016). For the purposes of the experiments in this dissertation proposal, we implemented a mouse model of MIA using PIC administration on E12.5 to examine the effect of maternal immune insult on offspring physiology and behavior.

Aims

Here, these experiments examine the role of gut microbiota and diet have on circadian rhythms. Detailed chronobiological techniques are employed to examine gut microbiota (Chapter 3) and high fat diet (Chapter 4), and their influence on circadian rhythms. Following, circadian rhythms of offspring born with sickness during pregnancy were examined in mice that possess different gut microbiota composition (Chapter 5). Finally, Siberian hamsters show robust circadian and circannual oscillations in immune function. How these two timescales interact has not been studied. To this end, diurnal and seasonal changes in innate and adaptive immune function were examined (Chapter 6). The circadian network, gut microbiota, and the immune system are intimately intertwined. Examining these interactions furthers our understanding of the complexities of organismal biology.

Chapter 2: Methods and Procedures Common to Several Experiments

Circadian Manipulations

Mouse locomotor activity (LMA) and/or core body temperature (Tb) were recorded during multiple circadian manipulations to measure both entrainment to environmental cues (i.e., light and food) and endogenous, free-running rhythms (i.e., constant darkness). Below, standard chronobiology metrics are first defined, followed by environmental manipulations that measure several aspects of the circadian network.

Circadian Chronotyping Metrics

Actogram. Mouse activity is visualized using actograms. The x-axis indicates time-of-day, while the y-axis indicates successive days of the experiment. The top bar indicates when lights are either on (yellow/white) or off (black). See Figure 3 for example of an actogram.

Onset, offset, and alpha (α). Activity onset time indicates the time that the active phase (i.e., waking) begins. Activity offset time indicates the time that the inactive phase (i.e., rest) begins. The time elapsed between activity onset and activity offset is the duration of the active phase, defined as alpha (α). For core body temperature, duration spent above daily Tb mean (temperature alpha duration) was calculated by the difference of the time body temperature rose above the daily mean (onset) and the time it fell below the daily mean (offset). See Figure 4 for visualization of activity onset, offset, and alpha for locomotor activity.

Onset tau. When a mouse in placed in constant lighting conditions (constant darkness; see below), the mouse begins to 'free-run' at the speed of its endogenous circadian rhythm, tau. The speed or tau (τ) of the clock can be quantified using activity data collected from mice housed in constant darkness. The absence of cyclic changes in the environment (i.e., lack of a light:dark

cycle) allows observation of endogenous circadian rhythms. The speed of onset tau is calculated using ClockLab's automated system and is measured by a least-means-squared line drawn through consecutive days of onset activity time, and the slope of that line is the endogenous speed of the central pacemaker. A researcher blinded to treatment group confirmed ClockLab's estimations, and corrected mistakes if any were present. See Figure 5 for visualization of quantification of onset tau.

Lomb-Scargle Periodogram (LSP). The Lomb-Scargle Peridogram (LSP) is a Fourier-based power spectrum estimator used to detect and characterize periodicity in timeseries data and can accommodate unequally-spaced time series. It also allows for the analysis of data that are missing values due to equipment failure (Refinetti, Cornélissen, & Halberg, 2007). Two outputs of this algorithm are pertinent to chronobiology. First, the period (i.e., speed or tau) of the periodicity is identified. Second, the power of the LSP at the 24 hr period is determined. Both the speed and power provide insights to the structure of the timeseries data, where an increase in power indicates greater amplitude in the data structure (VanderPlas 2018).

Non-parametric circadian rhythm amplitude (NPCRA). Non-parametric circadian rhythms amplitude (NPCRA; RA; relative amplitude) is quantified by comparing periods of lowest and highest activity (van Someren et al 1996).

$$\mathrm{RA} = \frac{(\mathrm{M\ Avg} - \mathrm{L\ Avg})}{(\mathrm{M\ Avg} + \mathrm{L\ Avg})}$$

Where M Avg is the average activity of the most active 10-hour period of locomotor activity data. L Avg is the average activity of the least active 5-hour period. Increases in RA indicate a larger difference between the periods of most and least daily activity.

Entrainment to Photocycles

To document baseline circadian entrainment, locomotor activity (LMA) and core body temperature (Tb) data were acquired while mice were maintained in a 12:12 light:dark cycle. Analyses were performed on 12 days of uninterrupted LMA and Tb data. For LMA: onset time, offset time, duration of the active phase (α duration), Lomb-Scargle periodogram (LSP) power in the circadian range (~24hr), non-parametric circadian rhythm amplitude (NPCRA), and total daily were determined. See Figure 3 for an example of an example raster plot of locomotor activity of a mouse in a 12:12 light:dark cycle.

Constant Conditions

The release of mice into constant darkness (DD) allows the measurement of endogenous circadian rhythms (See Chapter 1's *Free-Running Rhythms*). Analyses of endogenous circadian rhythms of mice placed in constant darkness were performed on 11 days of uninterrupted LMA and Tb data. For LMA: LSP was used to determine free-running period (τ) and amplitude in the circadian range. Additionally, free-running tau using onset was calculated using ClockLab's automated system. Alpha (α) duration (duration of active phase, in hours) was also calculated. For Tb, duration spent above daily mean (temperature alpha duration), Tb during they active phase (α Tb), and Tb during the rest phase (ρ Tb) were calculated. See Figure 5 for an example of an example raster plot of locomotor activity of a mouse in constant darkness.

Jet-Lag Manipulation

To evaluate the speed at which the circadian clock responds to a full shift of the photocycle, mice were subjected to a 6-hour phase advance jet-lag manipulation. Mice were first

entrained to standard 12:12 light:dark cycle conditions, with lights on from 6:00 AM (Zeitgeber time 0, ZT00) to 6:00 PM (Zeitgeber time 12, ZT12) prior to the jet-lag manipulation. On the day of the phase advance, dark onset occurred 6 hours earlier. Daily onset times were determined using ClockLab's automated system. A researcher blind to treatment group confirmed ClockLab's estimations and corrected mistakes if any were present. To account for each mouse's baseline phase relationship relative to lights off, adjustment to the phase shift for each day was quantified as a difference in baseline mean onset time and the post-shift day's onset time (delta onset). Complete adjustment to the new light:dark cycle was quantified as a 5.7 hr (95%) phase advance from the mean activity onset time at baseline, prior to the shift. See Figure 6 for schematic of jet-lag manipulation.

Delaying (pZT15) Light Pulse

To evaluate non-parametric phase resetting responses of the circadian clock in response to discrete light pulses, mice in constant darkness (DD) were subjected to 15 mins of light exposure during the early subjective night. Mice were maintained in a standard 12:12 light:dark cycle for 13 days prior to constant darkness before the light pulse. The day before the light pulse, lights did not turn on. On the day of the light pulse, lights were turned on for 15 minutes at the beginning of the projected 3rd hour of the dark (i.e., 51 hours after the last dark onset). This is projected Zeitgeber Time 15 (pZT15), or 15 hours after projected lights on. Onset and offset times were determined using ClockLab's automated system. A researcher blind to treatment group confirmed ClockLab's estimations, and correct mistakes if any were present. Magnitude of phase advance was determined by the displacement between activity onset day of light pulse and

activity onset predicted by a regression line fit to post-pulse activity onsets, excluding the first three days post-pulse days to allow for transients.

Advancing (pZT22) Light Pulse

To evaluate resetting of the circadian clock in response to discrete light pulses, mice in DD were subjected to 15 mins of light exposure during the late subjective night. Mice were maintained in a standard 12:12 light:dark cycle for 17 days prior to constant darkness before the light pulse. The day before the light pulse, lights did not turn on. On the day of the light pulse, lights were turned on for 15 minutes at the beginning of the projected 10th hour of the dark (i.e., 58 hours after the last dark onset). This is projected Zeitgeber Time 22 (pZT22), or 22 hours after projected lights on. Onset and offset times were determined using ClockLab's automated system. A researcher blind to treatment group confirmed ClockLab's estimations and corrected them for mistakes if any were present. Magnitude of phase advance was determined by the displacement between activity onset day of light pulse and activity onset predicted by a regression line fit to post-pulse activity onsets, excluding the first three days post-pulse days to allow for transients.

Food Anticipatory Activity

To examine contributions of gut microbiota to the food entrainable oscillator (FEO), mice were subjected to a timed-feeding protocol (see Chapter 1's *Food Entrainable Oscillator*). Light and feeding behavior are normally concordant, where nocturnal rodents eat majority of their food during the dark (active) phase. In order to disentangle the food-entrained and light-entrained oscillators, mice are deprived food during their dark phase, and only given food in the light

phase. Locomotor activity fragments and a component of the activity profile aligns with the new feeding time. This results in an increase in activity in the light phase, a time in which mice are normally inactive. This increased activity prior to feeding during the light phase is known as food anticipatory behavior (FAA). Increases in FAA indicate increased behavioral shifts to food cues.

To measure FAA in the laboratory, mice were entrained to a 12:12 light:dark cycle (lights off at ZT12). For all days of the experiment prior to the start of training, mice were fed food ad libitum. On the first day of food entrainment, food was removed beginning at the onset of light, then made available only during ZT08 to ZT16. The second day of training, food was available between ZT08 to ZT12. The following 10-12 days of training, food was available only from ZT08 to ZT12. After training, food was made available for two days starting at ZT08 until ZT12 52 hours later. After ~2 days of ad libitum food, mice were food deprived starting at ZT12 until ZT12 48hrs later, at which point all mice were returned to ad libitum diets. By convention (Mistlberger 1994), activity occurring during the 3 hours immediately prior to the expected or actual food delivery was coded as FAA. To account for individual differences in locomotor activity, FAA was calculated as a quotient of the total number of activity counts during the 3 hour FAA window divided by the sum of the total activity from the FAA's light phase and the following dark phase activity. See Figure 7 for FAA schedule.

Chapter 3: Influence of Gut Microbiota on Circadian Rhythms

Introduction

Circadian rhythms are ubiquitous in nature. From cyanobacteria to eukaryotes, all kingdoms possess examples of convergent evolution for biological timing of physiological processes, with distinct mechanisms for internalizing geological time (Pittendrigh & Daan 1976d, Takahashi et al 2008). In mammals, the circadian network is composed of multiple circadian oscillators – a central pacemaker housed in the hypothalamic suprachiasmatic nucleus (SCN) which confers phase of the light:dark cycle to many peripherally oscillating tissues (Bartness et al 2001). In peripheral (non-SCN) oscillators that cannot entrain to photic (i.e., light) cues may instead rely on tissue-to-tissue communication within an organism and cell-to-cell communication within a specific tissue. This concept of a 'web of pacemakers' (Figure 1) is well-accepted despite a lack of defined pathways for communication between tissues (Schibler & Sassone-Corsi 2002). Contained in each mammalian cell are autonomous core clock genes composed of a molecular autoregulatory feedback loop that oscillates with a period of about 24 hrs (Ko & Takahashi 2006). Together, circadian clocks in the central and peripheral tissues maintain specific phase relationships with each other that coordinate behavior and physiology optimized to specific times of day (Takahashi et al 2008).

In addition to the mammalian molecular clock, there are trillions of microorganisms, living in and on the body, referred to as the microbiome or the microbiota. Many of these microbes also possess their own autoregulatory feedback loops (Eelderink-Chen et al 2021, Parkar et al 2019, Sartor et al 2019). Recent estimates suggest the body harbors a nearly equal ratio of microbe to host cells (Sender et al 2016), and the gut microbiome plays important roles in digestion, metabolism and immune function (Belkaid & Hand 2014, Nicholson et al 2012), all

of which exhibit circadian periodicity (Panda 2016, Scheiermann et al 2013). Indeed, germ free (GF) mice raised in complete absence of microbes exhibit a unique metabolic and immune states relative to their conventionally-raised SPF counterparts harboring complex microbial communities, displaying resistance to Western diet-induced obesity and compromised immune function (Backhed et al 2007). Only recently has it been identified that gut microbiota community membership and function are sensitive to host circadian disruption (i.e., jet-lag, timed feeding), and that microbially-derived components as well as small molecules can feedback onto both the host intestinal and hepatic (i.e., liver) molecular clock network to influence metabolic outcomes (Leone et al 2015, Thaiss et al 2014, Zarrinpar et al 2014). Previous examples of the integration between biological clocks in symbiotic systems and behavioral rhythmic outputs have been described in marine life, including between the sea anemone *Aiptasia diaphana* and its algal symbiont *Symbiodinium* (Sorek et al 2018) where a presence of its symbiont, the anemone it's circadian period can change to 24 hrs from 12 hrs. Additionally, the Hawaiian bobtail squid *Euprymna scolopes* has its symbiont bacterial bioluminescent *Vibrio fischeri* that colonizes the squid's light organ (McFall-Ngai 2014). Despite this knowledge, whether and how these interactions between mammalian host circadian networks and gut microbes translate into changes in host behavioral rhythms has remained unexplored.

To explore the impact gut microbiota elicits on host behavioral rhythms in a mammalian circadian system, experiments to test the hypothesis that gut microbes contribute to host behavioral circadian rhythms were designed. To this end, we acquired continuous locomotor activity (LMA) and body temperature (Tb) radiotelemetry data from germ free (GF), conventionalized germ free (ex-GF), and conventionally-raised specific pathogen free (SPF)

mice. These data reveal the mammalian circadian network and behavioral outputs are dramatically influenced by the presence of gut microbes, where GF mice exhibited unique entrainment to a 12:12 light:dark cycle (LD) and differential endogenous rhythms in constant darkness (DD). Further, a timed-feeding paradigm that quantified food anticipatory activity (FAA) showed that GF mice exhibited augmented FAA, which was reversed to SPF levels in ex-GF mice. Similar to observations of lower transkingdom symbiotic relationships, the symbiont microbes that colonize the mammalian gut can modulate the host circadian network, transforming behavioral rhythms in response to environmental influences.

Methods

Animals

Male C57BL6/J specific pathogen free (SPF) mice were purchased from the Jackson Laboratories (JAX), bred, and maintained in The University of Chicago animal vivarium upon arrival under conventional housing conditions. Germ free (GF) mice were bred and maintained in sterile, flexible film isolators. Germ free conventionalized mice (ex-GF) were reared in sterile flexible film isolators, removed under sterile conditions, and inoculated with 150uL of cecal content slurry in sterile PBS (100mg cecal contents/mL of PBS) obtained from sex-matched SPF mice five weeks prior to data collection via oral gavage. These ex-GF mice possessed a microbiome composition indistinguishable from SPF mice. All mice were maintained in the same or neighboring vivarium rooms under their respective conditions on a 12:12 light:dark cycle (lights off at 6:00 PM CST) unless otherwise noted. Ambient temperature and relative humidity were held constant at 19 ± 2°C and 53% ± 10%, respectively. Autoclaved pine shavings were provided to both all mice and autoclaved water was freely available throughout

the experiment. Mice were freely fed *ad libitum* unless otherwise noted and SPF, GF, and ex-GF mice were provided with autoclaved normal rodent chow (NC; LabDiet 5k67) at the start of LMA and Tb collection. Three groups of mice in total were examined: SPF (n=18), GF (n=16), and ex-GF (n=6). Experiments were conducted in two rounds. In round 1: SPF mice (SPF; n=10) and germ-free (GF) mice (GF; n=8); 11 to 18 weeks of age at the start of 12:12 light:dark data collection began. In round 2: SPF (n=8), GF (n=8), conventionalized mice (ex-GF; n=6), 17 to 24 weeks of age at the start of a 12:12 light:dark cycle data collection. All procedures were approved by The University of Chicago Animal Care and Use Committee.

Surgical Procedures

Mouse locomotor activity (LMA) and core body temperature (Tb) were collected using implanted transmitters. Germ free, SPF, and ex-GF male mice were anesthetized with dexdomitor (1mg/kg, i.p.; Henry Shein) and ketamine (75mg/kg, i.p.; Henry Shein) and were implanted (i.p.) with pre-calibrated radio-telemetric transmitters (G2 E-mitters; Starr Life Sciences; Oakmont, PA, USA). Anti-sedative atipamezole (5mg/kg; Henry Shein) was administered following surgery. Additionally, subcutaneous (s.c.) buprenorphine analgesic was administered immediately following surgery and at 12-hour intervals for 48 hours. Implanted devices wirelessly transmitted LMA and Tb to receiver boards (ER-4000 Energizer/Receiver; Starr Life Sciences) placed under the cages. LMA and Tb data were acquired using VitalView software (Starr Life Sciences) and stored for offline analyses. Cumulative locomotor activity and Tb data were analyzed using ClockLab v6.0.53 (Actimetrics, Evanston, IL) in 6-minute bins.

Circadian Phenotyping

In Round 1's order of circadian manipulations: entrainment to 12:12 LD cycle, jet-lag, pZT15 light pulse, pZT22 light pulse, constant darkness, food entrainment (Figure 8). Round 2's order of circadian manipulations: entrainment 12:12 LD cycle, constant darkness, jet-lag, and food entrainment (Figure 9). See Chapter 2 for other details on procedures.

Statistical Analyses

Analyses of variance (ANOVAs) were performed to decrease chances of Type I error. If a statistically significant F-statistic was achieved, unpaired T-tests were performed using Statview 5.0 (SAS Institute, Cary, NC). Datapoints that lied outside 3±SD of the mean were omitted from statistical analysis (encompassing less than 0.4% of data) to meet necessary conditions for parametric tests. Differences were considered significant if $P \leq 0.05$. Studies were conducted in two rounds (see 'Animals' and 'Circadian Phenotyping'). Datasets from both rounds were combined when no statistical differences were observed between rounds. No differences were observed between rounds except for the simulated jet-lag study, when mice were exposed to a 6 hr phase shift. The data in the jet-lag study were analyzed separately by round.

Results

Entrainment to 12:12 Light:Dark Cycle

Locomotor Activity. Gut microbiota influenced mouse activity in 12:12 LD photocycle (Figure 10). Onset time (time that daily activity bout began; time of 'waking') was later in GF mice compared to SPF mice ($p<0.05$; Figure 10B). GF mice showed an earlier offset time (time

that daily activity bout ended; time of 'sleeping') compared to SPF mice ($p<0.001$; Figure 10B). Alpha duration (α_{LMA}; time elapsed between onset and offset time; 'active duration') was shorter in GF mice compared to SPF mice ($p<0.0001$; Figure 10B). Total daily activity did not differ between groups ($p>0.05$); though, when activity during the light phase was quantified, GF mice showed less activity compared to SPF mice ($p<0.01$; Figure 10C). GF mice showed less variability in onset time compared to SPF mice ($p<0.05$; Figure 10D). No differences were observed in offset variability ($p>0.60$). GF mice showed increased LSP power (see Chapter 2 for LSP details) in the circadian (~24 hr) domain compared to SPF mice ($p<0.0001$; Figure 10E). GF mice also showed increased amplitude in non-parametric measures of circadian rhythm amplitude (NPCRA; see Chapter 2 for details; $p<0.001$; Figure 10E). Conventionalized (ex-GF) mice showed values indistinguishable from SPF mice (Figure 10).

Body Temperature. Body temperature showed no differences in LSP circadian power between GF and SPF mice ($p>0.10$). Onset time (time that core body temperature rises above the daily mean) was the same of SPF and GF mice ($p>0.05$; Figure 11B). However, offset time was earlier in GF mice compared to SPF mice ($p<0.001$; Figure 11B). Alpha duration (α_{Tb}; duration in hours core body temperature remains above its daily mean) was shorter in GF mice compared to SPF mice ($p<0.0001$; Figure 11B). Daily mean temperature was lower in GF mice compared to SPF mice ($p<0.001$; Figure 11C). When separated by dark (active) and light (rest) phases, body temperature of GF mice was lower than SPF mice during both alpha and rho ($p<0.01$, both comparisons; Figure 11C). Ex-GF mice showed onset and offset times indifferent from SPF mice ($p>0.05$; Figure 11B). Ex-GF mice showed lower mean compared to SPF mice in daily mean temperature ($p<0.05$) and mean temperature during the dark phase ($p<0.05$; Figure 11C). See Table 1 for more details of the influence of microbiota on entrainment to 12:12 light:dark cycle.

Endogenous Circadian Rhythms in Constant Darkness

Locomotor Activity. Onset τ was longer in GF mice compared to SPF mice ($p<0.05$, both comparisons; Figure 12B). Offset tau F statistic did not reach significance, but means showed similar means as onset tau ($p<0.05$; Table 1). Total daily counts did not differ between GF and SPF mice ($p>0.10$; Table 1), though GF mice showed less activity during the rest phase compared to SPF mice ($p<0.05$; Figure 12C). Alpha duration was shorter in GF mice compared to SPF mice ($p<0.0001$; Figure 12D). No differences in onset variability were observed ($p>0.30$; Figure 12E), though GF mice tended to show less offset variability ($p=0.0502$; Table 1). LSP period did not differ between groups (Table 1). LSP power was increased in GF mice compared to SPF mice ($p<0.01$; Figure 12F). In NPCRA, GF mice show higher relative amplitude compared to SPF mice ($p<0.0001$; Figure 12F). Ex-GF mice did not differ from SPF mice in any comparisons. See Table 1 for more details of the influence of microbiota on endogenous circadian rhythms.

Body Temperature. Compared to SPF mice, GF mice tended to show longer period using spectral analysis LSP ($p=0.055$; Table 1). LSP amplitude was higher in GF mice compared to SPF mice ($p<0.05$; Table 1). Onset and offset tau tended to be longer in GF compared to SPF mice ($p>0.05$, both comparisons; Table 1). Onset error tended to be higher in GF mice relative to SPF mice ($p>0.05$), while offset variability was without effect ($p>0.70$; Table 1). Alpha (α_{Tb}) duration was shorter in GF mice compared to SPF mice ($p<0.01$; Table 1). Mean daily core body temperature was lower in GF mice relative to SPF mice ($p<0.0001$; Figure 12G). No differences between SPF and ex-GF mice were observed except in daily mean body temperature, where ex-GF mice showed hypothermia similar to GF mice in the active phase ($p<0.01$, ex-GF v SPF mice; Figure 12G).

Re-Entrainment to Shifted Light:Dark Cycle in Jet-Lag Protocol

Locomotor Activity. In round 1, GF mice re-entrained to the new light:dark cycle faster than SPF mice ($F_{11,176}$=6.943, $p<0.0001$; Figure 13A-B). However, in round 2, no difference in rate of re-entrainment to the jet-lag paradigm was observed ($F_{11,143}$=1.487, $p>0.10$; Figure 13C-D). Data from conventionalized (ex-GF) mice did not differ from SPF or GF mice in round 2 (data not shown).

Body Temperature. No differences in rate of re-entrainment were observed in round 1 ($F_{11,132}$=1.654; $p>0.05$) or 2 ($F_{11,132}$=0.719; $p>0.70$). Data from conventionalized (ex-GF) mice did not differ from SPF or GF mice (body temperature data in response to phase shift not shown).

Responses to Acute Light Pulses

Locomotor activity. No differences in magnitude of phase delay were observed in response to a 15 min light pulse at ZT15 between SPF and GF mice for neither LMA ($p>0.30$) or T_b ($p>0.30$). Magnitude of phase delay in response to a 15 min light pulse at ZT22 showed no difference between SPF and GF mice for neither LMA ($p>0.50$) or T_b ($p>0.30$; Figure 14).

Entrainment to Timed-Feeding Protocol

Locomotor Activity. During training, more activity in the FAA was evident in GF mice compared to SPF mice. Following training, on the first probe day of total food deprivation, no differences were observed between GF and SPF mice ($p>0.10$; Figure 15A-B), while GF mice showed about twice as much FAA compared to SPF mice ($p<0.01$; Figure 15C). Data from conventionalized (ex-GF) mice did not differ from SPF mice.

Physiological Measures and Feeding Behavior

Throughout the experiment, change in body mass from baseline between SPF and GF mice did not differ ($F_{1,70}$=0.003; p>0.90). When normalized by body mass, SPF mice showed increased food intake compared to GF mice ($F_{1,42}$=13.552; p<0.01; Figure 16A). Food intake did not differ between SPF and ex-GF mice, though GF mice showed less food intake compared to SPF mice (p<0.05, Figure 16B) When normalized to terminal body weight, epididymal fat mass from GF mice weighed less than those of SPF mice (p<0.01; Figure 16C). When normalized to terminal body mass, livers from GF mice weight less than those of SPF mice (p<0.01; Figure 16D).

Discussion

The present report suggests an important role of the intestinal microbiota in driving host behavioral circadian rhythms. These data show that microbiota serve to stabilize the circadian network. Precedence for the symbiotic relationship between host and microbe in the context of behavioral rhythms and the circadian network has been set in the context of marine life (McFall-Ngai 2014, Sorek et al 2018), which has provided key insights into the importance of this bi-directional interaction. The complexity of this dynamic relationship is further intensified in a mammalian system. However, in the present study provides evidence that gut microbes play a crucial role in driving mammalian host circadian rhythms through the use of a GF murine system. Here, GF mice possess shorter alpha duration in both photocycle and constant darkness conditions as well as a slower clock speed and augmented FAA compared to SPF mice, all of which were restored to SPF levels by the introduction of a complex gut microbiota community later in life in ex-GF mice. These data reveal that, from a behavioral perspective, introduction of

gut microbiota in adulthood alters two fundamental aspects of the circadian network: (i) how the circadian network entrains to environmental cues (i.e., food) and (ii) the speed of the endogenous clock. Given that GF mice are more perturbed in response to environmental stimuli, this provides overall support for the notion that GF mice possess a lower amplitude within the circadian network.

Here the circadian network's stability was probed via several strategies (i.e., jet-lag and timed feeding paradigms) in the presence and absence of gut microbes. One method to probe the amplitude (strength) of the circadian network is to quantify re-entrainment of a mouse's behavioral rhythms to a phase shift in the light:dark cycle. In Round 1, Faster re-entrainment to the new light:dark cycle are consistent with the presence of a lower amplitude (more easily shifted or weaker) circadian network. However, the inconsistent results indicate that the light-entrained component of the circadian network was unaltered, as no differences were observed in the jet-lag protocol and acute light pulses. Together, these data indicate that mice lacking microbiota do not shift their circadian network differently in response to photic stimuli.

Feeding is temporally coordinated by the food entrainable oscillator (FEO), one component of the circadian network (Mistlberger 1994, Storch & Weitz 2009). While the SCN entrains to photic cues (dawn and dusk), temporal changes in feeding patterns have little influence on SCN circadian oscillations (Storch & Weitz 2009). The FEO tracks daily changes in food availability, independent of the central circadian packer (i.e., SCN). When mice are provided food only during the rest phase, they show increased activity preceding food delivery, a time of day mice normally show relatively little activity when fed ad libitum (Mistlberger 1994). Increases in food anticipatory activity (FAA) are consistent with the idea that the FEO, a component of the mammalian circadian network, is more easily shifted (or is of lower

amplitude). While specific brain nuclei and peripheral tissues housing the FEO have yet to be defined, the FEO tracks daily changes in food availability, independent of the SCN. The present data indicate an important role of intestinal microbiota in the FEO, given that FAA is augmented in GF mice compared to both SPF and ex-GF counterparts. These data suggest that gut microbes increase the amplitude of the FEO component of the circadian network as larger shifts in food anticipatory behavior are observed in mice lacking gut microbes and can be restored to SPF levels upon conventionalization in ex-GF mice.

It is worth underscoring that amplitude has been used with two different meanings in the present Chapter. Circadian amplitude measured by LSP power spectrum or non-parametric circadian rhythm amplitude (NPCRA) are both measures of the waveform of locomotor activity. GF mice possess increased amplitude in the LSP power and NPCRA – both measures of the shape of the activity timeseries. In contrast, when tested during our FAA protocol, the FEO component of circadian network of GF mice lacking gut microbiota showed decreased amplitude, seen by its increased sensitivity to environmental perturbations (i.e., food). Oscillators with increased amplitude are more resistant to environmental perturbations. Consider a small pendulum (low amplitude oscillator) swinging versus a large pendulum (higher amplitude oscillator), it will take less energy to disturb the small pendulum compared to the large one. Lower amplitude oscillators can be disturbed more easily. Here, we find that GF mice that lack microbiota mice show more day-time FAA, a bigger shift in activity during the time-feeding protocol compared to SPF mice. This bigger shift suggests that GF mice have a lower amplitude circadian network, more easily perturbed by environmental stimuli. Importantly, the functional stability of the circadian network is not necessarily defined by algorithmic decomposition of waveforms.

While the mechanisms for tissue-to-tissue communication in the circadian network remain to be elucidated, it is plausible that a combination of neuronal and humoral signaling mechanisms allow coherence between the numerous oscillating clocks within a mammal. Microbially-derived products, such as short-chain fatty acids (SCFAs) including butyrate, produced in the distal colon, may contribute to shifting host molecular circadian networks, which could translate to host behavioral rhythm outputs. For instance, compared to control media, exposure of hepanoids (liver-derived stem cells) to butyrate *in vitro* results in a 180-degree (i.e., 12 hour) shift in the expression of a core clock gene, *bmal1*, in only one cycle (Leone et al 2015). Further, injection of GF mice with butyrate at ZT14, but not at ZT02, produces a shift in the *per2:bmal1* mRNA ratio in the liver, which could be one mechanism for humoral signal transmission for peripheral tissue-to-tissue communication (Leone et al 2015). Further supporting this notion that microbially-derived products can impact circadian networks was revealed in a study where timed administration of SCFAs at the beginning of the dark phase entrained peripheral tissue PER2::luc rhythms faster in response to a new light:dark cycle (Tahara et al 2018). Whether and how the time-dependent effects of SCFAs on the molecular clock in peripheral tissues contributes to host circadian behavioral rhythms remains to be determined. Additionally, the signals from gut microbes may communicate to the brain in order to influence behavior, which could be mediated by the vagal enteric nervous system, which could be further explored using the current system in future studies.

Limitations of the study include the inability implicate or exclude specific microbial community members as main drivers of the effects we observe. However, future studies involving monoassociation or conventionalization with defined microbial communities coupled with different dietary intake could provide valuable insights into which microbes (i.e., butyrate-

producing community members) are most important for either stabilizing or destabilizing the circadian network. Additionally, we surprisingly did not observe a faster adjustment in GF mice in response to jet-lag in experimental round 2. Instead, we observed no differences between GF, SPF, and ex-GF animals. One explanation for the lack of congruency between experimental rounds is that round 2 mice were up to 7 weeks older than mice from round 1, where round 2 mice were slower to re-entrain compared to round 1 mice (Figure 13). This is in line with previous reports that indicate that older mice re-entrain more slowly to jet-lag as compared to younger mice (Sellix et al 2012). Whether and how gut microbes impact aging specifically in the context of circadian re-entrainment remains unexplored, however, comparing the jet-lag data from both experimental rounds suggest that faster phase resetting in GF mice could also be dependent on age, while other circadian phenotypes (such as 12:12 LD cycle entrainment, endogenous rhythms and FAA) are not as dependent on age. In photocyclic and constant darkness, GF mice show increase LSP amplitude and decreased alpha (α) duration, but restored to SPF values in conventionalized ex-GF mice. It is important to note that while GF mice exhibited increases in spectral LSP analysis in the circadian period (~24 hrs), this is not a quantification of the stability of the circadian network (as probed in jet-lag and timed feeding), but a quantification of the best fit to a sinusoidal waveform with a ~24 hr period.

The overall goal of these initial studies was to test the hypothesis that gut microbes provide inputs into the host circadian network. The majority of differences between SPF and GF mice were restored to SPF levels in the ex-GF mice, which includes GF mice displaying shorted alpha (α) duration, increased LSP power and augmented FAA, compared to SPF mice. The restoration of SPF-like phenotypes upon reintroduction of gut bacteria in conventionalized ex-GF mice provides evidence that gut bacteria serve as an important factor in ‘normal’ circadian

network functions. Together, this report is the first to indicate a direct role of gut microbiota on the mammalian host circadian behavioral rhythms, supporting the concept that gut microbes should be included in the hierarchical transkingdom control of the circadian network.

Chapter 4: Influence of High Fat Diet on Circadian Rhythms

Abstract

The purpose of this Chapter was to examine the role of high fat diet (HFD) on circadian rhythms, both dependent on and independent of gut microbiota. The circadian clock coordinates the timing of daily behavior and physiology. Studies that have examined the role of high fat diet on behavioral rhythms showed that a high fat diet lengthens the period of free-running locomotor activity rhythms in constant darkness (Kohsaka et al 2007), while other reports have showed a shortening or no change in period (Mendoza et al 2008, Pendergast et al 2013, Yokoyama et al 2020). Further, high fat diet dampens the amplitude of circadian rhythms in adipose (fat) tissue (Kohsaka et al 2007). While these reports indicate a role of HFD on circadian rhythms - varying with diet, mouse strain, and age of HFD presentation - it is unknown if the role of HFD on circadian rhythms is a result of HFD acting directly on the host or mediated by gut microbiota reacting to a HFD. As detailed in Chapter 1, the adverse effects of HFD are, at times, mediated by the gut microbiota. Diet can influence the immune system and, in turn, host physiology and behavior, either directly or via gut microbiota. Germ free (GF) mice produce less immunoglobulin when fed an elemental diet (containing hydrolysed amino acids, purified lipids and carbohydrates) compared to GF mice fed autoclaved food, which contain dead bacterial material. Specifically, GF mice fed an elemental diet have reduced levels of serum IgG and IgA, and fewer splenic IgG-producing cells and circulating leukocytes. When challenged with bacterial mimicking stimulus, LPS, mice that were fed an autoclaved diet mounted a stronger specific IgG response compared to mice fed an elemental diet, but neither GF group had a response as robust as SPF mice (Macpherson & Harris 2004).

High fat diet disrupts behavioral circadian rhythms in mice and HFD alters re-entrainment to a phase advance in the light:dark cycle compared to normal chow-fed, control mice. Previous reports of the effects of HFD on behavioral rhythms have been performed in specific pathogen free (SPF) mice with a normal gut microbiota (Kohsaka et al 2007, Mendoza et al 2008), which does not exclude the hypothesis that the effects of HFD on behavior is independent of gut microbiota. If HFD in GF mice alters behavioral rhythms, absent of commensal bacteria, this outcome would suggest that the influence of HFD on behavioral rhythms does not require gut microbiota. If HFD does not alter behavioral rhythms in GF mice, this outcome would suggest that gut microbiota is necessary in the expression of HFD-induced alterations in circadian rhythms. To understand the mediating effects of gut microbiota on circadian rhythms as a result of HFD, we exposed control SPF and GF mice to normal chow (NC) or a HFD. Mice fed HFD show an increased mean body temperature compared to NC-fed mice. Interestingly and in contrast some previous studies (Kohsaka et al 2007, Mendoza et al 2008, Pendergast et al 2013, Yokoyama et al 2020), the present report showed HFD results in a shortened period of free running rhythms. Finally, HFD abolished food anticipatory activity in mice both SPF and GF mice. These data suggest that HFD can influence circadian rhythms, independent of gut microbiota.

Methods

Animals

The SPF and GF mice fed normal chow from Chapter 3 were used in the current chapter. Male C57BL6/J specific pathogen free (SPF) mice were purchased from the Jackson Laboratories and maintained in The University of Chicago animal vivarium upon arrival under

conventional housing conditions. Germ free (GF) mice were bred and maintained in sterile, flexible film isolators. All mice were maintained in the same or neighboring vivarium rooms under their respective conditions on a 12:12 light:dark cycle (lights off at 6:00 PM CST) unless otherwise noted. Ambient temperature and relative humidity were held constant at 19 ± 2°C and 53% ± 10%, respectively. Autoclaved pine shavings were provided and autoclaved water was freely available throughout the experiment. Mice were fed ad libitum unless otherwise noted and both SPF and GF mice were provided with either autoclaved normal rodent chow (NC; LabDiet 5k67) or fed an irradiated purified high-fat diet containing 37.5% anhydrous milk fat (HFD; Envigo Harlan Teklad TD.97222 customized diet) at the start of LMA and Tb collection. Four groups of mice in total were examined: SPF-NC (n=18), GF-NC (n=16), SPF-HF (n=8), and GF-HF (n=8). All procedures were approved by The University of Chicago Animal Care and Use Committee.

Surgical Procedures

Mice were implanted with wireless radiotelemetry devices (G2 E-mitters; Starr Life Sciences; Oakmont, PA, USA) to continuously record locomotor activity (LMA) and temperature (Tb) data as indicated in Chapter 3.

Circadian Phenotyping

Experiments were conducted in two rounds. In Round 1's order of circadian manipulations: entrainment to 12:12 LD cycle, jet-lag, pZT15 light pulse, pZT22 light pulse, constant darkness, food entrainment (Figure 8). Round 2's order of circadian manipulations: entrainment 12:12 LD cycle, constant darkness, jet-lag, and food entrainment (Figure 9). In

round 1: SPF mice fed normal chow (SPF-NC; n=10) and germ free (GF) mice fed normal chow (GF-NC; n=8); 11 to 18 weeks of age at the start of 12:12 light:dark data collection began. In round 2: SPF-NC (n=8), GF-NC (n=8), SPF mice fed high fat chow (SPF-HFD; n=8), and GF mice fed high fat chow (GF-HFD; n=8); 17 to 24 weeks of age at the start of a 12:12 light:dark cycle data collection. See Chapter 2 for further details.

Statistical Analyses

Analyses of variance (ANOVAs) were performed to decrease chances of Type I error. If a statistically significant F-statistic was achieved, unpaired T-tests were performed using Statview 5.0 (SAS Institute, Cary, NC). Datapoints that lied outside 3±SD of the mean were omitted from statistical analysis (encompassing less than 0.4% of data) to meet necessary conditions for parametric tests. Differences were considered significant if $P \leq 0.05$. Studies were conducted in two rounds (see 'Animals' and 'Circadian Phenotyping'). Datasets from both rounds were combined when no statistical differences were observed between rounds. No differences were observed between rounds.

Results

Entrainment to 12:12 Light:Dark Cycle

Locomotor Activity. Diet influences mouse activity in 12:12 LD photocycle. Onset time was phase advanced in mice fed HFD (microbes $F_{1,46}=4.826$, $p<0.05$; Figure 17). HFD mice showed a later offset time compared to NC-fed mice (microbes $F_{1,46}=4.417$, $p<0.05$; Figure 17). Alpha duration (α; duration of active phase) was lengthened in HFD mice compared to NC-fed mice ($F_{1,46}=7.884$, $p<0.01$; Figure 17), where GF-HFD had an alpha lengthened relative to GF-

NC mice ($p<0.01$) to values similar to SPF-NC ($p>0.05$) and SPF-HFD ($p>0.10$). Diet was without effect on total daily activity counts ($F_{1,46}=0.640$, $p>0.40$), nor when binned by light ($F_{1,46}=0.131$, $p>0.70$; Figure 17B) or dark ($F_{1,46}=2.803$, $p>0.10$; Figure 17B) phases. No effect of diet was observed in onset variability ($F_{1,46}=0.093$, $p>0.70$; Figure 17C). However, offset variability was increased in HFD mice relative to NC-fed mice ($F_{1,46}=4.287$, $p<0.05$). LSP power was not altered as a result of diet (microbes $F_{1,46}=1.427$, $p>0.20$); nor was nonparametric amplitude of circadian rhythms (microbes $F_{1,46}=0.893$, $p=0.3495$). See Table 2 for more on the influence of HFD on circadian rhythms.

Body Temperature. Diet influenced daily rhythms in body temperature. HFD mice showed decreased LSP circadian amplitude ($F_{1,44}=7.076$, $p<0.05$; Table 2). Onset time was earlier in HFD mice relative to NC mice ($F_{1,44}=12.651$, $p<0.001$; Figure 18A). Offset time was without effect ($F_{1,46}=1.103$, $p>0.20$; Figure 18A). Alpha (α) duration was lengthen as a result of HFD ($F_{1,44}=15.032$, $p<0.001$), and expanded alpha in GF-HFD compared to GF-NC mice ($p<0.001$; Figure 18A). Temperature was higher in HFD mice compared to NC-fed mice ($F_{1,44}=20.373$, $p<0.0001$), with increased temperature in both SPF ($p<0.0001$) and GF ($p<0.05$) mice; this daily increase was present in the light phase ($F_{1,44}=38.819$, $p<0.0001$; Figure 18B), but not the dark phase ($F_{1,44}=3.937$, $p>0.05$; Figure 18B). See Table 2 for more on the influence of HFD on circadian rhythms.

Endogenous Circadian Rhythms in Constant Darkness

Locomotor Activity. Onset tau was shortened in HFD mice compared to NC mice ($F_{1,45}=17.668$, $p=0.0001$; SPF-NC v SPF-HFD, $p<0.001$; GF-NC v GF-HFD, $p<0.05$; Figure 19A). Offset tau did not reach significance ($F_{1,45}=0.212$, $p>0.60$). Total daily activity counts

were not influenced by diet (microbes $F_{1,45}$=0.020, p=0.8872; Figure 19B), regardless of if it was binned by active phase ($F_{1,45}$=0.003, p=0.9551; Figure 19B) or rest phase ($F_{1,45}$=0.809, p=0.3731; Figure 19B). Similar to photocycle data, alpha (α) duration was lengthened in HFD mice ($F_{1,45}$=9.744, p<0.01) with a ~1 hr lengthening of alpha in GF-HFD mice compared to those fed NC (p<0.001; Figure 19C). Onset variability was reduced in HFD-fed mice compared to NC-fed mice ($F_{1,45}$=4.394, p<0.05; Figure 19D), though without effect on offset variability ($F_{1,45}$=0.574, p=0.4525; Table 2). LSP spectral analysis showed reduced amplitude in HFD mice compared to NC mice ($F_{1,45}$=5.491, p<0.05; Figure 19E). Non-parametric measures of circadian amplitude did were reduced in GF-HFD compared to GF-NC mice (p<0.05; Figure 19E). See Table 2 for more on the influence of HFD on circadian rhythms.

Body Temperature. No differences in free-running period quantified using LSP spectral analysis were observed as a result of diet ($F_{1,44}$=4.029, p=0.0509). Amplitude was reduced in SPF and GF mice fed a HFD compared to those fed NC (p<0.001, both comparisons). HFD shortened free-running period in SPF (p<0.01) and GF (p<0.05) mice compared to NC-fed mice. Offset tau was not influenced by diet ($F_{1,44}$=0.827, p=0.3682). No differences were observed in onset variability ($F_{1,44}$=0.335, p=0.5656) or offset variability ($F_{1,44}$=3.461, p=0.0695). Alpha duration was expanded in GF-HFD compared to GF-NC mice (p<0.001; Table 2). Both SPF and GF mice fed HFD showed hyperthermia compared to NC-fed mice (SPF: p<0.01; GF: p<0.0001; Figure 19F). See Table 2 for more on the influence of HFD on circadian rhythms.

Re-Entrainment to Shifted Light:Dark Cycle in Jet-Lag Protocol

Locomotor Activity. HFD accelerated re-entrainment of the LMA rhythm to simulated jet-lag (diet $F_{1,286}$ =6.599, $p<0.05$; Figure 20A), independent of microbial status (microbes $F_{1,286}$=1.123; p=0.2990; Figure 20A).

Entrainment to Timed-Feeding Protocol

Locomotor Activity. High fat diet attenuated food anticipatory activity on the probe trial of activity ($F_{1,44}$=11.780; $p<0.01$). GF-HFD mice showed less FAA compared to GF-NC mice ($p<0.05$; Figure 20B), while SPF mice showed similar trends (p=0.0590; Figure 20B).

Physiological Measures and Feeding Behavior

Somatic, ingestive and physiological responses to HFD depend on commensal microbes. HFD increased delta body mass only in SPF mice, but not GF mice (Figure 21A). SPF-NC mice consumed more calories compared to the other three groups, throughout most of the experiment (Figure 21B). As previously reported, both epididymal fat pad mass and liver mass increased with high fat feeding (Figure 21C-D).

Discussion

An important role of the circadian system is to maintain adequate phase adjustments to daily changes in light. The circadian network greatly influences several aspects of physiology, with particularly strong effects on metabolic function (Panda 2016). Metabolic cues under certain feeding conditions can modulate the circadian synchronization to light (Mendoza 2007). All previous reports of circadian rhythms changes as a result of different diets, all have been in

the presence of a ‘normal’ gut microbiota composition (e.g. (Kohsaka et al 2007, Mendoza et al 2010, Mendoza et al 2008)). Previous reports do not distinguish the contributing factors of (1) the direct effects of HFD on circadian rhythms or (2) effects of HFD mediated through intestinal microbiota. This is the first study testing the contributing effects of HFD on circadian rhythms, independent of gut microbes. We report that HFD can have a direct effect on circadian rhythms in LMA and core body temperature: entrainment to 12:12 LD photocycle, constant darkness, simulated jet-lag paradigm, and food anticipatory behavior.

Previous reports showed different effects of HFD on circadian rhythms. Changes in endogenous clock speed (τ), ratio of activity during the active and inactive phase, and adjustment to jet-lag changes with HFD feeding (Kohsaka et al 2007, Mendoza et al 2008, Pendergast et al 2013, Yokoyama et al 2020). In a previous report, mice fed a HFD showed lower active (dark) phase wheel-running activity in a 12:12LD photocycle (3440±443 versus 6156±865 wheel rotations). However, the present report showed no differences on daily activity as a result of HFD feeding (Figure 17). In constant darkness, HFD-fed mice showed a slower τ in one report (~23.8 versus ~23.6 hrs); mice began their HFD (45% fat in HFD; 16% fat in NC) feeding at 4 weeks of age (Kohsaka et al 2007). Another article found a longer τ period in activity in HFD-fed mice compared to those fed NC (24±0.20 versus 23.8±0.02 hrs, respectively); mice were fed HFD (53% fat in HFD; 12% fat in NC) beginning at 6 weeks (Mendoza et al 2008). In common with these pervious reports (Kohsaka et al 2007, Mendoza et al 2008), HFD altered circadian τ, however the direction of the effect in the present report was in the opposite direction where HFD-fed mice showed a shorted τ compared to NC-fed mice (Figure 19). In the present study, mice fed HFD displayed a faster endogenous τ compared to NC-fed mice; mice were 17 to 24 weeks of age at the start of HFD feeding. These differences in a photocycle and constant

darkness may be attributable to the later age at which HFD was implemented or the later age at which mice were tested in the present report, presentation of HFD, or HFD composition. The developmental stage at which diet manipulations are introduced may impact the magnitude of their effects on the circadian system, in common with other behavioral and physiological systems (Boitard et al 2012, Del Olmo & Ruiz-Gayo 2018, Murray & Chen 2019), where our present report may have presented HFD after a developmental window for period lengthening effects.

If diet can confer a direct effect on the circadian system, independent of intestinal microbiota, it is conceivable that specific molecules in food may either speed up or slow down the circadian network, or perhaps it may make the circadian network either hyper- or hypo-sensitive to environmental cues, *Zeitgebers*. Despite the differential findings compared to those observed in previous reports, clearly diet can have profound effects on mouse behavioral rhythms, both in the presence or absence of intestinal microbiota.

Further studies could determine which microbial species or food contents serve as the most powerful *Zeitgebers* for the circadian network. Additionally, the method by which the diet signal influence the circadian system still need elucidation. Insulin or leptin could both be intermediatory molecules that allow high fat diet to confer their effect on the circadian system (Kohsaka et al 2007, Voigt et al 2014). While no specific afferent mechanisms from the periphery to the central nervous system have been elucidated here - vagal afferent signals or diffusible molecules may be influencing the brain - it is clear that diet can influence both the endogenous and entrained components of the circadian network.

Chapter 5: Influence of Maternal Immune Activation on Circadian Rhythms

Introduction

Autism spectrum disorder (ASD) is a chronic disease with a prevalence rate of 1 in 54 children (Maenner et al 2020). This neurodevelopmental disorder manifests early in development, characterized by developmental deficits that produce impairments in personal, social, academic, or occupational function. Autism spectrum disorder is diagnosed with deficits in social communication are accompanied by excessively repetitive behaviors and restricted interests (APA 2013). Disrupted sleep and circadian rhythms are observed in up 78% of patients with ASD (Couturier et al 2005, Souders et al 2009). In addition to ASD, those suffering from several neurodevelopmental disorders are at increased risk for circadian disruption (Jagannath et al 2013, Walker et al 2020). Further, aberrant circadian rhythms are comorbid in ASD patients (Luciana et al 2019) and may be involved in the development of the disorders (Missig et al 2020, Wintler et al 2020).

Infections during pregnancy can lead to adverse outcomes for offspring. Epidemiological data reveal a positive correlation of maternal levels of cytokines IL-8 and TNFα with neurodevelopmental disorders (Brown et al 2004, Buka et al 2001). Indeed, environmental fetal programming is known to alter early fetal brain development and increase risk of ASD (Atladottir et al 2010, Jiang et al 2016, Lee et al 2015). Given the connection between proinflammatory cytokines and abnormal development, systemic inflammation may induce these aberrant behavioral phenotypes. Correlations from epidemiological studies implicating maternal infection to abnormal development are supported by rodent models of maternal immune activation (Boksa 2010, Estes & McAllister 2016, Kentner et al 2019).

Rodent models of maternal immune activation (MIA) have been utilized to explore the neurobiology underlying subsets of individuals diagnosed with autism spectrum disorder (ASD) (Bilbo & Schwarz 2012, Schwartzer et al 2013, Shi et al 2003, Smith et al 2007). Offspring mice born from mothers with an infection during pregnancy show increased anxiety-related and repetitive behaviors (Hsiao et al 2013, Kentner et al 2019), characteristic of a subset of individuals diagnosed with ASD (Schwartzer et al 2013). Importantly, gut microbiota species, segmented filamentous bacteria (SFB), has been shown as critical in the expression of MIA-typical behaviors in mice (Kim et al 2017). SFBs participate in the effects of MIA on some ASD-like behaviors in mice. In addition to MIA, we examined the effects of SFBs on CRs from mice obtained from two sources known for the differential presence of this intestinal species: Jackson laboratories (JAX) mice which are absent of intestinal SFB and Taconic Biosciences (Tac) mice that possess intestinal SFB (Ivanov et al 2008). The aim of the present report was to measure circadian rhythms (CRs) in mice born of maternal illness. To this end, pregnant mice obtained from JAX or Tac were injected with either saline (control 0.9% NaCl) or viral mimic dsRNA PIC (double-stranded polyinosinic:polycytidylic acid; 20mg/kg) on embryonic day 12.5 (E12.5; 12.5 days following egg fertilization), and adult offspring circadian rhythms were characterized in a 12:12 light:dark photocycle, constant darkness, and phase shifting manipulations. Both mouse vendor and sex influenced several aspects of CRs, whereas MIA was with little effect. These findings show that vendor source has a significant effect on CRs where JAX mice displayed a shorter alpha duration and increased LSP power, compared to Tac mice. Additionally, these data support previous reports showing that sex differences play a role in the circadian system where females show an expanded alpha and increased LSP power, however MIA was without effect.

Methods

Animals

C57BL/6J mice were purchased from The Jackson Laboratory (JAX; stock#: 000664; facility RB15 or MP15) or Taconic Biosciences (Tac). Male and female age-matched mice were delivered at 7 weeks of age were allowed at least one week of acclimate to the facility before pairing males and females for breeding. Mice were housed in a 12:12 light:dark cycle, unless noted for the experiment. Mice were allowed free access to food and water. Mouse cages contained irradiated 1/8" corncob bedding (Envigo catalog number: 7902.25) and mice were fed irradiated 18% rodent diet chow (Envigo catalog number: 2918) housed in 19 ± 2 degrees Celsius and 53 ± 10% humidity. All procedures were approved by the Animal Care and Use Committee at The University of Chicago.

Generation of Offspring

Female mice were 8-10 weeks of age at time of mating. Male and female mice from the same vendor (JAX male with JAX female & Tac male with Tac female) were co-housed overnight. Less than 30 minutes prior to the onset of darkness (i.e., nocturnal rodent's active phase), one male mouse was placed into a cage with up to 4 female mice overnight. The following morning, the male was separated from the female mice, and the females were examined for presence of vaginal plugs. The presence of a vaginal plug marked that day as embryonic day 0 (E0) and the female was weighed for a baseline body mass. Pregnant mice were weighed again on day 12.5 and if a 15% increased from baseline body mass was observed, the female was injected with either sterile 0.9% NaCl saline or PIC (20mg/kg) (Sigma: P9582) between ZT02 and ZT03 (the 2nd and 3rd hours of the light phase). If females did not gain 15%

body mass compared to baseline, then that female was regrouped with other female mice that were not pregnant. Offspring mice were kept with their mother to nurse until they were weaned at 21 days of age. If a runt was born, the pup was weaned at 28 days of age at the latest. Collection of circadian rhythm analyses began at 21 weeks of age. See Figure 22 for experimental timeline.

Locomotor Activity Recording

To monitor circadian rhythms, mice were single housed. Passive infrared motion sensors (PIR) were mounted 22 cm above the floor of the home cage. Motion detectors recorded a movement event when 3 of 27 zones were crossed within the cage. Continuous locomotor counts were collected into 1-minute bins and recorded using ClockLab Acquisition (Actimetrics, Evanston, IL) or VitalView (Starr Life Sciences; Oakmont, PA) software.

Circadian Phenotyping

Circadian phenotypes were determined from uninterrupted PIR activity data. Mice were first exposed to a 12:12 light:dark cycle (12 days), followed by constant darkness (10 days) conditions to explore endogenous circadian rhythms, then masking effects of light were examined, and finally exposed to a 15 minute acute light pulse at pZT15 (Figure 23). See Chapter 2 for details on circadian manipulations. Analysis were performed using ClockLab Analysis (Actimetrics, Evanston, IL). Onset and offset times were calculated using ClockLab Analysis software; data were checked by eye; if ClockLab automated software incorrectly identified an onset or offset time, this datapoint was corrected by a scorer blind to treatment group. Onset time, offset time, alpha duration, onset tau and offset tau were calculated using the

daily onset/offset time data. Additionally, Lomb-Scargle periodogram (LSP) spectral analysis was performed. Alpha (α) duration is calculated by the amount of time (in hours) elapsed between the activity onset and activity offset.

Masking Effects of Shifted Photocycle

The shift in the photocycle was completed by advancing the light phase, thereby shortening the dark phase to 6 hours on the day of the shift. This experiment is in is contrast to previous chapters, where the phase advance of the 12:12 LD photocycle is typically completed through advancing the onset of darkness, so that the light phase is 6 hours on the day of the shift. The difference between the two is important to note, where the presence of light is the first perturbation in the lighting cycle in the former, the absence of light is the first perturbation in the lighting cycle in the latter.

Statistical Analyses

Analyses of variance (ANOVAs) were performed to decrease chances of type I error. Three factors for the model were included: MIA (maternal injection of saline or PIC), sex (female or male), and vendor (Jackson Laboratories or Taconic Bioscience). If a statistically significant ANOVA was determined, unpaired T-tests were performed using Statview 5.0 (SAS Institute, Cary, NC). Datapoints that lied outside 3±SD of the mean were omitted from statistical analysis. Data where onset or offset could not be quantified due to by a researcher blind to treatment group were also omitted. Omitted data compassed less than 3.5% datapoints (83 of 2480). Differences were considered significant if $P \leq 0.05$.

Results

Entrainment to 12:12 Light:Dark Cycle

In a 12:12 light:dark photocycle, the Lomb-Scargle periodogram (LSP) showed a main effect of sex, where females possessed greater circadian power compared to males ($F_{1,106}$=37.731, p<0.0001; Figure 24A), without effect of MIA ($F_{1,106}$=0.343, p>0.50) or vendor ($F_{1,106}$=5.87, p>0.05). A main effect of sex was observed in total daily activity counts where females showed more activity ($F_{1,106}$=27.017, p<0.0001), but no differences were observed for MIA ($F_{1,106}$=0.096, p>0.70) or vendor ($F_{1,106}$=1.317, p<0.20). The same effects were observed in the active phase counts (sex: $F_{1,106}$=24.343, p<0.0001; MIA: $F_{1,106}$=0.168, p>0.60; vendor: $F_{1,106}$=1.996, p>0.10; Figure 24B) and dark phase (sex: $F_{1,106}$=19.142, p<0.0001; MIA: $F_{1,106}$=0.052, p>0.80; vendor: $F_{1,106}$=0.155, p>0.60; Figure 24B) counts. Females showed a longer alpha phase duration (hours of active phase) compared to males ($F_{1,106}$=7.723, p<0.01); and Tac mice showed a longer alpha compared to JAX mice ($F_{1,106}$=10.379, p<0.01; Figure 24C); without effect of MIA ($F_{1,106}$=0.562, p>0.40; Figure 24C).

Endogenous Circadian Rhythms in Constant Darkness

A main effect of vendor was observed in tau (free-running period in constant darkness) where JAX mice had a longer tau compared to Tac mice ($F_{1,104}$=4.714, p<0.05), without effect of MIA ($F_{1,104}$=3.756, p>0.05) or sex ($F_{1,104}$=1.918, p>0.10; Figure 25A). LSP circadian power was greater in JAX mice compared to Tac mice ($F_{1,104}$=6.367, p<0.05). Further, females showed increased circadian power compared to males ($F_{1,104}$=65.772, p<0.0001), without effect of MIA ($F_{1,104}$=0.574, p=0.4505; Figure 25B). Similar to recordings in the 12:12 LD cycle, female mice showed more activity compared to males ($F_{1,104}$=39.910, p<0.0001). Additionally, a main effect

of vendor was observed on total activity counts, where JAX mice showed more activity compared to Tac mice ($F_{1,104}$=13.112, p=0.0005), without effect of MIA ($F_{1,104}$=0.019, p=0.8898). The same effects were observed in the active phase counts (sex: $F_{1,104}$=39.227, p<0.0001; MIA: $F_{1,104}$=0.006, p<0.90; vendor: $F_{1,104}$=15.046, p=0.0002) and dark phase counts (sex: $F_{1,104}$=28.197, p<0.0001; MIA: $F_{1,104}$=0.083, p>0.70; vendor: $F_{1,104}$=5.010, p<0.05; Figure 25C). Alpha duration in constant darkness did not have a main effect on any the three factors (sex: $F_{1,104}$=0.0001, p>0.90; MIA: $F_{1,104}$=0.004, p>0.90; vendor: $F_{1,104}$=0.806, p>0.30; Figure 25D).

Masking Effects of Shifted Photocycle

No differences in masking effects of a shifted photocycle were observed. Decreases in activity as a result of light exposure during a time when mice expected darkness did not differ between groups (sex: $F_{1,105}$=5.477, p<0.05; MIA: $F_{1,105}$=0.827, p>0.30; vendor: $F_{1,105}$=0.388, p>0.50; Figure 26A).

Response to Phase Delaying Light Pulse

The acute light pulse at ZT15 was without effect by vendor ($F_{1,105}$=1.373, p=0.2439) or MIA ($F_{1,105}$=0.3185). However, female mice showed a greater magnitude phase delay compared to male mice ($F_{1,105}$=7.814, p<0.01; Figure 26B).

Open Field Test

In the open field test (OFT), female mice showed more time spent inside the center arena compared to male mice (sex: $F_{1,103}$=4.305, p<0.05; MIA: $F_{1,103}$=0.620, p>0.40, vendor:

$F_{1,103}$=1.970, p>0.10; Figure 27A). In the OFT, more time spent in the center of the arena is interpreted as more exploratory behavior or less anxiety-related behavior. Frequencies of entries into the center were also greater in female mice compared to male mice (sex: $F_{1,103}$=21.227, p<0.0001), with a main effect of vendor where JAX mice showed more entries into the center compared to Tac mice (vendor: $F_{1,103}$=13.614, p<0.001; MIA: $F_{1,103}$=1.443, p>0.20; Figure 27B). No differences in latency to enter the center area were observed (sex: $F_{1,103}$=0.018, p>0.80; vendor: $F_{1,103}$=2.602, p>0.10; MIA: $F_{1,103}$=0.627, p>0.40; Figure 27C).

Discussion

Aberrant circadian rhythms are a prominent feature of several neuropsychiatric disorders (APA 2013). With sleep disturbances documented in up to 78% of patients diagnosed with autism spectrum disorder (Couturier et al 2005), it is important to examine circadian rhythms circadian rhythms in animal models for neuropsychiatry. Several animal models attempt to recapitulate the behavioral phenotypes of human psychopathology, each with their own promises and shortcomings of construct validity (Nestler & Hyman 2010). Here, we examined circadian rhythms in an animal model of neuropsychiatric disorders shown to recapitulate several aspects of autism spectrum disorder using maternal immune activation (MIA) (Bilbo & Schwarz 2012, Choi et al 2016, Smith et al 2007). Circadian activity was quantified in 12:12 light:dark cycle, constant darkness, a masking manipulation, and phase delaying light pulse.

In the current report, the effect of MIA had little effect compared to the effects of sex and mouse vendor. No differences as a result of MIA were present in LSP power, activity counts, or alpha (α) duration in a 12:12 light:dark photocycle. Further, no differences in endogenous onset tau (τ), LSP power, activity counts, or alpha were seen in constant darkness. Sex differences

were consistent across both photocyclic and constant darkness conditions. LSP power was greater in females compared to males, activity was greater in females (LD: Figure 24; DD: Figure 25). Additionally, females showed a faster onset tau in constant darkness (Figure 25). One previous report showed differences in circadian rhythms as a result of MIA (Delorme et al 2021), where mice were injected with 5mg/kg PIC on E9.5. MIA males showed a longer alpha (α) in a 12:12 light:dark cycle and constant darkness compared to control males. MIA males also showed more daily activity in a 12:12 light:dark cycle, as well as more subjective day activity in constant darkness (Delorme et al 2021). However MIA females showed no differences in a 12:12 light:dark cycle or constant darkness (Delorme et al 2021). Sex differences were reported in endogenous period (τ), alpha longer, and total activity counts with significant F-statistics, however means for groups separated by sex were not performed; rather, males and females were grouped in pairwise comparisons (Delorme et al 2021). These differences may be explained by the time of viral mimic injection, or viral mimic vendor (Kentner et al 2019). While others have found an effect of MIA on circadian rhythms, differences between previous reports and the current findings may stem from the use of running wheels in contrast to passive infrared sensors, as the use of running wheels to record activity rhythms can feedback into and modulate circadian organization (Pendergast et al 2014). Interestingly, the mice in the previous report were used ordered from JAX, a vendor known for their lack of SFBs (Ivanov et al 2008). Given the many facilities JAX houses mice in in North America, it is possible that some JAX facilities house mice with intestinal SFBs while others do not (Ivanov 2017). The present report provides evidence that MIA has little effect on circadian rhythms. However, given the high rate of mouse MIA results depending on cage bedding, sex, time of injection, and PIC molecular weight

(Kentner et al 2019), it may be worth further investigation before discounting MIA as a modulator of offspring circadian rhythms.

Chapter 6: Circadian and Circannual Timescales Interact to Generate Seasonal Changes in Immune Function

Introduction

Properties of biological systems vary over multiple timescales in nature: annual, circadian, ultradian. Recurrent daily and seasonal rhythms in immunity are well-documented (Martin et al 2008, Scheiermann et al 2018). Whereas circadian rhythms are generated by endogenous cell- and tissue-level circadian clocks and are synchronized to the solar day by light, the mechanisms that generate annual rhythms in immunity and entrain them to a period of one year remain to be fully identified. In the laboratory, simulated seasonal changes in day length are sufficient to trigger trait-specific enhancement and suppression of immune function in many vertebrates (Nelson 2004).

Annual changes in immune function are trait- and species-specific, and afford opportunities to assess how climatic variables affect biology (Stevenson & Prendergast 2015, Stevenson et al 2015) in a comparative context. Immune activation has metabolic costs (Demas et al 1997), and energetically-expensive immune responses are attenuated in winter (Bilbo et al 2002a, Nelson 2004, Prendergast et al 2004). In hamsters, for example, cellular (Baillie & Prendergast 2008, Bilbo et al 2002a, Prendergast et al 2004), behavioral (Bilbo et al 2002b) and febrile (Wen et al 2007) responses to pathogen infection are suppressed in short days. In contrast, skin hypersensitivity responses are augmented in short days, indicative of enhanced T cell dependent immune function in winter (Bilbo et al 2002a). In common with most photoperiod-driven physiology, these short-day responses are melatonin-dependent (Freeman et al 2007, Wen et al 2007). Indeed, in melatonin-deficient C57BL/6J mice (Goto et al 1989) photoperiodic, but not circadian, immunomodulation is absent (Yellon & Tran 2002).

Photoperiod also modifies circadian waveform and amplitude (Evans et al 2012, Pittendrigh & Daan 1976a). Long and short day lengths alter the timing and expression levels of clock genes within subregions of the master circadian pacemaker in the suprachiasmatic nucleus (SCN; (Evans et al 2013, Hastings 2001, Johnston et al 2005, Steinlechner et al 2002, Yan & Silver 2008)); daily SCN phase output, in turn, rapidly entrains peripheral physiological circadian rhythms. The phase and amplitude of circadian rhythms in melatonin secretion and locomotor activity, for example, change predictably following transfer from long to short days (Elliott & Tamarkin 1994, Illnerova et al 1984, Vanecek et al 1990). These changes reflect rapid effects of circadian entrainment to photoperiod on the network of molecular oscillators that constitute the core circadian pacemaker (Pittendrigh & Daan 1976a), and it is this short latency that distinguishes these from other photoperiod-driven traits such as body size, gonad size and function, and behavioral thresholds, which require weeks-to-months to transition between seasonal phenotypes (Prendergast et al 2002a, Prendergast et al 2002b).

Seasonal changes in immune function may reflect long-term adaptations to changes in photoperiod (Figure 28A-C), alternatively, they may arise merely from entrainment-driven changes in phase alignment of daily immunological rhythms (Figure 28D), or they may be generated by waveform modifications (Figure 28E&F), or any combination of these. Characterizing diurnal waveforms in physiology at a resolution sufficient to discriminate among these mechanisms requires measurements to be obtained at multiple phases over the circadian cycle, but such measures have not been performed. In a systematic review of all published research on photoperiodic changes in immune function in hamsters (the modal animal model for mammalian photoperiodic immunology research (Stevenson & Prendergast 2015); we identified 53 peer-reviewed manuscripts which collectively reported on 129 distinct measures of immune

responses to photoperiod (see Methods). Among these, none examined immune function or challenged the immune system at more than one time of day; moreover, 22 of the 53 reports (42% of total) did not specify the time of day at which measures were obtained.

There is no unconfounded matching of phase across photoperiods. Thus, to determine whether photoperiodic differences in immunity captured in static measures reflect long-term seasonal adaptations vs. artifacts of phase alignment, we examined multiple immune measures at high frequency (3 h) intervals in hamsters following adaptation to long and short days. If trait differences between photoperiod groups persist irrespective of phase alignment, this would exclude the hypothesis that seasonal immunomodulation merely reflects acute effects of phase alignment.

Methods

Meta-Analysis

A meta-analysis of the peer-reviewed empirical literature was performed. It was restricted to Siberian hamsters (*Phodopus sungorus*) and Syrian (*Mesocricetus auratus*) hamsters, as these model species are commonly used to examine photoperiodic changes in immune function. Two databases were surveyed: ISI Web of Knowledge and PubMed Central, using the search terms: "immune" and "photoperiod" and "hamster" with publication dates between January 2001 and February 2019, which yielded a total of 113 articles. Review papers, reports unrelated to photoperiodism and immune function, and those that did not use Siberian or Syrian hamsters were omitted. Methods and Results sections of each article were examined, and papers that investigated responses of the immune system to actual or simulated seasonal changes in photoperiod were included, yielding a total of 53 articles for analysis. Figures, tables, text, and

supplementary information were examined to extract relevant data. Each immunological trait and the time of measurement or immunological challenge was extracted.

Animals

Male Siberian hamsters (*Phodopus sungorus*) were born and raised in a long-day (LD; 15 h light, 9 h dark; 15L:9D; lights off at 17:00 CST) photoperiod. Hamsters were housed in polypropylene cages (28 x 17 x 12 cm), on wood-fiber bedding (Sani-Chips, Harlan, USA), with cotton nesting material available. Food (Teklad, Harlan, USA) and filtered tap water were provided *ad libitum*; ambient temperature was held at 19 ±2 ^{o}C with humidity at 52 ±10 %. Hamster ages at the onset of each experiment (week 0) were as follows: experiment 1: 75-204 days of age (154 ± 45 days); experiment 2: 138-185 days of age (160 ± 15 days); experiment 3: 83-188 days of age (132 ± 28 days); experiment 3 supplement: 389-460 days of age (424 ± 22). All procedures were approved by the Institutional Animal Care and Use Committee of the University of Chicago.

Photoperiod Manipulations and Determination of Photoperiod Responsiveness

At the beginning of each experiment (week 0) male hamsters were singly-housed and either transferred from their natal LD photoperiod into a short-day (SD; 9L:15D; lights off at 17:00) photoperiod (experiment 1: n=31; experiment 2: n=117; experiment 3: n=80), or remained in LD (experiment 1: n=22; experiment 2: n=87; experiment 3: n=64). A dim (<1 lux) green light remained continuously illuminated in all photoperiods to facilitate entrainment of the circadian system to experimental photoperiods (Evans et al 2007).

Somatic and reproductive responses to LD and SD treatments were confirmed in all hamsters via changes in body mass and testis size. To assess reproductive responses, the length and width (in mm) of the right testis were obtained using analog calipers through the abdominal skin in hamsters under light isoflurane anesthesia (~3% in O_2) on week 0 and again on week 6 (experiments 1 and 3) or on weeks 0, 3 and 6/8 (experiment 2, hereafter: 'week 6'). Estimated testis volume (ETV) was calculated as the product of the square of testis width and testis length. ETV is positively correlated (R^2>0.9) with testis weight, circulating testosterone and spermatogenesis (Gorman & Zucker 1995, Schlatt et al 1995). Hamsters exhibiting a decrease in ETV of >50% between week 0 and 6 in SD were identified as photoperiod-responsive and were included in all subsequent experiments. In each study, immune challenges were timed in order to equate the midpoint of treatments across studies to approximately week 8.

Anesthesia

Anesthesia was required for humane blood collection via the retro-orbital route (Experiment 1), and to relax hamsters sufficiently to permit pinna measurements. Experiments in rats, mice and honeybees have documented circadian phase shifts in response to isoflurane (see Sebastian et al. 2019 for review). We did not attempt to control for any such effects, but we view them as unlikely to have confounded the data reported here: circadian shifting effects have been reported after treatments that entail 4-6 hours of continuous isoflurane anesthesia, whereas in the present paradigm hamsters were exposed to isoflurane gas for no more than 1-2 minutes. Moreover, isoflurane-induced phase shifts in body temperature and activity habituated by the second exposure (Song et al, 2016).

Experiment 1 - Peripheral Blood Leukocyte Concentrations

Blood Collection. Blood (~100 µl) was obtained under light isoflurane anesthesia from the right retro-orbital sinus using heparinized collection tubes. A dim (<1 lux) red light was used to facilitate dark-phase collections. Each hamster was randomly assigned to be bled at 4 of 8 times of day (ZT 1.5, ZT 4.5, ZT 7.5, ZT 10.5, ZT 13.5, ZT 16.5, ZT 19.5, or ZT 22.5; n=9-11 per ZT [ZT= 'Zeitgeber time'; hours after lights on]). Following each blood draw, hamsters were administered 0.5 ml of sterile saline (s.c.). Blood collections were performed in pseudo-random order, in a room separate from the general animal colonies, and following the procedure, hamsters were isolated from the colony until all collections were completed. Animal handling during the blood collection was kept to a minimum (<2 min). Blood samples were deposited into heparinized (50 units) microcentrifuge tubes, mixed gently, and a 25 µl aliquot of whole heparinized blood was removed for leukocyte determination (PBL assay).

Peripheral Blood Leukocyte (PBL) Assay. PBLs were obtained from whole blood via hemolysis with 3% acetic acid at a 1:20 dilution, and enumeration in duplicate on a hemocytometer at 400× magnification by an experimenter blind to the hamster's photoperiod group. Lysed samples were kept at room temperature for <3 h before leukocyte counts were determined. Distinct leukocyte subtypes are not identifiable with this method, but the PBL assay reliably identifies environmentally-induced; for example, photoperiod (Bilbo et al 2002a), stress (Prendergast et al 2013) changes in blood leukocyte concentrations. In several studies of hamster leukocytogenesis, total leukocyte concentration correlates positively with photoperiodic changes in specific leukocyte subtypes, including total lymphocytes, T-cells, and NK cells (Bilbo et al 2002a, Wen et al 2007). Diurnal leukocyte trafficking requires clock-driven migration of PBLs out of the

circulation to skin, organs, and lymph nodes (Dhabhar et al 1995). The PBL assay thus provides a rapid and omnibus indicator of effects of circadian rhythmicity on the capacity for immunosurveilliance in the blood. Applied longitudinally, this measure provides an accurate indicator of daily and stress-induced leukocyte trafficking (Dhabhar et al 1995, Dhabhar et al 1994).

Body Mass and Testis Volume Determinations. At the time of blood collection in Experiment 1, body mass (±0.1 g) and estimated testis volume (see above for ETV methods) were also determined. In addition, to verify that testis measurements were not influenced by ambient lighting, following the final PBL blood draw, testis measurements were recorded from each hamster during both the light and the dark phases of the LD or SD photoperiod (as appropriate).

Experiment 2 - Innate Immune Responses to Endotoxin

LPS-Induced Sickness Responses. Hamsters were administered lipopolysaccharide (LPS) from gram-negative bacteria (*Escherichia coli*), which mimics systemic bacterial infection. LPS-induced sickness responses require the coordinated activity of innate immune cells and pathways, which integrate pathogen-associated molecule recognition, Toll-like receptor signaling, proinflammatory cytokine expression, and changes in metabolism, behavior and motivational state (Hart 1988). The measurement of acute phase responses to LPS in Siberian hamsters has been described in detail elsewhere (Prendergast et al 2004, Wen et al 2007). Briefly, body mass and food intake values were recorded daily beginning on week 7. After 3 d of baseline measurements, hamsters were injected i.p. with either bacterial LPS (625 µg/kg; isolated from *Escherichia coli* strain 026:B6, L8274, Sigma, USA) or sterile 0.9% saline (0.1 mL). This

dose of LPS is commonly used in studies of Siberian hamsters (Baillie & Prendergast 2008, Wen et al 2007) which, compared to mice, require a somewhat higher dose to elicit robust sickness responses (Bilbo et al 2002b, Prendergast et al 2015). Separate groups of LD and SD hamsters were administered LPS or saline injections at one of 8 different times of day (ZT 1.5, ZT 4.5, ZT 7.5, ZT 10.5, ZT 13.5, ZT 16.5, ZT 19.5, or ZT 22.5; n = 8-11 hamsters per ZT per photoperiod). Food intake and body mass were recorded every 24 h following injection for 5 d (hereafter: 'post-injection day'; 'P.I.D.'). LPS and saline treatments were administered in a block-randomized design: hamsters were randomly assigned to an initial LPS or saline treatment group, and treatments were delivered in a counterbalanced design, with successive injections separated by 14 days. Hamsters remained within a single ZT group for both injections. One SD hamster lost more than 30% of its body mass following LPS treatment, a highly atypical response (for any photoperiod or time-of-day), and it was removed from further study.

Experiment 3 - Adaptive Immune Responses to Antigen

DNFB-Induced DTH Responses. Hamsters were sensitized and challenged with cutaneous application of 2,4-dinitro-1-fluorobenze (DNFB), which elicits a delayed-type (Type IV) hypersensitivity (DTH) response. DTH responses require immunological memory and thus provide an integrative assay of T cell-dependent immune function. DTH-associated cutaneous inflammation is reliably measured by changes in pinna thickness after DNFB challenge to the dorsal pinna. DTH methods have been described extensively elsewhere (Prendergast et al 2004). Briefly, to elicit DTH, 25 µl DNFB (Sigma, D1529; 0.5% v/v in 4:1 acetone:oil vehicle) was applied to the shaved dorsum on two successive days of week 8; each of these sensitization treatments was performed at the midpoint of the light phase (LD: ZT 7.5; SD: ZT 4.5). One week

later, separate groups of LD and SD hamsters were challenged with 20 µl of a diluted DNFB solution (0.2% [v/v]) applied to the right pinna at one of 8 different times of day (ZT 1.5, ZT 4.5, ZT 7.5, ZT 10.5, ZT 13.5, ZT 16.5, ZT 19.5, or ZT 22.5; n = 6-9 hamsters per ZT per photoperiod). At the same time as DNFB treatments, a control vehicle (4:1 acetone:oil; 20 ul) was applied to the right pinna, and each hamster served as its own control (Bilbo et al 2002a). Solutions were made fresh <20 min prior to use. Pinna thicknesses were measured just prior to DNFB challenge and again every 24 h (at the ZT of the challenge) for the next 6 d in lightly anesthetized hamsters using a constant-loading dial micrometer (±0.01 mm; Mitutoyo, Tokyo, Japan). Baseline (just prior to DNFB challenge) pinna thickness measurements did not vary significantly over the course of the day (LD: $F_{7,45}$=0.72, P=0.65; SD: $F_{7,62}$=1.36, P=0.24), thus we interpret daily rhythms in ear thicknesses observed after DNFB challenge as reflecting DTH inflammatory responses, rather than an interaction between spontaneous daily rhythms in pinna water content and DTH-induced edema.

Lastly, a supplemental experiment examined whether the phase of DNFB sensitization affected DTH magnitude. Using DTH methods described above, hamsters housed in LD (15L:9D; n=51) were sensitized to DNFB at the mid-light phase (ZT 7; n=26) or during the mid-dark phase (ZT 19; n=25), and were challenged one week later at either ZT 7 or ZT 19, resulting in 4 experimental groups: sensitization at ZT 7 and challenge at ZT 7 (ZT 7 – ZT 7, n=13), ZT 7 – ZT 19 (n=13), ZT 19 – ZT 7 (n=12), and ZT 19 – ZT 19 (n=13). As in the main experiment, pinna thicknesses were measured on the day of challenge and daily thereafter for 6 days.

Measurement Validation

To determine whether circadian variation in testis volume reflected differences in measurement accuracy during the light and dark phases, ETVs were determined on a separate group of LD and SD hamsters under full room illumination, and again minutes later, with the room lights turned off with the assistance of dim red illumination. ETVs obtained in the dark were strongly and positively correlated with those obtained under full illumination: R^2=0.913, df=38, P<0.001. As in other reports (Gorman & Zucker 1995, Schlatt et al 1995), ETV was strongly correlated with testis mass: R^2=0.911, df=38, P<0.001. To ensure that any daily changes in pinnae thickness determinations were not artifacts of accuracy differences in the light and dark phases, DTH was induced in a separate group of hamsters and pinna thicknesses were determined in the light phase, and again 2 h later (to provide sufficient time for edema to be restored) with room lights extinguished and with the assistance of dim red illumination. Pinnae thicknesses obtained in the light and dark were strongly positively correlated: R^2=0.872, df=34, P<0.001.

Lastly, in Experiment 3 pinnae thicknesses were determined at 3 h intervals for 6 consecutive days, requiring two experimenters working in tandem. To evaluate inter-rater consistency, DTH was induced in a group of hamsters (n=70), and pinnae thicknesses were determined on all animals by both experimenters (KGO, BJP), separated by an interval of 2 h. Pinnae thicknesses were strongly and positively correlated between the two investigators (R^2=0.9164, df=69, P<0.001).

Statistical Analyses

Longitudinal PBL, body mass and ETV (Experiment 1), food intake and body mass (Experiment 2), and pinna thickness (Experiment 3) were analyzed using repeated measures factorial ANOVA, with photoperiod and treatment/measurement time as between-subjects variables. In Experiment 2, the ANOVA model also included injection type (LPS, SAL) as a between-subjects variable.

To test the hypothesis that circadian phase alignment constitutes a meaningful source of the variance in immunological photoperiodism, we examined how 3 distinct temporal alignments affected the measured immune responses: (1) ZT alignment [ZT]: aligned LD and SD values relative to the onset of the light phases for each photoperiod; (2) Dark Onset [DkO]: aligned group values relative to the onset of darkness; (3) Midpoint [MP]: aligned values relative to the midpoint of the light phase. ETV and body mass were examined in a similar manner. Where justified by a significant F-statistic, values were compared using unpaired t-tests (Statview 5; SAS Institute, Cary, NC). Differences were considered significant if $P \leq 0.05$.

CircWave (courtesy of R. Hut; www.huttlab.nl); was used to quantify rhythms in multiple dependent variables with one or two sine wave functions; F, P and R^2 values were identified for each curve fit (Zhou et al 2014). In Experiment 1, PBL concentrations, ETV and body mass were evaluated. In Experiment 2, two integrative metrics captured the acute robustness and the overall net magnitude of the anorexic response to LPS: (1) amplitude of the peak (day +1) anorexic response and (2) area under the curve of the anorexic response during the 5 days after LPS treatment (AUC_{FI}). In Experiment 3, AUC of the DTH (AUC_{DTH}) and the magnitude of the skin inflammatory response on day +1 (the approximate day of peak DTH) were assessed.

Results

Meta-Analysis of Immunological Photoperiodism Research

The analysis identified 53 peer-reviewed, empirical reports on photoperiodic changes in immune function in hamsters. Among the 129 trait measurements therein, none was obtained at more than one phase of the daily cycle. In 21 of the 53 reports (accounting for 60 of the 129 traits; 40% of total reports; 47% of total traits) measures or treatments were performed within ±2 h of the onset of darkness. In addition, 22 of 53 reports (42%) failed to indicate the time of day when measurements were obtained.

Experiment 1 - Peripheral Blood Leukocyte (PBL) Concentrations

Adaptation to Photoperiod. 18 of 31 (58.1%) hamsters exhibited gonadal regression in SD and were included in the study. ETV and body mass each differed between LD and SD (ETV: $F_{1,38}$=34.4, P<0.001, Figure 29A; body mass: $F_{1,38}$=10.9, P<0.001, Figure 29B).

PBL Concentrations. Collapsed across all collection times, PBL counts were greater in SD than LD hamsters (i.e., a main effect of photoperiod; $F_{1,144}$=24.7, P<0.001; Figure 30A). When collection times were aligned by light onset (ZT) there was a significant interaction between photoperiod and time ($F_{7,144}$=32.5, P<0.001; Figure 30B); alignment by dark onset (DkO; $F_{7,144}$=16.4, P<0.001; Fig 6.3C) and light phase midpoint (MP; $F_{7,144}$=26.6, P<0.001) each yielded a categorically similar statistical outcome (Figure 30B-D). Pairwise comparisons indicated that PBL concentrations were greater in SD than LD at 5 discrete time points when aligned by DkO (Figure 30C), at 3 time points when aligned by ZT (Figure 30B), and at 4 time

points when aligned by MP (Figure 30D). DkO alignment also yielded 2 time points at which PBL concentrations were greater in LD (Figure 30C).

Daily Rhythms in PBL Concentrations. Daily rhythms were evident in blood leukocyte concentrations in both LD ($F=40.76$, $P<0.001$, $R^2=0.49$) and SD ($F=58.16$, $P<0.001$, $R^2=0.63$). In LD, PBLs concentrations reached peak levels at ZT 5.6 ±3.0 (mean ± SD), and in SD PBLs peaked at ZT 5.5 ±3.0. Daily rhythms were not observed in testis size ($F<1.5$, $P>0.2$, $R^2<0.05$, all analyses) or in body mass ($F<1.3$, $P>0.2$, $R^2<0.04$, all analyses).

Testis Size and Body Mass. ETV was smaller in SD relative to LD ($F_{1,144}=1321.2$, $P<0.001$; Figure 31A). Circadian phase alignment did not interact with photoperiod to affect ETV (ZT: ($F_{7,144}=1.42$, $P>0.20$, Figure 31B; DkO: $F_{7,144}=0.73$, $P>0.60$, Figure 31C; MP: $F_{7,144}=0.96$, $P>0.40$, Figure 31D). ETVs were significantly greater in LD relative to SD hamsters at all 8 timepoints, regardless of alignment (Figure 31B-D). SD hamsters also weighed less than LD hamsters ($F_{1,144}=54.4$, $P<0.001$; Figure 32A), and none of the 3 phase alignments impacted the effect of photoperiod on body mass (ZT: $F_{7,144}=0.4$, $P>0.90$, Figure 32B; DkO: $F_{7,144}=0.7$, $P>0.60$, Figure 32C; MP: $F_{7,144}=0.5$, $P>0.80$, Figure 32D). LD hamsters weighed more than SD hamsters at all 8 timepoints in the ZT and DkO alignments, and at 7 of 8 timepoints in the MP alignment (Figure 32B-D).

Experiment 2 - Innate Immune Challenge

Adaptation to Photoperiod. Reproductive photoresponsiveness was evident in 80 of 117 (68%) SD hamsters on week 6; the remaining 37 hamsters were excluded from further study. One LD

hamster (of 87) had a relatively small (ETV = 146) testis on week 6 and was also removed from study. Among photoresponsive hamsters, SD inhibited ETV and body mass during photoperiodic adaptation (ETV: $F_{2,632}$=102.2, P<0.001, Figure 29C; BW: $F_{6,1896}$=134.1, P<0.001, Figure 29D).

Effects of Photoperiod and Phase Alignment on LPS-Induced Anorexia. LPS-induced changes in food intake were reduced in SD hamsters ($F_{5,1405}$=9.80, P<0.001), both in magnitude and persistence (Figure 33A). When aligned by ZT, photoperiod, injection type and circadian phase interacted to affect food intake (photoperiod x injection x phase; $F_{35,1405}$=1.90, P<0.005; Figure 33B); SD attenuated anorexic responses to LPS at 5 distinct phases of the cycle (ZT 1.5, P<0.005; ZT 4.5, P<0.001; ZT 13.5, P<0.01; ZT 16.5, P<0.05; ZT 22.5, P<0.05) and tended to do so at one additional phase (ZT 7.5, P=0.056). When aligned by DkO, the photoperiod x injection x circadian phase interaction was significant ($F_{35,1405}$=1.59, P<0.05; Figure 33C); SD adaptation attenuated anorexic response to LPS at 5 phases of the cycle (DkO+4.5 h, P<0.05; DkO+7.5 h, P<0.01; DkO+13.5, P<0.01; DkO+16.5 h, P<0.05; DkO+22.5 h, P<0.05). Lastly, the photoperiod x injection x phase interaction was also evident when photoperiods were aligned by midpoint (MP) of the light cycle ($F_{35,1405}$=1.48, P<0.05; Figure 33D). SD reduced anorexia magnitude relative to LD at 5 phases: the midpoint of the light phase (MP, P<0.05), 6 h before MP (MP-6; P<0.05), MP-3 (P<0.05), 6 hours after MP (MP+6; P<0.05) and MP+9 (P<0.001), and tended to do so at one additional phase (MP-9, P=0.084).

Daily Rhythms in Sickness Responses to LPS. In LD, there was a clear daily rhythm in the response to LPS as measured by acute (peak) anorexic responses on day +1 (F=4.24, P<0.05, R^2=0.10), but in SD hamsters no such rhythm was evident (F=0.67, P>0.5). Daily rhythms were

not evident in AUC_{FI} in either day length (LD: F=2.86, P>0.05; SD: F=0.2, P>0.80).

Experiment 3 - Adaptive Immune Challenge

Adaptation to Photoperiod. 70 of 80 (87.5%) hamsters were reproductively responsive to SD and included in this study. One (of 64) LD hamster had a relatively small ETV of 230, and was also removed from further study. ETV and body mass responses differed significantly between LD and SD hamsters during photoperiodic adaptation (ETV: $F_{1,121}$=305.2, P<0.001, Figure 29E; BW: $F_{7,847}$=59.1, P<0.001; Figure 29F).

Effects of Photoperiod and Circadian Phase Alignment On DTH. DTH reactions were augmented in SD relative to LD ($F_{6,726}$=5.90, P<0.001; Figure 34A). Circadian time did not interact with photoperiod to affect DTH, regardless of phase alignment (ZT alignment: $F_{42,642}$=1.3, P>0.05; DkO alignment: $F_{42,642}$=0.9, P>0.50; MP alignment: $F_{42,642}$=1.1, P>0.30; Figure 34B-D). When aligned by ZT, DTH responses were greater in SD relative to LD when hamsters were challenged at ZT 7.5 (P=0.001), ZT 19.5 (P<0.001) and ZT 22.5 (P<0.005; Figure 34B). When aligned by DkO, SD enhanced DTH in hamsters challenged at DkO+4.5 h (P<0.001), DkO+7.5 h (P<0.005), DkO+22.5 h (P<0.05), and tended to enhance DTH at DkO+16.5 h (P=0.07; Figure 34C). Lastly, when aligned by MP, SD enhanced DTH at MP-9 (P<0.001), MP±12 (P<0.001), and tended to enhance DTH at MP+3 (P=0.08; Figure 34D).

Daily Rhythms in DTH. Diurnal rhythms in AUC_{DTH} were identified in LD (F=4.83, P=0.01, R^2=0.16) and in SD (F=2.61, P<0.05, R^2=0.16 [2 sines]). In LD hamsters, AUC_{DTH} was greatest in hamsters challenged at ZT 7.5 and smallest in hamsters challenged at ZT 19.5; whereas in SD,

the largest and smallest AUC_{DTH} values were in hamsters challenged at ZT 7.5 and 13.5, respectively (waveforms not illustrated).

Supplemental Experiment. Sensitization time did not affect DTH ($F_{6,282}$=1.50, P>0.15), but challenge time did ($F_{6,282}$=2.37, P<0.05); specifically. DTH reactions were greater in hamsters challenged during the light phase ZT 7. There was no interaction between sensitization and challenge time on DTH ($F_{6,282}$=0.50, P>0.80; Figure 35).

Discussion

Adaptation to winter photoperiods increased blood leukocyte concentrations, attenuated sickness responses to a simulated gram-negative bacterial infection, and augmented skin DTH reactions, consistent with prior reports of diverse immunological effects of changes in day length (Stevenson & Prendergast 2015). Diurnal changes in immune function were also identified. These data permitted examination of how the seasonally-changing waveforms of daily rhythms in immunity factor in the identification of photoperiodic immune responses. Mean daily levels about which circadian oscillations revolved differed between SD and LD in a trait-specific manner (PBLs: SD>LD; anorexia: LD>SD; DTH: SD>LD), and alignment of these immunological waveforms to standard phase markers (ZT, DkO, MP) framed unique, phase-dependent differences between winter and summer immunophenotypes, but in no instance did a circadian phase alignment eliminate photoperiodic differences in any measure of immunity. The persistence of clear and distinct photoperiodic immunophenotypes irrespective of phase alignment permits rejection of the hypothesis that seasonal immunomodulation merely reflects acute, entrainment-driven, effects of circadian phase alignment, and is consistent with the

hypothesis that seasonal changes in immune function are a result of seasonal adaptations to photoperiod and involve longer-term changes in the norms of reaction to immunological stimuli.

Daily rhythms in constitutive measures of immunity (e.g., circulating leukocytes, lymphocyte subpopulations) are well-documented in laboratory mammals (Depres-Brummer et al 1997, Dhabhar et al 1994) and humans (Born et al 1997, Dimitrov et al 2009). The severity of multiple aspects of innate immune activation by bacteria or LPS – including the activation of cellular and humoral inflammatory cascades (Gibbs et al 2012b, Marpegan et al 2009), sickness behaviors (Franklin et al 2007, Marpegan et al 2009, Prendergast et al 2015), and morbidity and mortality (Marpegan et al 2009, Shackelford & Feigin 1973) – vary over the circadian cycle. Likewise, adaptive immune responses, e.g., responses to immunization and DTH reactions (Pownall et al 1979) and many T cell and B cell functions (Fortier et al 2011, Silver et al 2012), change over the course of the day, with peak phases that depend on species and trait. The present data extend these observations by generating high-resolution circadian and circannual maps of multiple dimensions of immune function (immunocompetence, innate immunity, antigen-specific adaptive immune function) in a single species.

PBL concentrations exhibited diurnal rhythms in both photoperiods, peaking ~5-6 h after lights on (Fig. 7), a waveform similar to that reported in nocturnal rats (Depres-Brummer et al 1997) and opposite of diurnal human subjects (Dimitrov et al 2009). Leukocyte dynamics during the early light phase were similar in both photoperiods: rising over the first 4.5 h, then precipitously declining over the next 12 h, regardless of whether a transition to darkness occurred during this interval (as it did in SD). We have previously documented that the PBL rhythm persists with a similar waveform in hamsters housed under continuous darkness (Prendergast et al 2013), indicating that this is a true, endogenous circadian rhythm, and not

solely a masking effect of light. The tight temporal correspondence of the PBL peaks in LD and SD supports the conjecture that the onset of illumination, rather than the onset of darkness, serves as the primary zeitgeber for the daily PBL rhythm.

A robust daily rhythm in sickness responses to LPS was identified in LD, but not SD. This indicates that the time of day at which LPS is recognized by the immune system impacts symptom severity for days to come, well after the insult itself has passed. Acute anorexia was greatest in LD hamsters receiving LPS at ZT 4.5 (~90% inhibition of food intake on day +1) and least severe at ZT 16.5, (~55% inhibition). LPS inhibits food intake via stimulation of vagal afferents, and also through cytokine signaling to the brain (Konsman & Dantzer 2001) which ultimately upregulates expression of hypothalamic anorexigenic neuropeptides (e.g., proopiomelanocortin; (Asarian & Langhans 2010). It is not clear from these data whether the daily rhythm in anorexia is a consequence of circadian modulation of cytokine responses, as has been described *in vitro* and *in vivo* (Gibbs et al 2012b, Marpegan et al 2009), or arises as a result of time constraints on peripherally-derived anorexic signals reaching food intake and satiety centers of the hypothalamus, or a combination of these processes. Hamsters in LD accomplish the majority (~60%) of their daily food intake during the 9 h dark phase (Prendergast & Bradley, unpublished data). A lag, or hysteresis, of just a few hours between LPS treatment and the onset of anorexia would be sufficient for a ZT 16.5 injection to effectively miss the majority of the day +1 nocturnal feeding interval. In contrast, LPS at ZT 4.5 would be better positioned in time to engage an anorexic state in advance of this feeding interval. Lethargic responses were also more severe in female Siberian hamsters challenged during the early light phase as compared to those treated in the early evening (Prendergast et al 2015). We are unaware of reports that have documented daily rhythms in anorexia with the resolution reported here, but the present

behavioral data resonate with the identification of greater cytokine responses, lethargy and mortality in male mice challenged with septic doses of LPS at ZT 11 than at ZT 19 (Marpegan et al 2009).

Lastly, T cell-dependent adaptive inflammatory responses (DTH reactions) were greater in SD than LD (Fig. 10). Sensitization time did not affect DTH magnitude; this allowed inferences to be made from the use of a single sensitization phase (mid-day) across all photoperiod and challenge ZT groups. In common with experiments 1 and 2, no circadian phase alignment eliminated the effects of photoperiod on DTH. DTH did, however, exhibit robust diurnal modulation in LD hamsters, and a more complex waveform (2 sines) was fitted to the AUC_{DTH} in SD. In LD hamsters, DTH_{AUC} was ~10 fold higher at ZT 7.5 relative to ZT 19.5, similar in waveform to the daily rhythm in DTH to oxazolone described in male rats, but greater in amplitude (Pownall et al 1979). DTH skin inflammatory responses require priming and clonal expansion of antigen-specific T cells by antigen presenting cells in the draining lymph nodes. The factors that determine the strength of this T cell response are not fully understood, but require recognition of MHC-bound antigen fragments by the T cell receptor (TCR; (Esser et al 2014, Sewell 2012)). TCR-dependent intracellular signaling and T cell-dependent integrative organismal immune responses in male C57BL6/J mice exhibit clear circadian rhythms (Fortier et al 2011), but whether daily changes in T cell responses alone account for the DTH rhythms described here is not known.

Photoperiod-driven changes in circadian waveforms are well-documented (Pittendrigh & Daan 1976a). Adaptation to long and short days alters the locomotor activity waveform of nocturnal rodents (Pittendrigh & Daan 1976a); including Siberian hamsters (Prendergast et al 2013), SCN neurophysiology (Margraf & Lynch 1993), neuroendocrine function (Sumova et al

1995) and patterns of gene expression (Johnston et al 2005, Nuesslein-Hildesheim et al 2000, Yan & Silver 2008). Photoperiod alters organismal-level circadian rhythms in behavior and endocrine function by altering interactions among components of the SCN oscillator network (Evans et al 2013, Evans et al 2015). The present data extend this observation to multiple, distinct aspects of immune function. Following adaptation to short days, the amplitude of the PBL rhythm increased, diurnal rhythms in the anorexic response to LPS became undetectable, and the DTH response developed a more complex daily waveform. Together the data indicate that changes in pacemaker waveform that occur in the CNS are paralleled by seasonal changes in the immune system.

The clinical relevance of photoperiodic changes in the immune system is not well-established. Predictable seasonal variations in disease prevalence and severity manifest in humans and in non-human animals (Fisman 2007, Martinez-Bakker & Helm 2015; Stevenson et al. 2015), and the human immune system exhibits widespread seasonal transcriptomic changes (Dopico et al. 2015). But the extent to which seasonal patterns of human immune activity reflect interactions among: [1] masking responses to environmentally-driven cycles (e.g., allergens, parasite activity), [2] endogenous self-sustained host circannual rhythms, and [3] photoperiod-driven changes in host immune activity, is not well-understood. A better understanding of neuroimmune mechanisms exhibited by highly seasonal species may, in turn, afford insights into the proximate factors that generate human seasonal rhythms in health and disease.

In summary, we documented striking changes in the waveforms of daily rhythms in constitutive, innate and adaptive immune function following adaptation to seasonal changes in day length. Photoperiod effects on immune function did not depend on a specific phase alignment to manifest. Conversely, for all immunological traits, and under all alignment

schemes, there existed times of day when LD and SD hamsters were indistinguishable from one another, unlike the more categorical seasonal phenotypes evident in body fat and reproductive state. These data are nevertheless consistent with the conclusion that photoperiodic immunophenotypes do not merely reflect circadian phase realignments, but rather are instantiated by long-term changes in the physiological set points around which those oscillations occur. Seasonal changes in biology are seldom sampled at more than one phase of the circadian cycle. The high-frequency sampling approach described here may be useful in characterizing how seasonal and circadian timescales interact to affect physiology.

Chapter 7: General Discussion

Here I plan to summarize the main findings of each Chapter, integrate these data to provide general insights on transkingdom interactions that influence behavior across the lifespan, and provide future directions of this body of work.

The gut microbiota plays important roles in digestion, metabolism and immune function (Belkaid & Hand 2014, Nicholson et al 2012), all of which exhibit circadian periodicity (Panda 2016, Scheiermann et al 2013). The mammalian circadian network consists of rhythmic structures in the brain and periphery interacting to sustain organismal-level rhythms. Billions of potential autonomous oscillators reside in microbes throughout the body, but their contribution to generation and entrainment of mammalian behavioral and thermoregulatory circadian rhythms remains unknown. In Chapter 3, the role of microbiota on host circadian rhythms in locomotor activity and temperature was examined. Germ free (GF) mice lacking gut microbiota exhibit altered circadian rhythms compared to normal, bacterially replete SPF mice under photocyclic and constant darkness conditions. Additionally, GF mice display lower amplitude circadian rhythms, quantified by shifts in the daily activity waveform following timed feeding compared to normal. In theory, lower amplitude oscillators shift more quickly in response to external perturbations. Estimates suggest the human body harbors a nearly equal ratio of microbe to host cells (Sender et al 2016). While characterization of circadian rhythms of the majority of microbial species housed in the intestinal tract have not been defined, some such as cyanobacteria have shown to possess a 24-hour period (Paranjpe & Sharma 2005). If other bacterial species also possess a 24 hour circadian rhythm, these signals may be integrated to the organismal circadian network; the results from Chapter 3 support this inference, as the absence of microbiota resulted in altered circadian rhythms in GF mice, and microbiota reconstitution of

GF mice restored circadian phenotypes to SPF levels in ex-GF mice, showing microbiota as sufficient to restoring normal circadian rhythms. Together, these data identify fundamental contributions of the microbiota towards promoting circadian network coherence despite environmental challenges.

Future studies can examine the mechanisms by which gut microbiota influence circadian rhythms. Communication from the enteric nervous system that lines the gastrointestinal system to the brain via the vagus nerve is one pathway worth exploring. In order to test the hypothesis that the signal from microbiota are communicated to the central nervous system and, in turn, the suprachiasmatic nucleus of the hypothalamus, a subdiaphragmatic vagotomy (SDx) could be performed in ex-GF mice prior to reconstitution with normal, SPF cecal contents. Circadian phenotypes could be examined in SPF mice, GF mice, ex-GF mice, and ex-GF-SDx mice. If similar chronotypes are observed in GF and ex-GF-SDx mice, these results would suggest that the vagus nerve is a necessary mode of communication between the gastrointestinal tract and the circadian network. If similar circadian rhythms are seen in SPF, ex-GF, and ex-GF-SDx mice, this would support the hypothesis that the vagus nerve is not a necessary communication pathway in which microbiota influence circadian rhythms. In addition to the vagus nerve, signals from the microbiota-containing gastrointestinal tract can be transmitted to the brain by means of neural, endocrine, immune, and humoral links. Isolation and administration of single or group of signaling molecules from the aforementioned systems may contribute to the altered circadian rhythms in GF mice compared to SPF and ex-GF mice.

There may be a sensitive period in which the introduction of gut microbiota in GF mice can reversibly change circadian rhythms to match SPF values. Similar to previous reports (Sudo et al 2004) on the influence of microbiota on physiology, where GF mice show an exaggerated

HPA-axis response in a restraint stress test compared to SPF mice when inoculation occurred at 6 weeks of age, but not at 14 weeks of age. Reintroduction of showed a similar reversible effect on behavior, where ex-GF mice in Chapter 3 were introduced to SPF cecal contents at 12 to 19 weeks of age. Examining the presence of a sensitive period in which introduction of SPF cecal contents could be completed at different ages. Introduction of SPF cecal contents to GF mice at 4, 6, 12, 18, or 24 months of age would allow examination of a sensitive period of microbiota to influence circadian rhythms. While comparing ex-GF mice to age-matched GF and SPF mice would allow us to determine if there is a sensitive period for microbiota to influence circadian rhythms in the murine model lifespan.

Logical extensions of the current report may explore sex differences in germ free female and male mice. Male biased studies where only males are included in their report outnumber female-only studies 5.5 to 1 (Beery & Zucker 2011). Due to breeding constraints, the current GF mice in Chapters 3 and 4 only allowed the study of male mice. Sex differences are well-defined in rodent models, with many of these differences hormone-dependent (Blattner & Mahoney 2014, Hsu et al 2010, Krizo & Mintz 2014). Future endeavors could examine the interacting effects of sex and microbiota on circadian rhythms.

Other future studies could examine the role of matching circadian rhythms of host and microbes on Darwinian fitness. Convergent evolution has shown circadian rhythms are present in organisms across kingdoms, from bacteria to mammalian species (Paranjpe & Sharma 2005). Given the symbiotic relationship developed between bacteria and mammals over evolutionary time and the importance of circadian rhythms in Darwinian fitness, a stable phase relationship between the mammalian host and intestinal microbes may benefit both symbionts. To test the hypothesis that microbiota and host organisms with the same tau (τ) contribute to Darwinian

fitness, the colonization of a GF mice via mono-association of a single cyanobacterial species with tau (τ) lengths of 22, 24, or 28 hours (Ouyang et al 1998) into a wild type mouse with a 24 hour tau (τ), then longevity of each group documented. Circadian clock with periods that do not match their environment have negative consequences for fitness (Ouyang et al 1998, Spoelstra et al 2016). If there are no differences in the survival curves of mice containing bacteria with a 22, 24, or 28 hour tau (τ), this would suggest that matching rhythms in microbe and host are not involved in fitness. If a survival curve shows that ex-GF mice monoassociated with cyanobacteria with a 22 or 28 hour tau (τ) live shorter lives than mice inoculated with a 24 hour tau (τ), suggests that circadian rhythms of similar lengths in both the host and microbes are important for host fitness.

High fat diet (HFD) can have profound effects on immune function, metabolism, and digestion. Further, HFD can quickly alter microbiota populations (Leone et al 2015). Previous publications have reported circadian rhythms in HFD-fed mice (Kohsaka et al 2007, Mendoza et al 2008, Pendergast et al 2013, Yokoyama et al 2020), though the influence of HFD on circadian rhythms has not been examined in GF mice. Chapter 4 examined if HFD acts directly on the host or the effects of HFD are mediated by gut microbiota. In the current experiments, both SPF and GF mice fed HFD showed changes in circadian rhythms compared to mice fed a normal chow (NC). These results indicate that the effects of HFD can manifest independent of gut microbiota. Similar to the aforementioned proposed studies to examine the effects of microbiota on host circadian rhythms, future studies can include SDx manipulations to examine the role of the vagus nerve in HFD-induced changes in circadian rhythms, HFD introduction at different ages to explore sensitive periods for effects of HFD on circadian rhythms, and sex differences in HFD-fed mice in both male and females. Further, an elemental diet of a single or group of

carbohydrate or protein molecules could narrow down the contributing effects of specific molecules to behavioral rhythms if soluble mediators are contributing to the HFD-induced changes in circadian rhythms.

Epidemiological data reveal a positive correlation of maternal levels of proinflammatory cytokines IL-8 and TNFα with neurodevelopmental disorders (Brown et al 2004, Buka et al 2001). Indeed, environmental fetal programming is known to alter early fetal brain development and increase risk of ASD (Atladottir et al 2010, Jiang et al 2016, Lee et al 2015). Further, aberrant circadian rhythms are comorbid in ASD patients (Luciana et al 2019) and may be involved in the development of this disorder (Missig et al 2020, Wintler et al 2020). Maternal immune activation (MIA) has been shown to alter behavior as well as disrupt neural development in the cortex and lower brain regions in offspring (Garay et al 2013). The changes in freely-behaving, rhythmic behavior resulting from MIA's neurodevelopmental disruptions had not been documented. In Chapter 5, circadian rhythms of offspring born of pregnant females exposed to MIA were compared to mice born of females injected with 0.9% saline. MIA had no effects on circadian rhythms. However, differences in mouse vendor, known for their differential expression of intestinal microbe SFB, influenced both activity and the speed of the endogenous clock, tau (τ). Differences in vendors that are known for their differential expression of intestinal microbe SFB influenced both activity and the speed of the endogenous clock, tau (τ). Future directions investigating which commensal microbes (i.e., SFBs) influence circadian rhythms could be completed by monoassociation studies in GF mice, to determine specific bacterial species that influence the circadian network. Further, dissection of the differences between mice obtained from Jackson Laboratories (JAX) or Taconic Biosciences (Tac) may also elucidate differences observed in circadian rhythms between these mice. Further work to examine

circadian rhythms in MIA offspring may introduce different immunogenic molecules that bind to different toll-like receptors (e.g., lipopolysaccharide or parasite) with higher doses at difference stages of development of female gestation (e.g., embryonic day 9.5). As previous reports have observed differences in MIA and control offspring circadian rhythms using running wheel data (Delorme et al 2021), it may be worth exploring different methods of recording locomotor activity (e.g., telemetry, beam breaks, or running wheels) in offspring mice for future experiments.

Circannual and circadian timescales interact to produce trait-specific photoperiodic alterations in immune function (Onishi et al 2020). There exist robust daily rhythms in immune function in mammals, as the immune system is primed to mount an optimal immune response at a time-of-day (Scheiermann et al 2018, Scheiermann et al 2013). Additionally, photoperiodic changes in the immune system of Siberian hamsters have been well-documented: short day (SD) hamsters show attenuated innate immune response to LPS and augmented immune response to DNFB, compared to LD hamsters (Bilbo et al 2002b, Nelson & Demas 1996, Prendergast et al 2004, Stevenson & Prendergast 2015). However, the interaction between annual and daily waveforms in immune function have not been examined. For any trait that changes over the course of the day, comparisons between different daylengths are complicated by phase alignment, as circadian phase cannot be perfectly equated across different photoperiods. In Chapter 6, data support previous publications of photoperiodic changes in immune function (Bilbo et al 2002b, Nelson & Demas 1996, Prendergast et al 2004, Stevenson & Prendergast 2015), while extending these seasonal differences to persist in any phase alignment. Chapter 6 includes only male Siberian hamsters (Onishi et al 2020), and female Siberian hamsters should

be included in future reports. Additionally, studies could examine the effects of photoperiodic and circadian responses to viral mimics or parasites.

Together, the data presented in this program show transkingdom interactions – commensal gut microbiota and host behavior, as well as pathogenic immunogens and host immune response – influence behavior across the lifespan.

References

Actor JK, Ampel NM. 2009. Hypersensitivity: T Lymphocyte-mediated (Type IV). *eLS*

AL-Ayadhi LY, Mostafa GA. 2012. Elevated serum levels of interleukin-17A in children with autism. *J Neuroinflamm* 9

Albers HE. 1981. Gonadal hormones organize and modulate the circadian system of the rat. *Am J Physiol* 241: R62-6

Albrecht U. 2012. Timing to perfection: the biology of central and peripheral circadian clocks. *Neuron* 74: 246-60

Alesci S, Martinez PE, Kelkar S, Ilias I, Ronsaville DS, et al. 2005. Major depression is associated with significant diurnal elevations in plasma interleukin-6 levels, a shift of its circadian rhythm, and loss of physiological complexity in its secretion: clinical implications. *J Clin Endocrinol Metab* 90: 2522-30

Anforth HR, Bluthe RM, Bristow A, Hopkins S, Lenczowski MJP, et al. 1998. *Biological activity and brain actions of recombinant rat interleukin-1 alpha and interleukin-1 beta*. 279-88 pp.

APA. 2013. Diagnostic and statistical manual of mental disorders (5th ed.).

Arendt J. 2010. Shift work: coping with the biological clock. *Occup Med (Lond)* 60: 10-20

Arpaia N, Campbell C, Fan X, Dikiy S, van der Veeken J, et al. 2013. Metabolites produced by commensal bacteria promote peripheral regulatory T-cell generation. *Nature* 504: 451-5

Asarian L, Langhans W. 2010. A new look on brain mechanisms of acute illness anorexia. *Physiol Behav* 100: 464-71

Atarashi K, Tanoue T, Ando M, Kamada N, Nagano Y, et al. 2015. Th17 Cell Induction by Adhesion of Microbes to Intestinal Epithelial Cells. *Cell* 163: 367-80

Atladottir HO, Thorsen P, Ostergaard L, Schendel DE, Lemcke S, et al. 2010. Maternal infection requiring hospitalization during pregnancy and autism spectrum disorders. *J Autism Dev Disord* 40: 1423-30

Bäckhed F, Ding H, Wang T, Hooper LV, Koh GY, et al. 2004. The gut microbiota as an environmental factor that regulates fat storage. *Proceedings of the National Academy of Sciences of the United States of America* 101: 15718-23

Backhed F, Manchester JK, Semenkovich CF, Gordon JI. 2007. Mechanisms underlying the resistance to diet-induced obesity in germ-free mice. *Proc Natl Acad Sci U S A* 104: 979-84

Baillie SR, Prendergast BJ. 2008. Photoperiodic regulation of behavioral responses to bacterial and viral mimetics: a test of the winter immunoenhancement hypothesis. *J Biol Rhythms* 23: 81-90

Baldridge MT, Nice TJ, McCune BT, Yokoyama CC, Kambal A, et al. 2015. Commensal microbes and interferon-lambda determine persistence of enteric murine norovirus infection. *Science* 347: 266-9

Balmer ML, Schurch CM, Saito Y, Geuking MB, Li H, et al. 2014. Microbiota-derived compounds drive steady-state granulopoiesis via MyD88/TICAM signaling. *J Immunol* 193: 5273-83

Balsalobre A, Brown SA, Marcacci L, Tronche F, Kellendonk C, et al. 2000. Resetting of circadian time in peripheral tissues by glucocorticoid signaling. *Science* 289: 2344-7

Banchereau J, Briere F, Caux C, Davoust J, Lebecque S, et al. 2000. Immunobiology of dendritic cells. *Annu Rev Immunol* 18: 767-811

Banks WA. 2009. The blood-brain barrier in psychoneuroimmunology. *Immunol Allergy Clin North Am* 29: 223-8

Barajon I, Serrao G, Arnaboldi F, Opizzi E, Ripamonti G, et al. 2009. Toll-like receptors 3, 4, and 7 are expressed in the enteric nervous system and dorsal root ganglia. *J Histochem Cytochem* 57: 1013-23

Barrett E, Ross RP, O'Toole PW, Fitzgerald GF, Stanton C. 2012. gamma-Aminobutyric acid production by culturable bacteria from the human intestine. *J Appl Microbiol* 113: 411-7

Bartness TJ, Song CK, Demas GE. 2001. SCN efferents to peripheral tissues: implications for biological rhythms. *J Biol Rhythms* 16: 196-204

Bateson P, Gluckman P, Hanson M. 2014. The biology of developmental plasticity and the Predictive Adaptive Response hypothesis. *J Physiol* 592: 2357-68

Beery AK, Zucker I. 2011. Sex bias in neuroscience and biomedical research. *Neurosci Biobehav Rev* 35: 565-72

Bel S, Hooper LV. 2015. Immunology: A bacterial nudge to T-cell function. *Nature* 526: 328-30

Belkaid Y, Hand TW. 2014. Role of the microbiota in immunity and inflammation. *Cell* 157: 121-41

Benveniste J, Lespinats G, Adam C, Salomon JC. 1971. Immunoglobulins in intact, immunized, and contaminated axenic mice: study of serum IgA. *J Immunol* 107: 1647-55

Bercik P, Denou E, Collins J, Jackson W, Lu J, et al. 2011a. The intestinal microbiota affect central levels of brain-derived neurotropic factor and behavior in mice. *Gastroenterology* 141: 599-609, 09 e1-3

Bercik P, Park AJ, Sinclair D, Khoshdel A, Lu J, et al. 2011b. The anxiolytic effect of Bifidobacterium longum NCC3001 involves vagal pathways for gut-brain communication. *Neurogastroenterol Motil* 23: 1132-9

Bilbo SD, Dhabhar FS, Viswanathan K, Saul A, Yellon SM, Nelson RJ. 2002a. Short day lengths augment stress-induced leukocyte trafficking and stress-induced enhancement of skin immune function. *Proc Natl Acad Sci U S A* 99: 4067-72

Bilbo SD, Drazen DL, Quan N, He L, Nelson RJ. 2002b. Short day lengths attenuate the symptoms of infection in Siberian hamsters. *Proc Biol Sci* 269: 447-54

Bilbo SD, Schwarz JM. 2012. The immune system and developmental programming of brain and behavior. *Front Neuroendocrinol* 33: 267-86

Blattner MS, Mahoney MM. 2014. Estrogen receptor 1 modulates circadian rhythms in adult female mice. *Chronobiology International* 31: 637-44

Bluthé RM, Walter V, Parnet P, Layé S, Lestage J, et al. 1994. Lipopolysaccharide induces sickness behaviour in rats by a vagal mediated mechanism. *Comptes Rendus De L'academie Des Sciences. Serie III, Sciences De La Vie* 317: 499-503

Boitard C, Etchamendy N, Sauvant J, Aubert A, Tronel S, et al. 2012. Juvenile, but not adult exposure to high-fat diet impairs relational memory and hippocampal neurogenesis in mice. *Hippocampus* 22: 2095-100

Boksa P. 2010. Effects of prenatal infection on brain development and behavior: a review of findings from animal models. *Brain Behav Immun* 24: 881-97

Born J, Lange T, Hansen K, Molle M, Fehm HL. 1997. Effects of sleep and circadian rhythm on human circulating immune cells. *J Immunol* 158: 4454-64

Bravo JA, Forsythe P, Chew MV, Escaravage E, Savignac HM, et al. 2011. Ingestion of Lactobacillus strain regulates emotional behavior and central GABA receptor expression in a mouse via the vagus nerve. *Proc Natl Acad Sci U S A* 108: 16050-5

Brown AS, Hooton J, Schaefer CA, Zhang H, Petkova E, et al. 2004. Elevated maternal interleukin-8 levels and risk of schizophrenia in adult offspring. *Am J Psychiatry* 161: 889-95

Brown MB, von Chamier M, Allam AB, Reyes L. 2014. M1/M2 macrophage polarity in normal and complicated pregnancy. *Front Immunol* 5: 606

Brown SA, Zumbrunn G, Fleury-Olela F, Preitner N, Schibler U. 2002. Rhythms of Mammalian Body Temperature Can Sustain Peripheral Circadian Clocks. *Current Biology* 12: 1574-83

Brun P, Giron MC, Qesari M, Porzionato A, Caputi V, et al. 2013. Toll-like receptor 2 regulates intestinal inflammation by controlling integrity of the enteric nervous system. *Gastroenterology* 145: 1323-33

Buffington SA, Di Prisco GV, Auchtung TA, Ajami NJ, Petrosino JF, Costa-Mattioli M. 2016. Microbial Reconstitution Reverses Maternal Diet-Induced Social and Synaptic Deficits in Offspring. *Cell* 165: 1762-75

Buka SL, Tsuang MT, Torrey EF, Klebanoff MA, Wagner RL, Yolken RH. 2001. Maternal Cytokine Levels during Pregnancy and Adult Psychosis. *Brain, Behavior, and Immunity* 15: 411-20

Butler MP, Karatsoreos IN, LeSauter J, Silver R. 2012. Dose-dependent effects of androgens on the circadian timing system and its response to light. *Endocrinology* 153: 2344-52

Camerini V, Panwala C, Kronenberg M. 1993. Regional specialization of the mucosal immune system. Intraepithelial lymphocytes of the large intestine have a different phenotype and function than those of the small intestine. *The Journal of Immunology* 151: 1765-76

Cani PD, Amar J, Iglesias MA, Poggi M, Knauf C, et al. 2007. Metabolic endotoxemia initiates obesity and insulin resistance. *Diabetes* 56: 1761-72

Cani PD, Bibiloni R, Knauf C, Waget A, Neyrinck AM, et al. 2008. Changes in gut microbiota control metabolic endotoxemia-induced inflammation in high-fat diet-induced obesity and diabetes in mice. *Diabetes* 57: 1470-81

Cani PD, Knauf C, Iglesias MA, Drucker DJ, Delzenne NM, Burcelin R. 2006. Improvement of glucose tolerance and hepatic insulin sensitivity by oligofructose requires a functional glucagon-like peptide 1 receptor. *Diabetes* 55: 1484-90

Cannon WB. 1929. Organization for Physiological Homeostasis. *Physiological Reviews* 9: 399-431

Cantarel BL, Lombard V, Henrissat B. 2012. Complex carbohydrate utilization by the healthy human microbiome. *PLoS One* 7: e28742

Careaga M, Taylor SL, Chang C, Chiang A, Ku KM, et al. 2018. Variability in PolyIC induced immune response: Implications for preclinical maternal immune activation models. *J Neuroimmunol* 323: 87-93

Challet E. 2019. The circadian regulation of food intake. *Nat Rev Endocrinol* 15: 393-405

Choi GB, Yim YS, Wong H, Kim S, Kim H, et al. 2016. The maternal interleukin-17a pathway in mice promotes autism-like phenotypes in offspring. *Science* 351: 933-9

Clarke G, Grenham S, Scully P, Fitzgerald P, Moloney RD, et al. 2013. The microbiome-gut-brain axis during early life regulates the hippocampal serotonergic system in a sex-dependent manner. *Mol Psychiatry* 18: 666-73

Costedio MM, Hyman N, Mawe GM. 2007. Serotonin and its role in colonic function and in gastrointestinal disorders. *Dis Colon Rectum* 50: 376-88

Couturier JL, Speechley KN, Steele M, Norman R, Stringer B, Nicolson R. 2005. Parental perception of sleep problems in children of normal intelligence with pervasive developmental disorders: prevalence, severity, and pattern. *J Am Acad Child Adolesc Psychiatry* 44: 815-22

Daan S, Damassa D, Pittendrigh CS, Smith ER. 1975. An effect of castration and testosterone replacement on a circadian pacemaker in mice (Mus musculus). *Proc Natl Acad Sci U S A* 72: 3744-7

Daan S, Pittendrigh CS. 1976. A Functional analysis of circadian pacemakers in nocturnal rodents. II. Variability of phase response curves. *Journal of comparative physiology* 106: 253-66

Dahlgren J, Samuelsson AM, Jansson T, Holmang A. 2006. Interleukin-6 in the maternal circulation reaches the rat fetus in mid-gestation. *Pediatr Res* 60: 147-51

Dantzer R, Kelley KW. 2007. Twenty years of research on cytokine-induced sickness behavior. *Brain Behav Immun* 21: 153-60

Dantzer R, O'Connor JC, Freund GG, Johnson RW, Kelley KW. 2008. From inflammation to sickness and depression: when the immune system subjugates the brain. *Nat Rev Neurosci* 9: 46-56

Davidson AJ, Poole AS, Yamazaki S, Menaker M. 2003. Is the food-entrainable circadian oscillator in the digestive system? *Genes Brain Behav* 2: 32-9

Davis JO, Phelps JA, Bracha HS. 1995. Prenatal development of monozygotic twins and concordance for schizophrenia. *Schizophr Bull* 21: 357-66

de Lartigue G, de La Serre CB, Raybould HE. 2011. Vagal afferent neurons in high fat diet-induced obesity; intestinal microflora, gut inflammation and cholecystokinin. *Physiol Behav* 105: 100-5

Del Olmo N, Ruiz-Gayo M. 2018. Influence of High-Fat Diets Consumed During the Juvenile Period on Hippocampal Morphology and Function. *Front Cell Neurosci* 12: 439

Delorme TC, Srivastava LK, Cermakian N. 2021. Altered circadian rhythms in a mouse model of neurodevelopmental disorders based on prenatal maternal immune activation. *Brain Behav Immun*

Demas GE, Chefer V, Talan MI, Nelson RJ. 1997. Metabolic costs of mounting an antigen-stimulated immune response in adult and aged C57BL/6J mice. *Am J Physiol* 273: R1631-7

Depres-Brummer P, Bourin P, Pages N, Metzger G, Levi F. 1997. Persistent T lymphocyte rhythms despite suppressed circadian clock outputs in rats. *Am J Physiol-Reg I* 273: R1891-R99

Derecki NC, Cardani AN, Yang CH, Quinnies KM, Crihfield A, et al. 2010. Regulation of learning and memory by meningeal immunity: a key role for IL-4. *J Exp Med* 207: 1067-80

Desai MS, Seekatz AM, Koropatkin NM, Kamada N, Hickey CA, et al. 2016. A Dietary Fiber-Deprived Gut Microbiota Degrades the Colonic Mucus Barrier and Enhances Pathogen Susceptibility. *Cell* 167: 1339-53 e21

Dhabhar FS, Miller AH, McEwen BS, Spencer RL. 1995. Effects of stress on immune cell distribution. Dynamics and hormonal mechanisms. *J Immunol* 154: 5511-27

Dhabhar FS, Miller AH, Stein M, McEwen BS, Spencer RL. 1994. Diurnal and acute stress-induced changes in distribution of peripheral blood leukocyte subpopulations. *Brain Behav Immun* 8: 66-79

Diaz Heijtz R, Wang S, Anuar F, Qian Y, Bjorkholm B, et al. 2011. Normal gut microbiota modulates brain development and behavior. *Proc Natl Acad Sci U S A* 108: 3047-52

Dimitrov S, Benedict C, Heutling D, Westermann J, Born J, Lange T. 2009. Cortisol and epinephrine control opposing circadian rhythms in T cell subsets. *Blood* 113: 5134-43

DuBois EF. 1921. The Basal Metabolism in Fever. *JAMA: The Journal of the American Medical Association* 77: 352-57

Eckburg PB, Bik EM, Bernstein CN, Purdom E, Dethlefsen L, et al. 2005. Diversity of the human intestinal microbial flora. *Science* 308: 1635-8

Eelderink-Chen Z, Bosman J, Sartor F, Dodd AN, Kovacs AT, Merrow M. 2021. A circadian clock in a nonphotosynthetic prokaryote. *Sci Adv* 7

Eilam O, Zarecki R, Oberhardt M, Ursell LK, Kupiec M, et al. 2014. Glycan degradation (GlyDeR) analysis predicts mammalian gut microbiota abundance and host diet-specific adaptations. *MBio* 5

Elliott JA, Tamarkin L. 1994. Complex circadian regulation of pineal melatonin and wheel-running in Syrian hamsters. *J Comp Physiol A* 174: 469-84

Erny D, Hrabe de Angelis AL, Jaitin D, Wieghofer P, Staszewski O, et al. 2015. Host microbiota constantly control maturation and function of microglia in the CNS. *Nat Neurosci* 18: 965-77

Esser PR, Kimber I, Martin SF. 2014. Correlation of contact sensitizer potency with T cell frequency and TCR repertoire diversity. *Experientia supplementum (2012)* 104: 101-14

Estes ML, McAllister AK. 2016. Maternal immune activation: Implications for neuropsychiatric disorders. *Science* 353: 772-7

Evans JA, Elliott JA, Gorman MR. 2007. Circadian effects of light no brighter than moonlight. *J Biol Rhythms* 22: 356-67

Evans JA, Elliott JA, Gorman MR. 2012. Individual differences in circadian waveform of Siberian hamsters under multiple lighting conditions. *J Biol Rhythms* 27: 410-9

Evans JA, Leise TL, Castanon-Cervantes O, Davidson AJ. 2011. Intrinsic regulation of spatiotemporal organization within the suprachiasmatic nucleus. *PLoS One* 6: e15869

Evans JA, Leise TL, Castanon-Cervantes O, Davidson AJ. 2013. Dynamic interactions mediated by nonredundant signaling mechanisms couple circadian clock neurons. *Neuron* 80: 973-83

Evans JA, Suen TC, Callif BL, Mitchell AS, Castanon-Cervantes O, et al. 2015. Shell neurons of the master circadian clock coordinate the phase of tissue clocks throughout the brain and body. *BMC Biol* 13: 43

Exton MS. 1997. Infection-induced anorexia: active host defence strategy. *Appetite* 29: 369-83

Feillet CA, Ripperger JA, Magnone MC, Dulloo A, Albrecht U, Challet E. 2006. Lack of food anticipation in Per2 mutant mice. *Curr Biol* 16: 2016-22

Fisher RE, Steele M, Karrow NA. 2012. Fetal programming of the neuroendocrine-immune system and metabolic disease. *J Pregnancy* 2012: 792934

Follett BK. 2015. "Seasonal changes in the neuroendocrine system": some reflections. *Front Neuroendocrinol* 37: 3-12

Fortier EE, Rooney J, Dardente H, Hardy MP, Labrecque N, Cermakian N. 2011. Circadian variation of the response of T cells to antigen. *J Immunol* 187: 6291-300

Franklin AE, Engeland CG, Kavaliers M, Ossenkopp KP. 2007. The rate of behavioral tolerance development to repeated lipopolysaccharide treatments depends upon the time of injection during the light-dark cycle: a multivariable examination of locomotor activity. *Behav Brain Res* 180: 161-73

Freedman MS, Lucas RJ, Soni B, von Schantz M, Munoz M, et al. 1999. Regulation of mammalian circadian behavior by non-rod, non-cone, ocular photoreceptors. *Science* 284: 502-4

Freeman DA, Teubner BJ, Smith CD, Prendergast BJ. 2007. Exogenous T3 mimics long day lengths in Siberian hamsters. *Am J Physiol Regul Integr Comp Physiol* 292: R2368-72

Friedman JM, Halaas JL. 1998. Leptin and the regulation of body weight in mammals. *Nature* 395: 763-70

Fuller PM, Lu J, Saper CB. 2008. Differential rescue of light- and food-entrainable circadian rhythms. *Science* 320: 1074-7

Furness JB, Rivera LR, Cho HJ, Bravo DM, Callaghan B. 2013. The gut as a sensory organ. *Nat Rev Gastroenterol Hepatol* 10: 729-40

Gao Z, Yin J, Zhang J, Ward RE, Martin RJ, et al. 2009. Butyrate improves insulin sensitivity and increases energy expenditure in mice. *Diabetes* 58: 1509-17

Garay PA, Hsiao EY, Patterson PH, McAllister AK. 2013. Maternal immune activation causes age- and region-specific changes in brain cytokines in offspring throughout development. *Brain Behav Immun* 31: 54-68

Gaspari AA, Katz SI, Martin SF. 2016. Contact Hypersensitivity. *Current Protocols in Immunology* 113: 4.2.1-4.2.7

Gibbs JE, Blaikley J, Beesley S, Matthews L, Simpson KD, et al. 2012a. The nuclear receptor REV-ERBalpha mediates circadian regulation of innate immunity through selective regulation of inflammatory cytokines. *Proc Natl Acad Sci U S A* 109: 582-7

Gibbs JE, Blaikley J, Beesley S, Matthews L, Simpson KD, et al. 2012b. The nuclear receptor REV-ERBα mediates circadian regulation of innate immunity through selective regulation of inflammatory cytokines. *Proceedings of the National Academy of Sciences* 109: 582-87

Giulian D YD, Woodward J, Brown DC, Lachman LB. 1988. Interleukin-1 is an astroglial growth factor in the developing brain. *Journal of Neuroscience*: 709-14

Gorman MR, Zucker I. 1995. Testicular Regression and Recrudescence without Subsequent Photorefractoriness in Siberian Hamsters. *Am J Physiol-Reg I* 269: R800-R06

Goto M, Oshima I, Tomita T, Ebihara S. 1989. Melatonin content of the pineal gland in different mouse strains. *J Pineal Res* 7: 195-204

Gray D. 2002. A role for antigen in the maintenance of immunological memory. *Nat Rev Immunol* 2: 60-5

Griffiths EA, Duffy LC, Schanbacher FL, Qiao H, Dryja D, et al. 2004. In vivo effects of bifidobacteria and lactoferrin on gut endotoxin concentration and mucosal immunity in Balb/c mice. *Dig Dis Sci* 49: 579-89

Guerin LR, Prins JR, Robertson SA. 2009. Regulatory T-cells and immune tolerance in pregnancy: a new target for infertility treatment? *Hum Reprod Update* 15: 517-35

Haghikia A, Jorg S, Duscha A, Berg J, Manzel A, et al. 2015. Dietary Fatty Acids Directly Impact Central Nervous System Autoimmunity via the Small Intestine. *Immunity* 43: 817-29

Hansson GC. 2012. Role of mucus layers in gut infection and inflammation. *Curr Opin Microbiol* 15: 57-62

Harris MA, Reddy CA, Carter GR. 1976. Anaerobic bacteria from the large intestine of mice. *Appl Environ Microbiol* 31: 907-12

Hart BL. 1988. Biological basis of the behavior of sick animals. *Neurosci Biobehav Rev* 12: 123-37

Hart BL. 2011. Behavioural defences in animals against pathogens and parasites: parallels with the pillars of medicine in humans. *Philos Trans R Soc Lond B Biol Sci* 366: 3406-17

Hastings M. 2001. Modeling the molecular calendar. *J Biol Rhythms* 16: 117-23

Hatori M, Vollmers C, Zarrinpar A, DiTacchio L, Bushong EA, et al. 2012. Time-restricted feeding without reducing caloric intake prevents metabolic diseases in mice fed a high-fat diet. *Cell Metab* 15: 848-60

He B, Hoang TK, Wang T, Ferris M, Taylor CM, et al. 2017. Resetting microbiota by Lactobacillus reuteri inhibits T reg deficiency-induced autoimmunity via adenosine A2A receptors. *J Exp Med* 214: 107-23

Heldmaier G, Steinlechner S, Rafael J. 1982. Nonshivering thermogenesis and cold resistance during seasonal acclimatization in the Djungarian hamster. *Journal of comparative physiology* 149: 1-9

Hendrickson A, Boothe R. 1976. Morphology of the retina and dorsal lateral geniculate nucleus in dark-reared monkeys (Macaca nemestrina). *Vision Res* 16: 517-21

Honda K, Takeda K. 2009. Regulatory mechanisms of immune responses to intestinal bacteria. *Mucosal Immunol* 2: 187-96

Hoogerwerf WA, Hellmich HL, Cornelissen G, Halberg F, Shahinian VB, et al. 2007. Clock gene expression in the murine gastrointestinal tract: endogenous rhythmicity and effects of a feeding regimen. *Gastroenterology* 133: 1250-60

Hsiao EY, McBride SW, Chow J, Mazmanian SK, Patterson PH. 2012. Modeling an autism risk factor in mice leads to permanent immune dysregulation. *Proc Natl Acad Sci U S A* 109: 12776-81

Hsiao EY, McBride SW, Hsien S, Sharon G, Hyde ER, et al. 2013. Microbiota modulate behavioral and physiological abnormalities associated with neurodevelopmental disorders. *Cell* 155: 1451-63

Hsiao EY, Patterson PH. 2011. Activation of the maternal immune system induces endocrine changes in the placenta via IL-6. *Brain Behav Immun* 25: 604-15

Hsu CT, Patton DF, Mistlberger RE, Steele AD. 2010. Palatable meal anticipation in mice. *PLoS One* 5

Hut RA, Beersma DG. 2011. Evolution of time-keeping mechanisms: early emergence and adaptation to photoperiod. *Philos Trans R Soc Lond B Biol Sci* 366: 2141-54

Illnerova H, Hoffmann K, Vanecek J. 1984. Adjustment of pineal melatonin and N-acetyltransferase rhythms to change from long to short photoperiod in the Djungarian hamster Phodopus sungorus. *Neuroendocrinology* 38: 226-31

Irving WL, James DK, Stephenson T, Laing P, Jameson C, et al. 2000. Influenza virus infection in the second and third trimesters of pregnancy: a clinical and seroepidemiological study. *BJOG* 107: 1282-9

Ivanov, II. 2017. Microbe Hunting Hits Home. *Cell Host Microbe* 21: 282-85

Ivanov, II, Atarashi K, Manel N, Brodie EL, Shima T, et al. 2009. Induction of intestinal Th17 cells by segmented filamentous bacteria. *Cell* 139: 485-98

Ivanov, II, Frutos Rde L, Manel N, Yoshinaga K, Rifkin DB, et al. 2008. Specific microbiota direct the differentiation of IL-17-producing T-helper cells in the mucosa of the small intestine. *Cell Host Microbe* 4: 337-49

Iwasaki A, Medzhitov R. 2004. Toll-like receptor control of the adaptive immune responses. *Nat Immunol* 5: 987-95

Jagannath A, Peirson SN, Foster RG. 2013. Sleep and circadian rhythm disruption in neuropsychiatric illness. *Curr Opin Neurobiol* 23: 888-94

Janeway CA, Jr., Medzhitov R. 2002. Innate immune recognition. *Annu Rev Immunol* 20: 197-216

Jechura TJ, Walsh JM, Lee TM. 2000. Testicular hormones modulate circadian rhythms of the diurnal rodent, Octodon degus. *Horm Behav* 38: 243-9

Jiang HY, Xu LL, Shao L, Xia RM, Yu ZH, et al. 2016. Maternal infection during pregnancy and risk of autism spectrum disorders: A systematic review and meta-analysis. *Brain Behav Immun* 58: 165-72

Johansson ME, Phillipson M, Petersson J, Velcich A, Holm L, Hansson GC. 2008. The inner of the two Muc2 mucin-dependent mucus layers in colon is devoid of bacteria. *Proc Natl Acad Sci U S A* 105: 15064-9

Johnson CH. 1999. Forty years of PRCs--what have we learned? *Chronobiol Int* 16: 711-43

Johnson JD, O'Connor KA, Watkins LR, Maier SF. 2004. The role of IL-1beta in stress-induced sensitization of proinflammatory cytokine and corticosterone responses. *Neuroscience* 127: 569-77

Johnston JD, Ebling FJ, Hazlerigg DG. 2005. Photoperiod regulates multiple gene expression in the suprachiasmatic nuclei and pars tuberalis of the Siberian hamster (Phodopus sungorus). *Eur J Neurosci* 21: 2967-74

Kallikourdis M, Betz AG. 2007. Periodic accumulation of regulatory T cells in the uterus: preparation for the implantation of a semi-allogeneic fetus? *PLoS One* 2: e382

Kawate T, Abo T, Hinuma S, Kumagai K. 1981. Studies of the bioperiodicity of the immune response. II. Co-variations of murine T and B cells and a role of corticosteroid. *The Journal of Immunology* 126: 1364-67

Kentner AC, Bilbo SD, Brown AS, Hsiao EY, McAllister AK, et al. 2019. Maternal immune activation: reporting guidelines to improve the rigor, reproducibility, and transparency of the model. *Neuropsychopharmacology* 44: 245-58

Kim KA, Gu W, Lee IA, Joh EH, Kim DH. 2012. High fat diet-induced gut microbiota exacerbates inflammation and obesity in mice via the TLR4 signaling pathway. *PLoS One* 7: e47713

Kim S, Kim H, Yim YS, Ha S, Atarashi K, et al. 2017. Maternal gut bacteria promote neurodevelopmental abnormalities in mouse offspring. *Nature* 549: 528-32

Kluger M, Rothenburg B. 1979. Fever and reduced iron: their interaction as a host defense response to bacterial infection. *Science* 203: 374-6

Kluger MJ. 1978. The Evolution and Adaptive Value of Fever: Long regarded as a harmful by-product of infection, fever may instead be an ancient ally against disease, enhancing resistance and increasing chances of survival. *American Scientist* 66: 38-43

Ko CH, Takahashi JS. 2006. Molecular components of the mammalian circadian clock. *Hum Mol Genet* 15 Spec No 2: R271-7

Kohsaka A, Laposky AD, Ramsey KM, Estrada C, Joshu C, et al. 2007. High-fat diet disrupts behavioral and molecular circadian rhythms in mice. *Cell Metab* 6: 414-21

Konsman JP, Dantzer R. 2001. How the immune and nervous systems interact during disease-associated anorexia. *Nutrition* 17: 664-68

Konsman JP, Parnet P, Dantzer R. 2002. Cytokine-induced sickness behaviour: mechanisms and implications. *Trends Neurosci* 25: 154-9

Korem T, Zeevi D, Suez J, Weinberger A, Avnit-Sagi T, et al. 2015. Growth dynamics of gut microbiota in health and disease inferred from single metagenomic samples. *Science* 349: 1101-06

Krizo JA, Mintz EM. 2014. Sex differences in behavioral circadian rhythms in laboratory rodents. *Front Endocrinol (Lausanne)* 5: 234

Kuljis DA, Loh DH, Truong D, Vosko AM, Ong ML, et al. 2013. Gonadal- and sex-chromosome-dependent sex differences in the circadian system. *Endocrinology* 154: 1501-12

L. A. Scheving LA, Yeh YC, Tsai TH, Scheving LE. 1980. Circadian Phase-Dependent Stimulatory Effects of Epidermal Growth Factor on Deoxyribonucleic Acid Synthesis in the Duodenum, Jejunum, Ileum, Caecum, Colon, and Rectum of the Adult Male Mouse*. *Endocrinology* 106: 1498-503

Lammas DA, Casanova JL, Kumararatne DS. 2000. Clinical consequences of defects in the IL-12-dependent interferon-gamma (IFN-gamma) pathway. *Clin Exp Immunol* 121: 417-25

Lamont EW, Diaz LR, Barry-Shaw J, Stewart J, Amir S. 2005. Daily restricted feeding rescues a rhythm of period2 expression in the arrhythmic suprachiasmatic nucleus. *Neuroscience* 132: 245-8

Lange T, Dimitrov S, Born J. 2010. Effects of sleep and circadian rhythm on the human immune system. *Ann N Y Acad Sci* 1193: 48-59

Lee BK, Magnusson C, Gardner RM, Blomstrom A, Newschaffer CJ, et al. 2015. Maternal hospitalization with infection during pregnancy and risk of autism spectrum disorders. *Brain Behav Immun* 44: 100-5

Leone V, Gibbons SM, Martinez K, Hutchison AL, Huang EY, et al. 2015. Effects of diurnal variation of gut microbes and high-fat feeding on host circadian clock function and metabolism. *Cell Host Microbe* 17: 681-9

Lin HV, Frassetto A, Kowalik EJ, Jr., Nawrocki AR, Lu MM, et al. 2012. Butyrate and propionate protect against diet-induced obesity and regulate gut hormones via free fatty acid receptor 3-independent mechanisms. *PLoS One* 7: e35240

Liu C, Weaver DR, Strogatz SH, Reppert SM. 1997. Cellular construction of a circadian clock: period determination in the suprachiasmatic nuclei. *Cell* 91: 855-60

Logan RW, Sarkar DK. 2012. Circadian nature of immune function. *Mol Cell Endocrinol* 349: 82-90

Lu Y, Fan C, Li P, Lu Y, Chang X, Qi K. 2016. Short Chain Fatty Acids Prevent High-fat-diet-induced Obesity in Mice by Regulating G Protein-coupled Receptors and Gut Microbiota. *Sci Rep* 6: 37589

Luciana P, Caio Sergio Galina S, Regina Pekelmann M, Sanseray da Silveira C-M. 2019. Dysregulation of Circadian Rhythms in Autism Spectrum Disorders. *Current Pharmaceutical Design* 25: 4379-93

Macpherson AJ, Harris NL. 2004. Interactions between commensal intestinal bacteria and the immune system. *Nat Rev Immunol* 4: 478-85

Macpherson AJ, Hunziker L, McCoy K, Lamarre A. 2001. IgA responses in the intestinal mucosa against pathogenic and non-pathogenic microorganisms. *Microbes Infect* 3: 1021-35

Macpherson AJ, Uhr T. 2004. Induction of protective IgA by intestinal dendritic cells carrying commensal bacteria. *Science* 303: 1662-5

Maenner M, Shaw K, Baio J. 2020. Prevalence of Autism Spectrum Disorder Among Children Aged 8 Years — Autism and Developmental Disabilities Monitoring Network, 11 Sites, United States, 2016. MMWR Surveill Summ 2020: No. SS-4

Maier SF, Watkins LR. 1998. Cytokines for psychologists: implications of bidirectional immune-to-brain communication for understanding behavior, mood, and cognition. *Psychol Rev* 105: 83-107

Mandal M, Marzouk AC, Donnelly R, Ponzio NM. 2010. Preferential development of Th17 cells in offspring of immunostimulated pregnant mice. *J Reprod Immunol* 87: 97-100

Margraf RR, Lynch GR. 1993. Melatonin injections affect circadian behavior and SCN neurophysiology in Djungarian hamsters. *Am J Physiol* 264: R615-21

Marpegan L, Leone MJ, Katz ME, Sobrero PM, Bekinstein TA, Golombek DA. 2009. Diurnal variation in endotoxin-induced mortality in mice: correlation with proinflammatory factors. *Chronobiology International* 26: 1430-42

Martin LB, Weil ZM, Nelson RJ. 2008. Seasonal changes in vertebrate immune activity: mediation by physiological trade-offs. *Philos Trans R Soc Lond B Biol Sci* 363: 321-39

Mayer EA. 2011. Gut feelings: the emerging biology of gut-brain communication. *Nat Rev Neurosci* 12: 453-66

McEwen BS, Wingfield JC. 2010. What is in a name? Integrating homeostasis, allostasis and stress. *Horm Behav* 57: 105-11

McFall-Ngai M. 2014. Divining the essence of symbiosis: insights from the squid-vibrio model. *PLoS Biol* 12: e1001783

Meijer JH, Schwartz WJ. 2003. In search of the pathways for light-induced pacemaker resetting in the suprachiasmatic nucleus. *J Biol Rhythms* 18: 235-49

Mendoza J. 2007. Circadian clocks: setting time by food. *J Neuroendocrinol* 19: 127-37

Mendoza J, Albrecht U, Challet E. 2010. Behavioural food anticipation in clock genes deficient mice: confirming old phenotypes, describing new phenotypes. *Genes Brain Behav* 9: 467-77

Mendoza J, Pevet P, Challet E. 2008. High-fat feeding alters the clock synchronization to light. *J Physiol* 586: 5901-10

Meyer U, Feldon J, Fatemi SH. 2009. In-vivo rodent models for the experimental investigation of prenatal immune activation effects in neurodevelopmental brain disorders. *Neurosci Biobehav Rev* 33: 1061-79

Meyer U, Murray PJ, Urwyler A, Yee BK, Schedlowski M, Feldon J. 2008a. Adult behavioral and pharmacological dysfunctions following disruption of the fetal brain balance between pro-inflammatory and IL-10-mediated anti-inflammatory signaling. *Mol Psychiatry* 13: 208-21

Meyer U, Nyffeler M, Yee BK, Knuesel I, Feldon J. 2008b. Adult brain and behavioral pathological markers of prenatal immune challenge during early/middle and late fetal development in mice. *Brain Behav Immun* 22: 469-86

Missig G, McDougle CJ, Carlezon WA, Jr. 2020. Sleep as a translationally-relevant endpoint in studies of autism spectrum disorder (ASD). *Neuropsychopharmacology* 45: 90-103

Mistlberger RE. 1994. Circadian food-anticipatory activity: formal models and physiological mechanisms. *Neurosci Biobehav Rev* 18: 171-95

Mistlberger RE, Yamazaki S, Pendergast JS, Landry GJ, Takumi T, Nakamura W. 2008. Comment on "Differential rescue of light- and food-entrainable circadian rhythms". *Science* 322: 675; author reply 75

Mizuno T, Sawada M, Suzumura A, Marunouchi T. 1994. Expression of cytokines during glial differentiation. *Brain Res* 656: 141-46

Mohawk JA, Green CB, Takahashi JS. 2012. Central and peripheral circadian clocks in mammals. *Annu Rev Neurosci* 35: 445-62

Moore JG, Wolfe M. 1973. The relation of plasma gastrin to the circadian rhythm of gastric acid secretion in man. *Digestion* 9: 97-105

Morin LP, Fitzgerald KM, Zucker I. 1977. Estradiol shortens the period of hamster circadian rhythms. *Science* 196: 305-7

Mowat AM, Agace WW. 2014. Regional specialization within the intestinal immune system. *Nat Rev Immunol* 14: 667-85

Mueller C, Macpherson AJ. 2006. Layers of mutualism with commensal bacteria protect us from intestinal inflammation. *Gut* 55: 276-84

Mueller FS, Polesel M, Richetto J, Meyer U, Weber-Stadlbauer U. 2018. Mouse models of maternal immune activation: Mind your caging system! *Brain Behav Immun* 73: 643-60

Murray S, Chen EY. 2019. Examining Adolescence as a Sensitive Period for High-Fat, High-Sugar Diet Exposure: A Systematic Review of the Animal Literature. *Front Neurosci* 13: 1108

Neal MD, Leaphart C, Levy R, Prince J, Billiar TR, et al. 2006. Enterocyte TLR4 mediates phagocytosis and translocation of bacteria across the intestinal barrier. *J Immunol* 176: 3070-9

Nelson RJ. 2004. Seasonal immune function and sickness responses. *Trends Immunol* 25: 187-92

Nelson RJ, Demas GE. 1996. Seasonal changes in immune function. *Q Rev Biol* 71: 511-48

Nelson RJ, Demas GE. 2004. Seasonal Patterns of Stress, Disease, and Sickness Responses. *Current Directions in Psychological Science* 13: 198-201

Nestler EJ, Hyman SE. 2010. Animal models of neuropsychiatric disorders. *Nat Neurosci* 13: 1161-9

Nicholson JK, Holmes E, Kinross J, Burcelin R, Gibson G, et al. 2012. Host-gut microbiota metabolic interactions. *Science* 336: 1262-7

Nuesslein-Hildesheim B, O'Brien JA, Ebling JP, Maywood ES, Hastings MH. 2000. The circadian cycle of mPER clock gene products in the suprachiasmatic nucleus of the Siberian hamster encodes both daily and seasonal time. *European Journal of Neuroscience* 12: 2856-64

O'Boyle CJ, MacFie J, Mitchell CJ, Johnstone D, Sagar PM, Sedman PC. 1998. Microbiology of bacterial translocation in humans. *Gut* 42: 29-35

O'Donnell KJ, Meaney MJ. 2017. Fetal Origins of Mental Health: The Developmental Origins of Health and Disease Hypothesis. *Am J Psychiatry* 174: 319-28

Oliveira-Nascimento L, Massari P, Wetzler LM. 2012. The Role of TLR2 in Infection and Immunity. *Front Immunol* 3: 79

Onishi KG, Maneval AC, Cable EC, Tuohy MC, Scasny AJ, et al. 2020. Circadian and circannual timescales interact to generate seasonal changes in immune function. *Brain Behav Immun* 83: 33-43

Ortega-Cava CF, Ishihara S, Rumi MA, Kawashima K, Ishimura N, et al. 2003. Strategic compartmentalization of Toll-like receptor 4 in the mouse gut. *J Immunol* 170: 3977-85

Ouyang Y, Andersson CR, Kondo T, Golden SS, Johnson CH. 1998. Resonating circadian clocks enhance fitness in cyanobacteria. *Proc Natl Acad Sci U S A* 95: 8660-4

Özogul F. 2011. Effects of specific lactic acid bacteria species on biogenic amine production by foodborne pathogen. *International Journal of Food Science & Technology* 46: 478-84

Palin K, McCusker RH, Strle K, Moos F, Dantzer R, Kelley KW. 2008. Tumor necrosis factor-alpha-induced sickness behavior is impaired by central administration of an inhibitor of c-jun N-terminal kinase. *Psychopharmacology (Berl)* 197: 629-35

Palmer C, Bik EM, DiGiulio DB, Relman DA, Brown PO. 2007. Development of the human infant intestinal microbiota. *PLoS Biol* 5: e177

Panda S. 2016. Circadian physiology of metabolism. *Science* 354: 1008-15

Panda S, Sato TK, Castrucci AM, Rollag MD, DeGrip WJ, et al. 2002. Melanopsin (Opn4) Requirement for Normal Light-Induced Circadian Phase Shifting. *Science* 298: 2213-16

Paolicelli RC, Bolasco G, Pagani F, Maggi L, Scianni M, et al. 2011. Synaptic Pruning by Microglia Is Necessary for Normal Brain Development. *Science* 333: 1456-58

Paranjpe DA, Sharma VK. 2005. Evolution of temporal order in living organisms. *J Circadian Rhythms* 3: 7

Parkar SG, Kalsbeek A, Cheeseman JF. 2019. Potential Role for the Gut Microbiota in Modulating Host Circadian Rhythms and Metabolic Health. *Microorganisms* 7

Paul MJ, Indic P, Schwartz WJ. 2015. Social synchronization of circadian rhythmicity in female mice depends on the number of cohabiting animals. *Biol Lett* 11: 20150204

Pelleymounter MA, Cullen MJ, Baker MB, Hecht R, Winters D, et al. 1995. Effects of the obese gene product on body weight regulation in ob/ob mice. *Science* 269: 540-3

Pendergast JS, Branecky KL, Huang R, Niswender KD, Yamazaki S. 2014. Wheel-running activity modulates circadian organization and the daily rhythm of eating behavior. *Front Psychol* 5: 177

Pendergast JS, Branecky KL, Yang W, Ellacott KL, Niswender KD, Yamazaki S. 2013. High-fat diet acutely affects circadian organisation and eating behavior. *Eur J Neurosci* 37: 1350-6

Pittendrigh CS. 1960. Circadian rhythms and the circadian organization of living systems. *Cold Spring Harb Symp Quant Biol* 25: 159-84

Pittendrigh CS. 1993. Temporal organization: reflections of a Darwinian clock-watcher. *Annu Rev Physiol* 55: 16-54

Pittendrigh CS, Daan S. 1976a. A functional analysis of circadian pacemakers in nocturnal rodents. *Journal of comparative physiology* 106: 333-55

Pittendrigh CS, Daan S. 1976b. A functional analysis of circadian pacemakers in nocturnal rodents. I. The Stability and Lability of Spontaneous Frequency. *Journal of comparative physiology* 106: 223-52

Pittendrigh CS, Daan S. 1976c. A functional analysis of circadian pacemakers in nocturnal rodents. IV. Entrainment Pacemaker as clock. *Journal of comparative physiology* 106: 291-331

Pittendrigh CS, Daan S. 1976d. A functional analysis of circadian pacemakers in nocturnal rodents. V. Pacemaker Stucuture A Clock for All Seasons. *Journal of comparative physiology* 106: 333-55

Pittendrigh CS, Minis DH. 1972. Circadian systems: longevity as a function of circadian resonance in Drosophila melanogaster. *Proc Natl Acad Sci U S A* 69: 1537-9

Pousset F. 1994. Developmental expression of cytokine genes in the cortex and hippocampus of the rat central nervous system. *Brain Res Dev Brain Res* 81: 143-6

Pownall R, Kabler PA, Knapp MS. 1979. The time of day of antigen encounter influences the magnitude of the immune response. *Clin Exp Immunol* 36: 347-54

Prendergast BJ, Bilbo SD, Nelson RJ. 2004. Photoperiod controls the induction, retention, and retrieval of antigen-specific immunological memory. *Am J Physiol Regul Integr Comp Physiol* 286: R54-60

Prendergast BJ, Cable EJ, Patel PN, Pyter LM, Onishi KG, et al. 2013. Impaired leukocyte trafficking and skin inflammatory responses in hamsters lacking a functional circadian system. *Brain Behav Immun* 32: 94-104

Prendergast BJ, Cable EJ, Stevenson TJ, Onishi KG, Zucker I, Kay LM. 2015. Circadian Disruption Alters the Effects of Lipopolysaccharide Treatment on Circadian and Ultradian Locomotor Activity and Body Temperature Rhythms of Female Siberian Hamsters. *J Biol Rhythms* 30: 543-56

Prendergast BJ, Mosinger B, Jr., Kolattukudy PE, Nelson RJ. 2002a. Hypothalamic gene expression in reproductively photoresponsive and photorefractory Siberian hamsters. *Proc Natl Acad Sci U S A* 99: 16291-6

Prendergast BJ, Onishi KG, Zucker I. 2014. Female mice liberated for inclusion in neuroscience and biomedical research. *Neurosci Biobehav Rev* 40: 1-5

Prendergast BJ, Wynne-Edwards KE, Yellon SM, Nelson RJ. 2002b. Photorefractoriness of immune function in male Siberian hamsters (Phodopus sungorus). *J Neuroendocrinol* 14: 318-29

Quan N, Whiteside M, Herkenham M. 1998. Time course and localization patterns of interleukin-1beta messenger RNA expression in brain and pituitary after peripheral administration of lipopolysaccharide. *Neuroscience* 83: 281-93

Rabasa C, Dickson SL. 2016. Impact of stress on metabolism and energy balance. *Current Opinion in Behavioral Sciences* 9: 71-77

Ralph MR, Foster RG, Davis FC, Menaker M. 1990. Transplanted Suprachiasmatic Nucleus Determines Circadian Period. *Science* 247: 975-78

Rescigno M. 2011. The intestinal epithelial barrier in the control of homeostasis and immunity. *Trends Immunol* 32: 256-64

Ribeiro AC, Ceccarini G, Dupre C, Friedman JM, Pfaff DW, Mark AL. 2011. Contrasting effects of leptin on food anticipatory and total locomotor activity. *PLoS One* 6: e23364

Robertson SA. 2005. Seminal plasma and male factor signalling in the female reproductive tract. *Cell Tissue Res* 322: 43-52

Roenneberg T, Merrow M. 2016. The Circadian Clock and Human Health. *Curr Biol* 26: R432-43

Ruan JW, Statt S, Huang CT, Tsai YT, Kuo CC, et al. 2016. Dual-specificity phosphatase 6 deficiency regulates gut microbiome and transcriptome response against diet-induced obesity in mice. *Nat Microbiol* 2: 16220

Saberi M, Woods NB, de Luca C, Schenk S, Lu JC, et al. 2009. Hematopoietic cell-specific deletion of toll-like receptor 4 ameliorates hepatic and adipose tissue insulin resistance in high-fat-fed mice. *Cell Metab* 10: 419-29

Salzman NH. 2011. Microbiota-immune system interaction: an uneasy alliance. *Curr Opin Microbiol* 14: 99-105

Samuelsson AM, Ohrn I, Dahlgren J, Eriksson E, Angelin B, et al. 2004. Prenatal exposure to interleukin-6 results in hypertension and increased hypothalamic-pituitary-adrenal axis activity in adult rats. *Endocrinology* 145: 4897-911

Sano T, Huang W, Hall JA, Yang Y, Chen A, et al. 2015. An IL-23R/IL-22 Circuit Regulates Epithelial Serum Amyloid A to Promote Local Effector Th17 Responses. *Cell* 163: 381-93

Sartor F, Eelderink-Chen Z, Aronson B, Bosman J, Hibbert LE, et al. 2019. Are There Circadian Clocks in Non-Photosynthetic Bacteria? *Biology (Basel)* 8

Sasaki Y, Sakai M, Miyazaki S, Higuma S, Shiozaki A, Saito S. 2004. Decidual and peripheral blood CD4+CD25+ regulatory T cells in early pregnancy subjects and spontaneous abortion cases. *Mol Hum Reprod* 10: 347-53

Savage DC. 1970. Associations of indigenous microorganisms with gastrointestinal mucosal epithelia. *Am J Clin Nutr* 23: 1495-501

Schafer DP, Lehrman EK, Kautzman AG, Koyama R, Mardinly AR, et al. 2012. Microglia sculpt postnatal neural circuits in an activity and complement-dependent manner. *Neuron* 74: 691-705

Scheiermann C, Gibbs J, Ince L, Loudon A. 2018. Clocking in to immunity. *Nat Rev Immunol* 18: 423-37

Scheiermann C, Kunisaki Y, Frenette PS. 2013. Circadian control of the immune system. *Nat Rev Immunol* 13: 190-8

Scheiermann C, Kunisaki Y, Lucas D, Chow A, Jang JE, et al. 2012. Adrenergic nerves govern circadian leukocyte recruitment to tissues. *Immunity* 37: 290-301

Scheving LA. 2000. Biological clocks and the digestive system. *Gastroenterology* 119: 536-49

Scheving LE, Burns ER, Pauly JE, Tsai TH. 1978. Circadian variation in cell division of the mouse alimentary tract, bone marrow and corneal epithelium. *Anat Rec* 191: 479-86

Schibler U, Ripperger J, Brown SA. 2003. Peripheral circadian oscillators in mammals: time and food. *J Biol Rhythms* 18: 250-60

Schibler U, Sassone-Corsi P. 2002. A web of circadian pacemakers. *Cell* 111: 919-22

Schlatt S, De Geyter M, Kliesch S, Nieschlag E, Bergmann M. 1995. Spontaneous recrudescence of spermatogenesis in the photoinhibited male Djungarian hamster, Phodopus sungorus. *Biol Reprod* 53: 1169-77

Schroeder BO, Birchenough GMH, Stahlman M, Arike L, Johansson MEV, et al. 2018. Bifidobacteria or Fiber Protects against Diet-Induced Microbiota-Mediated Colonic Mucus Deterioration. *Cell Host Microbe* 23: 27-40 e7

Schwartzer JJ, Careaga M, Onore CE, Rushakoff JA, Berman RF, Ashwood P. 2013. Maternal immune activation and strain specific interactions in the development of autism-like behaviors in mice. *Transl Psychiatry* 3: e240

Sekirov I, Russell SL, Antunes LC, Finlay BB. 2010. Gut microbiota in health and disease. *Physiol Rev* 90: 859-904

Sellix MT, Evans JA, Leise TL, Castanon-Cervantes O, Hill DD, et al. 2012. Aging differentially affects the re-entrainment response of central and peripheral circadian oscillators. *J Neurosci* 32: 16193-202

Sender R, Fuchs S, Milo R. 2016. Revised Estimates for the Number of Human and Bacteria Cells in the Body. *PLoS Biol* 14: e1002533

Sewell AK. 2012. Why must T cells be cross-reactive? *Nat Rev Immunol* 12: 669-77

Shackelford PG, Feigin RD. 1973. Periodicity of susceptibility to pneumococcal infection: influence of light and adrenocortical secretions. *Science* 182: 285-7

Shearman LP, Sriram S, Weaver DR, Maywood ES, Chaves I, et al. 2000. Interacting molecular loops in the mammalian circadian clock. *Science* 288: 1013-9

Shi L, Fatemi SH, Sidwell RW, Patterson PH. 2003. Maternal influenza infection causes marked behavioral and pharmacological changes in the offspring. *J Neurosci* 23: 297-302

Shi L, Tu N, Patterson PH. 2005. Maternal influenza infection is likely to alter fetal brain development indirectly: the virus is not detected in the fetus. *Int J Dev Neurosci* 23: 299-305

Shin Yim Y, Park A, Berrios J, Lafourcade M, Pascual LM, et al. 2017. Reversing behavioural abnormalities in mice exposed to maternal inflammation. *Nature* 549: 482-87

Shishov VA, Kirovskaya TA, Kudrin VS, Oleskin AV. 2009. Amine neuromediators, their precursors, and oxidation products in the culture of Escherichia coli K-12. *Applied Biochemistry and Microbiology* 45: 494-97

Silver AC, Arjona A, Hughes ME, Nitabach MN, Fikrig E. 2012. Circadian expression of clock genes in mouse macrophages, dendritic cells, and B cells. *Brain Behav Immun* 26: 407-13

Slack E, Hapfelmeier S, Stecher B, Velykoredko Y, Stoel M, et al. 2009. Innate and adaptive immunity cooperate flexibly to maintain host-microbiota mutualism. *Science* 325: 617-20

Small PM, Täuber MG, Hackbarth CJ, Sande MA. 1986. Influence of body temperature on bacterial growth rates in experimental pneumococcal meningitis in rabbits. *Infection and Immunity* 52: 484-87

Smith PM, Howitt MR, Panikov N, Michaud M, Gallini CA, et al. 2013. The microbial metabolites, short-chain fatty acids, regulate colonic Treg cell homeostasis. *Science* 341: 569-73

Smith SE, Li J, Garbett K, Mirnics K, Patterson PH. 2007. Maternal immune activation alters fetal brain development through interleukin-6. *J Neurosci* 27: 10695-702

Sorek M, Schnytzer Y, Waldman Ben-Asher H, Caspi VC, Chen CS, et al. 2018. Setting the pace: host rhythmic behaviour and gene expression patterns in the facultatively symbiotic cnidarian Aiptasia are determined largely by Symbiodinium. *Microbiome* 6: 83

Souders MC, Mason TB, Valladares O, Bucan M, Levy SE, et al. 2009. Sleep behaviors and sleep quality in children with autism spectrum disorders. *Sleep* 32: 1566-78

Spoelstra K, Wikelski M, Daan S, Loudon AS, Hau M. 2016. Natural selection against a circadian clock gene mutation in mice. *Proc Natl Acad Sci U S A* 113: 686-91

Steinlechner S, Jacobmeier B, Scherbarth F, Dernbach H, Kruse F, Albrecht U. 2002. Robust circadian rhythmicity of Per1 and Per2 mutant mice in constant light, and dynamics of Per1 and Per2 gene expression under long and short photoperiods. *J Biol Rhythms* 17: 202-9

Stephan FK. 2002. The "Other" Circadian System: Food as a Zeitgeber. *Journal of Biological Rhythms* 17: 284-92

Stephan FK, Swann JM, Sisk CL. 1979. Anticipation of 24-hr feeding schedules in rats with lesions of the suprachiasmatic nucleus. *Behav Neural Biol* 25: 346-63

Stephan FK, Zucker I. 1972. Circadian rhythms in drinking behavior and locomotor activity of rats are eliminated by hypothalamic lesions. *Proc Natl Acad Sci U S A* 69: 1583-6

Stevenson TJ. 2017. Environmental and hormonal regulation of epigenetic enzymes in the hypothalamus. *J Neuroendocrinol* 29

Stevenson TJ, Prendergast BJ. 2015. Photoperiodic time measurement and seasonal immunological plasticity. *Front Neuroendocrinol* 37: 76-88

Stevenson TJ, Visser ME, Arnold W, Barrett P, Biello S, et al. 2015. Disrupted seasonal biology impacts health, food security and ecosystems. *Proc Biol Sci* 282: 20151453

Stokkan KA, Yamazaki S, Tei H, Sakaki Y, Menaker M. 2001. Entrainment of the circadian clock in the liver by feeding. *Science* 291: 490-3

Storch KF, Weitz CJ. 2009. Daily rhythms of food-anticipatory behavioral activity do not require the known circadian clock. *Proc Natl Acad Sci U S A* 106: 6808-13

Sudo N, Chida Y, Aiba Y, Sonoda J, Oyama N, et al. 2004. Postnatal microbial colonization programs the hypothalamic-pituitary-adrenal system for stress response in mice. *J Physiol* 558: 263-75

Sumova A, Travnickova Z, Peters R, Schwartz WJ, Illnerova H. 1995. The Rat Suprachiasmatic Nucleus Is a Clock for All Seasons. *Proceedings of the National Academy of Sciences of the United States of America* 92: 7754-58

Suzuki H, Jeong KI, Itoh K, Doi K. 2002. Regional variations in the distributions of small intestinal intraepithelial lymphocytes in germ-free and specific pathogen-free mice. *Exp Mol Pathol* 72: 230-5

Suzuki K, Oida T, Hamada H, Hitotsumatsu O, Watanabe M, et al. 2000. Gut cryptopatches: direct evidence of extrathymic anatomical sites for intestinal T lymphopoiesis. *Immunity* 13: 691-702

Svensson-Arvelund J, Ernerudh J. 2015. The Role of Macrophages in Promoting and Maintaining Homeostasis at the Fetal-Maternal Interface. *Am J Reprod Immunol* 74: 100-9

Tahara Y, Kuroda H, Saito K, Nakajima Y, Kubo Y, et al. 2012. In vivo monitoring of peripheral circadian clocks in the mouse. *Curr Biol* 22: 1029-34

Tahara Y, Yamazaki M, Sukigara H, Motohashi H, Sasaki H, et al. 2018. Gut Microbiota-Derived Short Chain Fatty Acids Induce Circadian Clock Entrainment in Mouse Peripheral Tissue. *Sci Rep* 8: 1395

Takahashi JS, Hong HK, Ko CH, McDearmon EL. 2008. The genetics of mammalian circadian order and disorder: implications for physiology and disease. *Nat Rev Genet* 9: 764-75

Thaiss CA, Zeevi D, Levy M, Zilberman-Schapira G, Suez J, et al. 2014. Transkingdom control of microbiota diurnal oscillations promotes metabolic homeostasis. *Cell* 159: 514-29

Tilburgs T, Roelen DL, van der Mast BJ, de Groot-Swings GM, Kleijburg C, et al. 2008. Evidence for a Selective Migration of Fetus-Specific CD4+CD25bright Regulatory T Cells from the Peripheral Blood to the Decidua in Human Pregnancy. *The Journal of Immunology* 180: 5737-45

Tognini P, Thaiss CA, Elinav E, Sassone-Corsi P. 2017. Circadian Coordination of Antimicrobial Responses. *Cell Host Microbe* 22: 185-92

Tolhurst G, Heffron H, Lam YS, Parker HE, Habib AM, et al. 2012. Short-chain fatty acids stimulate glucagon-like peptide-1 secretion via the G-protein-coupled receptor FFAR2. *Diabetes* 61: 364-71

van Dam AM, Brouns M, Louisse S, Berkenbosch F. 1992. Appearance of interleukin-1 in macrophages and in ramified microglia in the brain of endotoxin-treated rats: a pathway for the induction of non-specific symptoms of sickness? *Brain Res* 588: 291-6

Van Reeth K. 2000. Cytokines in the pathogenesis of influenza. *Vet Microbiol* 74: 109-16

van Someren EJ, Hagebeuk EE, Lijzenga C, Scheltens P, de Rooij SE, et al. 1996. Circadian rest-activity rhythm disturbances in Alzheimer's disease. *Biol Psychiatry* 40: 259-70

VanderPlas JT. 2018. Understanding the Lomb–Scargle Periodogram. *The Astrophysical Journal Supplement Series* 236

Vanecek J, Kosar E, Vorlicek J. 1990. Daily changes in melatonin binding sites and the effect of castration. *Mol Cell Endocrinol* 73: 165-70

Vela J. 2002. Interleukin-1 Regulates Proliferation and Differentiation of Oligodendrocyte Progenitor Cells. *Molecular and Cellular Neuroscience* 20: 489-502

Viswanathan K, Dhabhar FS. 2005. Stress-induced enhancement of leukocyte trafficking into sites of surgery or immune activation. *Proceedings of the National Academy of Sciences of the United States of America* 102: 5808-13

Vitkovic L, Konsman JP, Bockaert J, Dantzer R, Homburger V, Jacque C. 2000. Cytokine signals propagate through the brain. *Molecular Psychiatry* 5: 604-15

Voigt RM, Forsyth CB, Green SJ, Mutlu E, Engen P, et al. 2014. Circadian disorganization alters intestinal microbiota. *PLoS One* 9: e97500

Voigt RM, Summa KC, Forsyth CB, Green SJ, Engen P, et al. 2016. The Circadian Clock Mutation Promotes Intestinal Dysbiosis. *Alcohol Clin Exp Res* 40: 335-47

Wachulec M, Li H, Tanaka H, Peloso E, Satinoff E. 1997. Suprachiasmatic Nuclei Lesions Do Not Eliminate Homeostatic Thermoregulatory Responses in Rats. *Journal of Biological Rhythms* 12: 226-34

Walker WH, 2nd, Walton JC, DeVries AC, Nelson RJ. 2020. Circadian rhythm disruption and mental health. *Transl Psychiatry* 10: 28

Wan W, Wetmore L, Sorensen CM, Greenberg AH, Nance DM. 1994. Neural and biochemical mediators of endotoxin and stress-induced c-fos expression in the rat brain. *Brain Res Bull* 34: 7-14

Wang Y, Devkota S, Musch MW, Jabri B, Nagler C, et al. 2010. Regional mucosa-associated microbiota determine physiological expression of TLR2 and TLR4 in murine colon. *PLoS One* 5: e13607

Wang Z, Xiao G, Yao Y, Guo S, Lu K, Sheng Z. 2006. The role of bifidobacteria in gut barrier function after thermal injury in rats. *J Trauma* 61: 650-7

Watkins LR, Wiertelak EP, Goehler LE, Mooney-Heiberger K, Martinez J, et al. 1994. Neurocircuitry of illness-induced hyperalgesia. *Brain Res* 639: 283-99

Welsh DK, Takahashi JS, Kay SA. 2010. Suprachiasmatic nucleus: cell autonomy and network properties. *Annu Rev Physiol* 72: 551-77

Wen JC, Dhabhar FS, Prendergast BJ. 2007. Pineal-dependent and -independent effects of photoperiod on immune function in Siberian hamsters (Phodopus sungorus). *Horm Behav* 51: 31-9

Wikoff WR, Anfora AT, Liu J, Schultz PG, Lesley SA, et al. 2009. Metabolomics analysis reveals large effects of gut microflora on mammalian blood metabolites. *Proc Natl Acad Sci U S A* 106: 3698-703

Wilke CM, Bishop K, Fox D, Zou W. 2011. Deciphering the role of Th17 cells in human disease. *Trends Immunol* 32: 603-11

Williams K, Mackenzie JS. 2009. Influenza infections during pregnancy in the mouse. *Journal of Hygiene* 79: 249-57

Wintler T, Schoch H, Frank MG, Peixoto L. 2020. Sleep, brain development, and autism spectrum disorders: Insights from animal models. *J Neurosci Res* 98: 1137-49

Wu WL, Hsiao EY, Yan Z, Mazmanian SK, Patterson PH. 2017. The placental interleukin-6 signaling controls fetal brain development and behavior. *Brain Behav Immun* 62: 11-23

Xuan IC, Hampson DR. 2014. Gender-dependent effects of maternal immune activation on the behavior of mouse offspring. *PLoS One* 9: e104433

Yamaguchi S, Isejima H, Matsuo T, Okura R, Yagita K, et al. 2003. Synchronization of cellular clocks in the suprachiasmatic nucleus. *Science* 302: 1408-12

Yan L, Silver R. 2008. Day-length encoding through tonic photic effects in the retinorecipient SCN region. *Eur J Neurosci* 28: 2108-15

Yellon SM, Tran LT. 2002. Photoperiod, reproduction, and immunity in select strains of inbred mice. *J Biol Rhythms* 17: 65-75

Yokoyama Y, Nakamura TJ, Yoshimoto K, Ijyuin H, Tachikawa N, et al. 2020. A high-salt/high fat diet alters circadian locomotor activity and glucocorticoid synthesis in mice. *PLoS One* 15: e0233386

Young. 2001. Time zones: a comparative genetics of circadian clock.

Zarrinpar A, Chaix A, Yooseph S, Panda S. 2014. Diet and feeding pattern affect the diurnal dynamics of the gut microbiome. *Cell Metab* 20: 1006-17

Zhou L, Lopes JE, Chong MM, Ivanov, II, Min R, et al. 2008. TGF-beta-induced Foxp3 inhibits T(H)17 cell differentiation by antagonizing RORgammat function. *Nature* 453: 236-40

Zhou P, Ross RA, Pywell CM, Liangpunsakul S, Duffield GE. 2014. Disturbances in the murine hepatic circadian clock in alcohol-induced hepatic steatosis. *Sci Rep* 4: 3725

Zoetendal EG, Akkermans ADL, Akkermans-van Vliet WM, De Visser JAGM, De Vos WM. 2001. The Host Genotype Affects the Bacterial Community in the Human Gastrointestinal Tract. *Microbial Ecology in Health & Disease* 13

Zou J, Chassaing B, Singh V, Pellizzon M, Ricci M, et al. 2018. Fiber-Mediated Nourishment of Gut Microbiota Protects against Diet-Induced Obesity by Restoring IL-22-Mediated Colonic Health. *Cell Host Microbe* 23: 41-53 e4

Zwietering MH, de Koos JT, Hasenack BE, de Witt JC, van't Riet K. 1991. Modeling of bacterial growth as a function of temperature. *Applied and Environmental Microbiology* 57: 1094-101

Appendix A: Figures

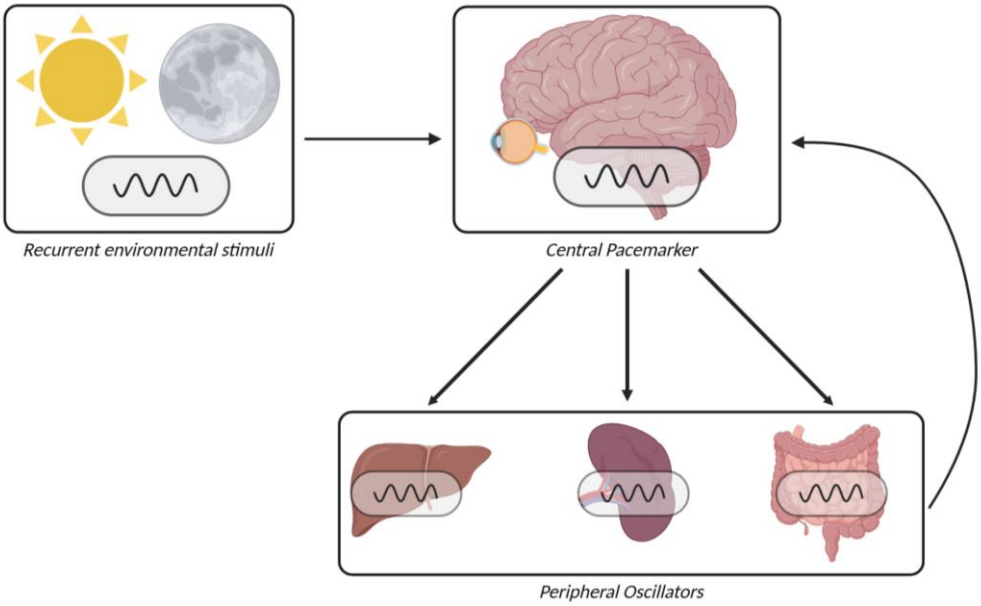

Figure 1 - Web of circadian pacemakers
The central circadian pacemaker located in the hypothalamic suprachiasmatic nucleus (SCN) and entrains to the environmental light:dark cycle. Time-of-day information is conferred to peripheral tissues and oscillators. Further, peripheral oscillators can influence the circadian network via non-light cues such as social interaction or food entrainment. Created with BioRender.com.

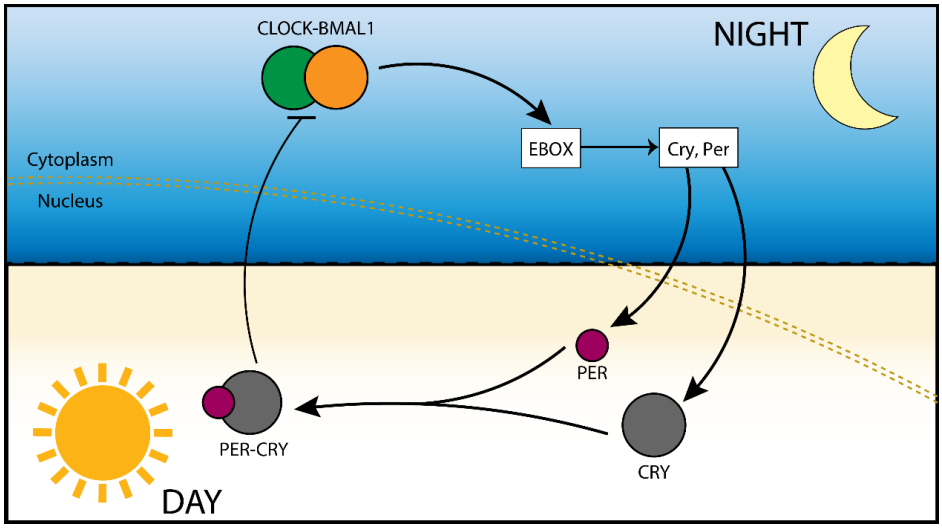

Figure 2 - Transcription-translation feedback loop
Schematic view of molecular clock contained within each mammalian cell. The circadian TTFL revolves around the timed transcription of PERIOD (PER) and CRYPTOCHROME (CRY) genes, activated by BMAL/CLOCK dimers, and subsequent accumulation of PER and CRY proteins that progressively inhibit BMAL1/CLOCK dimer activity in the cytoplasm. The degradation of PER and CRY proteins removes the inhibition from BMAL1/CLOCK and begins a new 24 hour cycle.

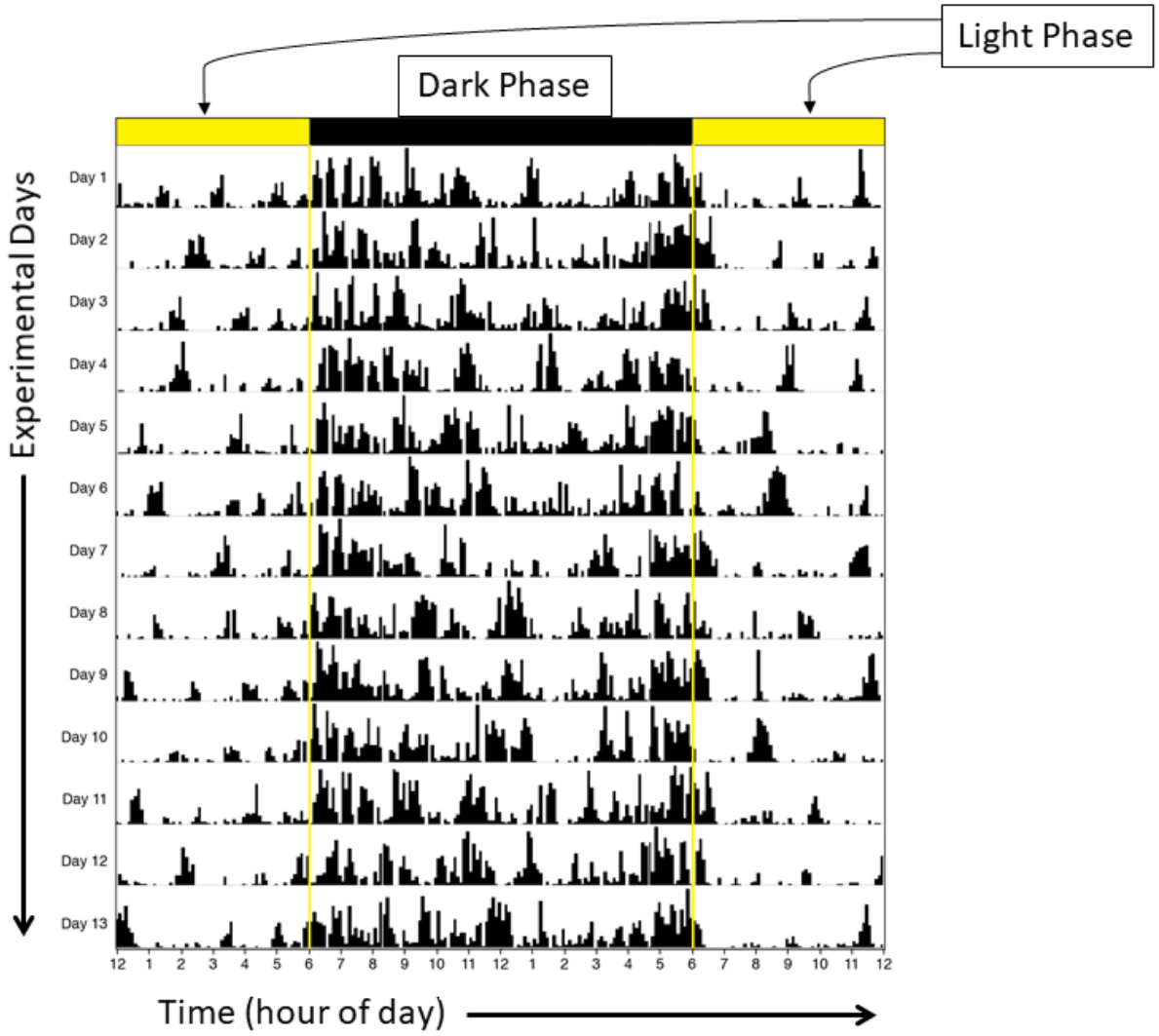

Figure 3 - 12:12 light:dark cycle actogram example
A raster plot of mouse locomotor activity. Time of the day is plotted on the x-axis, successive days are plotted on each row starting from the top; 24 hours of activity are plotted on each row. The higher the bar graphs indicates more activity during that time and day of the experiment. The mouse is held in 12 hours of light and 12 hours of darkness. For nocturnal rodents such as mice, the majority of the daily activity occurs during the dark phase.

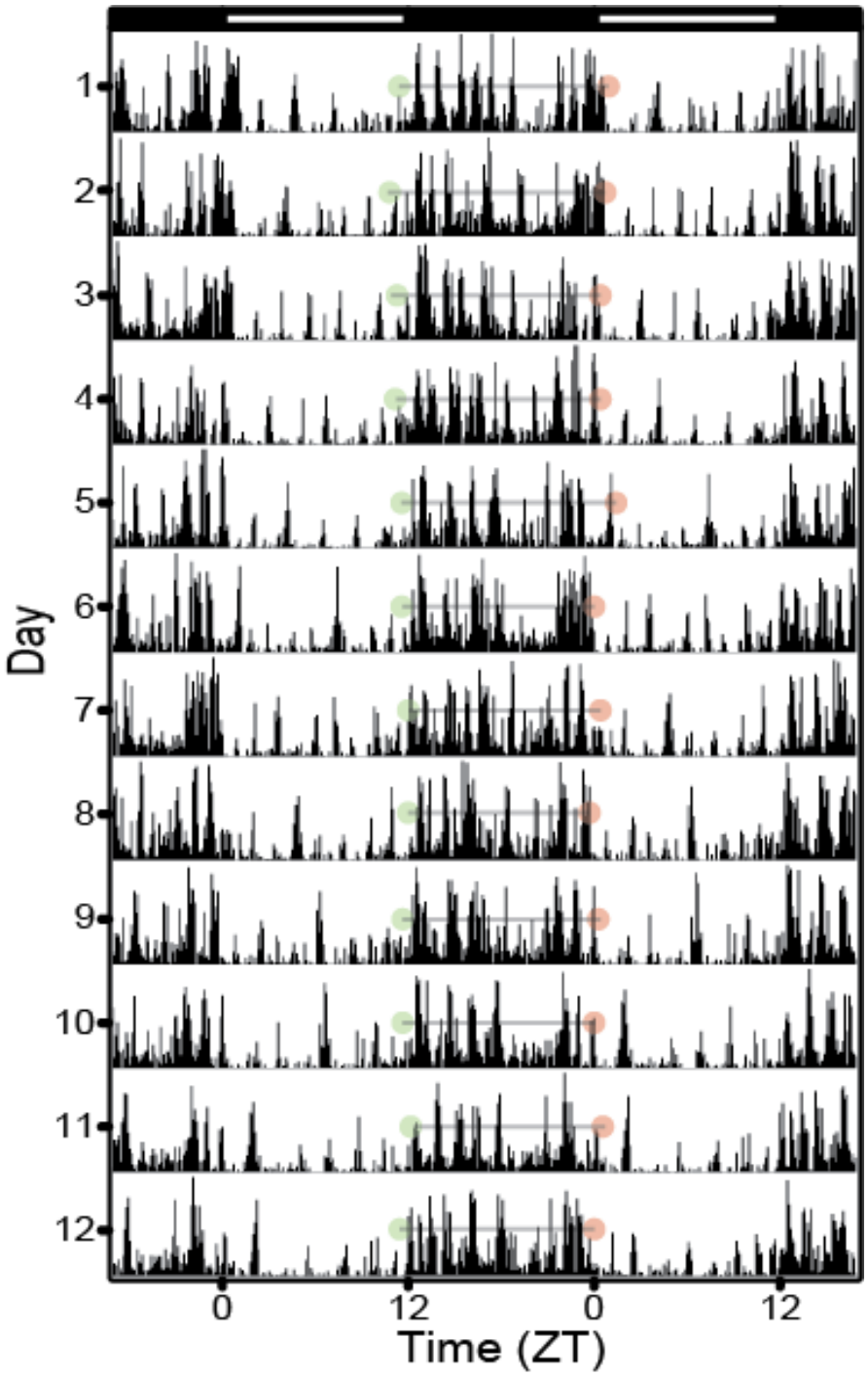

Figure 4 - Activity onset, activity offset, and alpha (α) duration visualization
Double-plotted actogram of mouse locomotor activity of a mouse housed in a 12:12 light:dark cycle. Each row contains 48 hours of locomotor activity data. The green circle indicates 'activity onset', the red circle indicates 'activity offset', and the black line spanning between activity onset and offset indicates alpha duration.

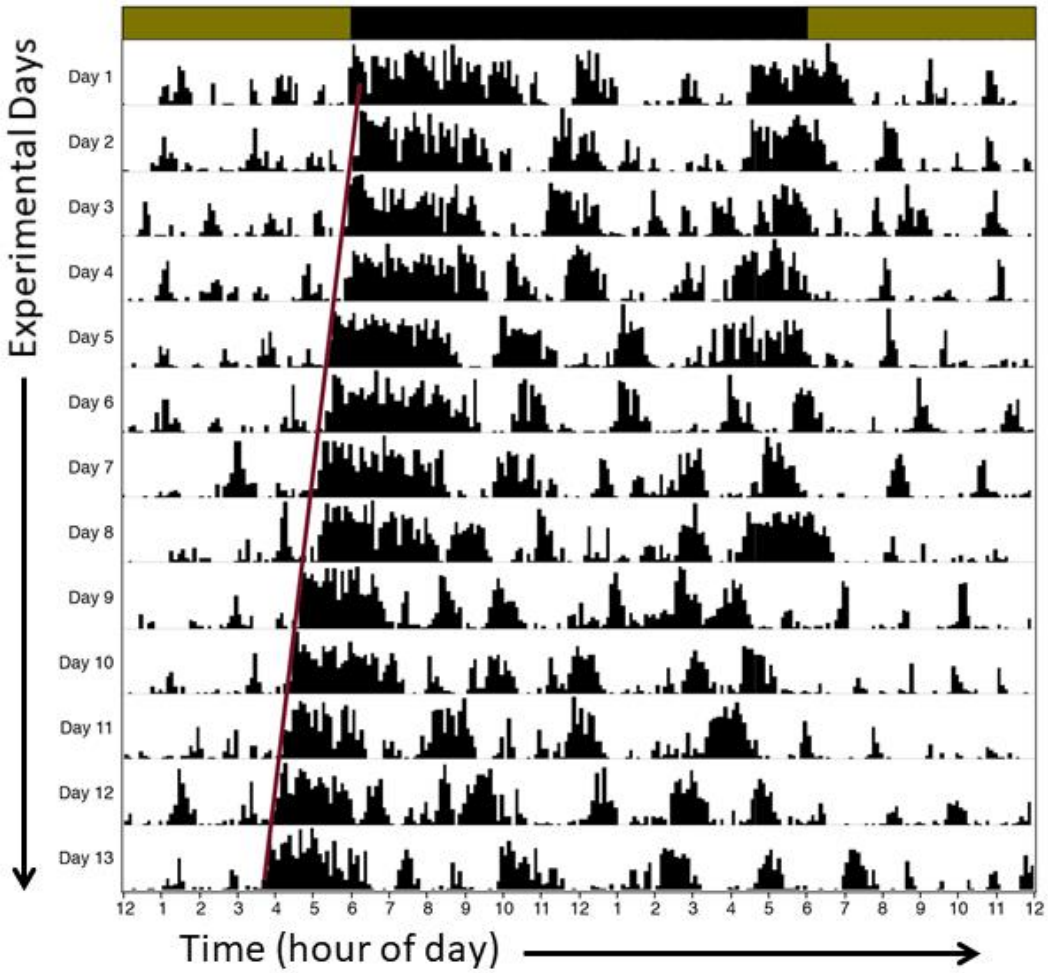

Figure 5 - Constant darkness actogram example
When mice are transferred a light:dark cycle into constant darkness, circadian rhythms drift out of phase with the outside world and "free run" with their own endogenous circadian clock speed (also called period or tau). The light:dark bar has a darker yellow shade, indicating the light:dark cycle the day prior to the mouse's release into constant darkness. By putting animals into constant darkness, it allows us to quantify one fundamental diagnostic feature of the circadian network: the speed of the clock or its period. The maroon line drawn is a least-means-squared fit to activity onset time. Note: in this example actogram, activity onset occurs earlier and earlier on consecutive days of the experiment; this earlier onset indicates a free-running period (or tau; τ) that is shorter than 24 hours.

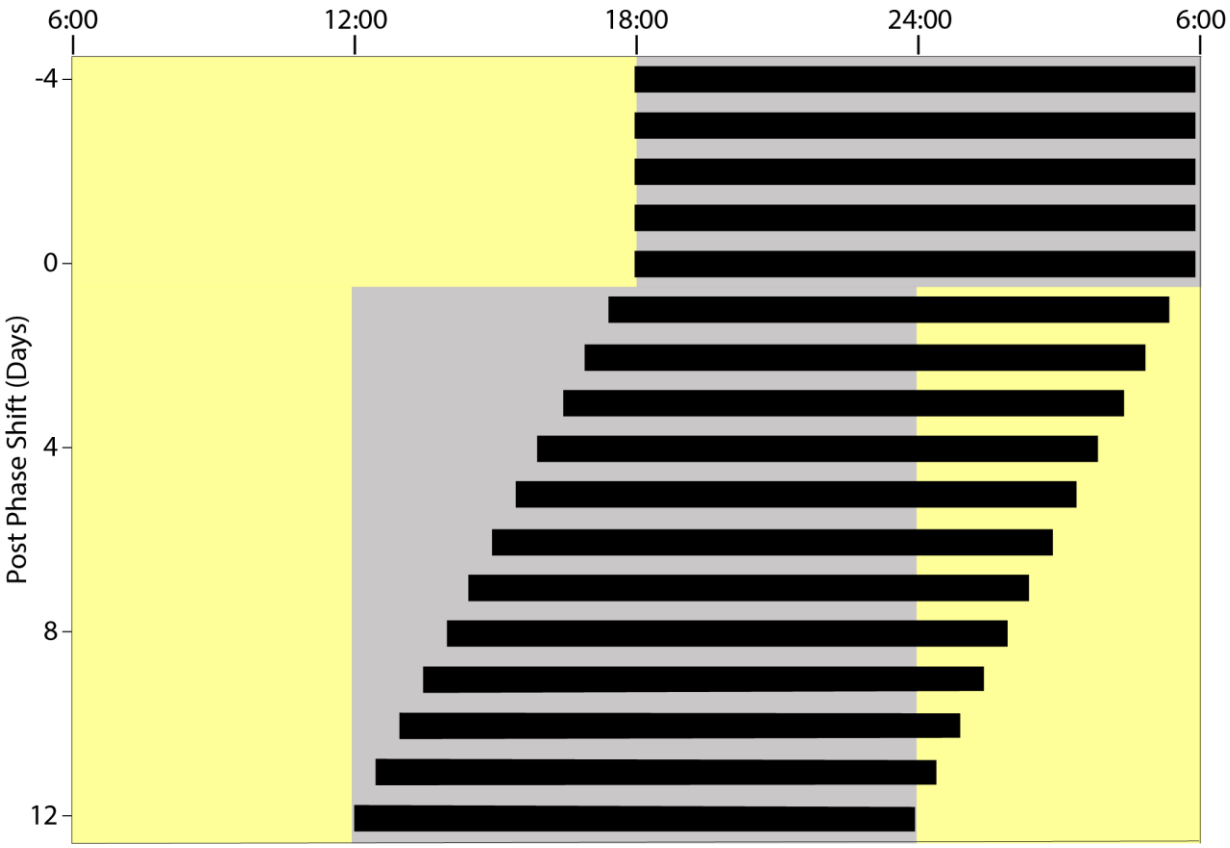

Figure 6 - Jet-lag manipulation schematic

To evaluate the speed at which the circadian system responds to shifts in the light:dark cycle, the light:dark cycle is shifted by 6-hours and the latency to shift to the onset of activity to the new photocycle is recorded. Each row represents another day of the experiment, the x-axis depicts time. In this paradigm, the dark phase is 6 hours earlier on the day of the shift.

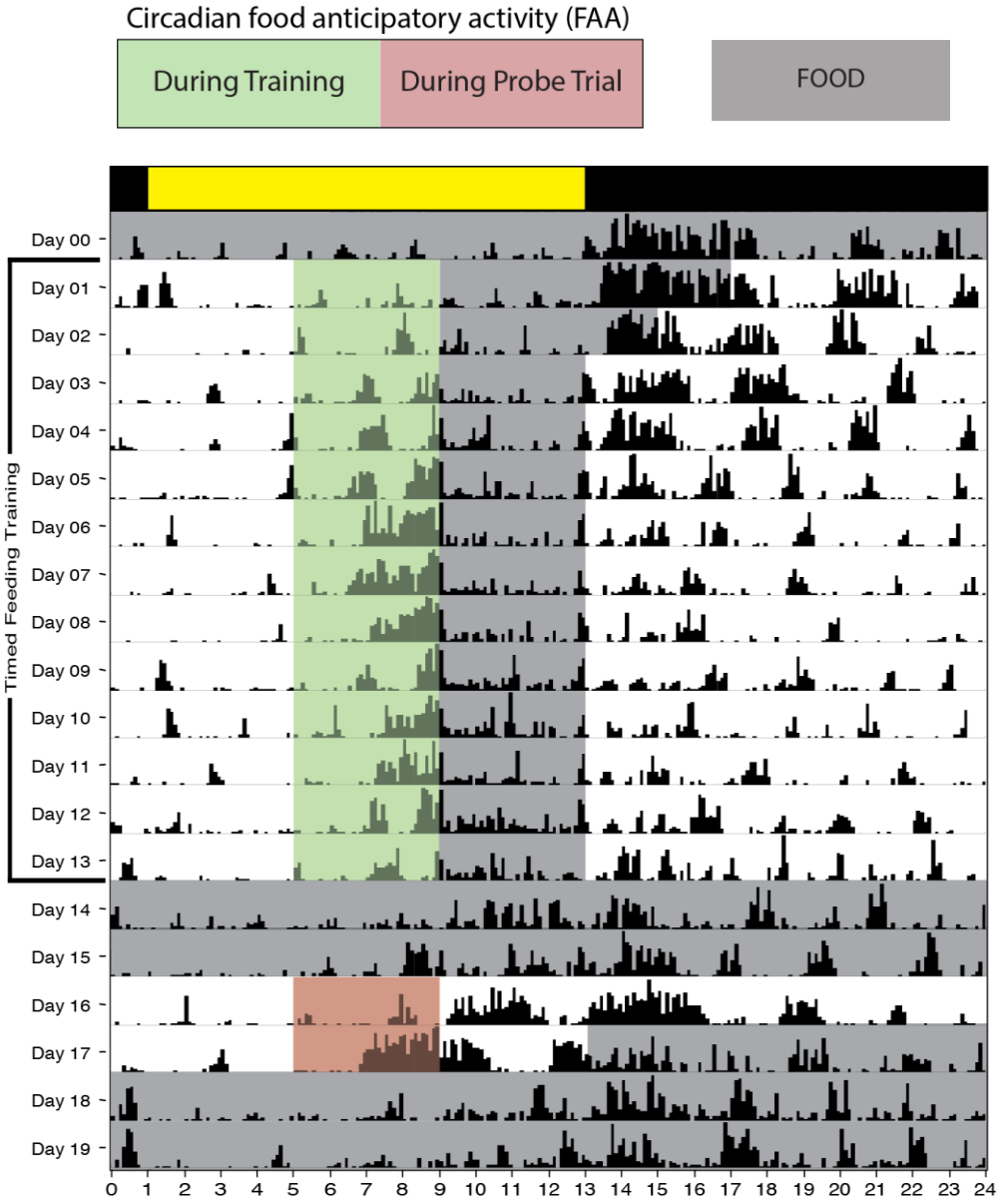

Figure 7 - Food anticipatory activity schedule

Representative actogram of the shift of activity during timed-feeding to elicit food anticipatory activity (FAA). On Day 0, food (grey shading) is available throughout the day and majority of locomotor activity is consolidated to the dark phase. On Day 1 of the experiment, food is available for 8 hrs. On Day 2, food is available for 6 hrs. On Days 3 through 13, food is available for 4 hrs of the light phase. As days of timed-feeding continue, more activity is observed prior to the delivery of food. FAA is calculated as a quotient of the total number of activity counts during the 3 hr FAA window on Day 17 divided by the sum of the total activity from the FAA's light phase and the following dark phase activity.

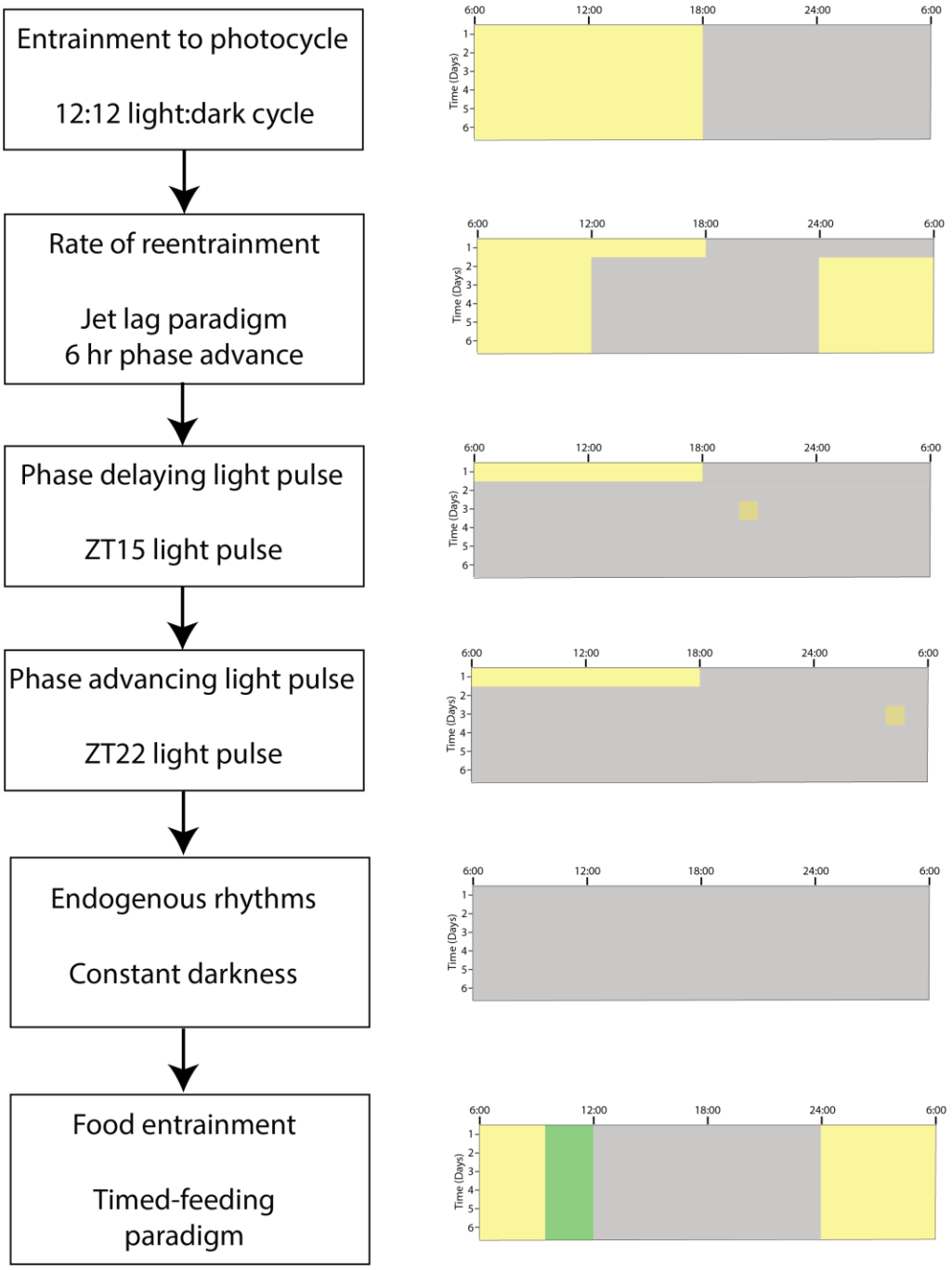

Figure 8 - Experimental timeline for round 1
In round 1: SPF mice fed normal chow (SPF-NC; n=10) and germ-free (GF) mice fed normal chow (GF-NC; n=8); 11 to 18 weeks of age at the start of 12:12 light:dark data collection began.

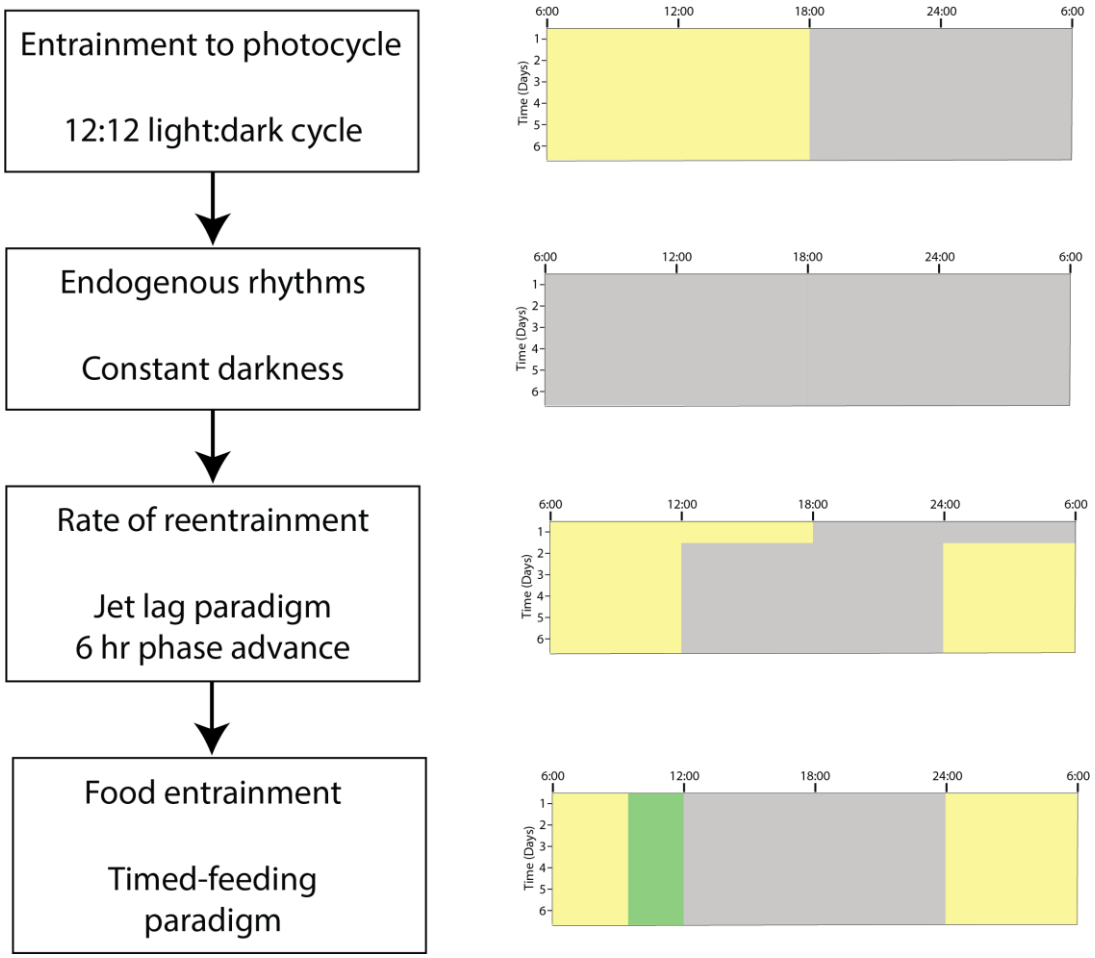

Figure 9 - Experimental timeline for round 2
In round 2: SPF-NC (n=8), SPF-HFD (n=8), GF-NC (n=8), GF-HFD (n=8), and conventionalized mice (ex-GF-NC; n=6), 17 to 24 weeks of age at the start of a 12:12 light:dark cycle data collection.

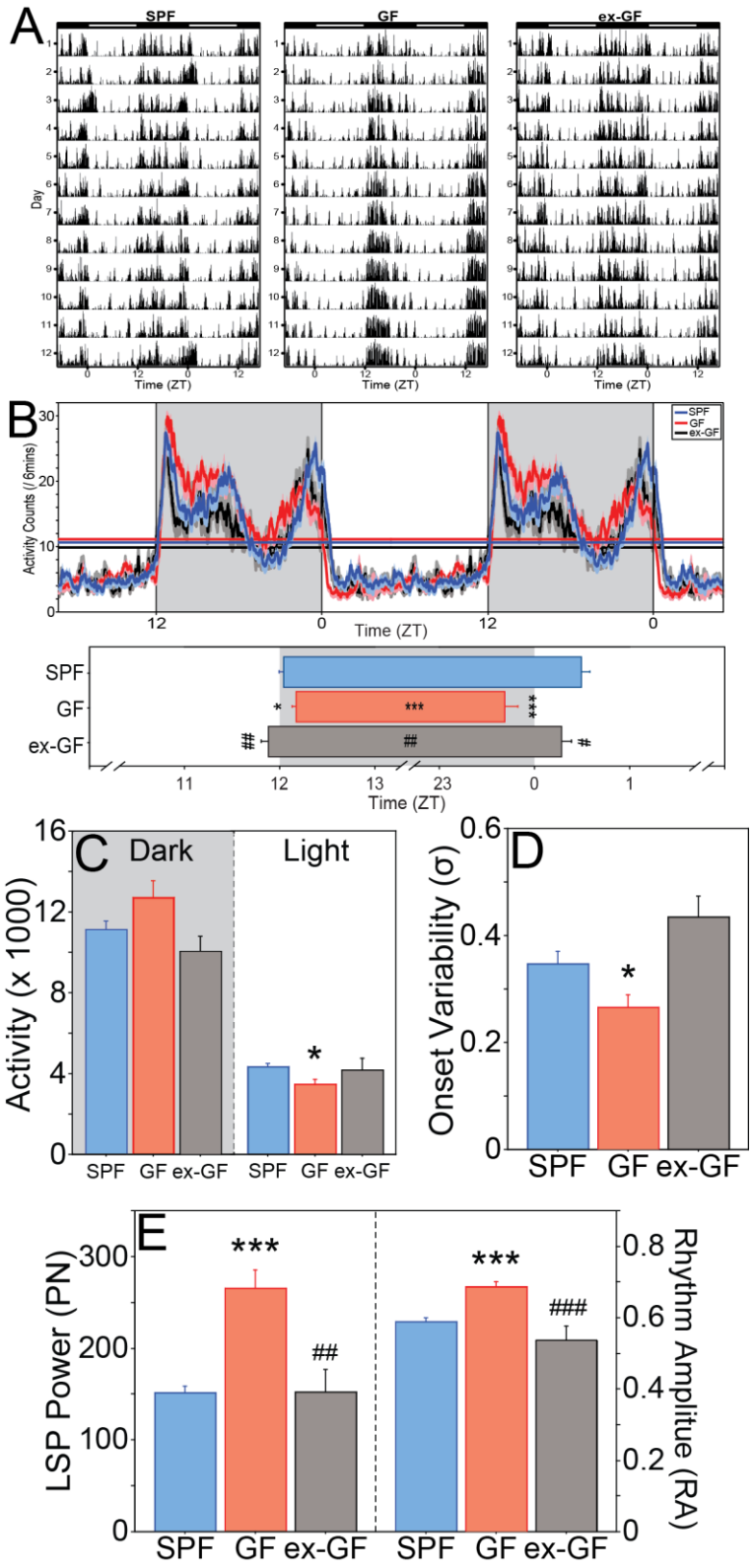

Figure 10 - Circadian rhythms in a 12:12 LD photocycle

Figure 10 - Circadian rhythms in a 12:12 LD photocycle (Continued)
(A) Double-plotted home cage locomotor activity (LMA) record of representative SPF (left panel), GF (middle panel) and ex-GF (right panel) mice housed in a 12L:12D photocycle (LD). Time is indicated on the horizontal axis, as are light (white) and dark (black) phases of the LD photocycle. (B) Double-plotted LMA waveform profile (mean ±SEM daily activity in 6 min bins) of SPF, GF, and ex-GF mice in LD (top panel); mean +SEM onset and offset of daily locomotor activity of SPF, GF and ex-GF mice in LD (bottom panel); onset and offset are represented by the beginning and end of each bar, respectively. (C) Mean +SEM total activity counts of SPF, GF and ex-GF mice in the dark (shaded) and light (unshaded) phases of the LD cycle. (D) Mean +SEM variability in activity onsets of SPF, GF and ex-GF mice in LD. (E) Mean +SEM circadian power (left panel) and rhythmic amplitude (right panel) of SPF, GF and ex-GF mice in LD. SPF: n=18; GF: n=16; ex-GF: n=6. *P<0.05, ***P<0.001 v SPF mice; #P<0.05, ##P<0.01, ###P<0.001 v GF mice.

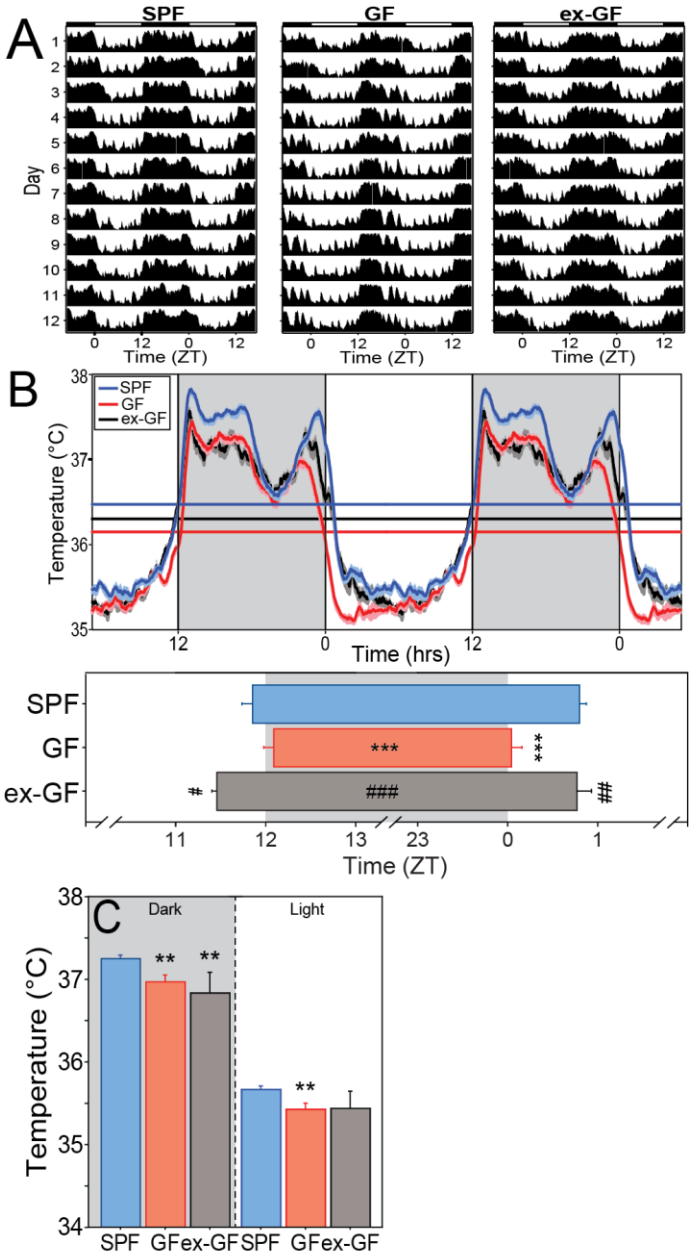

Figure 11 - Circadian rhythms and homeostatic maintenance of core body temperature depend on the microbiome

(A) Representative, double-plotted records of core body temperature (Tb) in SPF (left panel), GF (middle panel), and ex-GF (right panel) mice housed in in a 12L:12D photocycle (LD). Actogram annotations as in Fig. 2. (B) Double-plotted Tb waveform profile (mean ±SEM Tb at 6 min intervals) of SPF, GF, and ex-GF mice in LD (top panel); mean +SEM beginning and end of nightly elevated Tb in SPF, GF and ex-GF mice in LD (bottom panel). (C) Mean +SEM Tb of SPF, GF and ex-GF mice in the dark (shaded) and light (unshaded) phases of the LD cycle. SPF: n=18; GF: n=15; ex-GF: n=4. **P<0.01, ***<0.001 v SPF mice; #P<0.05, ##P<0.01, ###P<0.001 v GF mice.

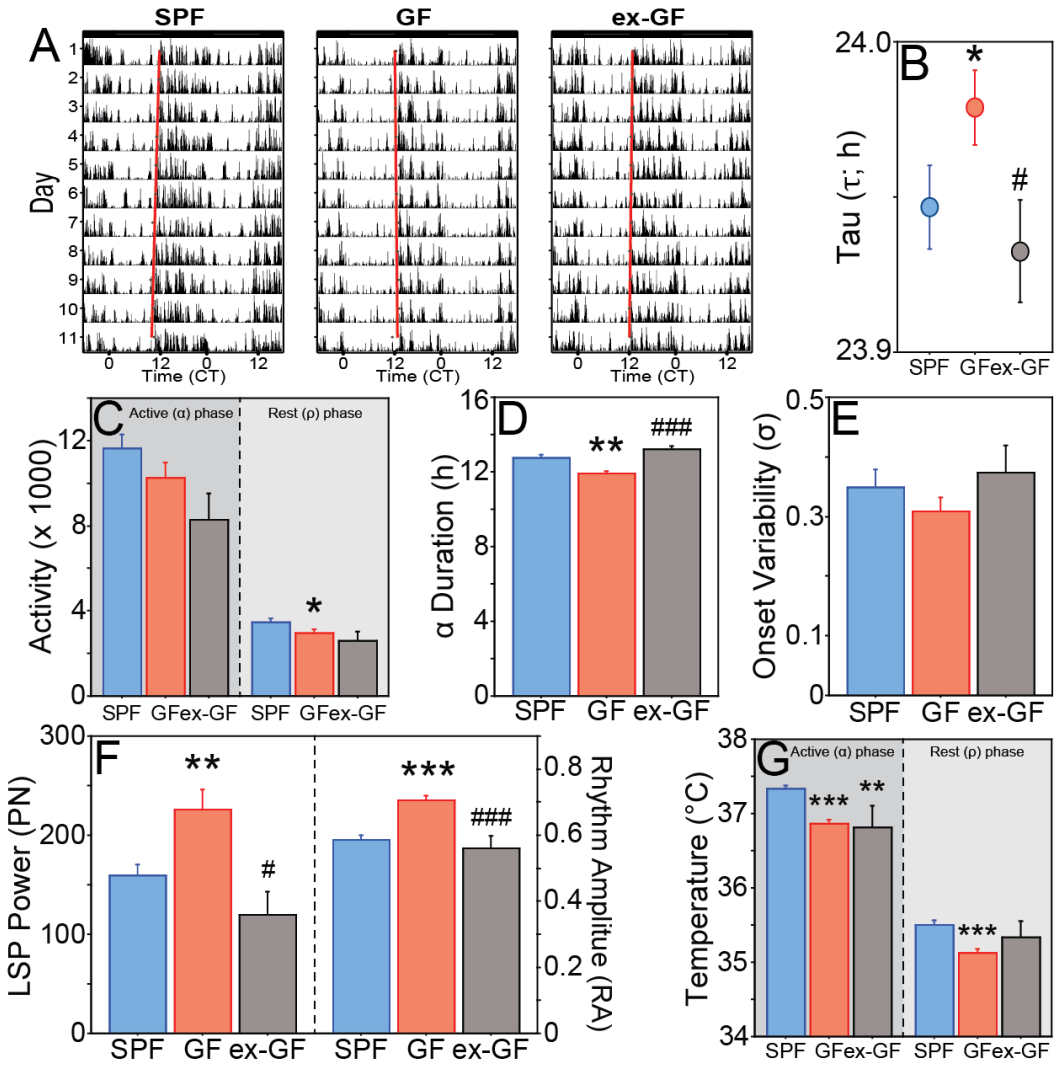

Figure 12 - Endogenous rhythms in constant darkness

(A) Representative, double-plotted home cage locomotor activity (LMA) record of SPF (left panel), GF (middle panel) and ex-GF (right panel) mice housed in continuous darkness (DD). Activity onsets are depicted with red circles, over which a regression line is plotted for the calculation of free-running circadian period (τ). (B) Mean ±SEM period (in h) of the free running circadian rhythm of LMA in DD. (C) Mean +SEM total activity counts during the subjective night (active phase; dark shading) and subjective day (inactive phase; lighter shading) of SPF, GF and ex-GF mice in DD. (D) Mean +SEM duration of the active phase during each circadian cycle (αLMA) of SPF, GF and ex-GF in DD. (E) Mean +SEM variability in activity onsets of SPF, GF and ex-GF mice in DD. (F) Mean +SEM circadian power (left panel) and rhythmic amplitude (right panel) of SPF, GF and ex-GF mice in DD. (G) Mean +SEM Tb of SPF, GF and ex-GF mice in DD during the subjective night (active phase; dark shading) and subjective day (inactive phase; lighter shading). LMA SPF: n=18; GF: n=16; ex-GF: n=5. Tb SPF: n=18; GF: n=15; ex-GF: n=4. *P<0.05, **P<0.01, ***P<0.001 v SPF mice; #P<0.05, ###P<0.001 v GF mice.

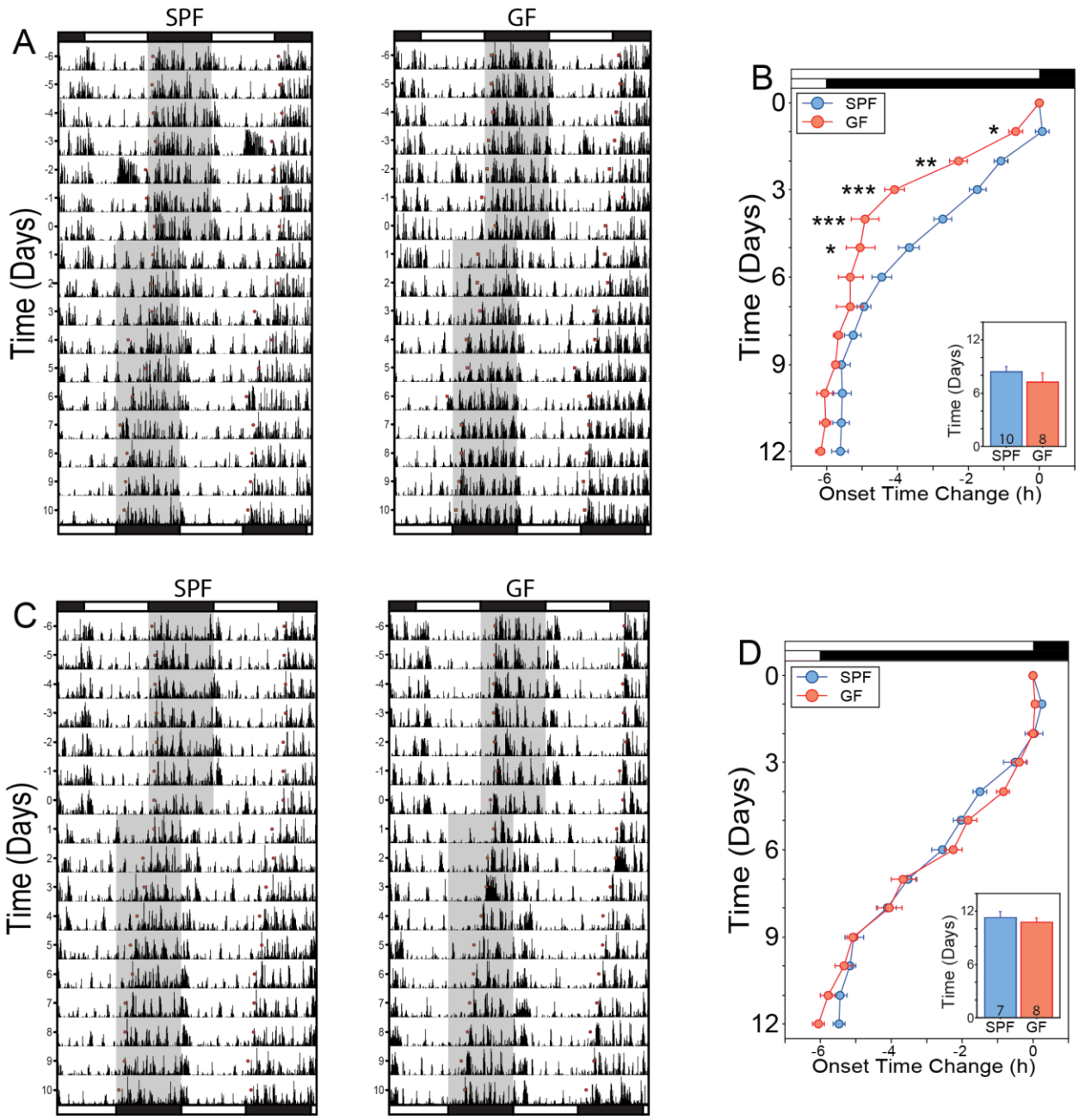

Figure 13 - Re-entrainment to phase advance of light:dark cycle

Data are depicted separately for the two experimental replication rounds. Round 1: panels A-B; Representative, double-plotted home cage activity (LMA) records of SPF (left record) and GF (right record) mice housed in a 12L:12D photocycle (LD) which was phase-advanced by 6 h via a shortening of the light phase on day 0 (ordinate axis). Round 2: panels C-D. Mean ±SEM activity onsets of SPF and GF mice immediately prior to (day 0) and following a 6 h advance shift of the photocycle; inset: mean +SEM number of days required to re-entrain to the 6 h shift for each round of the experiment. *P<0.05, **P<0.01, ***P<0.001 v corresponding SPF value.

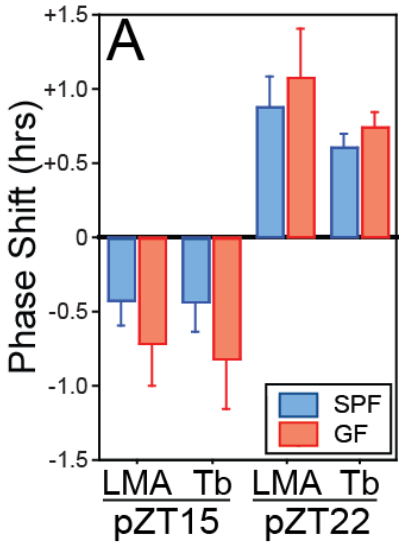

Figure 14 - Response to acute light pulses

(A) Circadian responses to photic Zeitgebers were evaluated using: (1) discrete pulses of light delivered 3 h or 10 h into the subjective night (projected Zeitgeber Time [pZT] in constant darkness at pZT15 and pZT22), which elicit phase advances and delays, respectively, in the circadian pacemaker. GF and SPF mice exhibited comparable delay (LMA, P>0.30; Tb, P>0.30) and advance (LMA, P>0.50; Tb, P>0.30) responses to acute light pulses at pZT15 and pZT22, respectively.

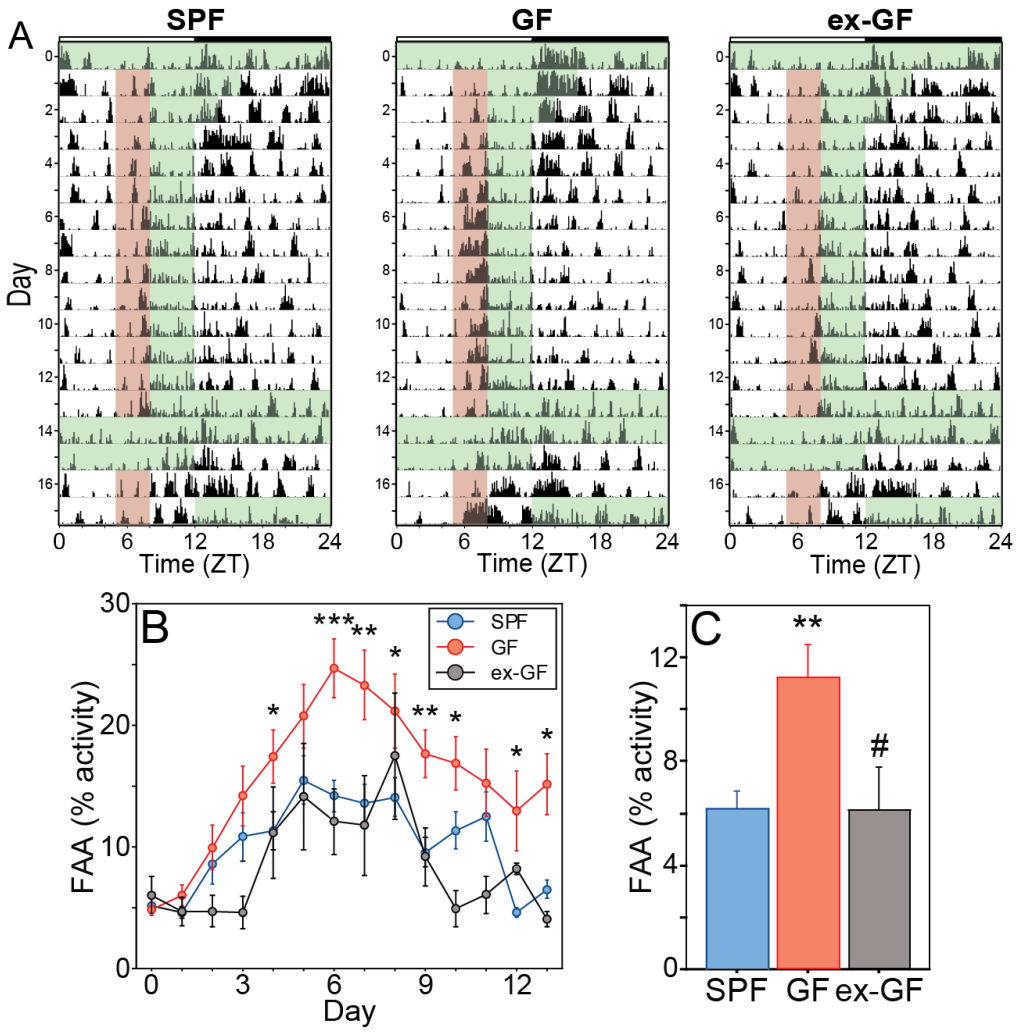

Figure 15 - Conventionalization of GF mice returns food anticipatory activity to SPF values
(A) Representative, single-plotted home cage locomotor activity (LMA) records of SPF (left panel), GF (middle panel), and ex-GF mice (right panel) subjected to the restricted feeding (RF) paradigm. Green shaded regions indicate intervals when food was available. Red shading indicates the 3 h interval of activity coded as food anticipatory activity (FAA), which emerged over the course of several days during RF. During the last 48 h of RF, mice were food deprived to elicit re-emergence of FAA (retention probe trial). (B) Mean ± SEM FAA of SPF, GF and ex-GF mice subjected to RF expressed as a percentage of total daily activity during the 10-12 days of RF. (C) Mean +SEM FAA on the 2nd day of the retention probe trial. SPF: n=18; GF: n=16; ex-GF: n=6. *P<0.05, **P<0.01, ***P<0.001 vs SPF mice; #P<0.05 v GF mice.

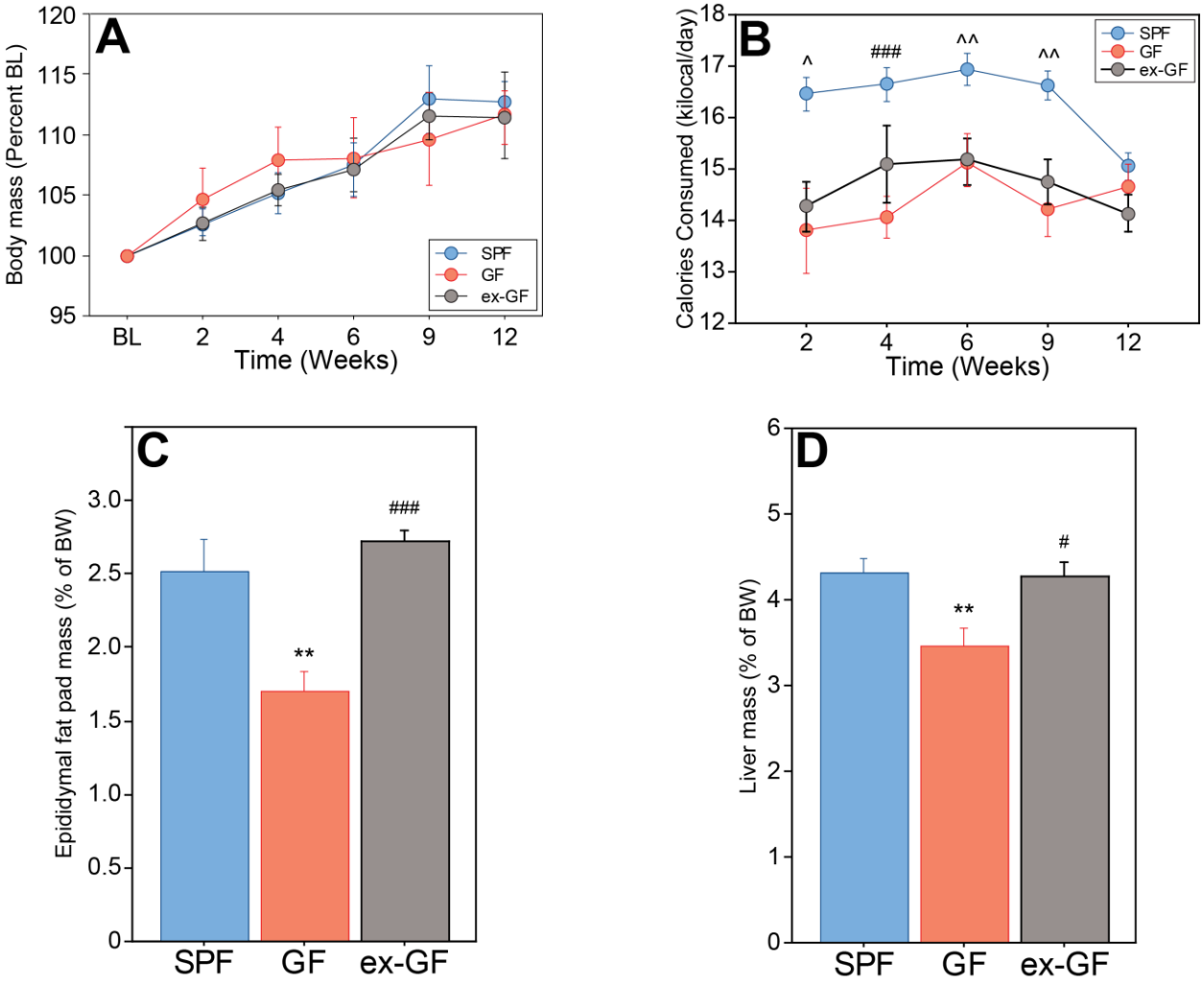

Figure 16 - Conventionalization of GF mice in ex-GF mice restores SPF values of physiology and behavior in previously GF mice

(A) No differences in body mass change from baseline were observed between SPF, GF, and ex-GF mice. (B) Ex-GF mice showed intermediate food consumption between SPF and GF mice. GF mice ate less compared to SPF mice. (C) Epididymal fat pad mass did not differ between SPF and ex-GF mice. Fat pad mass of GF mice weighed less than SPF and ex-GF mice. (D) Liver mass did not differ between SPF and ex-GF mice. Livers of GF mice weighted less than SPF and ex-GF mice. ^P<0.05, ^^P<0.01, ^^P<0.001 v GF and ex-GF. *P<0.05, **P<0.01, ***P<0.001 v SPF mice. #P<0.05, ###P<0.001 v GF mice.

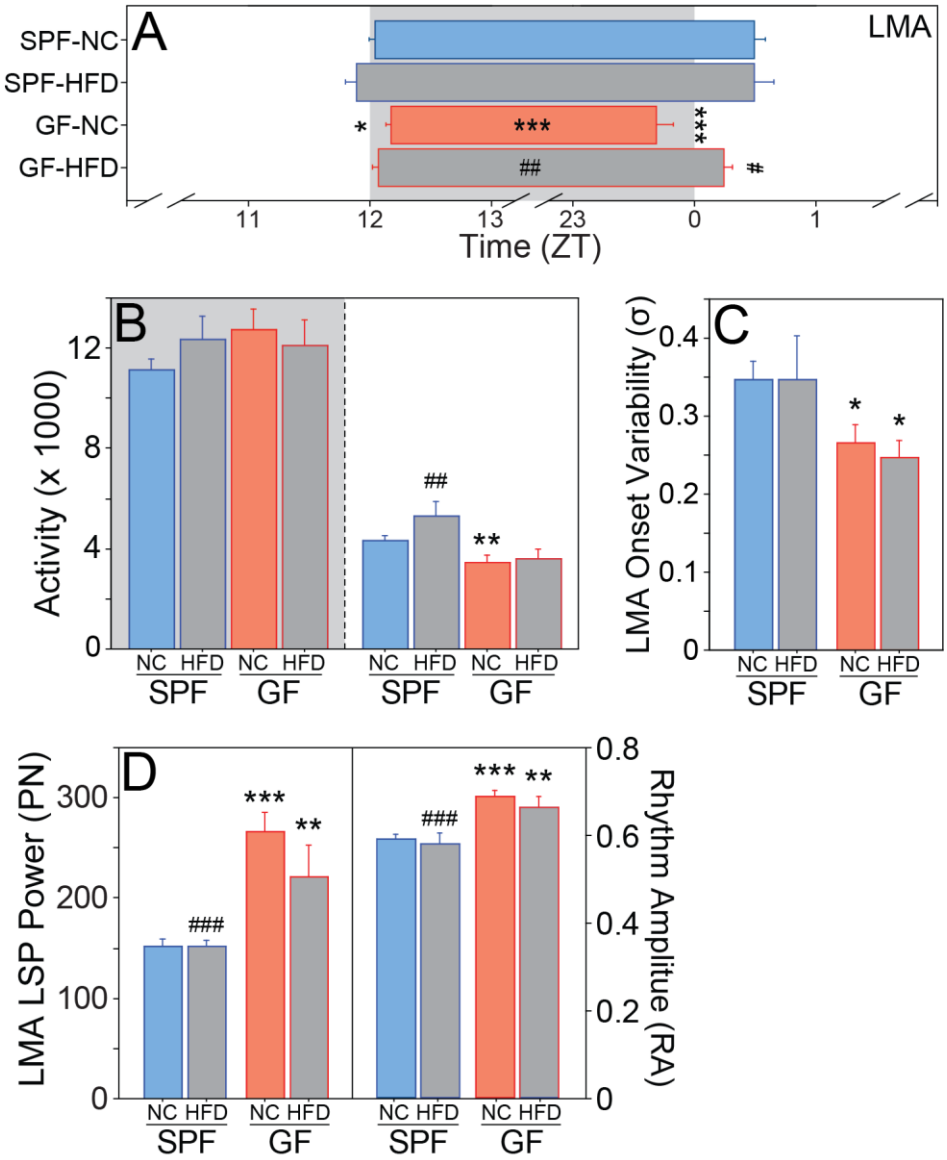

Figure 17 - High fat diet influences circadian rhythms in a 12:12 LD photocycle
(A) Onset and offset are represented by the beginning and end of each bar, respectively. (B) Mean +SEM total activity counts of SPF and GF mice fed a high fat diet (HFD) or normal chow (NC) in the dark (shaded) and light (unshaded) phases of the LD cycle. (C) Mean +SEM variability in activity onsets of mice fed different diets in LD. (D) Mean +SEM circadian power (left panel) and rhythmic amplitude (right panel) of mice LD. SPF-NC: n=18; SPF-HF: n=8; GF-NC: n=16; GF-HFD: n=8. *P<0.05, **P<0.01, ***P<0.001 v SPF mice; #P<0.05, ##P<0.01, ###P<0.001 v GF mice.

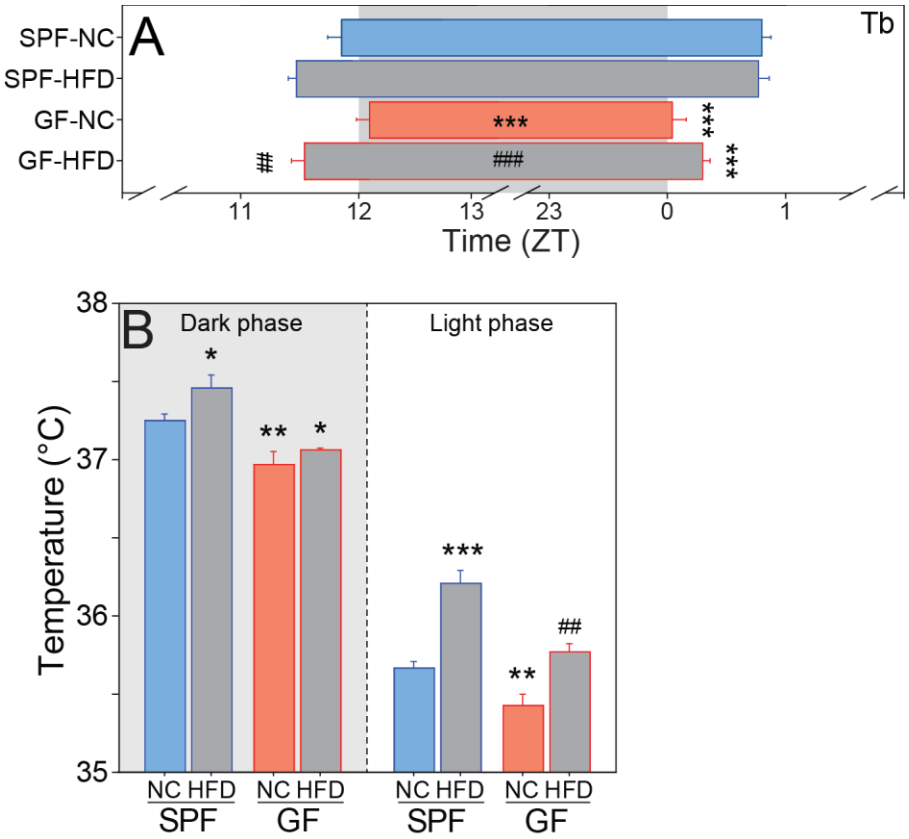

Figure 18 - Circadian rhythms and core body temperature are altered by diet, independent of microbiome

(A) Mean +SEM beginning and end of nightly elevated Tb in mice fed either NC or HFD in LD. (B) Mean +SEM Tb of SPF and GF mice fed either NC or HFD in the dark (shaded) and light (unshaded) phases of the LD cycle. SPF-NC: n=18; SPF-HFD: n=8; GF-NC: n=15; GF-HFD: n=7. *P<0.05, **P<0.01, ***<0.001 v SPF-NC mice; ##P<0.01, ###P<0.001 v GF-NC mice.

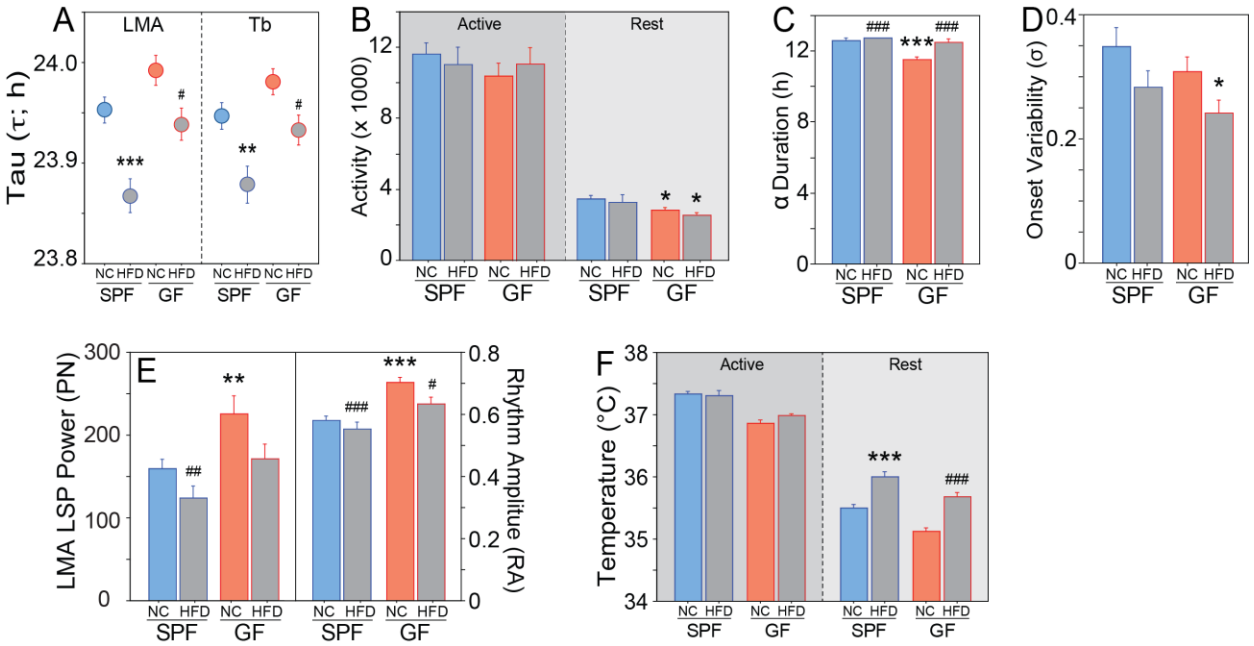

Figure 19 - High fat diet influences endogenous circadian rhythms in a constant darkness
(A) Mean ±SEM period (in h) of the free running circadian rhythm of LMA and Tb in DD. (B) Mean +SEM total activity counts during the subjective night (active phase; dark shading) and subjective day (inactive phase; lighter shading) of mice in DD. (C) Mean +SEM duration of the active phase during each circadian cycle (αLMA) of mice in DD. (D) Mean +SEM variability in activity onsets of mice in DD. (E) Mean +SEM circadian power (left panel) and rhythmic amplitude (right panel) of mice in DD. (F) Mean +SEM Tb of mice in DD during the subjective night (active phase; dark shading) and subjective day (inactive phase; lighter shading). SPF-NC: n=18; SPF-HFD: n=8; GF-NC: n=15-16; GF-HFD: n=7. *P<0.05, **P<0.01, ***<0.001 v SPF-NC mice; #P<0.05, ##P<0.01, ###P<0.001 v GF-NC mice.

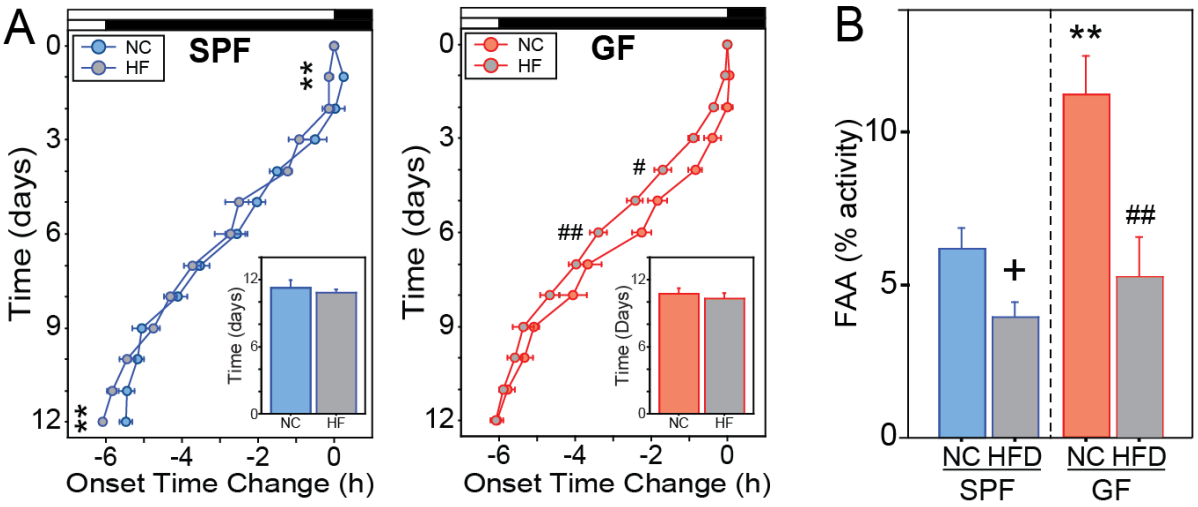

Figure 20 - High fat diet in jet-lag paradigm and food anticipatory activity
(A) Mean ±SEM activity onsets prior to (day 0) and following a 6 h advance shift of the photocycle of SPF (left panel) and GF (right panel) mice fed NC or HFD; insets: mean +SEM number of days required to re-entrain to the 6 h shift. (B) Mean +SEM food anticipatory activity (FAA) on the 2nd day of the retention probe trial of SPF and GF fed NC or HFD while subjected to the RF regimen. SPF-NC: n=8-18; SPF-HF: n=7-8; GF-NC: n=8-16; GF-HF: n=7. +P=0.059, *P<0.05, **P<0.01 v SPF-NC mice; #P<0.05, ##P<0.01 v GF-NC mice.

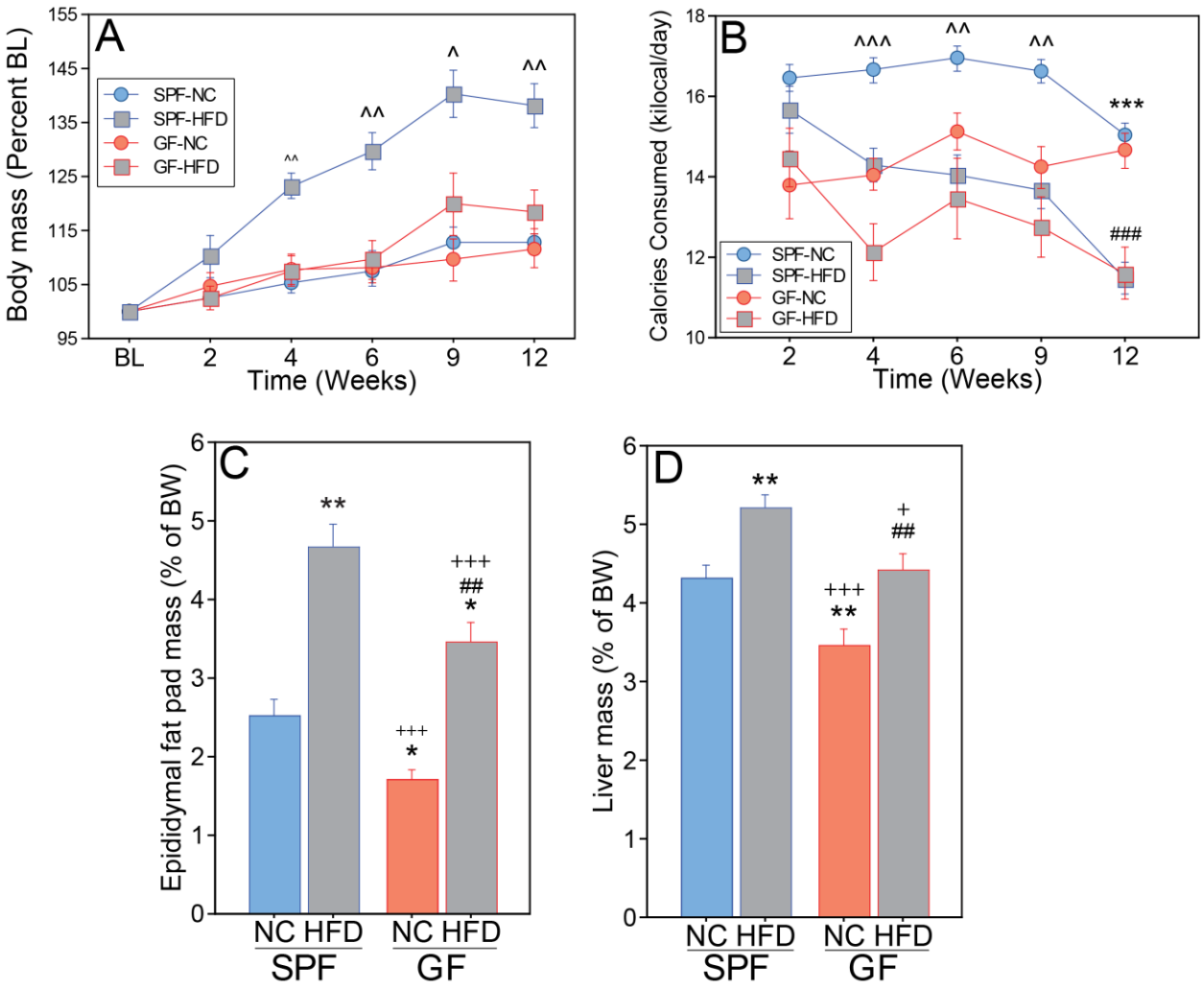

Figure 21 - Somatic, ingestive and physiological responses to high fat diet
Somatic, ingestive and physiological responses to high fat diet (HFD) depend on commensal microbes. (A) Mean ±SEM body masses indicate that SPF-HFD mice gained more weight compared to all other groups over the course of the experiment. Body mass did not differ from baseline between SPF, GF or ex-GF mice during the observation interval ($F_{2,95}$=0.02; P>0.90). (B) Mean ±SEM calorie intake data indicate that SPF-NC and GF-NC mice consumed more calories than SPF-HFD and GF-HFD, respectively. SPF mice consumed more kilocalories as compared to GF mice throughout the observation period ($F_{2,76}$=13.8; P<0.0001). (C) Mean +SEM epididymal fat, and (D) liver mass data indicate that the magnitude of HFD-induced increases in adiposity and hepatic hypertrophy were attenuated in GF mice. When normalized to terminal body mass, GF mice exhibited significantly lower epididymal fat pad and liver masses relative to those of SPF mice (P<0.01, P<0.01, respectively), and ex-GF mice were comparable to SPF mice (P>0.40; P>0.80; respectively). SPF-NC: n=13; SPF-HF: n=8; GF-NC: n=12; GF-HFD: n=7. ^P<0.05, ^^P<0.01 vs all other groups; **P<0.01, ***P<0.001 v SPF-NC; #P<0.05, ###P<0.001 v GF-NC; +P<0.05, +++P<0.001 v SPF-HFD.

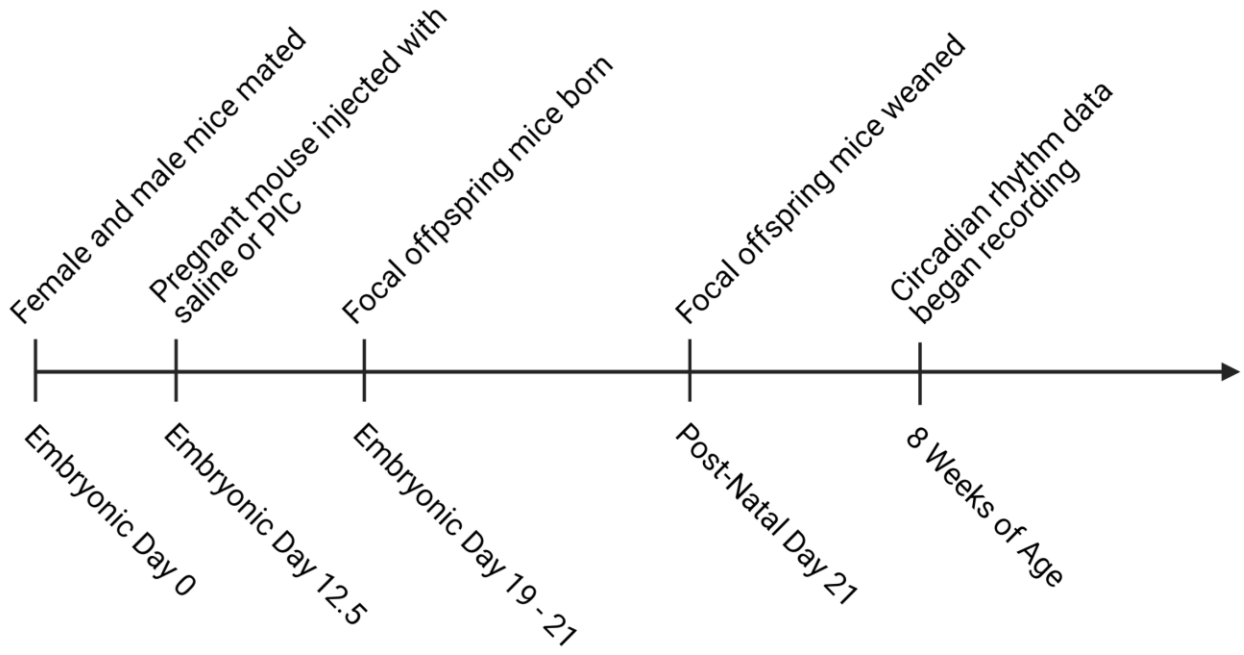

Figure 22 - Maternal immune activation timeline
Timeline for generating control and MIA offspring. Embronic day 0 is the day of mating. On embryonic day 12.5 (E12.5), pregnant female mice are injected with with saline (control group; 0.9% salt in physiological water) or PIC (experimental group; immunostimulant). The focal mice of this study are the offspring of injected pregnant female mice. Circadian recordings were performed in adult offspring mice. Made using BioRender.com.

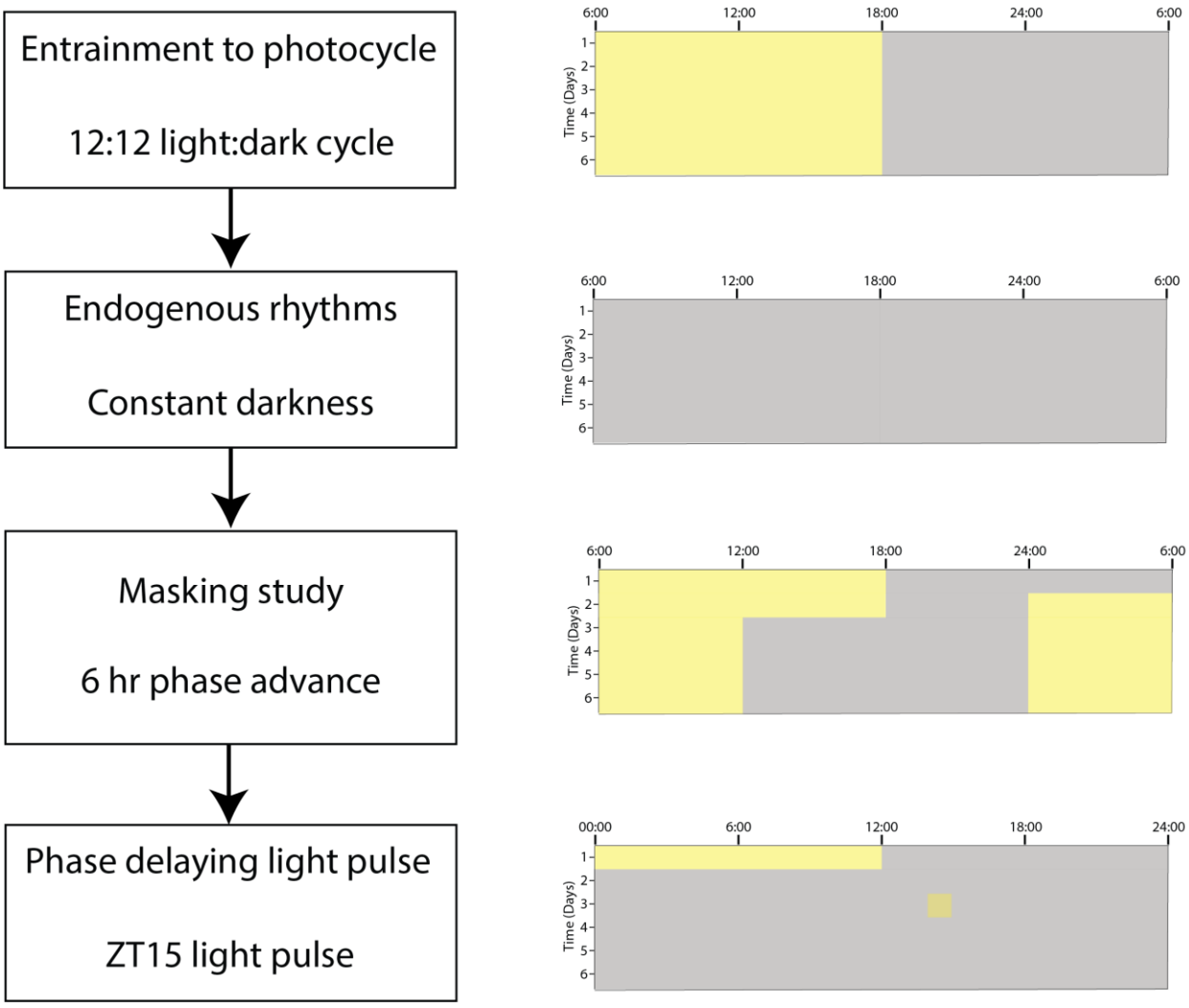

Figure 23 - Experimental Timeline

Female-JAX-saline, n=10; Female-Tac-saline, n=18; Male-JAX-saline, n=17; Male-Tac-saline, n=23; Female-JAX-MIA, n=12; Female-Tac-MIA, n=13; Male-JAX-MIA, n=9; Male-Tac-MIA, n=17.

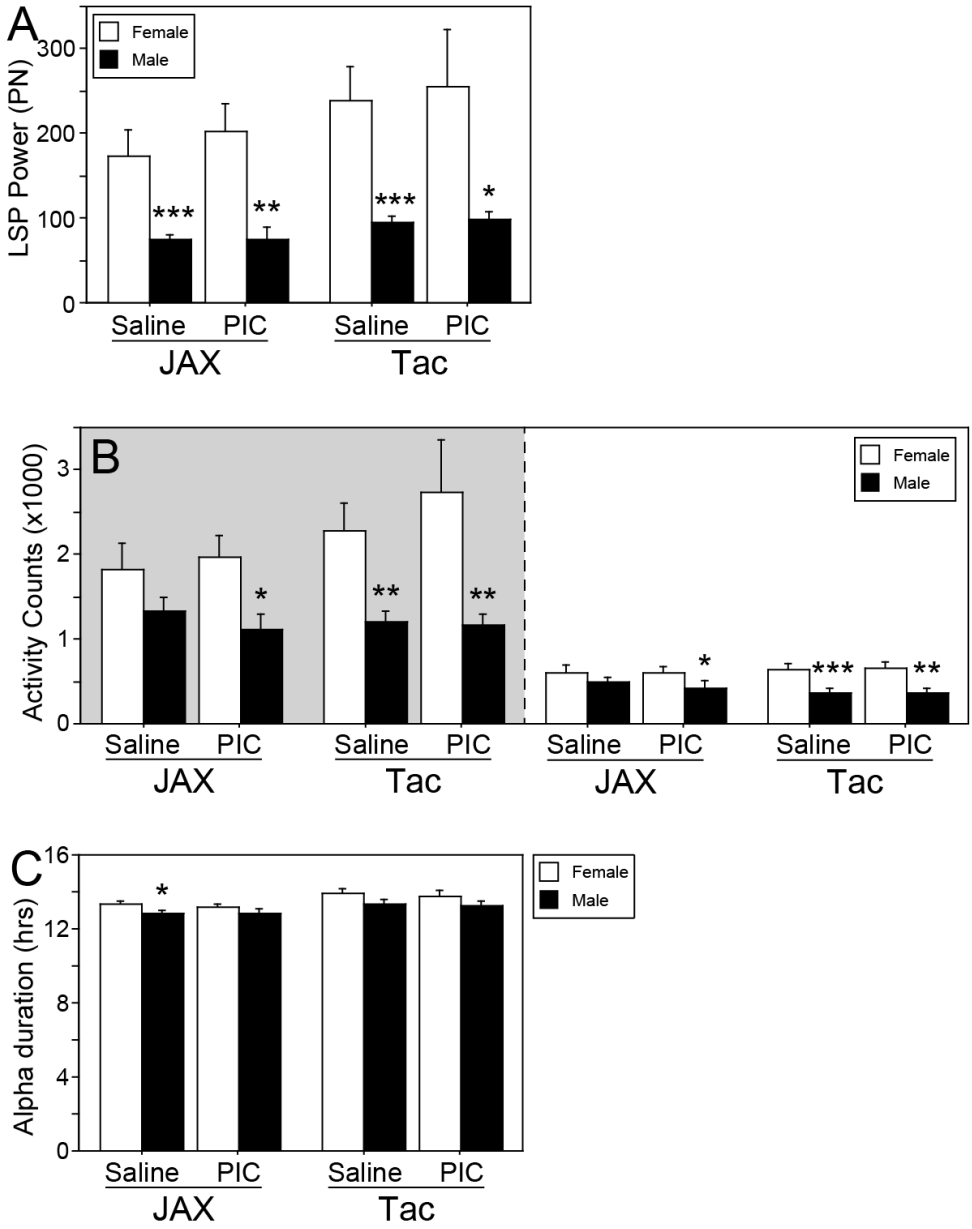

Figure 24 - Entrainment to 12:12 light:dark cycle

(A) Lomb-Scargle periodogram (LSP) showed a main effect of sex, where females possessed greater circadian power compared to males ($F_{1,106}$=37.731, p<0.0001), without effect of MIA ($F_{1,106}$=0.343, p>0.50) or vendor ($F_{1,106}$=5.87, p>0.05). A main effect of sex observed in the active phase (sex: $F_{1,106}$=24.343, p<0.0001; MIA: $F_{1,106}$=0.168, p>0.60; vendor: $F_{1,106}$=1.996, p>0.10) counts and dark phase (sex: $F_{1,106}$=19.142, p<0.0001; MIA: $F_{1,106}$=0.052, p>0.80; vendor: $F_{1,106}$=0.155, p>0.60) counts. (C) Females showed a longer alpha phase duration (hours of active phase) compared to males ($F_{1,106}$=7.723, p<0.01); and Tac mice showed a longer alpha compared to JAX mice ($F_{1,106}$=10.379, p<0.01); without effect of MIA ($F_{1,106}$=0.562, p>0.40). *P<0.05, **P<0.01, ***P<0.001 v sex-matched group.

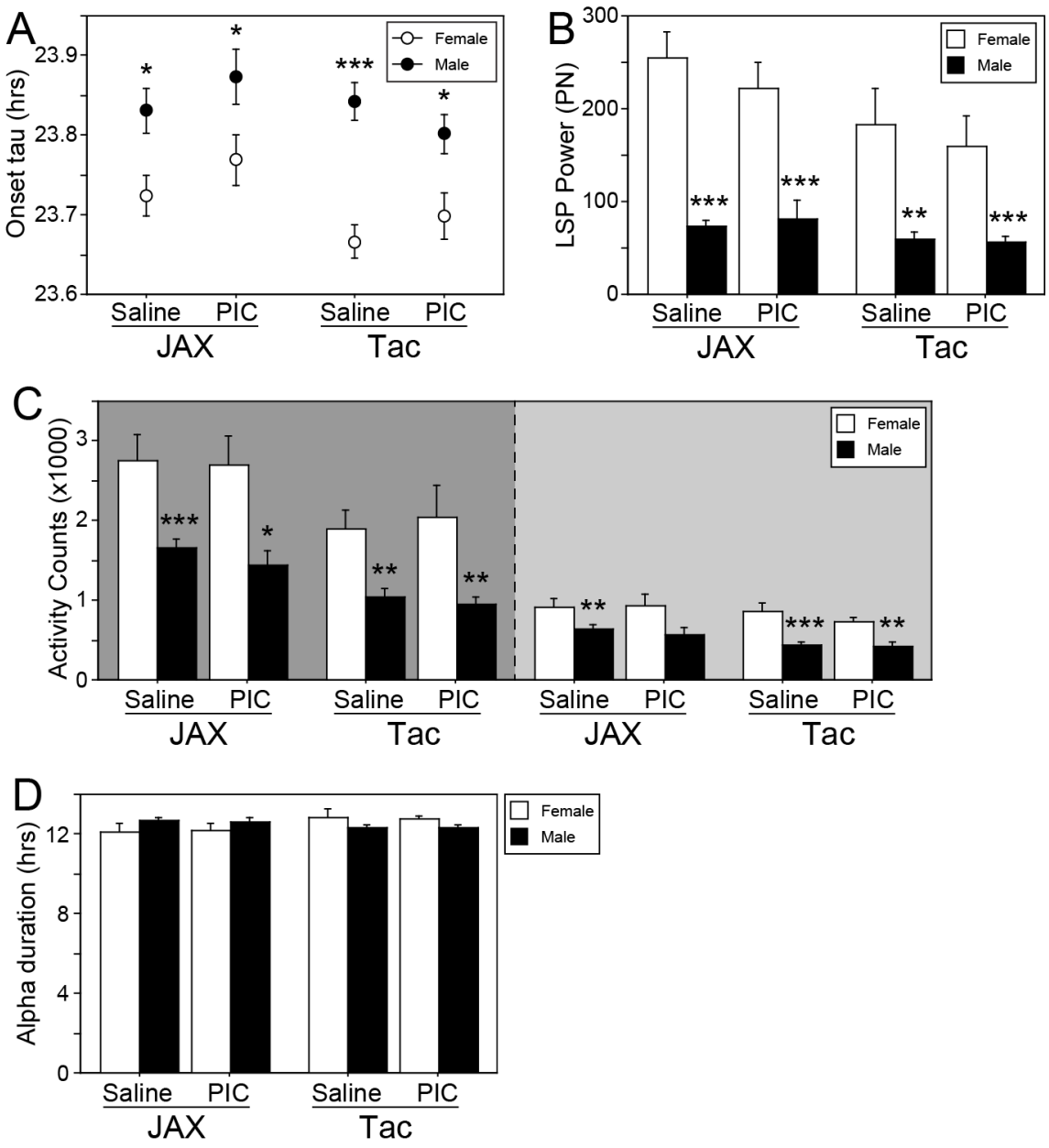

Figure 25 - Endogenous circadian rhythms in constant darkness

(A) A main effect of vendor was observed in tau (free-running period in constant darkness) where JAX mice had a longer tau compared to Tac mice ($F_{1,104}$=4.714, $p<0.05$), without effect of MIA ($F_{1,104}$=3.756, $p>0.05$) or sex ($F_{1,104}$=1.918, $p>0.10$). (B) LSP circadian power was greater in JAX mice compared to Tac mice ($F_{1,104}$=6.367, $p<0.05$). Females showed increased circadian power compared to males ($F_{1,104}$=65.772, $p<0.0001$), without effect of MIA ($F_{1,104}$=0.574, $p=0.4505$). (C) A main effect of sex was observed in the active phase counts (sex: $F_{1,104}$=39.227, $p<0.0001$; MIA: $F_{1,104}$=0.006, $p>0.90$; vendor: $F_{1,104}$=15.046, $p=0.0002$) and dark phase counts (sex: $F_{1,104}$=28.197, $p<0.0001$; MIA: $F_{1,104}$=0.083, $p>0.70$; vendor: $F_{1,104}$=5.010, $p<0.05$). (D) Alpha duration in constant darkness did not have a main effect on any the three factors (sex:

Figure 25 - Endogenous circadian rhythms in constant darkness (continued)
$F_{1,104}$=0.0001, p>0.90; MIA: $F_{1,104}$=0.004, p>0.90; vendor: $F_{1,104}$=0.806, p>0.30). *P<0.05, **P<0.01, ***P<0.001 v sex-matched group.

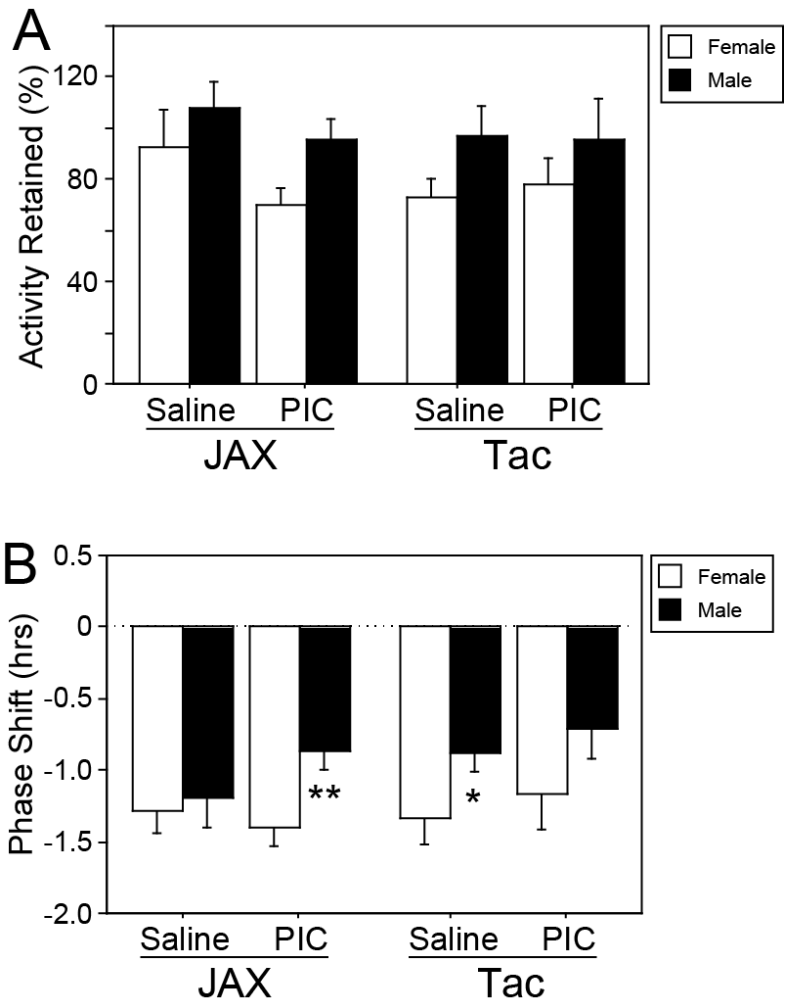

Figure 26 - Masking effect of light and acute light pulse

(A) No differences in masking effects of a shifted photocycle were observed. Decreases in activity as a result of light exposure during a time when mice expected darkness did not differ between groups (sex: $F_{1,105}=5.477$, $p<0.05$; MIA: $F_{1,105}=0.827$, $p>0.30$; vendor: $F_{1,105}=0.388$, $p>0.50$). (B) The acute light pulse at ZT15 was without effect by vendor ($F_{1,105}=1.373$, $p=0.2439$) or MIA ($F_{1,105}=0.3185$). However, female mice showed a greater magnitude phase delay compared to male mice ($F_{1,105}=7.814$, $p<0.01$). *P<0.05, **P<0.01, v sex-matched group.

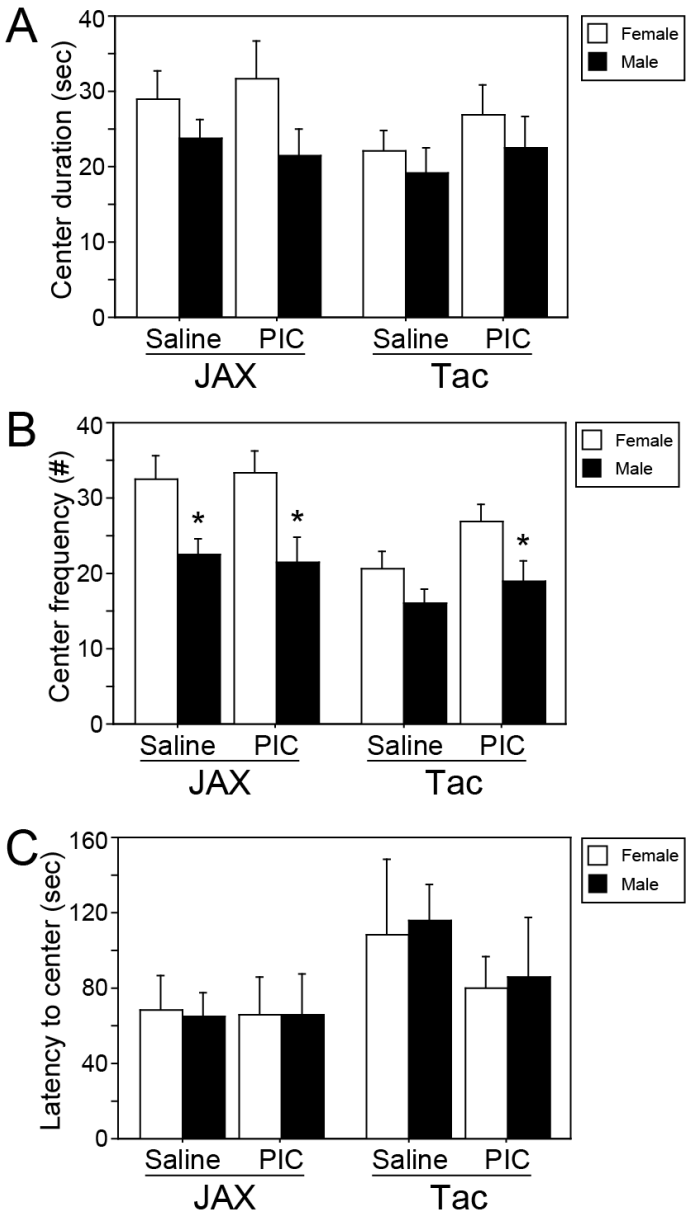

Figure 27 - Open field test

(A) Female mice spent more time inside the center arena compared to male mice (sex: $F_{1,103}=4.305$, $p<0.05$; MIA: $F_{1,103}=0.620$, $p>0.40$, vendor: $F_{1,103}=1.970$, $p>0.10$). In the OFT, more time spent in the center of the arena is interpreted as more exploratory behavior or less anxiety-related behavior. (B) Number of entries into the center were also greater in female mice compared to male mice (sex: $F_{1,103}=21.227$, $p<0.0001$), with a main effect of vendor where JAX mice showed more entries into the center compared to Tac mice (vendor: $F_{1,103}=13.614$, $p<0.001$; MIA: $F_{1,103}=1.443$, $p>0.20$). (C) No differences in latency to enter the center area were observed (sex: $F_{1,103}=0.018$, $p>0.80$; vendor: $F_{1,103}=2.602$, $p>0.10$; MIA: $F_{1,103}=0.627$, $p>0.40$). *$P<0.05$ v sex-matched group.

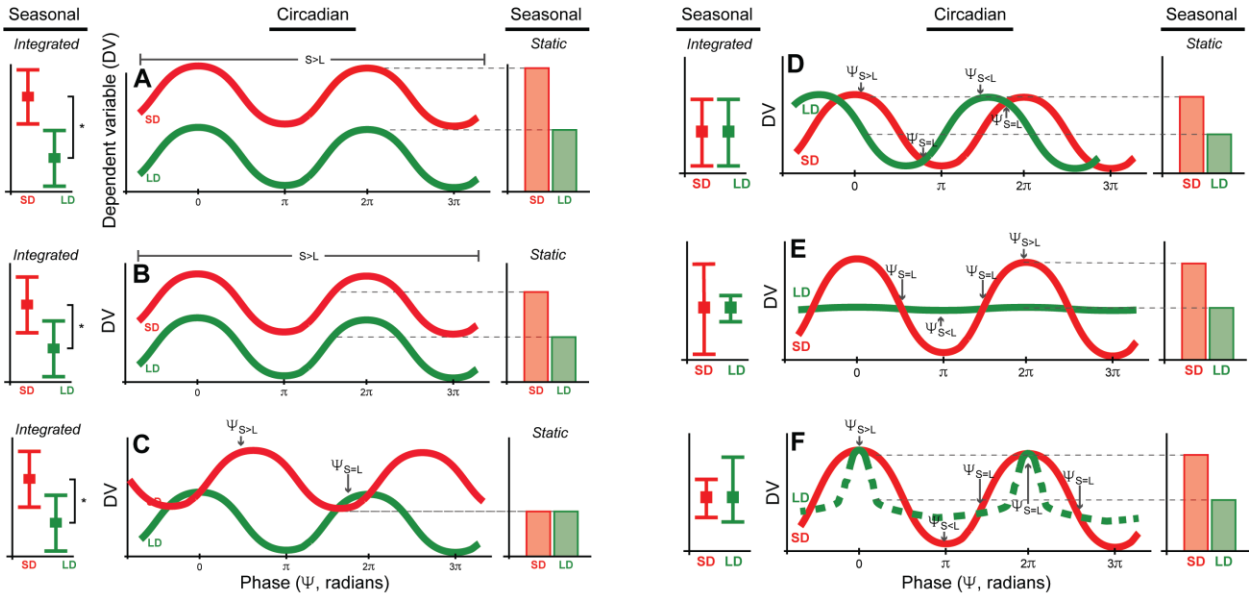

Figure 28 - Modeling interactions among circannual and circadian rhythms in seasonal immunomodulation

For any trait that changes over the course of the day, comparisons between photoperiod conditions are complicated by phase alignment, as circadian phase cannot be perfectly equated across different photoperiods. The common methodological approach of obtaining one measurement/sample at a single time of day (a 'static' measure) thus complicates data interpretation. This is illustrated in Figure 28: each panel depicts a hypothetical dependent variable ("DV"; e.g., immune function) measured after subjects adapted to long-day (LD; green) and short-day (SD; red) photoperiods. Within each lettered panel, the same DV is sampled at multiple resolutions: [1] a line chart in the center of each panel depicts the continuously-sampled trait ('circadian waveform'); [2] a dot plot to the left of each circadian waveform illustrates the mean (± range) daily value ('integrated' measure; equal to the mean of the continuously-sampled waveform); and [3] a bar plot to the right of each waveform illustrates the values that would be obtained from these oscillations if data were sampled at just one phase alignment ('static' sample; indicated by dashed lines).

(A) Panel A illustrates a scenario in which the DV is greater in SD than in LD (SD > LD) and the integrated and static DV measures agree with one another (congruence). The integrated measure indicates an omnibus effect of photoperiod (SD > LD; dot plot). Robust daily rhythms are evident, and their waveforms do not exhibit any overlap (line plot); thus any static sample of the DV, obtained at any phase (φ), would also indicate a SD > LD (bar plot). Panel A is an extreme example of a combination of seasonal and circadian chronotypes in which trait ranges exhibit no overlap, and thus there exists no circadian alignment in which a static sample would identify any relation other than SD > LD. (B) Panel B also illustrates congruent integrated and static measures. In this scenario, the daily waveforms exhibit substantial range overlap, but the SD > LD relation is maintained at all times because of their idiosyncratic phase alignment. Thus as in panel A, in this phase alignment, all static samples would indicate SD > LD. (C) Panel C depicts

Figure 28 - Modeling interaction among circannual and circadian rhythms in seasonal immunomodulation (continued)

waveforms with the same shapes and absolute values as in panel B, but with a different phase alignment. The integrated DV measure remains unchanged (SD > LD), but there now exist phases where a static sample would yield identical values in SD and LD; this underscores that when photoperiods differ, the choices of [1] phase alignment (e.g., by dark onset, by light onset, by photophase midpoint) and [2] sampling time collectively affect whether a Type II error is made, even if waveforms are similar between photoperiods. (D) Panel D also depicts the same waveforms as panel B, but now both phase alignment (as in panel C) and mean integrated value (SD = LD) are shifted. As a result, there now exist multiple time points at which a static sample would generate Type I errors (either in the form of SD > LD, or SD < LD). (E, F) Circadian waveforms are seldom comparable between different photoperiods. Thus, panels E and F illustrate the potential pitfalls associated with static DV samples under conditions in which photoperiod also modulates circadian waveform. Integrated daily means are identical (SD = LD) within each panel, but now either oscillation amplitude (panel E) or waveform (panel F) differs across photoperiods. This also yields Type I errors in both directions under static sampling. Only by sampling at multiple intervals across the circadian day can the likelihood of these errors be minimized and seasonal phenotypes clearly identified.

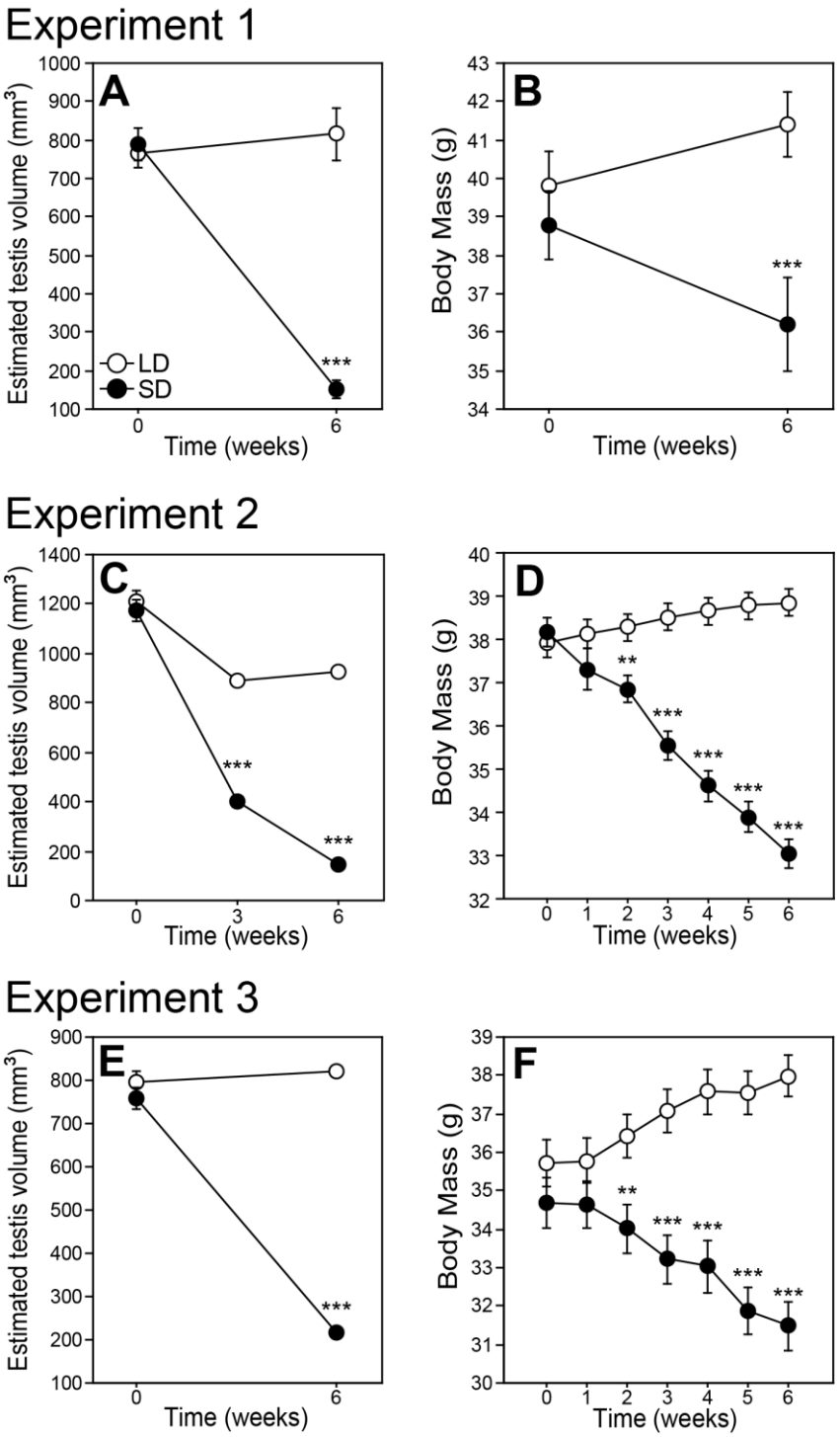

Figure 29 - Reproductive and somatic responses to photoperiod in experiments 1-3
Mean ± SEM (A) estimated testis volumes (ETV; mm3) and (B) body mass of male Siberian hamsters in Experiment 1 (PBL concentrations). Mean ± SEM (C) ETV and (D) body mass of male Siberian hamsters in Experiment 2 (LPS-induced innate inflammatory responses). Mean ± SEM (E) ETV and (F) body mass of male Siberian hamsters in Experiment 3 (adaptive DTH responses). **P<0.01, ***P<0.001 vs. LD value.

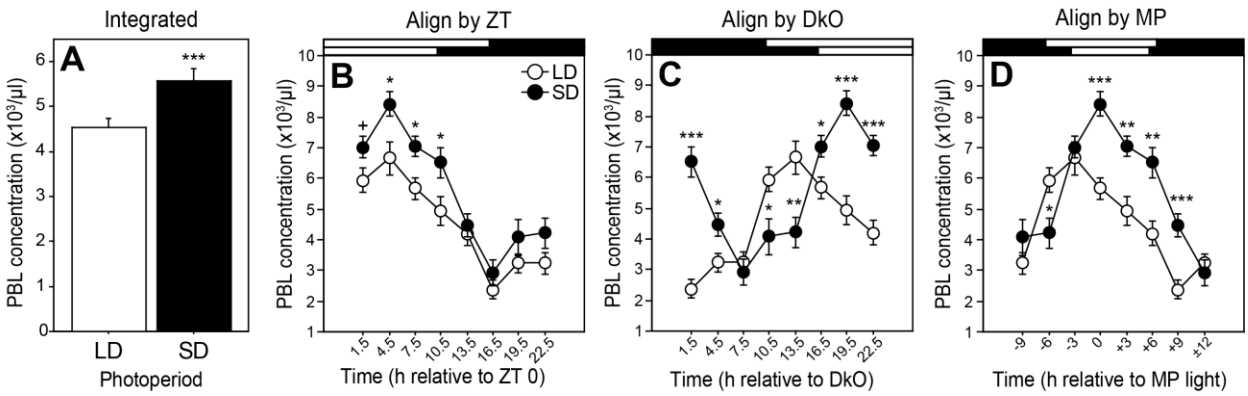

Figure 30 - Peripheral blood leukocytes (PBLs): effect of circadian phase alignment
(A) Integrated 24 h mean ± SEM of PBL concentrations in male Siberian hamsters following adaptation to LD (open symbols) or SD (filled symbols) photoperiods, calculated as the average of the 8 static PBL determinations within each photoperiod. (B) Mean ± SEM PBL concentrations of LD and SD hamsters obtained by static measurements at phases indicated along the abscissa, and with photoperiod treatment groups aligned by zeitgeber time (ZT). (C) Data from panel B aligned relative to the onset of darkness (DkO). (D) Data from panel B aligned relative to the midpoint of the light phase (MP). +P<0.10, *P<0.05, **P<0.01, ***P<0.001 vs. LD value.

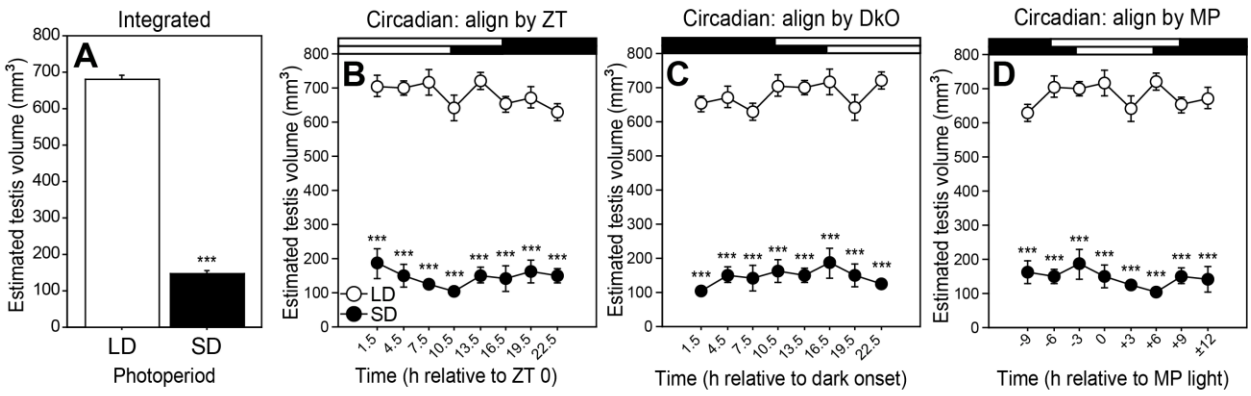

Figure 31 - Estimated testis volumes (ETVs): effect of circadian phase alignment
(A) Integrated 24 h mean ± SEM of ETV of male Siberian hamsters following adaptation to LD (open symbols) or SD (filled symbols) photoperiods, calculated as the average of the 8 static ETV determinations within each photoperiod. (B) Mean ± SEM ETV of LD and SD hamsters obtained by static measurements at phases indicated along the abscissa, and with photoperiod treatment groups aligned by zeitgeber time (ZT). (C) Data from panel B aligned relative to the onset of darkness (DkO). (D) Data from panel B aligned relative to the midpoint of the light phase (MP). ***P<0.001 vs. LD value.

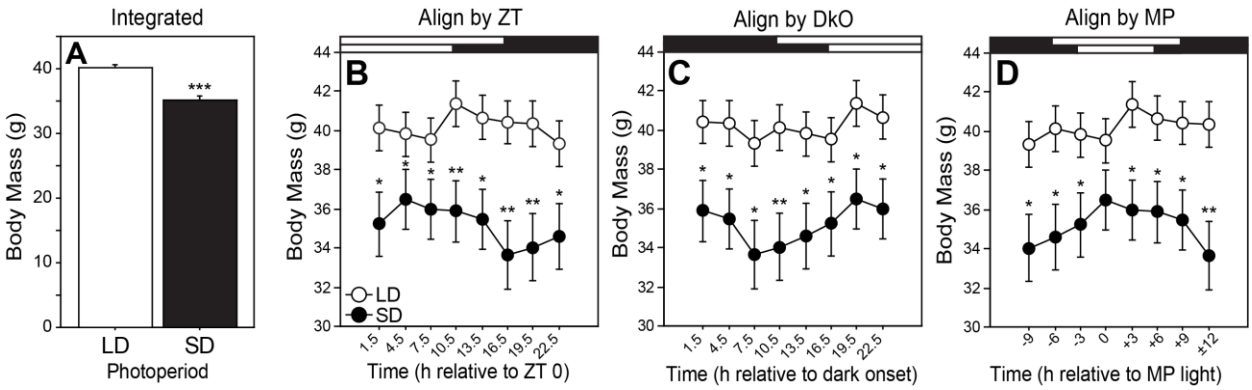

Figure 32 - Body mass: effect of circadian diurnal phase alignment

(A) Integrated 24 h mean ± SEM body mass of male Siberian hamsters following adaptation to LD (open symbols) or SD (filled symbols) photoperiods, calculated as the average of the 8 daily static body mass determinations within each photoperiod. (B) Mean ± SEM body mass of LD and SD hamsters obtained by static measurements at phases indicated along the abscissa, and with photoperiod treatment groups circadian aligned by zeitgeber time (ZT). (C) Data from panel B aligned relative to the onset of darkness (DkO). (D) Data from panel B aligned relative to the midpoint of the light phase (MP). *P<0.05, **P<0.01, ***P<0.001 vs. LD value.

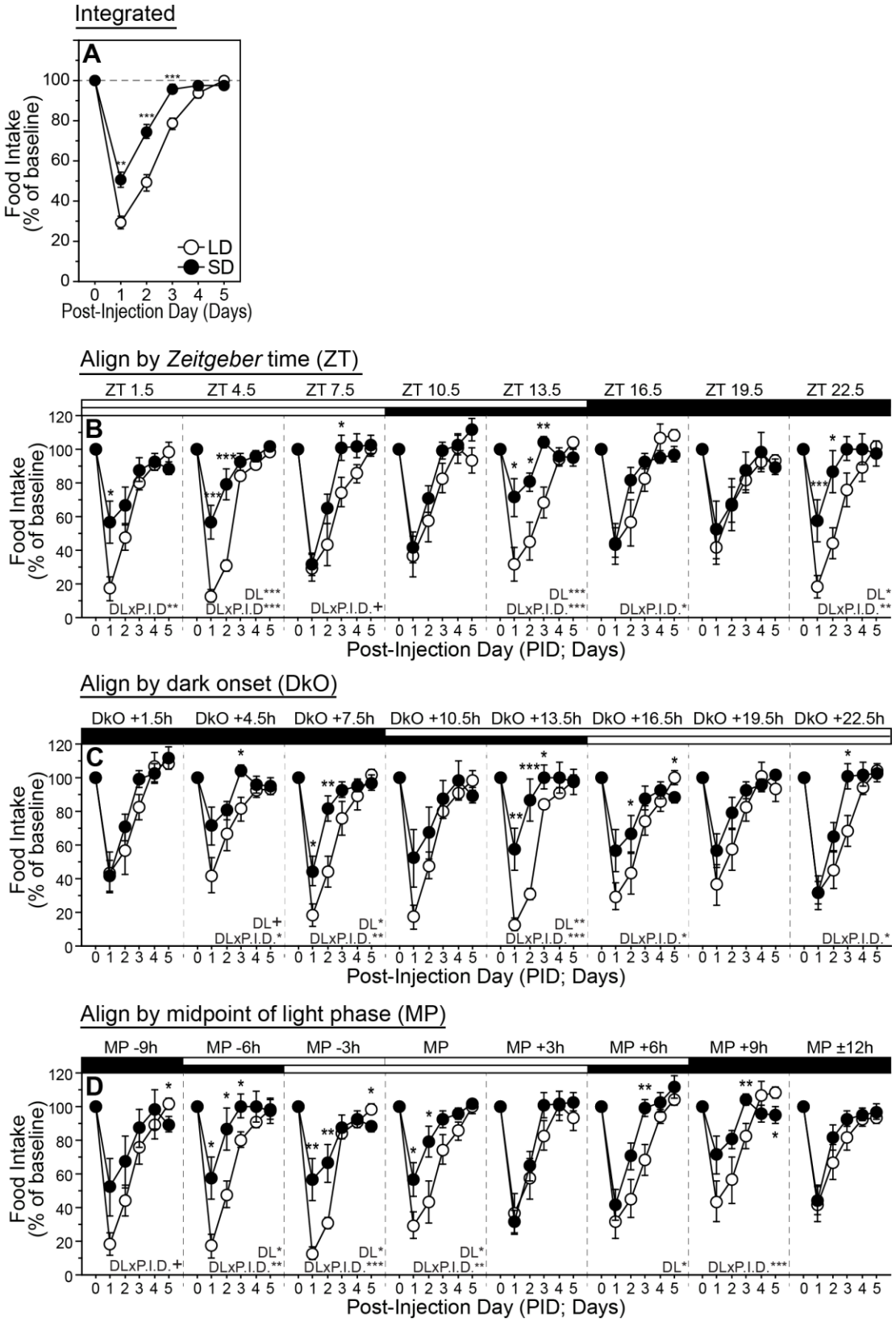

Figure 33 - Sickness behavior: effect of circadian phase alignment

Figure 33 - Sickness behavior: effect of circadian phase alignment (continued)
Mean ± SEM % change in food intake (anorexia; relative to baseline food intake) of male Siberian hamsters following adaptation to LD (open symbols) or SD (filled symbols) photoperiods and injection with LPS (625 µg/kg) at 1 of 8 phases of the circadian cycle. (A) Integrated, 24 h mean ± SEM anorexic responses, calculated as the average of the responses elicited by treatments delivered at all 8 phases within each photoperiod. (B) Mean ± SEM anorexia of LD and SD hamsters challenged with LPS at one of 8 phases (indicated above each panel), and with photoperiod treatment groups aligned by zeitgeber time (ZT). (C) Data from panel B aligned relative to the onset of darkness (DkO). (D) Data from panel B aligned relative to the midpoint of the light phase (MP). Within each panel, statistical significance and trends for the main effect of day length (DL) term and/or of the DL x 'post-injection day' interaction term (DL x P.I.D.) in the ANOVA are indicated with the following symbols: +P<0.10, *P<0.05, **P<0.01, ***P<0.001. Pairwise comparisons: *P<0.05, **P<0.01, ***P<0.001 vs. LD value.

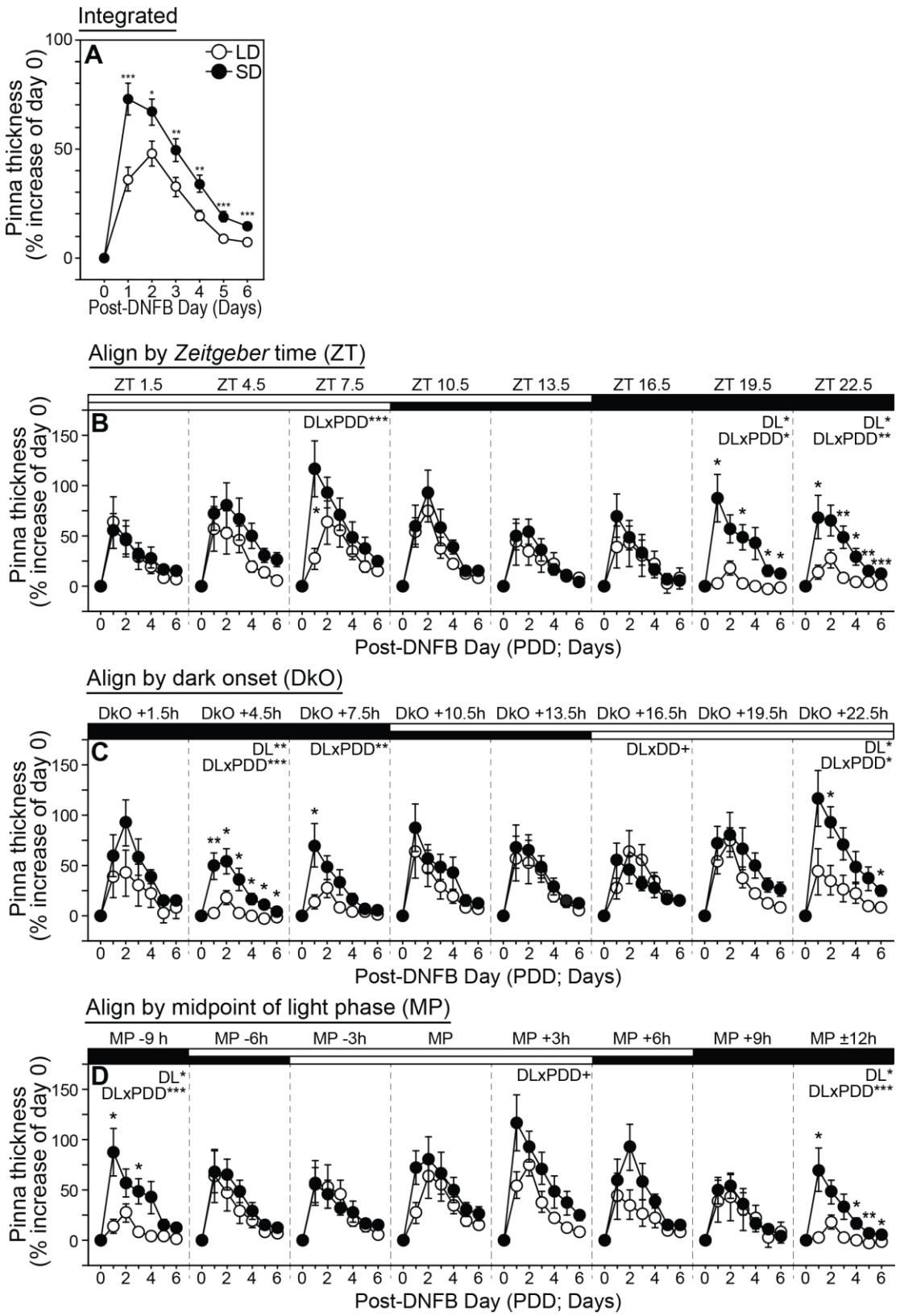

Figure 34 - DTH reactions: effect of circadian diurnal phase alignment

Figure 34 - DTH reactions: effect of circadian diurnal phase alignment (continued)
Mean ± SEM DTH skin inflammatory response (% increase in pinna thickness) of male Siberian hamsters housed in LD (open symbols) or SD (filled symbols) photoperiods, sensitized to DNFB, and challenged with DNFB at 1 of 8 phases of the circadian cycle. (A) Integrated, 24 h mean ± SEM DTH responses, calculated as the average of the responses elicited by treatments delivered at all 8 phases within each photoperiod. (B) Mean ± SEM DTH of LD and SD hamsters challenged with DNFB at one of 8 phases (indicated above each panel), and with photoperiod treatment groups aligned by zeitgeber time (ZT). (C) Data from panel B aligned relative to the onset of darkness (DkO). (D) Data from panel B aligned relative to the midpoint of the light phase (MP). Within each panel, statistical significance and trends for the main effect of day length (DL) term and/or of the DL x 'Post-DNFB Day' term (DL x P.D.D.) in the ANOVA are indicated with the following symbols: +P<0.10, *P<0.05, **P<0.01, ***P<0.001. Pairwise comparisons: *P<0.05, **P<0.01, ***P<0.001 vs. LD value.

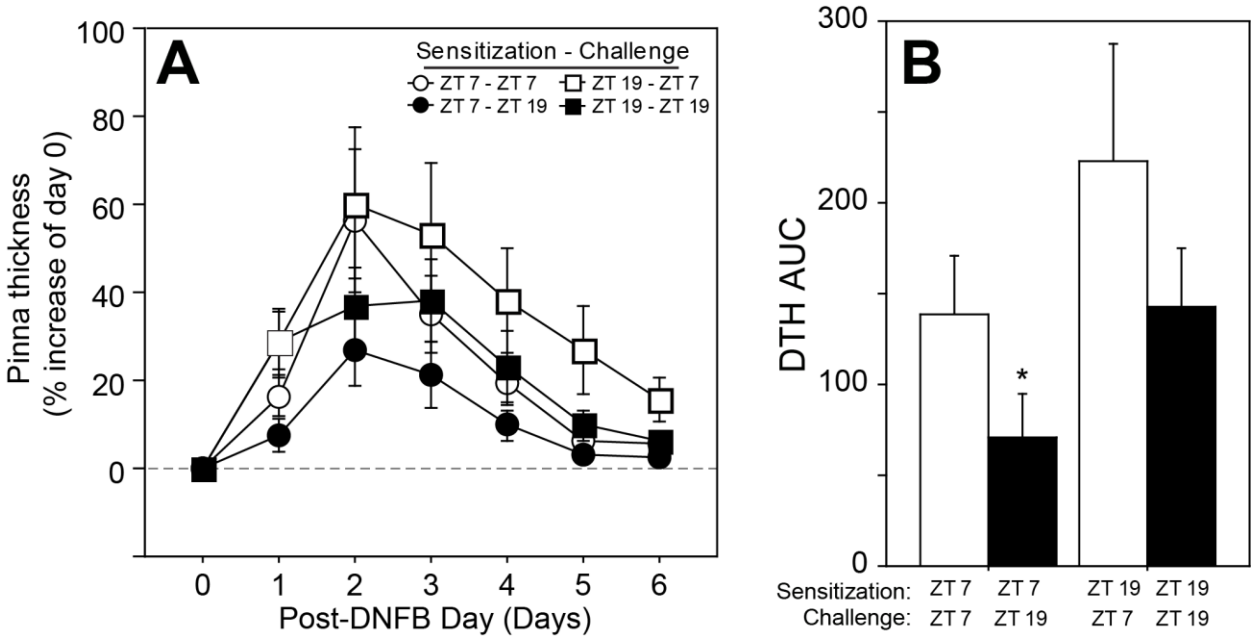

Figure 35 - Effects of sensitization time on circadian rhythms in response to DTH challenge (A) Mean ± SEM percentage increase in pinna thickness in male Siberian hamsters in experiment 3 supplement. Hamsters housed in a LD photoperiod (lights off at ZT15) were sensitized to DNFB at either ZT 7 or ZT 19, and were challenged with DNFB one week later, at either ZT 7 or ZT 19. (B) Area under the curve of the DTH response depicted in panel A (DTH-AUC). *P<0.05 vs. ZT7–ZT7 value.

Appendix B: Tables

Circadian manipulation	LMA/ T_b	Measure	Microbe F Statistic	Microbe P-Value	SPF-NC	GF-NC	ex-GF-NC
					n=18	n=16	n=6
12:12 light:dark cycle	LMA	LSP Power	17.495	<0.0001	151.639 (7.315)	265.580 (20.217) ***	152.278 (24.378) ##
12:12 light:dark cycle	LMA	Mean onset time	5.755	0.0067	19.041 (0.050)	19.174 (0.039) *	18.879 (0.076) ##
12:12 light:dark cycle	LMA	Onset time variability	7.362	0.002	0.347 (0.024)	0.266 (0.023) *	0.435 (0.039) ##
12:12 light:dark cycle	LMA	Mean offset time	14.024	<0.0001	7.494 (0.089)	6.688 (0.139)	7.281 (0.109)
12:12 light:dark cycle	LMA	Offset time variability	1.256	0.2966	0.445 (0.036)	0.472 (0.051)	0.571 (0.044)
12:12 light:dark cycle	LMA	Alpha duration	20.405	<0.0001	12.453 (0.090)	11.514 (0.135) ***	12.402 (0.148) ##
12:12 light:dark cycle	LMA	Total daily activity counts	0.818	0.449	15469 (489)	16167 (1065)	14220 (1069)
12:12 light:dark cycle	LMA	Dark phase counts	2.917	0.0666	11132 (416)	12711 (845)	10057 (738)
12:12 light:dark cycle	LMA	Light phase counts	3.468	0.0417	4336 (171)	3455 (267) **	4162 (591)
12:12 light:dark cycle	LMA	NCPRA (relative amplitude)	17.155	<0.0001	0.588 (0.011)	0.686 (0.014) ***	0.533 (0.044) ###
		`			n=18	n=15	n=4
12:12 light:dark cycle	T_b	LSP Power	1.044	0.3627	450.417 (27.736)	530.932 (48.455)	503.212 (101.174)
12:12 light:dark cycle	T_b	Mean onset time	3.323	0.0481	18.852 (0.119)	19.088 (0.111)	18.456 (0.058) #
12:12 light:dark cycle	T_b	Onset time variability	0.764	0.4737	0.354 (0.033)	0.386 (0.059)	0.478 (0.078)
12:12 light:dark cycle	T_b	Mean offset time	16.938	<0.0001	7.801 (0.074)	7.041 (0.121) ***	7.769 (0.163) #
12:12 light:dark cycle	T_b	Offset time variability	4.661	0.0163	0.431 (0.056)	0.507 (0.067)	0.832 (0.038) ** #
12:12 light:dark cycle	T_b	Alpha duration	20.696	<0.0001	12.949 (0.133)	11.953 (0.118) ***	13.313 (0.143) ###
12:12 light:dark cycle	T_b	Daily mean temp	6.904	0.003	36.47 (0.04)	36.14 (0.07) ***	36.15 (0.22) *
12:12 light:dark cycle	T_b	Dark phase mean temp	5.367	0.0094	37.24 (0.04)	36.97 (0.08) **	36.82 (0.25) *
12:12 light:dark cycle	T_b	Light phase mean temp	3.769	0.0332	35.66 (0.04)	35.42 (0.07) **	35.43 (0.20)
					n=18	n=16	n=5
Constant Darkness	LMA	LSP Period	0.403	0.6716	23.992 (0.026)	23.997 (0.027)	24.040 (0.046)
Constant Darkness	LMA	LSP Power	6.816	0.0031	159.136 (11.451)	225.452 (20.907) **	119.494 (23.600) #
Constant Darkness	LMA	Onset tau	4.236	0.0223	23.953 (0.013)	23.993 (0.015) *	23.916 (0.025) #
Constant Darkness	LMA	Onset error	0.885	0.4216	0.348 (0.030)	0.309 (0.023)	0.374 (0.045)
Constant Darkness	LMA	Offset tau	2.63	0.0859	23.941 (0.021)	24.002 (0.019)	23.950 (0.017)
Constant Darkness	LMA	Offset error	1.824	0.176	0.569 (0.040)	0.466 (0.029)	0.554 (0.109)
Constant Darkness	LMA	Alpha duration	16.564	<0.0001	12.604 (0.145)	11.533 (0.133) ***	12.318 (0.074) ##
Constant Darkness	LMA	Total daily activity counts	3.151	0.0548	15122 (825)	13217 (879)	10914 (1648)
Constant Darkness	LMA	Alpha phase counts	2.893	0.0684	11629 (641)	10398 (726)	8308 (1243)
Constant Darkness	LMA	Rho Phase Counts	3.679	0.0352	3434 (206)	2819 (163) *	2553 (426)
Constant Darkness	LMA	NCPRA (relative amplitude)	17.409	<0.0001	0.580 (0.015)	0.703 (0.016) ***	0.557 (0.041) ###
					n=18	n=15	n=4
Constant Darkness	T_b	LSP Period	2.153	0.1318	23.972 (0.017)	24.020 (0.017)	23.975 (0.032)
Constant Darkness	Tb	LSP Power	7.356	0.0022	441.018 (34.201)	559.354 (26.741) *	316.890 (38.354) ###
Constant Darkness	T_b	Onset tau	2.297	0.116	23.947 (0.013)	23.981 (0.013)	23.932 (0.017)
Constant Darkness	T_b	Onset error	1.546	0.2276	0.264 (0.024)	0.342 (0.036)	0.282 (0.099)
Constant Darkness	T_b	Offset tau	1.849	0.1729	23.946 (0.023)	24.001 (0.015)	23.973 (0.047)
Constant Darkness	T_b	Offset error	0.841	0.4402	0.482 (0.031)	0.463 (0.048)	0.578 (0.068)
Constant Darkness	T_b	Alpha duration	9.669	0.0005	12.738 (0.188)	11.916 (0.116) **	13.188 (0.184) ###
Constant Darkness	T_b	Daily mean temp	19.412	<0.0001	36.44 (0.04)	35.97 (0.03) ***	36.13 (0.23) *
Constant Darkness	T_b	Alpha phase mean temp	15.359	<0.0001	37.33 (0.04)	36.87 (0.05) ***	36.82 (0.29) **
Constant Darkness	T_b	Rho phase mean temp	9.098	0.0007	35.50 (0.06)	35.12 (0.05) ***	35.33 (0.22)

Table 1 - Gut microbiota contribute to circadian rhythms in 12:12 light:dark cycle and constant darkness

Mean (±SEM). *P<0.05 v SPF-NC, **P<0.01 v SPF-NC, ***P<0.001 v SPF-NC, #P<0.05 v GF-NC, ##P<0.01 v GF-NC, ###P<0.001 v GF-NC.

Circadian manipulation	Measure	Dependent variable	Diet F statistic	Diet P Value	Microbe x Diet F statistic	Microbe x Diet P Value	SPF-NC	GF-NC	SPF-HF	GF-HF
							n=18	n=16	n=8	n=8
12:12 light:dark cycle	LMA	LSP Power	1.427	0.2384	1.441	0.2361	151.639 (7.315)	265.580 (20.217)	151.746 (6.833)	221.250 (31.355)
12:12 light:dark cycle	LMA	Mean onset time	4.826	0.0331	0.173	0.679	19.041 (0.050)	19.174 (0.039) *	18.887 (0.090) ##	19.069 (0.052)
12:12 light:dark cycle	LMA	Onset time variability	0.093	0.7621	0.088	0.7676	0.347 (0.024)	0.266 (0.023)	0.347 (0.057)	0.247 (0.022)
12:12 light:dark cycle	LMA	Mean offset time	3.251	0.0779	1.492	0.2281	7.781 (0.172)	6.896 (0.298)	6.994 (0.201) *	6.745 (0.144)
12:12 light:dark cycle	LMA	Offset time variability	4.394	0.0416	4.417	0.0411	7.494 (0.089)	6.688 (0.139) ***	7.494 (0.161) ##	7.245 (0.070) #
12:12 light:dark cycle	LMA	Alpha duration	7.884	0.0073	3.042	0.0878	12.453 (0.090)	11.514 (0.135)	12.608 (0.234)	12.177 (0.111) ##
12:12 light:dark cycle	LMA	Total daily activity counts	0.64	0.4279	1.517	0.2243	15469 (489)	16167 (1065)	17620 (1494)	15710 (1264)
12:12 light:dark cycle	LMA	Alpha counts	0.131	0.7188	1.212	0.2767	11132 (416)	12711 (845)	12326 (956)	12109 (1008)
12:12 light:dark cycle	LMA	Rho counts	2.803	0.1009	1.521	0.2237	4336 (171)	3455 (267)	5294 (598)	3600 (377)
12:12 light:dark cycle	LMA	NCPRA (relative amplitude)	0.893	0.3495	0.202	0.6549	0.588 (0.011)	0.686 (0.014)	0.579 (0.024)	0.662 (0.024)
							n=18	n=15	n=8	n=7
12:12 light:dark cycle	Tb	LSP Power	7.076	0.0109	0.723	0.3997	450.417 (27.736)	530.932 (48.455)	309.417 (27.736)	424.557 (32.154)
12:12 light:dark cycle	Tb	Mean onset time	12.651	0.0009	0.39	0.5354	18.852 (0.119)	19.088 (0.111)	18.470 (0.070) ##	18.542 (0.109)##
12:12 light:dark cycle	Tb	Onset time variability	14.251	0.0005	1.642	0.2067	0.354 (0.033)	0.386 (0.059)	0.491 (0.033) *	0.663 (0.064) #
12:12 light:dark cycle	Tb	Mean offset time	1.103	0.2994	1.693	0.2	7.801 (0.074)	7.041 (0.121) ***	7.774 (0.086) ###	7.297 (0.062)
12:12 light:dark cycle	Tb	Offset time variability	2.321	0.1348	0.01	0.9202	0.431 (0.056)	0.507 (0.067)	0.547 (0.056)	0.609 (0.055)
12:12 light:dark cycle	Tb	Alpha duration	15.032	0.0003	2.238	0.1418	12.949 (0.133)	11.953 (0.118)	13.304 (0.116)	12.755 (0.148) ###
12:12 light:dark cycle	Tb	Daily mean temp	20.373	<0.0001	0.842	0.337	36.47 (0.04)	36.14 (0.07)	36.86 (0.08) ***	36.39 (0.03) #
12:12 light:dark cycle	Tb	Alpha mean temp	3.937	0.0535	0.689	0.4109	37.24 (0.04)	36.97 (0.08)	37.46 (0.08) *	37.05 (0.01)
12:12 light:dark cycle	Tb	Rho mean temp	38.819	<0.0001	1.928	0.1719	35.66 (0.04)	35.42 (0.07)	36.20 (0.07) ***	35.77 (0.05) ##
							n=18	n=16	n=8	n=7
Constant Darkness	LMA	LSP Period	2.337	0.1333	3.394	0.072	23.992 (0.026)	23.997 (0.027)	23.881 (0.041)	24.007 (0.025)
Constant Darkness	LMA	LSP Power	5.491	0.0236	0.276	0.6017	159.136 (11.451)	225.452 (20.907)	124.444 (13.904)	170.691 (18.308)
Constant Darkness	LMA	Onset tau	17.668	0.0001	0.896	0.3489	23.953 (0.013)	23.993 (0.015)	23.868 (0.017) ***	23.939 (0.016) #
Constant Darkness	LMA	Onset error	4.394	0.0417	0.002	0.9655	0.348 (0.030)	0.309 (0.023)	0.284 (0.030)	0.241 (0.022)
Constant Darkness	LMA	Offset tau	0.212	0.6475	0.262	0.6112	23.941 (0.021)	24.002 (0.019)	23.942 (0.031)	23.976 (0.028)
Constant Darkness	LMA	Offset error	0.574	0.4525	1.739	0.1939	0.569 (0.040)	0.466 (0.029)	0.541 (0.072)	0.569 (0.060)
Constant Darkness	LMA	Alpha duration	9.744	0.0031	6.014	0.0181	12.604 (0.145)	11.533 (0.133)	12.721 (0.193)	12.509 (0.191) ###
Constant Darkness	LMA	Total daily activity counts	0.02	0.8872	0.286	0.5956	15122 (825)	13217 (879)	14396 (1301)	13637 (1058)
Constant Darkness	LMA	Alpha counts	0.003	0.9551	0.558	0.459	11629 (641)	10398 (736)	11039 (963)	11084 (916)
Constant Darkness	LMA	Rho counts	0.809	0.3731	0.045	0.8326	3434 (206)	2819 (163)	3254 (451)	2527 (160)
Constant Darkness	LMA	NCPRA (relative amplitude)	6.414	0.0149	1.139	0.2915	0.580 (0.015)	0.703 (0.016)	0.552 (0.22)	0.633 (0.023) #
							n=18	n=15	n=8	n=7
Constant Darkness	Tb	LSP Period	4.029	0.0509	0.43	0.5155	23.972 (0.017)	24.020 (0.017)	23.919 (0.019)	23.993 (0.020)
Constant Darkness	Tb	LSP Power	33.758	<0.0001	0.441	0.5101	441.018 (34.201)	559.354 (26.741)	202.706 (32.535) ***	369.933 (32.209) ###
Constant Darkness	Tb	Onset tau	12.832	0.0008	0.387	0.5369	23.947 (0.013)	23.981 (0.013)	23.879 (0.018) **	23.933 (0.015) #
Constant Darkness	Tb	Onset error	0.335	0.5656	0.127	0.7237	0.264 (0.024)	0.342 (0.036)	0.256 (0.025)	0.310 (0.035)
Constant Darkness	Tb	Offset tau	0.827	0.3682	1.442	0.2363	23.946 (0.023)	24.001 (0.015)	23.894 (0.033)	24.009 (0.018)
Constant Darkness	Tb	Offset error	3.461	0.0695	0.008	0.9275	0.482 (0.031)	0.463 (0.048)	0.588 (0.054)	0.559 (0.094)
Constant Darkness	Tb	Alpha duration	12.712	0.0009	1.971	0.1673	12.738 (0.188)	11.916 (0.116)	13.147 (0.126)	12.856 (0.200) ###
Constant Darkness	Tb	Daily mean temp	34.18	<0.0001	1.177	0.284	36.45 (0.05)	35.98 (0.04)	36.71 (0.08) ###	36.36 (0.05) ***
Constant Darkness	Tb	Alpha mean temp	0.745	0.3927	1.391	0.2446	37.33 (0.05)	36.87 (0.08)	37.31 (0.08) ###	36.99 (0.02) ***
Constant Darkness	Tb	Rho mean temp	61.68	<0.0001	0.121	0.7297	35.50 (0.06)	35.13 (0.05)	36.00 (0.07) *** ###	35.68 (0.07) ###

Table 2 - High fat diet contribute to circadian rhythms in 12:12 light:dark cycle and constant darknesss

Mean (±SEM). *P<0.05 v SPF-NC, **P<0.01 v SPF-NC, ***P<0.001 v SPF-NC, #P<0.05 v GF-NC, ##P<0.01 v GF-NC, ###P<0.001 v GF-NC.